Biological and Medical Physics, Biomedical Engineering

Sharon Gerecht *Editor*

Biophysical Regulation of Vascular Differentiation and Assembly

Second Edition

Springer

Biological and Medical Physics, Biomedical Engineering

More information about this series at http://www.springer.com/series/3740

BIOLOGICAL AND MEDICAL PHYSICS, BIOMEDICAL ENGINEERING

The fields of biological and medical physics and biomedical engineering are broad, multidisciplinary and dynamic. They lie at the crossroads of frontier research in physics, biology, chemistry, and medicine. The Biological and Medical Physics, Biomedical Engineering Series is intended to be comprehensive, covering a broad range of topics important to the study of the physical, chemical and biological sciences. Its goal is to provide scientists and engineers with textbooks, monographs, and reference works to address the growing need for information.

Books in the series emphasize established and emergent areas of science including molecular, membrane, and mathematical biophysics; photosynthetic energy harvesting and conversion; information processing; physical principles of genetics; sensory communications; automata networks, neural networks, and cellular automata. Equally important will be coverage of applied aspects of biological and medical physics and biomedical engineering such as molecular electronic components and devices, biosensors, medicine, imaging, physical principles of renewable energy production, advanced prostheses, and environmental control and engineering.

Sharon Gerecht
Editor

Biophysical Regulation of Vascular Differentiation and Assembly

Second Edition

Springer

Editor
Sharon Gerecht
Department of Chemical and Biomolecular Engineering
Johns Hopkins Physical Sciences–Oncology Center and Institute for NanoBioTechnology
Baltimore, MD, USA

ISSN 1618-7210 ISSN 2197-5647 (electronic)
Biological and Medical Physics, Biomedical Engineering
ISBN 978-3-319-99318-8 ISBN 978-3-319-99319-5 (eBook)
https://doi.org/10.1007/978-3-319-99319-5

Library of Congress Control Number: 2018958962

This Springer imprint is published by the registered company Springer Nature Switzerland AG
The registered company address is: Gewerbestrasse 11, 6330 Cham, Switzerland

With heartfelt appreciation I dedicate this book to my parents, Ziva and Alexander Gerecht, whose unconditional support continually elevated me to new heights, both personally and professionally.

Preface

It has been 7 years since the first edition of *Biophysical Regulation of Vascular Differentiation and Assembly* in the series *Biological and Medical Physics, Biomedical Engineering*. With the significant changes that have occurred in the field in the interim, I am pleased to present this second edition.

Our first book presented the reader with an understanding of the concept of how biophysical cues in the microenvironment regulate vascular differentiation and assembly. Since then, many studies have focused on elucidating critical aspects in the microenvironment that regulate vascular development and growth, both in vitro and in vivo. Today, researchers are using increasingly sophisticated tools such as microfluidics, particles, biomaterials, and three-dimensional printing to recapitulate many biophysical cues in tissue culture systems. Some of these technologies are also being translated into animal models to validate mechanism and test potential therapeutics.

This book updates our previous work on a range of aspects governing the microvasculature related to normal and disease processes. The first chapter explores recent insights into how endothelial cell-pericyte interactions modulate tube morphogenesis and maturation (*Davis*). Chapters 2 and 3 detail how mechanical forces regulate vascularization in three-dimensional constructs (*Zohar*, *Landau*, *Levenberg*) and the means by which matrix properties and oxygen tension regulate vascular fate and assembly (*Blatchley, Abaci, Hanjaya-Putra, Gerecht*). The next chapter focuses on biophysical cues as they relate to vascular aging, and various culture systems for studying vascular aging (*Pitrez, Aires, Tomé, Ferreira, Ferreira*). Finally, in the realm of tissue engineering, the use of 3D printing to engineer complex vascularized tissue (*Yeung, Yesantharao, Ong, Hibino*) and harnessing of biophysical cues for therapeutic vasculature interfacing with the damaged brain (*Nih, Carmichael, Segura*) and infarcted heart (*Morrissette-McAlmon, Hawthorne, Snyder, Grayson*) are presented.

I am grateful to all the authors for their outstanding and timely contributions and Springer Nature for publishing this project. Special thanks to Christopher Coughlin,

the publishing editor of the book, for following up and supporting this second edition, and Ho Ying Fan and Kiruthika Kumar for excellent production work. Finally, I would like to thank Christine Schutzman who helped with editing the chapters and making this entire process seamless.

Baltimore, MD, USA Sharon Gerecht

Contents

Chapter 1
Molecular Control of Capillary Tube Morphogenesis and Maturation Through Endothelial Cell-Pericyte Interactions: Regulation by Small GTPase-Mediated Signaling, Kinase Cascades, Extracellular Matrix Remodeling, and Defined Growth Factors

George E. Davis

1.1 Introduction

Considerable progress has been made in our understanding of molecular events underlying the development of the vasculature and how it is regulated in postnatal life, particularly in the context of tissue injury and tumorigenesis [1, 18, 19, 30, 31, 36, 55, 89, 92]. A key point is that the major advances in the field appear to be directly related to our understanding of basic events that control these processes such as cell survival, proliferation, migration, invasion, and morphogenesis. Also, it should be pointed out that both in vitro and in vivo studies have played major roles in advancing this understanding, and it remains essential that both types of approaches are utilized to approach the complexities inherent in the developing and postnatal vasculature.

The molecular control of the vasculature is affected by many factors and signals, and in this chapter, we will focus on the influence of extracellular matrix (ECM), matrix metalloproteinases (MMPs), small GTPase-mediated signal transduction, defined growth factors, and endothelial cell (EC)-pericyte interactions in controlling vascular development and postnatal vascularization events. In general terms, the ECM is a fundamental regulator of vascularization, in that it presents a physical scaffold containing adhesive and growth factor modulatory signals that are necessary for blood vessels to form and mature [34, 35, 57, 58, 81, 89]. Vascular cell

G. E. Davis (✉)
Department of Molecular Pharmacology and Physiology,
University of South Florida School of Medicine, Tampa, FL, USA
e-mail: gedavis@health.usf.edu

S. Gerecht (ed.), *Biophysical Regulation of Vascular Differentiation and Assembly*, Biological and Medical Physics, Biomedical Engineering,
https://doi.org/10.1007/978-3-319-99319-5_1

recognition of ECM occurs through a variety of receptors including both integrin and non-integrin adhesion receptors [34, 58, 89, 97], and these mediate the complex signals that are delivered. There is considerable evidence that ECM can provide both stimulatory and inhibitory signals [34, 89], and thus, the ECM composition, the vascular cell types, and the biological context of the signaling dictate the cellular response that occurs. An important regulator of ECM structure and function are MMPs which can degrade matrix components [31, 33, 35, 47, 52] but can also release liberate factors such as growth factors and cytokines from these matrices to affect vascular cell behavior. Within the vascular wall, homotypic interactions between ECs [37] and heterotypic interactions of ECs and mural cells affect ECM production and deposition [92, 94], as well as its ability to be degraded by MMPs [87]. Many new studies are now focused on such interactions to understand how mural cells affect EC behavior during development and under various disease conditions [1, 5, 56, 92, 94]. In this chapter, we will review past and present work that addresses mechanisms by which ECM, MMPs, small GTPase signaling, defined growth factors, and EC-pericyte interactions influence vascular tube assembly and remodeling, tube stabilization, and vascular regression to control tissue vascularization in normal versus disease states.

1.2 Concepts in Vascular Tube Morphogenesis in 3D Extracellular Matrices

1.2.1 Extracellular Matrix and Vascular Morphogenesis

A critical regulator of vascular morphogenesis is the ECM which serves as a physical, mechanical, and agonistic substrate to affect survival, motility, invasion, and morphogenic events of both endothelial cells (ECs) and mural cells, including pericytes and vascular smooth muscle cells [1, 18, 34–36, 58, 81, 89, 92]. Interestingly, different types of ECM have distinct effects on the developing or mature vasculature, depending on the biologic context, with evidence for pro-morphogenic, pro-stabilization, or pro-regressive activities [31, 34, 35, 89]. Also, certain ECM environments may present quiescence signals to vascular cells that play an important role in vascular stabilization. Alteration in the ECM, through proteolysis or conformational changes, is known to generate matricryptic sites which activate cells, and thus, the ECM is a critical regulator of how cells perceive their environment and sense an injurious stimulus [24, 26]. Furthermore, the ECM is a scaffold that possesses adhesive signals for cells, by binding to both integrin and non-integrin surface receptors, but it also binds and presents specific growth factors to cells [34, 57, 58, 89]. The ECM also modulates the activation of specific growth factors and, thus, can modulate growth factor action to affect the vasculature [58]. It is clear that co-signaling between integrins and growth factor receptors is a critical regulator of vascularization events both during development and in postnatal life. The ECM is

also mechanosensitive and responds to mechanical forces generated by cells that exert tensional forces on this matrix. A key mechanosensitive ECM component is fibronectin which contains matricryptic sites that affect self-assembly reactions, particularly through the III-I domain [45, 77, 99, 106]. Interestingly, this domain is exposed in instances where fibronectin is absorbed into surfaces, such as cell surfaces or ECM [24, 26, 99], and appears to be particularly exposed when cells exert mechanical force on fibronectin through integrin-based interactions [106]. This facilitates fibronectin binding to itself which promotes the self-assembly reaction (i.e., including disulfide exchange to form covalent bonds between fibronectin molecules) necessary to form an insoluble matrix [77]. Since fibronectin is one of the few ECM proteins with clear mechanosensitive domains, it suggests that fibronectin may play a particularly important role in ECM assembly events that depend on mechanical forces, such as those observed during vascular morphogenic events in a variety of contexts [18, 94, 107].

1.2.2 Differential Effects of ECM Components on Vascular Tube Morphogenesis

Certain ECM components are potent stimulators of vascular tube morphogenesis, while others appear inhibitory. Interestingly, collagen type I, the most abundant ECM component in adult animals, is a potent stimulator of vascular tube morphogenesis in 3D matrices [34, 100] (Fig. 1.1). An accumulating view is that fibrillar collagen matrices are potent ECM agonists for these events. Another strong ECM agonist for EC tube morphogenesis is fibrin [78, 91], a provisional matrix component that is deposited along with fibronectin during tissue injury [34]. Interestingly, the collagen-binding integrins, α2β1 and α1β1, have been shown to control EC tube morphogenic events in vitro and in vivo in collagenous matrices [9, 28, 34, 88], while the fibrin-/fibronectin-binding integrins, αvβ3 and α5β1, have been shown to control tube morphogenesis in fibrin matrices [9, 11]. Because of the strong pro-morphogenic influence of collagen and fibrin matrices, these have predominantly been used to establish 3D EC tube morphogenic models [68, 78] that have strongly enhanced our knowledge concerning the molecular basis for EC tubulogenesis, sprouting, and tube maturation events. Overall, the ECM and integrin data strongly suggests that vascular tube morphogenesis is connected to integrin-mediated recognition of different pro-morphogenic ECM components and that multiple members of the integrin family can participate in stimulating EC tubulogenesis in 3D matrix environments [27, 34]. It does not appear that any particular integrin family member is special in its ability to affect tube morphogenesis. Their influence is dictated by the ECM environment in which the morphogenic process takes place. In contrast, it appears that laminin-rich matrices are likely to present inhibitory signals to endothelial cells to interfere with morphogenic events [34, 35, 71]. As blood vessels mature, laminin matrix deposits as a component of the vascular basement

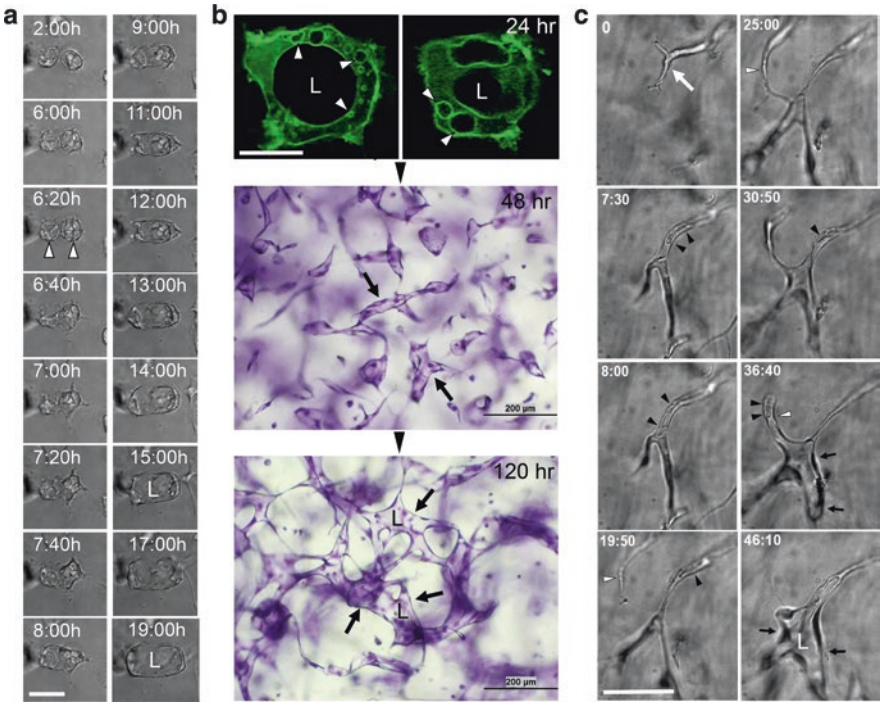

Fig. 1.1 Temporal analysis of endothelial tube formation events in 3D collagen matrices during vasculogenesis and angiogenic sprouting. (**a**) A time-lapse series is shown whereby two ECs are shown to form intracellular vacuoles that eventually coalescence inside each cell and then following cell-cell contact with the neighboring cells form a lumenal space in between the two cells. Vacuole fusion events are observed while they are contacting each other. L indicates EC lumen; arrowheads indicate vacuolating ECs. Bar equals 25 µm. (**b**) Confocal images of ECs expressing GFP-Rac1 fusion proteins that label intracellular vacuoles, the developing lumenal membrane, as well as the plasma membrane during lumen formation events at 24 h of culture. Upper panels- L indicates EC lumenal space, and arrowheads indicate intracellular vacuoles. Bar equals 20 µm. Over time ECs form interconnecting networks of tubes which are illustrated using fixed and toluidine-blue stained cultures. Arrows indicate tube structures; L indicates EC lumen; Bar equals 200 µm. (**c**) EC sprouting was stimulated by the combination of sphingosine-1-phosphate (1 µm) and SDF-1α (200 ng/ml) which were mixed in the collagen matrix. A time-lapse series (over a 46 h period) was taken beneath the surface of the monolayer to examine sprouting events and lumen development in assays mimicking angiogenesis. White arrow and arrowheads indicate EC tip cells that are sprouting through the 3D collagen matrices; black arrowheads indicate intracellular vacuoles that are observed particularly in ECs directly trailing tip cells; black arrows indicate the cell border of EC tubes; L indicates EC lumen. Bar equals 50 µm

membrane, a key ECM remodeling process which occurs as a result of EC-pericyte interactions during capillary tube assembly [94]. Vascular basement membrane assembly generally is thought to be a tube maturation stimulus, and hence, decreased morphogenesis is coincident with its appearance around the abluminal surface of EC-lined tubes. This point needs to be investigated in more detail, but early

information suggests that some laminin isoforms have inhibitory activity toward ECs during morphogenic events [71]. The vasculature appears to predominantly express laminin-8 (α4,β1,γ1- 411), laminin-9 (α4,β2,γ1-421), laminin-10 (α5, β1,γ1- 511), and laminin-11 (α5,β2,γ1- 521) isoforms [34, 50, 76]. In the past and more recently, we have reported that these subunits are differentially expressed by both ECs and pericytes during vascular tube morphogenesis and maturation events [12, 94]. The biological role of each isoform has not yet been elucidated in sufficient detail during these processes.

One critical question that similarly has not been investigated in sufficient detail is the nature of the embryonic ECM environment where vascular development takes place [35, 57]. It is clear that there is much less fibrillar collagen during development, while the matrices are known to be rich in glycosaminoglycans, such as hyaluronic acid, proteoglycans, and fibronectin. It appears that developing embryos strongly depend on the presence of fibronectin (perhaps its importance relates to its mechanosensitive ability to self-assemble) [57]. Fibronectin knockout mice show severe defects in vascular development along with other abnormalities [6, 42]. Fibronectin is also alternatively spliced, and several splice isoforms (IIIA and IIIB) appear to play a critical functional role to promote vascular tube assembly and maturation during development [6]. One of the problems with investigating such issues in a more molecular detail is that there currently are no 3D systems available that mimic an embryonic ECM environment, an important future direction for in vitro model development using vascular or other cell types.

1.3 Review of Work

1.3.1 Molecular Events Regulating Vascular Tube Morphogenesis and EC Sprouting in 3D Matrices

A major effort of our laboratory has been to elucidate the molecule and signaling requirements for ECs to form tube networks when suspended within 3D matrices and to sprout and form tubes from a monolayer surface into 3D matrices [34, 36, 60, 84] (Fig. 1.2). To this end, we have developed 3D matrix microassay systems to assess both of these phenomena in assays that mimic vasculogenesis and angiogenic sprouting events, using either collagen or fibrin matrices [29, 68]. Other laboratories have developed related systems to investigate these events [3, 78]. The majority of our work has focused on models that mimic embryonic vasculogenesis, whereby human ECs are seeded as single cells within a 3D matrix [28, 29, 36, 68]. Using appropriate media conditions, ECs undergo dramatic morphologic changes that lead to the development of interconnecting networks of EC-lined tubes (Fig. 1.1). For example, two ECs are observed in a time-lapse series to form intracellular vacuoles, which fuse within each cell and then through exocytic events; the two cells then interconnect to form a multicellular lumen structure (Fig. 1.1a). There is no

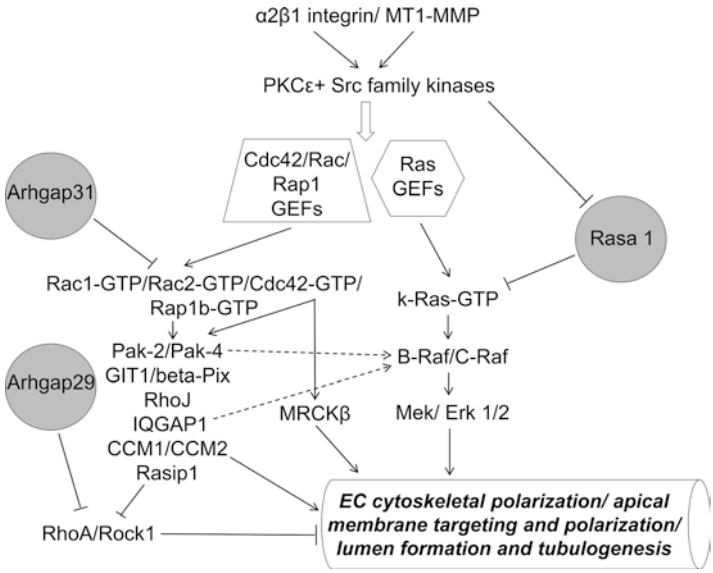

Fig. 1.2 EC tubulogenesis in 3D matrices is controlled by activation of a Cdc42-, Rac-, k-Ras, and Rap1b-dependent signaling cascade: a process antagonized by RhoA, Arhgap31, and Rasa1. A schematic diagram is shown illustrating key molecules and signals that regulate how EC lumen and tube formation occurs in 3D collagen matrices. These molecules and signals control EC cytoskeletal polarization (subapically distributed acetylated and detyrosinated tubulin; basally distributed F-actin) and the generation of the apical membrane which is decorated with key small GTPases including Cdc42, Rac1, Rac2, k-Ras, and Rap1b and the effectors c-Raf and Rasip1. EC tubulogenesis also requires MT1-MMP-dependent matrix proteolysis, a step that is co-dependent and coordinated with the indicated GTPase-, effector-, integrin-, and kinase-dependent signaling cascades. Intracellular vacuoles and vesicles (strongly labeled with Rac1 and k-Ras) traffic along subapically oriented acetylated tubulin tracks and then fuse together in a polarized perinuclear region (where acetylated tubulin co-localizes with Cdc42) to generate and expand the EC apical surface. Another aspect of this EC lumen signaling cascade is to suppress RhoA signaling, and key molecules that participate in this suppression are Cdc42, Rac isoforms, Pak2, Pak4, Rasip1 and its associated Gap, Arhgap29, and the CCM proteins CCM1 and CCM2

intermixing of cytoplasmic contents when this occurs, so the tube consists of adjacent ECs which interact through cell-cell adhesive contacts. In addition, the ECs are attached to the ECM to form the wall of a luminal space and need to maintain these adhesive contacts (i.e., both cell-ECM and cell-cell adhesion) to remain stable on this luminal wall. Intracellular vacuoles can be observed to form through integrin- and cytoskeletal-dependent pinocytic events, and these vacuoles target to a pericentrosomal location in a polarized fashion and then move to fuse with the developing luminal membrane as shown in Fig. 1.1b (upper panel) [8, 28, 30, 62–64, 104]. In Fig. 1.1b, intracellular vacuoles are strongly labeled with a GFP-Rac1 construct [8]. We previously observed labeling of intracellular vacuoles with GFP-Rac1, GFP-Cdc42, and GFP-RalA [8, 30, 79]. This GFP-Cdc42 was expressed using an

EC-specific promoter in zebrafish, revealing that intracellular vacuoles were observed and participate in the lumen formation process of intersegmental vessels during vascular development [62, 104]. Additional work in vivo reveals the clear presence of intracellular vacuoles as a major determinant of EC lumen formation in other species, including mouse and quail [36, 110].

Both Cdc42 and Rac1 are required for intracellular vacuole formation, as well as EC lumen and tube formation [8, 30, 67]. We have performed these experiments using either dominant-negative mutants of Cdc42 and Rac1 or specific siRNAs to these GTPases. Developing multicellular lumenal structures then interconnect into more extensive networks over time (Fig. 1.1b, middle and lower panels). Using an angiogenic sprouting model [9, 68], time-lapse images are shown which reveal how invading ECs interact, develop intracellular vacuoles, and migrate toward each other to form multicellular lumen and tube structures over time (Fig. 1.1c).

After much effort over many years, we have elucidated the molecular requirements and signaling pathways that underlie the ability of human ECs to form lumen and tube structures in 3D matrices [8, 25, 27, 36, 60, 63, 64, 79, 84, 87, 89, 93, 95]. Most of our studies have focused on collagen matrices, and, thus, a major requirement for these events is the α2β1 integrin, a collagen-binding integrin [28] (Fig. 1.2). Blocking antibodies directed to α2β1 markedly block lumen formation, as do α2 integrin subunit siRNAs. Interestingly, blocking antibodies directed to many other integrin subunits, including α5β1, a fibronectin receptor, have no effect in this system. Also, considerable work has shown that α2β1 integrin is important for vascularization events in vivo and in both developmental and postnatal life contexts [85, 88]. In contrast, when our studies utilized fibrin matrices, we identified that both αvβ3 and α5β1 were required for EC lumen and tube formation [11], while α2β1 was not shown to be involved. Interestingly, the first fibrin system that we developed was performed in the presence of serum. More recently, we developed a serum-free defined system in fibrin matrices, where fibronectin was added in with the matrix when it is polymerized [91]. Under these conditions, α5β1 was involved in the tube formation process, not αvβ3. This result suggests that serum-derived vitronectin might have been the reason why αvβ3 played a role in this first system [11]. Nonetheless, both of these integrins have been shown to be involved during vessel formation during development and in postnatal mice [57, 97]. Thus, an important point is that the in vitro models by our laboratory and others have very accurately predicted in vivo findings made by other groups. Another key point is that the in vitro model systems demonstrated first that multiple integrin chains could be utilized by ECs to control tube morphogenesis and second that there is little evidence to suggest that any particular integrin is unique or special in this property to regulate the morphogenic cascade necessary to form new blood vessels. The role of particular integrins in morphogenesis appears to be directly linked to the ECM environment (and the predominant ECM components) that are in contact with the ECs.

1.3.2 Functional Role of the Rho GTPases, Cdc42 and Rac1, and the Effectors, Pak2 and Pak4, in EC Tube Morphogenesis

An important question raised by the above studies is which downstream signaling pathways are activated by integrins to control these morphogenic processes (Fig. 1.2). Integrins were known to activate Rho GTPases among other molecules [49] such as a variety of kinases, including Src and focal adhesion kinase [34, 57, 89]. Our laboratory reported that Cdc42 was a critical GTPase controlling EC lumen formation [8] (Fig. 1.2). This was also the first report from any system implicating Cdc42 and tube formation. Subsequent studies have revealed that Cdc42 is a critical regulator of lumen formation from both ECs and epithelial cells [8, 25, 66, 67, 75, 79, 83] (Fig. 1.2). Very recently, EC-specific knockout of Cdc42 in mice resulted in embryonic lethality due to lack of EC lumen and tube formation. We reported a role for Rac1 in EC tubulogenesis [8, 66], while RhoA had no ability to stimulate these events. In contrast, expression of constitutively active RhoA leads to marked inhibition of EC lumen formation [8]. Both Cdc42 and Rac1 were shown to be activated during the morphogenic cascade in 3D collagen matrices [66, 83]. To address the question of downstream effectors that are responsible for the influence of Cdc42 and Rac1, we screened a series of known effectors using siRNA treatment of ECs. Major blocking phenotypes were observed using siRNAs to p21-activated kinase (Pak)-2 and Pak-4 [66]. Both EC tube formation and EC sprouting into 3D collagen matrices were markedly inhibited by these siRNAs. We also demonstrated that a time course of Pak-2 and Pak-4 activation, as indicated by phosphorylation, directly correlated with the EC lumen formation process [66]. It was further demonstrated that activated Pak-2 and Pak-4 could be demonstrated to be associated with activated Cdc42 during these events [66]. Expression of a dominant-negative mutant of either Pak-2 or Pak-4 was shown to completely inhibit EC lumen formation [66]. Interestingly, both Cdc42 and Rac1 are able to activate Pak-2, while Cdc42 selectively activates Pak-4 [17, 44]. Recent experiments have revealed important roles for both Pak-2 and Pak-4 during vascular development [44, 70, 98], which again corroborate the in vitro findings.

1.3.3 Functional Role for PKCε and Src in EC Tube Morphogenesis and Subsequent Pak Activation Events

Other known kinases that are activated by cell-ECM interactions include protein kinase C isoforms and Src family kinases. In our studies of EC lumen formation in 3D collagen matrices, we have shown that PKCε, but not PKCα or PKCδ, is involved in the process [66, 67]. siRNA suppression experiments or expression of

dominant-negative mutants of PKCε block lumen formation and downstream Src and Pak activation [67]. Interestingly, increased expression of PKCε strongly stimulates EC lumen and tube formation, and both increased Src, Pak-2, and Pak-4 phosphorylation events that directly correlate with its morphogenic influence [67] (Fig. 1.2). Our studies indicate that PKCε is upstream of Src activation, while Src activation is upstream of Pak activation [67]. Blockade of Src kinases by siRNA suppression; increased expression of the Src inhibitor, CSK (i.e., C-terminal Src kinase); or treatment with chemical inhibitors (e.g., PP2) completely interferes with EC tube formation. Expression of a dominant-negative Csk construct strongly increased lumen formation, again suggesting a positive role for Src in EC lumen formation [67]. Interestingly, Src and Pak kinases are known to active Raf kinases to affect processes such as cell survival which has previously been shown to influence angiogenesis in vivo [2], and we have recently shown that they are required for EC lumen formation [67]. Mouse knockout of B-Raf shows an embryonic lethal phenotype that is due to vascular abnormalities [43]. Of great interest is that we have shown that Raf kinase activation (of both C-Raf and B-Raf) occurs downstream of Src and Pak activation and controls EC tube morphogenic events along with survival [67] (Fig. 1.2). This is accompanied by Erk1/Erk2 activation which also directly correlates with the ability of these ECs to form tube networks. Interestingly, expression of a phosphatase, MKP-3, with selectivity for phospho-Erk1/Erk2, markedly decreases Erk phosphorylation and strongly blocks lumen formation [67]. A dominant-negative MEK kinase inhibitor also abrogates lumen formation and Erk1/Erk2 phosphorylation events. What is interesting about these results is that a known pathway to regulate both proliferation and survival is utilized by ECs to regulate a separate tubulogenic pathway in 3D matrices. In our systems there is little to no evidence for proliferation during these processes so the signaling cascade appears particularly focused on tube morphogenesis [12, 30]. Overall, this morphogenic pathway is coupled to cytoskeletal signaling (i.e., PKC, Src, Pak), survival (i.e., Raf), and transcriptional events (i.e., Erk) to coordinately control this process [30, 66, 67] (Fig. 1.2). Also, it is likely that these kinases are not limited to affecting only one of the critical functions during these events.

We have recently described a novel function for Src family kinases during EC lumen and tube assembly, which is to target and control the development of the apical membrane surface [64]. Marked intracellular vacuole membrane labeling with activated phospho-Src is observed which traffic along acetylated tubulin tracks to fuse in a subapical domain to create an apical membrane also decorated with activated Src isoforms [64]. Blockade of Src isoforms with PP2 completely blocks this process and siRNA suppression of Src, Fyn, and Yes, but not Lyn, interfere with EC lumen formation (Fig. 1.3). PP2 blocks lumen formation whether it is occurring during vasculogenic or angiogenic sprouting events, and interestingly, the addition of PP2 appears to markedly increase the number of EC tip cells as a result of this strong reduction in lumen formation [64].

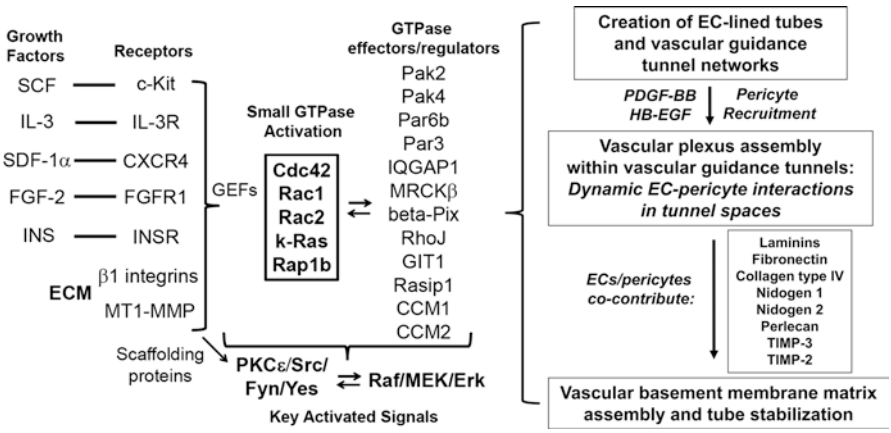

Fig. 1.3 Fundamental signaling molecules, events, and requirements for the establishment of human capillary tube networks. Human EC tube assembly requires a combination of Factors which are SCF, IL-3, SDF-1α, FGF-2, and insulin, which act through their receptors to activate small GTPases, their effectors, and key kinase cascades. These signaling pathways lead to EC cytoskeletal polarization, vacuole formation, trafficking, and fusion to create a polarized apical membrane surface within the tube networks (which reside within vascular guidance tunnels which are created through MT1-MMP-dependent proteolysis). The tubulogenic signaling cascade leads to production and release of PDGF-BB and HB-EGF which facilitates the recruitment of pericytes to the abluminal surface of EC-lined tubes and within vascular guidance tunnels. Dynamic EC-pericyte motility within tunnel spaces results in the deposition of the capillary basement membrane matrix between the two cell types, a key step in capillary tube development and maturation

1.3.4 Identification of New Small GTPases and Their Effectors Controlling EC Tube Morphogenesis

Recent studies have sought to identify additional small GTPases and downstream effectors that regulate the process of capillary tube morphogenesis. We demonstrated critical roles for k-Ras, Rac2, and Rap1b as well as a new series of effectors including Rasip1, IQGAP1, MRCKβ, GIT1, and beta-Pix (Fig. 1.2) [79]. siRNA suppression of these molecules individually or in combination resulted in marked defects in EC lumen and tube assembly [79]. In contrast, as in past studies, siRNA suppression of RhoA did not interfere with these processes. Interestingly, Rasip1 is known to interact with the RhoA-specific GTPase-activating protein (GAP), Arhgap29 [102], and siRNA suppression of this GAP lead to reduced lumen formation because of elevated RhoA activity [79]. Importantly, we also identified two additional GAPs that negatively regulate EC lumen formation, which are Arhgap31 (which inactivates Cdc42 and Rac1) and Rasa1 (which inactivates Ras isoforms) (Fig. 1.2). Combined siRNA suppression of Arhgap31 and Rasa1 led to marked increases in EC tube formation, suggesting an important combined role for Cdc42/Rac/k-Ras and possibly other Ras isoforms [79]. Combined siRNA suppression of Cdc42 with k-Ras leads to strong blockade of EC lumen and tube assembly [79].

Interestingly, previous collaborative studies revealed the role of another small GTPase, RhoJ, which also plays a role during these events [79, 105]. One of key remaining questions is to define the specific role for each of these individual GTPases. Together they appear to control membrane pinocytosis leading to intracellular vacuole formation, trafficking, and fusion of these vacuoles (and possibly other vesicular structures such as Weibel-Palade bodies) to contribute membrane to the developing apical surface. Interestingly, they appear to also regulate key cytoskeletal modifications such acetylation and detyrosination of tubulin which accumulates subapically to surround and regulate vacuole/vesicle transport (and thus direct new membrane) to the apical domain [79]. In addition, they may stimulate vesicle fusion and exocytic events to create this new polarized apical membrane. Clearly, more work is needed here to define the role of these GTPases and their downstream effectors at the different stages of this process. Of interest to this point is our finding that Rasip1, a Ras and Rap effector, strongly targets apically during the lumen formation process [79]. Apical targeting of Rac1, k-Ras, and Rap1b has also been observed, and interestingly, Cdc42 appears to accumulate predominantly subapically and can interestingly co-localize with acetylated tubulin in this subapical domain [79]. This co-localized region is where vacuole to vacuole fusion events occur to create and expand the apical membrane surface.

1.3.5 Cdc42 Coupling to Cell Polarity Pathways Controls EC Lumen and Tube Formation

A major function of Cdc42 is its ability to affect cell polarity signaling, by interfacing with the polarity proteins Par6, Par3, and atypical PKC isoforms [40, 73]. Cell polarity signaling controls directional cell motility that involves Cdc42 [40]. In fact, active Cdc42 (i.e., Cdc42-GTP) binds directly to Par6 which then couples to Par3, a scaffold protein that also interacts with atypical protein kinase C isoforms, such as PKCζ [73]. We reported that Cdc42-dependent EC lumen and tube formation was dependent on Par6b, Par3, and PKCζ [66] (Fig. 1.3). Thus, this work reveals a fundamental role for Cdc42-dependent polarity signaling in EC tubulogenesis. Par3 is known to interact with a number of other cell surface proteins including members of the junction adhesion molecule (Jam) family (i.e., Jam-A, Jam-B, and Jam-C) [38, 39]. Our most recent work reveals that Jam-B and Jam-C associate with Par3 in ECs to control EC lumen formation in 3D collagen matrices [83]. Furthermore, these Jam proteins co-assemble into a defined EC lumen signaling complex consisting of α2β1, MT1-MMP, Jam-C, Jam-B, Par3, Par6b, and Cdc42-GTP that is responsible for the ability of ECs to form tubes in 3D collagen matrices [83] (see later on). Disruption of any member of this complex markedly interferes with the ability of ECs to form tubes [83]. These lumen signaling complexes are also directly coupled to the kinase cascade discussed earlier including PKCε, Src, Pak, Raf, and Erk1/Erk2, since blockade of these complexes completely interferes with the

downstream kinase signaling necessary to regulate vascular tube morphogenesis [83]. Cdc42 and Par3 have also been shown to control lumen formation in epithelial cells, and a recent study shows that Par3 and β1 integrins co-regulate arteriolar lumen formation in vivo using a conditional β1 integrin subunit knockout mouse system [110]. Thus, this latter work again confirms our prior conclusions obtained in vitro showing that β1 integrins, Cdc42, and polarity proteins control the lumen and tube formation process in 3D matrix environments [30, 36, 66, 67, 79, 83, 95].

1.3.6 Key Role for Polarized Subapical Microtubule Modifications to Direct the Trafficking and Fusion of Pinocytic Vacuoles to Regulate Apical Membrane Development During EC Lumen Formation

Recent studies indicate that an important step in EC lumen and tube assembly is for the increased accumulation of posttranslationally modified tubulins (i.e., acetylated and detyrosinated tubulin) [63] (Fig. 1.2). Both of these modifications, which are associated with increased tubulin polymer stability, are upregulation during EC lumen formation and correlate with the lumen formation process. We demonstrated that the microtubule tip complex proteins, EB1, p150 glued, and Clasp1, play a key role in regulating lumen formation as well as the accumulation of both acetylated and detyrosinated tubulin [63]. In addition, we identified HDAC6 and sirtuin2 as negative regulators of lumen formation due to their ability to reduce tubulin acetylation via their activity as tubulin deacetylases. siRNA suppression of these deacetylases increased lumen formation, while increased expression of them decreased it [63]. Further support for this conclusion is that addition of the HDAC6 inhibitor, tubacin, leads to increased EC lumen and tube formation [79]. Of great interest here is that these modified tubulins accumulate in a polarized manner subapically during EC lumen and tube assembly, while in contrast, filamentous actin (F-actin) accumulates in a distinct basal location [64, 79]. This subapical polarized region where acetylated and detyrosinated tubulin accumulates is precisely the location where vacuole and vesicle fusion events occur, to control the development of the apical membrane surface during this process. Interestingly, Cdc42 shows strong co-localization with acetylated tubulin in these regions of vacuole/vesicle fusion [79]. Thus, one of the central features of the EC lumen formation process is the creation of cytoskeletal asymmetry and tracks where vesicles can be trafficked to this subapical domain, to polarize the lumen formation process. Furthermore, our data suggests that this subapical membrane accumulation of modified tubulins is necessary to stabilize the apical membrane and maintain a stable tube structure [63, 64, 79]. We demonstrated in past studies that disruption of microtubules led to rapid collapse of tube networks [10].

1.3.7 Critical Functional Role for MT1-MMP in EC Lumen and Tube Formation in 3D Collagen Matrices

Matrix metalloproteinases (MMPs) are a family of zinc-dependent metalloendopeptidases that degrade a variety of substrates, to affect the vasculature and other tissues [33, 47]. Their targets include the ECM, cytokines, and cell surface receptors, to affect vascularization as well as many other cellular responses [33, 47]. Our work and that of others have demonstrated a role for MT1-MMP (i.e., MMP-14) in EC morphogenic events in 3D matrix environments [21, 87, 95]. MT1-MMP is a transmembrane protein, and its cell surface expression is required for it to perform the localized ECM degradation necessary to control cell movement in 3D matrices. MT2-MMP is also able to participate in these types of events, while the function of MT3-MMP is less clear, although several studies show that it does not play a major role. Mouse knockout of MT1-MMP is compatible with embryogenesis, but the mice are small and ill and die within a month or two of birth [108]. Attempts to induce angiogenesis in these mice reveal that these responses do not occur [108]. Furthermore, aortic ring assays in 3D collagen matrices show no sprouting, in either 3D collagen or fibrin matrices using MT1-MMP knockout tissues compared to control [21]. Thus, this work demonstrates an important role for MT1-MMP in vascular morphogenic events in 3D matrices and during in vivo angiogenic responses (Fig. 1.4).

To elucidate the molecular mechanisms by which MT1-MMP controls vascular morphogenesis as well as cellular invasive events, our laboratory has examined this question using models of vasculogenesis and angiogenesis [9, 87, 95]. We have utilized protein and chemical MMP inhibitors as well as siRNA suppression approaches. In our first studies, we demonstrated that EC sprouting in response to sphingosine-1-phosphate (incorporated into the collagen matrices) was blocked by the broad spectrum inhibitor, GM6001, as well as tissue inhibitor of metalloproteinase (TIMP)-2, TIMP-3, and TIMP-4, but not TIMP-1 (Fig. 1.4a) [9]. Interestingly, MT-MMPs are insensitive to TIMP-1, but the other inhibitors utilized block their activity. When EC lumen and tube formation assays were performed, GM6001, TIMP-2, TIMP-3, and TIMP-4 blocked completely, while TIMP-1 had no influence. One important distinction among the TIMPs is that TIMP-3 is able to block the activity of MT-MMPs, but also many other members of the ADAM family of cell surface expressed metalloproteinases [7]. To functionally dissect which EC surface expressed metalloproteinases are relevant during EC sprouting and lumen formation, we performed siRNA suppression analysis. Our results suggest that the dominant metalloproteinase controlling these events is MT1-MMP (Fig. 1.4b), with a lesser influence of MT2-MMP during both sprouting and lumen formation [87, 95]. We observed a partial blocking effect of ADAM-15 siRNA knockdown in EC sprouting assays, using stromal-derived factor-1α as the invasion stimulus [87]. We did not observe an effect of either MT3-MMP or ADAM-17 siRNAs in our assays [87], although a recent study using a similar system revealed a potential role for ADAM-17 in modulating the invasion response [69]. The fact that TIMP-2 and

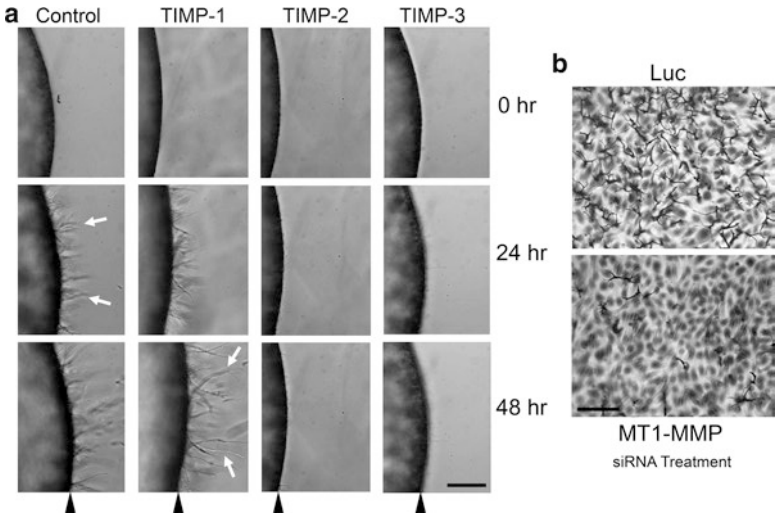

Fig. 1.4 MT1-MMP plays a critical role in EC sprouting in 3D collagen matrices from a monolayer surface in sprouting angiogenesis bioassays. (**a**) A time-lapse series was performed of EC sprouting viewed from the side into 3D collagen matrices where either no addition or recombinant TIMPs were added. Sphingosine-1-phosphate (1 μm) was added into the collagen matrix. Arrowhead indicates EC monolayer surface; arrows indicate EC sprouts. TIMP-2 and TIMP-3 block sprouting in an equivalent manner, while TIMP-1 has no blocking influence relative to the control. Bar equals 100 μm. (**b**) An siRNA suppression experiment was performed to examine the influence of an MT1-MMP siRNA versus a luciferase control. Sprouting assays were performed using the treated cells, and they were seeded on collagen matrices containing 1 μm sphingosine-1-phosphate. Cultures were fixed, stained, and photographed after 24 h. Bar equals 100 μm

TIMP-4 have dramatic blocking effects on both sprouting and lumen formation is more supportive of a major role for MT-MMPs, rather than ADAMs, since there is currently no evidence to suggest that they can block ADAM proteinases [7].

A further important experiment which demonstrates a role for MT1-MMP during EC tubulogenesis is that increased expression of MT1-MMP using viral vectors leads to marked increases in lumen formation that depends on its MMP catalytic domain [95]. Furthermore, addition of GM6001 to block MT1-MMP completely inhibits the stimulatory influence of the recombinant protein. In support of this result is that a catalytically dead full-length MT1-MMP construct (EA mutant) has no ability to stimulate EC lumen formation [95], while interestingly, it does not exert an inhibitory influence. In very recent experiments, we have further shown that increasing the expression of wild-type, full-length MT1-MMP increases both the rate and extent of EC lumen formation in 3D collagen matrices [83]. Of great interest is that we have created a construct that appears to be a dominant-negative mutant of MT1-MMP in this system where we mutated the active site and at the same time deleted its cytoplasmic tail [83]. When expressed in ECs, the cells are completely unable to make lumens in 3D collagen matrices. An additional finding is that

expression of wild-type MT1-MMP without its cytoplasmic tail markedly stimulates the rate and extent of EC lumen formation compared to full-length wild-type MT1-MMP expression [83]. A number of studies suggest that its cytoplasmic tail plays a role in endocytic recycling, and thus, deleting the tail increases cell surface expression, which in our case leads to additional increases in EC lumen formation events. Overall, these results demonstrate that MT1-MMP is a major regulator of EC lumen and tube formation and that it works closely in conjunction with the α2β1 integrin as well as Cdc42, Rac1, and other small GTPases to control this process.

1.3.8 MT1-MMP-Dependent EC Lumen and Tube Formation Leads to the Formation of a Network of Physical Spaces Within the ECM Termed Vascular Guidance Tunnels

During the course of the above studies, we made the novel observation that during EC lumen and tube formation, ECs are also creating a network of physical spaces that we term vascular guidance tunnels. These form as a result of MT1-MMP-mediated proteolysis of collagen matrices [95]. In every instance examined, there is a direct relationship between EC tube formation and the formation of vascular guidance tunnels [95]. Tunnels were first detected by staining the collagen type I matrix with a monoclonal antibody that recognizes native type I collagen and not denatured collagen (which is generated at 37 °C when it is cut with mammalian collagenases). The lumen and tube formation creates an extensive interconnecting network of these tunnel spaces within the 3D collagen matrices [95]. To further prove that these represent physical spaces in the ECM, they were microinjected with silicone oil [95]. Dramatic filling of networks was demonstrated showing that EC tube formation leads to the formation of interconnecting vascular guidance tunnel spaces. We further showed that the ECs produced twice as many tunnel spaces than were occupied by EC-lined tubes [95], raising the interesting possibility that vessel remodeling could occur through these pre-formed physical tunnel spaces. Although MT1-MMP was required for the formation of vascular guidance tunnel formation, once they were formed, blockade of MT1-MMP did not affect the ability of ECs to migrate within the spaces [95]. Thus, EC migration events which are necessary for EC tube formation are completely inhibited in 3D collagen matrices, if MT1-MMP is blocked from the beginning of culture. However, once vascular guidance tunnels have formed through MT1-MMP-mediated events, ECs are then able to migrate within these physical spaces in an MMP-independent manner [95]. Thus, vascular guidance tunnel spaces are similar to 2D matrix surfaces where EC motility is insensitive to MT1-MMP inhibition (siRNA or inhibitors) [95]. We also observed that while the creation of vascular guidance tunnels by ECs requires the α2β1 integrin, a native collagen-binding integrin, the motility of ECs within MT1-MMP-generated tunnels was not sensitive to inhibition with anti-α2 integrin subunit blocking antibodies. In contrast, EC motility was blocked using anti-αv subunit blocking antibodies [95] which are known to bind matricryptic RGD sites that are

present within unfolded collagen molecules following proteolysis [24, 26] (an event which controls the generation of the tunnel spaces).

Another important finding from this work is that inhibitors of EC lumen and tube formation, including anti-α2 and anti-β1 integrin blocking antibodies, chemical inhibitors of PKC and Src, as well as MT1-MMP inhibitors, completely abrogate the formation of vascular guidance tunnels [95]. Thus, the formation of EC tubes is an obligate step in the formation of vascular guidance tunnels, and thus, these processes are directly linked in some fundamental manner. Several critical questions arise from these studies, including how the lumen and tube formation processes are functionally connected with the cell surface proteolytic machinery to create vascular guidance tunnels. Very recent work, described below, provides some insights into these questions.

1.3.9 Cdc42 and MT1-MMP Are Functionally Interdependent Signaling Molecules Which Are Components of an EC Lumen Signaling Complex that Controls EC Tubulogenesis in 3D Extracellular Matrices

Several newer findings begin to shed light into how Cdc42-dependent signaling events, which activate kinase cascades and interact with cell polarity machinery (i.e., Par3, Par6, atypical PKC), intersect with MT1-MMP proteolysis to create EC lumens, tubes, and vascular guidance tunnels [66, 67, 83, 95]. One important point is that the EC lumen and tube formation is a 3D matrix-specific process [27], in that tubulogenesis does not occur on a 2D matrix surface. In contrast, EC motility can occur quite readily on a 2D matrix surface, while it also occurs in 3D matrices in a manner that depends on MT1-MMP proteolytic events. Importantly, MT1-MMP activity is not required for EC motility on a 2D matrix surface, as discussed above. With this introduction, our findings show that blockade of MT1-MMP activity using siRNA suppression or MT1-MMP inhibitors leads to marked interference with Cdc42 activation (a critical step necessary for activation of effectors such as Pak2, Pak4, and Par6 that leads to EC tubulogenesis) in 3D collagen matrices [83]. However, this blockade of MT1-MMP does not affect Cdc42 activation of ECs when they are seeded on 2D collagen surfaces, and coincidently, their motility is also not affected [83]. Expression of the dominant-negative MT1-MMP construct also markedly blocks lumen formation and Cdc42 activation [83]. Interestingly, the activation of RhoA, which is not involved in EC lumen and tube formation, is not affected by blockade of Cdc42 or MT1-MMP, nor is it affected by 2D vs. 3D collagen matrices. This data shows that MT1-MMP activity is directly coupled to Cdc42 activation in 3D, but not 2D, matrices to control the tube formation process [83]. The reverse is also true, in that blockade of Cdc42 using siRNA suppression leads to marked decreases in vascular guidance tunnel formation, a consequence of inactivation of MT1-MMP-dependent proteolysis [83]. Thus, this work suggests a

new hypothesis which states that Cdc42 and MT1-MMP are interdependent signaling molecules that control vascular morphogenic events specifically in a 3D matrix environment.

1.3.10 Critical Role for MMPs in the Molecular Control of Vascular Tube Regression Responses in 3D Collagen Matrices

A critically important direction of research is to understand how blood vessels regress under physiologic and pathophysiologic situations. Physiologic regression occurs with hyaloid vessels in the developing eye, in both the endometrium and ovaries during the menstrual cycle, and during vascular remodeling events in development [33]. Pathophysiologic regression characteristically occurs during wound repair and during disease processes such as hypertension and diabetes where vessel densities can decrease particularly in the distal limbs. Also, there have been considerable efforts to induce vascular tube regression responses, in the context of the tumor vasculature by disrupting VEGF and PDGF signaling [15]. An important point here is that it is critical to understand how vascular regression is controlled at the molecular level, in much the same way that the studies described earlier have been performed to determine how blood vessels form.

A variety of studies have identified MMPs that regulate vascular tube regression events [32, 86, 109]. A number of years ago, we identified the secreted MMPs MMP-1 and MMP-10 as being involved in vascular tube regression responses in vitro [32, 33, 35, 86]. We showed that these enzymes were secreted as proenzymes and that they need to be activated by serine proteases, such as plasminogen/plasmin or plasma kallikrein, in order to cause vascular tube collapse and regression [86]. Disruption of their activity by TIMP-1 (which blocks both MMP-1 and MMP-10) or blockade of serine protease activity leads to inhibition of the MMP-1- and MMP-10-dependent regression response. Other studies using the aortic ring model reached similar conclusions, with the exception that MT1-MMP was also found to be involved in both tube formation as well as regression [4]. We also identified ADAM-15 as being involved in the vascular regression response in a manner similar to that of MMP-1 and MMP-10 [87]. Interestingly, siRNA suppression of either MMP-1 or MMP-10 did not affect tube formation but markedly blocked tube regression, following addition of plasminogen or plasma kallikrein to the serum-free media system [86]. Also of note, a mouse knockout of histone deacetylase 7 (HDAC7) caused a vascular hemorrhage phenotype in vivo, during vascular development, which leads to embryonic lethality [20]. siRNA suppression of HDAC7 resulted in marked increases in MMP-10 and marked decreases in TIMP-1 expression which lead to the vascular developmental regression phenomenon [20]. Other work reveals that EC-specific knockout of the chromatin remodeling enzyme,

CHD4, leads to plasmin-dependent disruption of vascular integrity in both blood-derived and lymphatic EC-lined vessels during vascular development [22, 59].

Of great interest is that the MMP-1 and MMP-10 regression phenomena are strongly abrogated in our in vitro model when pericytes are added along with the ECs [87]. Pericyte recruitment to the tubes occurs, and they become much more resistant to pro-regressive stimuli. Thus, our model mimics that observed in vivo where EC tubes without pericytes are much more susceptible to regression [5, 13, 14]. Interestingly, tumor vessels have associated pericytes, but the interactions are abnormal. Despite these abnormalities the tumor vessels persist, which in this case may relate to the fact that many aggressive tumors overproduce TIMP-1 [101], which can interfere with the MMP-1 and MMP-10-dependent regression system [33]. We also observed that EC-pericyte interactions upregulate the production of EC TIMP-2 and pericyte TIMP-3 which together control how EC-pericyte interactions protect against pro-regressive MMP-1 and MMP-10, and also ADAM-15 [87]. Pericytes are a rich source of TIMP-3 [87] which is interesting because of its ECM-binding ability (i.e., ability to bind cell surfaces and basement membrane matrices) and its dual ability to inhibit soluble and membrane MMPs, as well as membrane ADAM proteinases [7]. In addition to interfering with pro-regressive stimuli, TIMP-3 and TIMP-2 block MT1-MMP, to interfere with further EC tube formation. Thus, these TIMPs contribute to vascular tube stabilization by inhibiting both vascular tube regression phenomena and further vascular tube morphogenesis. Additional support for this their latter influence, both TIMP-2 and TIMP-3 are antagonists of VEGFR2 [80, 90], an important EC signaling receptor. Interestingly, we have described the concept that VEGF does not directly stimulate vascular tube morphogenesis but that it primes ECs so that they respond in a more robust manner to a distinct set of downstream growth factors (see later on). Using this reasoning, TIMP-2 and TIMP-3 might be capable of suppressing EC priming and, thus, enhance EC tube stability in this manner.

1.3.11 Critical Functional Role for EC-Generated Vascular Guidance Tunnels During Blood Vessel Assembly in 3D Matrices

As shown in Fig. 1.2, ECs utilize a lumen signaling complex to form tubes in 3D matrices while at the same time generating networks of vascular guidance tunnel spaces. ECs are able to migrate through these spaces in an MMP-independent manner. We have also shown that ECs can regrow within these spaces following tube collapse. EC-lined tubes were treated with thrombin which reversibly causes tube collapse, leaving rounded up ECs within tunnel spaces [95]. After inhibition of thrombin with the thrombin inhibitor hirudin, the ECs regrow within tunnels to reassemble the collapsed tube [95]. Thus, pre-existing tunnel spaces are matrix conduits that allow for rearrangement of tubes and migration of ECs, and, thus, they are used

for tube remodeling events. In early vascular development, there is considerable evidence for dramatic tube network remodeling that occurs following the onset of flow [23, 72, 82], and we hypothesize that this is possible in large part due to the presence of vascular guidance tunnels which allows ECs to rapidly rearrange to accommodate the flows and pressure forces that are applied to the network. Also, at this stage of development, the ECM is likely to be elastic, and, thus, the forces generated may be able to expand lumen or tunnel width by mechanical distension. We have also shown that groups of cells comprising a tube structure can migrate together through tunnel spaces, to move and connect with adjacent EC tubes to regulate such vascular remodeling events [95]. As mentioned earlier, the EC lumen and tube formation process generates more vascular guidance tunnels than are utilized at any given time, which further suggests that this occurs to accommodate the necessary vascular remodeling events involved in generating a proper microcirculatory network.

Vascular guidance tunnels are also important to consider in the context of vascular tube regression and regrowth of vessels. One of the ways to eliminate the possibility of vascular regrowth following regression events would be to induce regression of both vascular tubes and vascular guidance tunnels. In fact, the MMP-1 and MMP-10 regression mechanism discussed earlier does cause the collapse of both structures. The presence of pericytes, which block the regression event, can thus protect not only the vascular tube structure but also the integrity of the vascular guidance tunnels. Of interest here is that tumor vessels are highly resistant to vascular regression, due to their production of regression inhibitors such as TIMP-1. Again, TIMP-1 is capable of protecting both the vessels and the tunnel spaces. Also, when tumors are treated with vascular regression agents, such as VEGF or VEGFR2 antagonists, vessels regress, but they can rapidly regrow (following withdrawal of the regression agent), in a similar fashion, to recapitulate the original pattern of vessels [74]. This appears to occur through the vascular guidance tunnels that were generated during initial tumor vessel formation. So an important therapeutic consideration here would be to devise approaches to induce vessel and vascular guidance tunnel regression. In this way vessel regrowth is less likely to occur, allowing for a better therapeutic opportunity to treat the tumors, their vascular supplies, and existing matrix conduits which facilitate vascular regrowth.

It is also important to consider how events such as arteriovenous identity might be regulated by vascular guidance tunnels. The tunnels represent a 2D matrix surface in a 3D matrix environment [95]. There is important data showing that ephrinB2 (an arterial marker) and EphB4 (a venous marker) represent a repulsive signaling pair, which appears early in development to control the development of A-V identity [46]. These repulsive interactions allow differential cell sorting, and, early in development, ECs expressing these markers are intermixed. Over time they sort out and become segregated to either the arterial or venous side [46, 53, 65]. They also appear to sort very early, even at the level of initial cardinal vein formation, due to sprouting from the developing aorta. This process is very analogous to what has been described for lymphatic sprouting and development from the cardinal vein [103]. Notch signaling appears to control this phenomenon, and, when

overactive Notch4 is produced in ECs, venous ECs inappropriately express ephrinB2, contributing to the development of arteriovenous malformations [65]. Of great interest is that many of these lesions will regress following withdrawal of the overactive Notch4. The important point to be made is that the repulsive ephrinB2-EphB4 interactions are occurring within vascular guidance tunnels (formed as a result of EC tube assembly), and the ability to sort following such interactions requires the ECs to move around on 2D matrices at the vessel wall surface. These interactions are secondary to ECs contacting each other.

However, the concept of vascular guidance tunnels extends to recruitment and sorting of mural cells within the vessel wall as well. EphrinB2 is expressed on vascular smooth muscle cells, with selectivity in arteries so similar repulsive interactions are likely to control this cell distribution as well [41]. What is interesting here is that this type of interaction would require that mural cell recruitment, to EC-lined tubes and within vascular tunnel spaces, occur in a polarized fashion exclusively on the EC abluminal surface. In fact, we have recently discovered that this is precisely what occurs during pericyte recruitment to EC-lined tubes. Within vascular guidance tunnels, they recruit to, and are localized only on, the EC tube abluminal surface [94]. Thus, mural cells could sort through repulsive interactions with each other but also secondary to repulsive interactions with ECs. The vascular guidance tunnel matrix conduit is a critical ECM structure necessary for these EC-EC, mural cell-mural cell, and EC-mural cell interactions to occur and to also allow the motility events required for proper sorting. In support of this possibility is that ECs and mural cells are highly dynamic during vascular tube assembly, and in fact, we have shown that both ECs and pericytes rapidly migrate in the ECM, as well as within vascular guidance tunnels during tube co-assembly and maturation events [94]. ECs have also been shown by a number of groups to be rapidly migrating in vivo during vascular development, to regulate both tube assembly and vascular remodeling [23, 72].

1.3.12 Pericyte Recruitment to Vascular Guidance Tunnels Induces Vascular Tube Stabilization

Many studies indicate that microvessels covered with pericytes are more stable to pro-regressive stimuli but also show reduced vascular permeability indicative of tube stabilization. Different vascular beds have varying pericyte numbers covering capillary networks, although many have approximately 20–25% coverage of pericytes relative to ECs. Individual pericytes can span across multiple ECs, resembling other types of supporting cells such as glia in the nervous system interacting with multiple neurons. Tissues such as the central nervous system, including the retina, have a very high pericyte to EC ratio which approaches 1:1. Thus, these interactions account in part for the blood-brain barrier with strongly increased permeability barrier functions relative to other vascular beds. Considerable work suggests that the

high VEGF environment of tumors is one reason why pericyte coverage is decreased compared to normal vascular beds [48, 61]. Treatment with VEGF antagonists has led to the finding that pericyte coverage increases, which results in improved microcirculatory function (i.e., vascular normalization) [61]. This approach represented a new strategy to improve drug delivery into the tumor microenvironment, since poor perfusion exists due to the abnormal microcirculatory network that is present.

1.3.13 Molecular Mechanisms Underlying Why Pericytes Are Able to Stabilize EC-Lined Tube Networks

A major question that has not been sufficiently addressed is why pericyte coverage stabilizes vessels and what their functions are when they arrive at the EC abluminal surface. To address this question, we established novel EC-pericyte coculture models in 3D collagen matrices (Fig. 1.5). We developed systems using either bovine retinal pericytes or human brain pericytes. In each case, the pericyte populations express the pericyte markers NG2 proteoglycan, 3G5 ganglioside, smooth muscle actin, and desmin. Perhaps the most important function of pericytes is to recruit to microvascular capillary beds. Using our model of EC vasculogenic tube assembly, we developed a system whereby we randomly mix together ECs and pericytes at a 5:1 or 5:1.25 ratio (i.e., 20–25% pericytes compared to 100% of ECs). Remarkably, the ECs form tube networks, and then, pericytes are recruited to these tubes [94] (Fig. 1.5). This ratio of ECs to pericytes is particularly optimal, and the reasons for this are currently not clear. It may be that too many pericytes (through their production of TIMP-3) [87] interfere with morphogenesis, by inhibiting MT1-MMP-dependent signaling, or that they are physically in the way and counteract the ability of ECs to find neighbors to properly form multicellular tubes. It is clear that too many pericytes can disrupt EC-pericyte tube co-assembly.

We further made the observation that EC tubes, from EC-only cultures, eventually became much wider than EC tubes from EC-pericyte cocultures. We examined this issue over time and observed that vascular diameters reached a range of 20–25 μm in EC-pericyte cocultures, which are vessel diameters observed in vivo during vasculogenesis, while EC-only cultures' diameters can reach 80–100 μm over a 5-day period [94]. Thus, pericytes have a marked ability to negatively regulate vascular tube diameters, which may have to do with the induction of TIMP-2 and TIMP-3. As discussed earlier, they are induced in EC-pericyte cocultures [87] and can inhibit and restrict EC lumen diameters. A number of studies indicate that vascular diameters are greater when pericyte recruitment is reduced or when ECM components such as fibronectin are knocked out of ECs during vasculogenesis in vivo [6, 42].

The mechanisms whereby pericytes are recruited to EC-lined tubes are still being investigated although past data supports the concept that PDGF-BB plays a role [5, 16, 54]. In past and ongoing studies from our laboratory, we have shown that pericyte recruitment is dependent on signals derived from the combined action

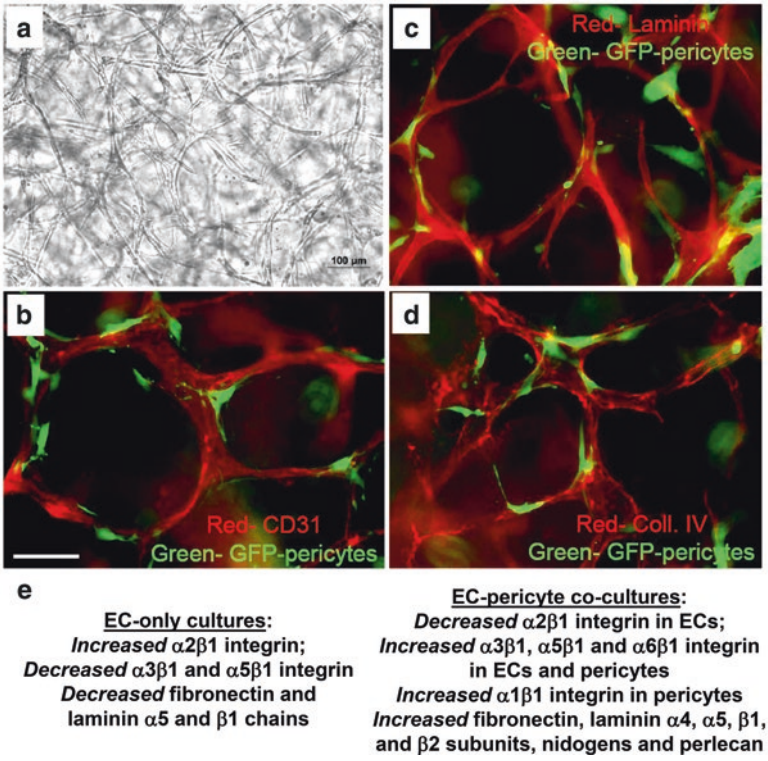

Fig. 1.5 EC-pericyte tube co-assembly in 3D collagen matrices leads to vascular basement membrane matrix deposition and tube stabilization. ECs were cocultured with bovine retinal pericytes (20% pericytes relative to 100% ECs) in 3D collagen matrices and after 5 days of culture were fixed and photographed (**a**) or were processed for immunofluorescence microscopy. The pericytes were labeled with GFP, while the ECs and extracellular matrix were stained with the indicated antibodies. Fluorescent images were overlaid to assess the relationship of the ECs and matrices with the presence of pericytes. (**b**) CD31 staining to detect EC-lined tubes. Bar equals 50 µm. (**c**) Laminin and (**d**) collagen type IV staining to detect vascular basement membrane matrix assembly. In the latter two cases, no detergent was utilized so that only extracellular antigens would be detected. (**e**) RT-PCR and Western blot analyses of EC-only versus EC-pericyte cocultures demonstrate marked changes in integrin and basement membrane matrix protein expressed during this process

of PDGF-BB and HB-EGF [96]. Blockade of these growth factors using blocking antibodies, receptor traps, or chemical disruption of their receptors revealed their involvement [96]. Importantly, we assessed pericyte motility and invasion under our serum-free media conditions and demonstrated that they failed to move, when cultured by themselves. In contrast, when pericytes were cocultured with ECs, pericyte motility ensued allowing for recruitment to EC-lined tubes [96]. This EC-dependent pericyte motility response was strongly abrogated by the combined blocking reagents directed at both PDGF-BB and HB-EGF [96]. These findings are consistent with work showing that EC-specific knockout of PDGF-BB leads to

about a 50% decrease in pericyte coverage of vessels [16]. Of interest is that these mice show primary defects in microvessel beds (where pericyte coverage is present), while larger vessels are much less affected. This microvascular deficiency phenotype manifests particularly in the kidney and central nervous system which strongly resembles that observed in diabetic microangiopathy [16]. Loss of pericytes is a major pathogenic cause of this type of microvascular disease [51]. It is important to further understand the signaling mechanisms which underlie pericyte recruitment to EC-lined tubes, to both identify other factors that regulate this recruitment as well as understand how pericytes invade 3D matrices to recruit to these tubes. This is currently a major research direction of our laboratory.

1.3.14 Pericyte Recruitment to EC-Lined Tubes Stimulates ECM Remodeling Events and Vascular Basement Membrane Matrix Assembly

Using our new model of EC-pericyte tube co-assembly, we sought to identify how pericytes contribute to vascular tube maturation and stabilization events. At different time points of tube co-assembly, we performed transmission electron microscopy and immunofluorescence microscopy to examine if basement membrane matrix assembly occurred [94]. In Fig. 1.5b, we show immunostaining for the EC marker CD31, while the pericytes stably express green fluorescent protein (GFP). This image shows EC tube networks that have associated pericytes at day 5 of culture. We also show a light microscopy image of the coculture system in Fig. 1.5a. As shown in Fig. 1.5c, d, there is marked deposition of laminin and collagen type IV, two critical basement membrane matrix components. In addition, we reported that fibronectin, nidogen-1, nidogen-2, and perlecan were also deposited around EC-lined tubes only when pericytes were cocultured with ECs [94] (Fig. 1.5e). We demonstrated that basement membrane matrices were observed by transmission electron microscopy, only when EC-pericytes were cocultured [94], and over many years we have never observed basement membrane deposition in the absence of pericytes in electron microscopic studies. Further, we confirmed our results in vivo and demonstrated that pericyte recruitment to developing quail EC tubes directly correlates with vascular basement membrane assembly, at day 7 of embryonic development [94]. Prior to pericyte recruitment, no vascular basement membranes around EC tubes were observed in vivo [94].

To perform the immunostaining experiments, we utilized detergent-free conditions so that we are examining only ECM that is deposited extracellularly [94] and not intracellular ECM molecules. We utilized this approach in our in vitro 3D cultures but also stained an in vivo tissue, the quail chorioallantoic membrane, in the same manner [94]. This is key point because we have shown that extracellular deposition of vascular basement membrane matrix is markedly stimulated by pericyte

recruitment [94]. Although increased production of individual basement membrane components was observed, this upregulation was not as marked as that observed in the immunostaining experiments. We utilized our human EC and bovine pericyte coculture system to determine which cell type produces particular ECM components over time, to regulate basement membrane matrix assembly (using species-specific RT-PCR primer sets) [94]. Major findings were that ECs increased the production of fibronectin selectively in the presence of pericytes (and not in their absence) and nidogen-1 was induced in pericytes that occurred selectively in the presence of ECs [94]. We also observed induction of particular laminin isoforms as well as perlecan at the mRNA level, which occurred through EC-pericyte interactions. Thus, EC-pericyte contacts during tube co-assembly events affected mRNA and protein levels for key basement membrane matrix molecules [94]. Interestingly, both fibronectin and nidogen-1 are known to bridge key molecules that compose the basement membrane matrix [34, 76, 89]. Fibronectin shows affinity for collagen type IV and perlecan, while nidogen-1 binds collagen type IV and laminin isoforms. It is possible that these ECM components initiate a nidus which leads to the assembly of the insoluble matrix surrounding the EC-lined tubes that control basement membrane deposition, as observed by electron microscopy. Most ECM proteins have self-assembly functions, but they need to interact with each other to create the complex meshwork that is characteristic of fully assembled basement membrane matrices. It is also intriguing that collagen type IV, a fundamental basement membrane component greatly responsible for its structural integrity, shows affinity for both fibronectin and nidogen-1, which are selectively affected by EC-pericyte interactions [94].

One question that is of great interest is how continuous basement membrane assembly is accomplished along EC-lined tubes, despite the fact that pericytes are only one-fifth to one-fourth of the total number of ECs. We believe that this occurs due to the motility of pericytes along the abluminal EC tube surface which scans along the tubes to stimulate the deposition of the basement membrane in a continuous manner [94]. Furthermore, the movement of both pericytes and ECs along each other, within vascular guidance tunnels, will almost certainly exert mechanical stress on the newly deposited ECM to facilitate basement membrane assembly. Thus, it is intriguing that fibronectin, a mechanosensitive ECM component whose assembly is facilitated by cell-exerted tensional forces, is a critical protein that only strongly deposits around EC-lined tubes when pericytes are present along the tube surface [94]. Another interesting possibility is that the presence of pericytes, along the EC abluminal surface (and in a polarized fashion) [94], may stimulate the directional secretion and deposition of basement membrane components from both cell types toward each other. Thus, both mechanical forces and vectorial secretion mechanisms may play a fundamental role in how pericyte recruitment to EC-lined tubes leads to vascular basement membrane matrix assembly, a major step toward further tube maturation and stabilization. As discussed above, the deposition of laminin isoforms may represent stimuli for ECs to stop undergoing morphogenesis and become a stable tube structure with a quiescent layer of ECs. Another molecule, TIMP-3, whose deposition in the basement membrane would lead to a similar

phenotype, binds basement membrane perlecan as well as other components, to suppress vascular morphogenesis [87]. The roles of these individual components need to be investigated in more detail in future studies.

1.3.15 Critical Functional Role for Fibronectin Matrix Assembly During Vascular Development

A series of studies indicate that fibronectin gene knockouts result in an embryonic lethal phenotype during vasculogenesis [42, 57]. Also, evidence has been presented that fibronectin alternative splicing (IIIA and IIIB isoforms) is important during these events [6]. Further work will be necessary to elucidate why these particular fibronectin isoforms are playing a role during these processes. Vessel diameters from these animals are extremely wide which, as discussed above, may be secondary to defects in proper EC-pericyte interactions causing abnormal basement membrane formation or reduced adhesiveness to these remodeled, but abnormal, matrices. EC-specific knockout of the α5 integrin also shows phenotypes that are manifested in a wider vessel phenotype, which appears to be further enhanced by knockout of αv integrins, another class of fibronectin receptors [57].

Since we observed strong fibronectin upregulation in ECs, as well as deposition selectively in EC-pericyte cocultures, we performed additional experiments to determine if fibronectin matrix assembly affected EC tube maturation events in this system. We incorporated a 70 kDa N-terminal fragment of fibronectin, which is known to block fibronectin matrix assembly [106], to assess if it had any influence during these events. Our work shows that disruption of fibronectin matrix assembly affects EC tube width by significantly increasing it [94], suggesting that deposited fibronectin may play a role in restricting vascular tube diameter. Interestingly, this treatment also markedly disrupted collagen type IV matrix deposition [94] while having a lesser influence on laminin assembly. In support of these findings are experiments showing that selective blockade of EC α5β1 integrin, a fibronectin receptor, also significantly increases vascular tube width in the EC-pericyte cocultures, but not in the EC-only cultures, where this receptor appears to play little role [94].

1.3.16 Important Functional Role for Collagen Type IV in EC-Pericyte Tube Co-Assembly and Maturation Events

In addition to the critical roles for fibronectin and nidogen-1, as bridging proteins for ECM assembly, collagen type IV is another key basement membrane component with affinity for both of these bridging molecules. Interestingly, pericyte-induced fibronectin assembly around developing tubes appears to be involved in collagen type IV assembly [94]. To assess which cell types contributed the collagen type IV

that was deposited extracellularly during these events, we performed siRNA suppression experiments revealing that ECs were the predominant source of collagen type IV [94]. Knockdown of collagen type IV in ECs strongly decreased collagen type IV assembly around tubes and resulting again in increased vascular tube width, an indicator of dysfunctional interactions between ECs and pericytes [94]. Knockdown of collagen type IV in pericytes had lesser, but nonetheless significant, inhibitory effects on both collagen type IV deposition and vessel tube width [94]. This suggests that both ECs and pericytes contribute collagen type IV during basement membrane assembly.

1.3.17 Pericyte TIMP-3 Contributes to Vascular Basement Membrane Matrix Assembly by Increasing Collagen Type IV Deposition or Stability

Another contributing role of pericytes during this process is the delivery of TIMP-3, a basement membrane and ECM-binding protein. As discussed earlier, TIMP-3 plays a critical role in pericyte-induced tube stabilization by blocking MMP-1, MMP-10, and ADAM-15, which promote vascular regression events as well as inhibiting further morphogenic events by blocking MT1-MMP [87]. In this work, we show that TIMP-3 plays yet another role, by facilitating collagen type IV assembly in EC-pericyte cocultures. siRNA suppression of pericyte TIMP-3 results in markedly decreased collagen type IV assembly [94], which may be due to less deposition or increased turnover due to lack of inhibition of MT1-MMP (which degrades type IV collagen). With decreased collagen type IV assembly around EC tubes, there was a significant increase in vessel diameter [94]. Thus, collagen type IV assembly may be a primary determinant of vascular tube diameter. It is particularly intriguing to consider that EC-only tubes, which are not surrounded by basement membranes, become very wide during morphogenic events. This suggests a lack of inhibitory signals. EC-pericyte co-assembled tubes are much narrower, suggesting that the inhibitory signals are delivered to ECs through interactions with the assembled basement membrane to suppress further morphogenesis and promote maturation. The marked differences in vessel diameter in these two situations demonstrate functional evidence for both the production and deposition of basement membrane matrices but also reveal that ECs recognize the proteins and respond by restricting tube diameter. Decreased vessel diameter and tube network areas are measurements that reflect the ability of pericytes to negatively regulate vascular tube morphogenesis while at the same time preventing pro-regressive stimuli from acting. Thus, EC tube diameter is also an important indicator of dysfunctional EC-pericyte interactions that lead to a variety of vessel abnormalities (which frequently show increased vessel diameter). In addition, it is well known that basement membranes can facilitate cell polarity functions, by enhancing cell-cell contacts mediated through junctional contacts, such as through adherens and tight junctional

proteins. Although the EC apical membrane domain has been difficult to define in molecular terms, the clear evidence of EC polarization in our coculture model is the deposition of basement membrane matrices specifically to the abluminal surface and the prior recruitment of pericytes to these same abluminal membranes [94].

1.3.18 Specific Upregulation of EC and Pericyte Integrins Recognizing Basement Membrane Matrices During EC-Pericyte Tube Co-Assembly in 3D Collagen Matrices

Again, using our coculture system with human ECs and bovine pericytes, we assessed how EC vs. pericyte integrins were regulated during this process. We assessed mRNA levels and performed function blocking experiments with anti-integrin monoclonal antibodies. As discussed above, blocking antibodies to the α5β1 integrin had function blocking effects that selectively occurred in the EC-pericyte cocultures but not the EC-only cultures [94]. Interestingly, the EC α5 integrin subunit was induced at the mRNA level in EC-pericyte cocultures, but not in EC-only cultures where it was downregulated. An important theme which emerged from these studies is that integrins which recognize the newly remodeled ECM assembling between ECs and pericytes were induced, while others that recognized collagen type I matrices, such as the α2 integrin subunit from ECs, were downregulated [94] (Fig. 1.5e). Thus, as basement membranes assemble around EC tubes, the direct interaction of ECs with collagen type I decreases, while their contact with basement membrane matrices increases. Concomitantly, we observed increases in the expression of integrin α5, α3, and α6 from ECs, which can recognize fibronectin, nidogens, and laminin isoforms, while α5, α3, α6, and α1 integrin subunits were increased, from pericytes which recognize fibronectin, nidogens, laminin isoforms, and collagen type IV [94]. We also observed functional effects of these integrins, since blocking antibodies to the α5, α3, α6, and α1 integrin all caused abnormalities in the tube maturation process, by significantly increasing tube width [94]. None of these antibodies have any influence on EC-only cultures, which are solely dependent on the collagen-binding integrin, α2β1 [28, 94]. This data strongly indicates that the purpose of the multiple β1 integrins, on the EC cell surface, is to recognize key ECM components they encounter at different stages of the tube morphogenic and maturation process. When they are exposed to collagen type I matrices, which serves as a strong agonist for tubulogenesis, they utilize collagen-binding integrins such as α2β1. However, when EC-lined tubes attract pericytes, ECM remodeling occurs that induces deposition of basement membrane matrices that are recognized by different sets of integrins such as α5β1 (a fibronectin receptor), α3β1 (a nidogen and laminin isoform receptor), α6β1 (a laminin isoform receptor), and α1β1 (a collagen type IV, collagen type I, and laminin receptor) [94]. Interestingly, α1β1 appears to be predominantly pericyte-derived during the

EC-pericyte tube co-assembly process. Thus, the effects of blocking antibodies that have been observed may be due to an inhibitory influence on pericyte recognition of basement membrane matrices during these events [94]. EC-dependence on α2β1, which is continuously observed over time in EC-only cultures is lost with time in EC-pericyte cocultures, as basement membrane matrix assembly occurs and exposure of ECs to collagen type I is strongly diminished. In conclusion, our findings show that EC-pericyte interactions control vascular basement membrane matrix assembly and that concomitant changes in EC and pericyte integrins occurs to recognize this newly remodeled matrix to facilitate further tube maturation and stabilization events.

1.3.19 Defining the Critical Growth Factors that Control Human Vascular Tube Morphogenesis and Pericyte Recruitment to EC-Lined Tubes

A central question in vascular biology is to elucidate the nature of the growth factors that are necessary to assemble the developing vasculature. Considerable data, particularly obtained from knockout mice or zebrafish, suggested a major role for VEGF [1]. Using serum-free defined models of vascular tube morphogenesis, we have assessed a role for VEGF and FGF-2, singly or in combination, in directly regulating EC tube assembly. Neither factor (alone or in combination) (i.e., VEGF+FGF) was able to support EC tubulogenesis [93]. Using a broad screen for growth factors, peptides, and other small molecules in a 96-well plate microassay format, we identified a single combination of five growth factors that leads to human EC lumen and tube network assembly. The five Factors are stem cell factor (SCF), interleukin-3 (IL-3), stromal-derived factor-1 alpha (SDF-1α), FGF-2, and insulin [93] (Fig. 1.3). Detailed screening of hundreds of additional combinations of molecules failed to identify any other mixture that supported this process [18]. Adding pericytes to ECs does not substitute for the Factor requirements [93]. Importantly, admixing pericytes with ECs under these Factor-driven defined conditions leads to EC tubulogenesis and marked pericyte recruitment as well as proliferation [93]. Of great interest is that pericytes proliferate, but ECs do not. In addition, this stimulated EC-pericyte tube co-assembly results in capillary maturation events, including basement membrane matrix assembly [93, 94]. Pericyte recruitment and basement membrane formation lead to narrower tube diameters, compared to EC-only cultures [94]. Using this Factor-driven system, we identified a key role for EC-derived PDGF-BB and HB-EGF, in pericyte recruitment and proliferation, during EC-pericyte tube co-assembly [96]. Disruption of recruitment using antagonists of PDGF-BB and HB-EGF (using blocking antibodies or receptor traps) leads to wider tubes, fewer pericytes, and markedly reduced basement membrane deposition [96]. Overall, these data strongly indicate that we have identified a key combination of five Factors that are necessary to stimulate the process of human capillary tube

assembly [18, 93]. These Factors, by acting on ECs, are also critical in facilitating pericyte recruitment (through PDGF-BB and HB-EGF) which is required for capillary basement membrane matrix assembly, a fundamental step in vessel maturation.

Finally, we have addressed a functional role for VEGF during these events, by acting as an upstream primer of EC responses to the Factors [93]. VEGF pretreatment leads to upregulation of c-Kit, IL-3Rα, and CXCR4, which are the key receptors necessary to act in conjunction with FGF and insulin receptors [93]. The addition of a combination of FGF and insulin together fails to support EC tubulogenesis. In contrast, addition of all five Factors leads to marked EC tubulogenesis. Importantly, VEGF pretreatment of ECs for 8 h or more leads to significant increases in their response to the downstream Factors [93]. Furthermore, VEGF priming also enhances pericyte recruitment responses, during EC-pericyte tube co-assembly [93]. This work strongly suggests that VEGF's functional role needs to be reinterpreted, in that it fails to directly stimulate EC tubulogenesis but can clearly act as an upstream EC primer/activator, which allows for enhanced responses to downstream Factors. The unique signaling features of VEGF priming must be investigated and distinguished from those supplied by the Factors, which separately leads to the major EC tubulogenic process. Thus, these unique signaling events control distinct steps in the process of EC tube morphogenesis which then leads to pericyte recruitment to establish capillary networks that mature over time.

1.4 Future Directions

It is clear that major advances have occurred over the past two decades in elucidating molecular mechanisms that underlie the ability of vessels to form, mature, and regress. In our view, it is this type of mechanistic research that will most likely lead to the generation of novel therapeutic strategies to manipulate blood vessels in the context of disease. It is also critical that both in vitro and in vivo approaches be continued and appreciated by individuals who focus on either side of these strategies. As the in vitro models and experimental strategies have evolved, it is more and more evident that very rapid advances are occurring in this area. Particular assay systems have repeatedly been shown to accurately reflect the biology of developing and postnatal vessels in vivo, and thus, these systems represent a critical experimental approach to rapidly advance the field.

In terms of key future directions, it is clear that more cytokine and growth factor research needs to be coupled with signal transduction studies to elucidate when and where particular molecules act to control the development, maturation, and stability of the vasculature. A key aspect of this question is how distinct growth factors or combinations (and their unique downstream signals) are necessary to create and maintain arteries, capillaries, veins, and the lymphatic vasculature. Our recent findings showing that five growth factors, SCF, IL-3, SDF-1α, FGF-2, and insulin, are required in combination to support human capillary tube assembly is an example of

this type of advance. The EC tubulogenic signaling cascade is highly complex and needs to be investigated in considerably more detail. A fundamental question, which remains unanswered, is what allows ECs to form lumen and tubes, while cells such as pericytes and fibroblasts cannot perform this function. In attempts to create the EC lineage from any other cell type, it is essential to determine whether the cells can form tubes in a 3D matrix environment, which is one of primary functional roles of ECs. It is likely that a detailed understanding of these processes will lead to important new opportunities to treat disease. Many of the most important acute and chronic diseases include a major component involving the dysfunction or breakdown of the vasculature (e.g., cancer, diabetes, tissue fibrosis, hypertension, atherosclerosis). Another important concept that needs to be stressed is that molecules (growth factors, ECM, receptors, MMPs) and downstream signaling molecules work together (i.e., multiprotein complexes), and it is critical to understand how such molecules and pathways temporally coordinate to control the observed biological responses. The single molecule analysis and approach that is inherent to many studies can be quite misleading in terms of our understanding of complex biological events. Systems approaches (i.e., RNAseq, non-coding RNA regulation, and proteomics analyzing protein-protein interactions with identification of key phosphorylation sites) are important directions in future work to identify new critical regulators of the pathways that control vascularization responses and to assess how these are altered in the context of vascular disease.

Acknowledgments This work was supported by NIH grants HL126518, HL128584, and HL136139 to G.E. Davis.

References

1. Adams, R. H., & Alitalo, K. (2007). Molecular regulation of angiogenesis and lymphangiogenesis. *Nature Reviews, 8*, 464–478.
2. Alavi, A., Hood, J. D., Frausto, R., Stupack, D. G., & Cheresh, D. A. (2003). Role of Raf in vascular protection from distinct apoptotic stimuli. *Science (New York, N.Y.), 301*, 94–96.
3. Aplin, A. C., Fogel, E., Zorzi, P., & Nicosia, R. F. (2008). The aortic ring model of angiogenesis. *Methods in Enzymology, 443*, 119–136.
4. Aplin, A. C., Zhu, W. H., Fogel, E., & Nicosia, R. F. (2009). Vascular regression and survival are differentially regulated by MT1-MMP and TIMPs in the aortic ring model of angiogenesis. *American Journal of Physiology, 297*, C471–C480.
5. Armulik, A., Abramsson, A., & Betsholtz, C. (2005). Endothelial/pericyte interactions. *Circulation Research, 97*, 512–523.
6. Astrof, S., Crowley, D., & Hynes, R. O. (2007). Multiple cardiovascular defects caused by the absence of alternatively spliced segments of fibronectin. *Developmental Biology, 311*, 11–24.
7. Baker, A. H., Edwards, D. R., & Murphy, G. (2002). Metalloproteinase inhibitors: Biological actions and therapeutic opportunities. *Journal of Cell Science, 115*, 3719–3727.
8. Bayless, K. J., & Davis, G. E. (2002). The Cdc42 and Rac1 GTPases are required for capillary lumen formation in three-dimensional extracellular matrices. *Journal of Cell Science, 115*, 1123–1136.

9. Bayless, K. J., & Davis, G. E. (2003). Sphingosine-1-phosphate markedly induces matrix metalloproteinase and integrin-dependent human endothelial cell invasion and lumen formation in three-dimensional collagen and fibrin matrices. *Biochemical and Biophysical Research Communications, 312*, 903–913.
10. Bayless, K. J., & Davis, G. E. (2004). Microtubule depolymerization rapidly collapses capillary tube networks in vitro and angiogenic vessels in vivo through the small GTPase Rho. *The Journal of Biological Chemistry, 279*, 11686–11695.
11. Bayless, K. J., Salazar, R., & Davis, G. E. (2000). RGD-dependent vacuolation and lumen formation observed during endothelial cell morphogenesis in three-dimensional fibrin matrices involves the alpha(v)beta(3) and alpha(5)beta(1) integrins. *The American Journal of Pathology, 156*, 1673–1683.
12. Bell, S. E., Mavila, A., Salazar, R., Bayless, K. J., Kanagala, S., Maxwell, S. A., et al. (2001). Differential gene expression during capillary morphogenesis in 3D collagen matrices: Regulated expression of genes involved in basement membrane matrix assembly, cell cycle progression, cellular differentiation and G-protein signaling. *Journal of Cell Science, 114*, 2755–2773.
13. Benjamin, L. E., Golijanin, D., Itin, A., Pode, D., & Keshet, E. (1999). Selective ablation of immature blood vessels in established human tumors follows vascular endothelial growth factor withdrawal. *The Journal of Clinical Investigation, 103*, 159–165.
14. Benjamin, L. E., Hemo, I., & Keshet, E. (1998). A plasticity window for blood vessel remodelling is defined by pericyte coverage of the preformed endothelial network and is regulated by PDGF-B and VEGF. *Development, 125*, 1591–1598.
15. Bergers, G., Song, S., Meyer-Morse, N., Bergsland, E., & Hanahan, D. (2003). Benefits of targeting both pericytes and endothelial cells in the tumor vasculature with kinase inhibitors. *The Journal of Clinical Investigation, 111*, 1287–1295.
16. Bjarnegard, M., Enge, M., Norlin, J., Gustafsdottir, S., Fredriksson, S., Abramsson, A., et al. (2004). Endothelium-specific ablation of PDGFB leads to pericyte loss and glomerular, cardiac and placental abnormalities. *Development, 131*, 1847–1857.
17. Bokoch, G. M. (2003). Biology of the p21-activated kinases. *Annual Review of Biochemistry, 72*, 743–781.
18. Bowers, S. L., Norden, P. R., & Davis, G. E. (2016). Molecular signaling pathways controlling vascular tube morphogenesis and pericyte-induced tube maturation in 3D extracellular matrices. *Advances in Pharmacology, 77*, 241–280. https://doi.org/10.1016/bs.apha.2016.04.005
19. Carmeliet, P. (2005). Angiogenesis in life, disease and medicine. *Nature, 438*, 932–936.
20. Chang, S., Young, B. D., Li, S., Qi, X., Richardson, J. A., & Olson, E. N. (2006). Histone deacetylase 7 maintains vascular integrity by repressing matrix metalloproteinase 10. *Cell, 126*, 321–334.
21. Chun, T. H., Sabeh, F., Ota, I., Murphy, H., McDonagh, K. T., Holmbeck, K., et al. (2004). MT1-MMP-dependent neovessel formation within the confines of the three-dimensional extracellular matrix. *The Journal of Cell Biology, 167*, 757–767.
22. Crosswhite, P. L., Podsiadlowska, J. J., Curtis, C. D., Gao, S., Xia, L., Srinivasan, R. S., et al. (2016). CHD4-regulated plasmin activation impacts lymphovenous hemostasis and hepatic vascular integrity. *The Journal of Clinical Investigation, 126*, 2254–2266. https://doi.org/10.1172/JCI84652
23. Czirok, A., Zamir, E. A., Szabo, A., & Little, C. D. (2008). Multicellular sprouting during vasculogenesis. *Current Topics in Developmental Biology, 81*, 269–289.
24. Davis, G. E. (2010). Matricryptic sites control tissue injury responses in the cardiovascular system: Relationships to pattern recognition receptor regulated events. *Journal of Molecular and Cellular Cardiology, 48*, 454–460. https://doi.org/10.1016/j.yjmcc.2009.09.002
25. Davis, G. E., & Bayless, K. J. (2003). An integrin and rho GTPase-dependent pinocytic vacuole mechanism controls capillary lumen formation in collagen and fibrin matrices. *Microcirculation, 10*, 27–44.

26. Davis, G. E., Bayless, K. J., Davis, M. J., & Meininger, G. A. (2000). Regulation of tissue injury responses by the exposure of matricryptic sites within extracellular matrix molecules. *The American Journal of Pathology, 156*, 1489–1498.
27. Davis, G. E., Bayless, K. J., & Mavila, A. (2002). Molecular basis of endothelial cell morphogenesis in three-dimensional extracellular matrices. *The Anatomical Record, 268*, 252–275.
28. Davis, G. E., & Camarillo, C. W. (1996). An alpha 2 beta 1 integrin-dependent pinocytic mechanism involving intracellular vacuole formation and coalescence regulates capillary lumen and tube formation in three-dimensional collagen matrix. *Experimental Cell Research, 224*, 39–51.
29. Davis, G. E., Kim, D. J., Meng, C. X., Norden, P. R., Speichinger, K. R., Davis, M. T., et al. (2013). Control of vascular tube morphogenesis and maturation in 3D extracellular matrices by endothelial cells and pericytes. *Methods in Molecular Biology, 1066*, 17–28. https://doi.org/10.1007/978-1-62703-604-7_2
30. Davis, G. E., Koh, W., & Stratman, A. N. (2007). Mechanisms controlling human endothelial lumen formation and tube assembly in three-dimensional extracellular matrices. *Birth Defects Research. Part C, Embryo Today, 81*, 270–285.
31. Davis, G. E., Norden, P. R., & Bowers, S. L. (2015). Molecular control of capillary morphogenesis and maturation by recognition and remodeling of the extracellular matrix: Functional roles of endothelial cells and pericytes in health and disease. *Connective Tissue Research, 56*, 392–402. https://doi.org/10.3109/03008207.2015.1066781
32. Davis, G. E., Pintar Allen, K. A., Salazar, R., & Maxwell, S. A. (2001). Matrix metalloproteinase-1 and -9 activation by plasmin regulates a novel endothelial cell-mediated mechanism of collagen gel contraction and capillary tube regression in three-dimensional collagen matrices. *Journal of Cell Science, 114*, 917–930.
33. Davis, G. E., & Saunders, W. B. (2006). Molecular balance of capillary tube formation versus regression in wound repair: Role of matrix metalloproteinases and their inhibitors. *The Journal of Investigative Dermatology. Symposium Proceedings, 11*, 44–56.
34. Davis, G. E., & Senger, D. R. (2005). Endothelial extracellular matrix: Biosynthesis, remodeling, and functions during vascular morphogenesis and neovessel stabilization. *Circulation Research, 97*, 1093–1107.
35. Davis, G. E., & Senger, D. R. (2008). Extracellular matrix mediates a molecular balance between vascular morphogenesis and regression. *Current Opinion in Hematology, 15*, 197–203.
36. Davis, G. E., Stratman, A. N., Sacharidou, A., & Koh, W. (2011). Molecular basis for endothelial lumen formation and tubulogenesis during vasculogenesis and angiogenic sprouting. *International Review of Cell and Molecular Biology, 288*, 101–165. https://doi.org/10.1016/B978-0-12-386041-5.00003-0
37. Dejana, E., Tournier-Lasserve, E., & Weinstein, B. M. (2009). The control of vascular integrity by endothelial cell junctions: Molecular basis and pathological implications. *Developmental Cell, 16*, 209–221.
38. Ebnet, K., Aurrand-Lions, M., Kuhn, A., Kiefer, F., Butz, S., Zander, K., et al. (2003). The junctional adhesion molecule (JAM) family members JAM-2 and JAM-3 associate with the cell polarity protein PAR-3: A possible role for JAMs in endothelial cell polarity. *Journal of Cell Science, 116*, 3879–3891.
39. Ebnet, K., Suzuki, A., Ohno, S., & Vestweber, D. (2004). Junctional adhesion molecules (JAMs): More molecules with dual functions? *Journal of Cell Science, 117*, 19–29.
40. Etienne-Manneville, S., & Hall, A. (2003). Cdc42 regulates GSK-3beta and adenomatous polyposis coli to control cell polarity. *Nature, 421*, 753–756.
41. Foo, S. S., Turner, C. J., Adams, S., Compagni, A., Aubyn, D., Kogata, N., et al. (2006). Ephrin-B2 controls cell motility and adhesion during blood-vessel-wall assembly. *Cell, 124*, 161–173.
42. Francis, S. E., Goh, K. L., Hodivala-Dilke, K., Bader, B. L., Stark, M., Davidson, D., et al. (2002). Central roles of alpha5beta1 integrin and fibronectin in vascular development in

mouse embryos and embryoid bodies. *Arteriosclerosis, Thrombosis, and Vascular Biology, 22*, 927–933.
43. Galabova-Kovacs, G., Matzen, D., Piazzolla, D., Meissl, K., Plyushch, T., Chen, A. P., et al. (2006). Essential role of B-Raf in ERK activation during extraembryonic development. *Proceedings of the National Academy of Sciences of the United States of America, 103*, 1325–1330.
44. Galan Moya, E. M., Le Guelte, A., & Gavard, J. (2009). PAKing up to the endothelium. *Cellular Signalling, 21*, 1727–1737.
45. Gao, M., Craig, D., Lequin, O., Campbell, I. D., Vogel, V., & Schulten, K. (2003). Structure and functional significance of mechanically unfolded fibronectin type III1 intermediates. *Proceedings of the National Academy of Sciences of the United States of America, 100*, 14784–14789.
46. Gerety, S. S., & Anderson, D. J. (2002). Cardiovascular ephrinB2 function is essential for embryonic angiogenesis. *Development, 129*, 1397–1410.
47. Gill, S. E., & Parks, W. C. (2008). Metalloproteinases and their inhibitors: Regulators of wound healing. *The International Journal of Biochemistry & Cell Biology, 40*, 1334–1347.
48. Greenberg, J. I., Shields, D. J., Barillas, S. G., Acevedo, L. M., Murphy, E., Huang, J., et al. (2008). A role for VEGF as a negative regulator of pericyte function and vessel maturation. *Nature, 456*, 809–813.
49. Hall, A. (2005). Rho GTPases and the control of cell behaviour. *Biochemical Society Transactions, 33*, 891–895.
50. Hallmann, R., Horn, N., Selg, M., Wendler, O., Pausch, F., & Sorokin, L. M. (2005). Expression and function of laminins in the embryonic and mature vasculature. *Physiological Reviews, 85*, 979–1000.
51. Hammes, H. P. (2005). Pericytes and the pathogenesis of diabetic retinopathy. *Hormone and Metabolic Research, 37*(Suppl 1), 39–43.
52. Handsley, M. M., & Edwards, D. R. (2005). Metalloproteinases and their inhibitors in tumor angiogenesis. *International Journal of Cancer, 115*, 849–860.
53. Herbert, S. P., Huisken, J., Kim, T. N., Feldman, M. E., Houseman, B. T., Wang, R. A., et al. (2009). Arterial-venous segregation by selective cell sprouting: An alternative mode of blood vessel formation. *Science (New York, N.Y.), 326*, 294–298.
54. Hirschi, K. K., Rohovsky, S. A., & D'Amore, P. A. (1998). PDGF, TGF-beta, and heterotypic cell-cell interactions mediate endothelial cell-induced recruitment of 10T1/2 cells and their differentiation to a smooth muscle fate. *The Journal of Cell Biology, 141*, 805–814.
55. Holderfield, M. T., & Hughes, C. C. (2008). Crosstalk between vascular endothelial growth factor, notch, and transforming growth factor-beta in vascular morphogenesis. *Circulation Research, 102*, 637–652.
56. Hughes, C. C. (2008). Endothelial-stromal interactions in angiogenesis. *Current Opinion in Hematology, 15*, 204–209.
57. Hynes, R. O. (2007). Cell-matrix adhesion in vascular development. *Journal of Thrombosis and Haemostasis, 5*(Suppl 1), 32–40.
58. Hynes, R. O. (2009). The extracellular matrix: Not just pretty fibrils. *Science (New York, N.Y.), 326*, 1216–1219.
59. Ingram, K. G., Curtis, C. D., Silasi-Mansat, R., Lupu, F., & Griffin, C. T. (2013). The NuRD chromatin-remodeling enzyme CHD4 promotes embryonic vascular integrity by transcriptionally regulating extracellular matrix proteolysis. *PLoS Genetics, 9*, e1004031. https://doi.org/10.1371/journal.pgen.1004031
60. Iruela-Arispe, M. L., & Davis, G. E. (2009). Cellular and molecular mechanisms of vascular lumen formation. *Developmental Cell, 16*, 222–231.
61. Jain, R. K. (2005). Normalization of tumor vasculature: An emerging concept in antiangiogenic therapy. *Science (New York, N.Y.), 307*, 58–62.
62. Kamei, M., Saunders, W. B., Bayless, K. J., Dye, L., Davis, G. E., & Weinstein, B. M. (2006). Endothelial tubes assemble from intracellular vacuoles in vivo. *Nature, 442*, 453–456.

63. Kim, D. J., Martinez-Lemus, L. A., & Davis, G. E. (2013). EB1, p150Glued, and Clasp1 control endothelial tubulogenesis through microtubule assembly, acetylation, and apical polarization. *Blood, 121*, 3521–3530. https://doi.org/10.1182/blood-2012-11-470179
64. Kim, D. J., Norden, P. R., Salvador, J., Barry, D. M., Bowers, S. L. K., Cleaver, O., et al. (2017). Src- and Fyn-dependent apical membrane trafficking events control endothelial lumen formation during vascular tube morphogenesis. *PLoS One, 12*, e0184461. https://doi.org/10.1371/journal.pone.0184461
65. Kim, Y. H., Hu, H., Guevara-Gallardo, S., Lam, M. T., Fong, S. Y., & Wang, R. A. (2008). Artery and vein size is balanced by notch and ephrin B2/EphB4 during angiogenesis. *Development, 135*, 3755–3764.
66. Koh, W., Mahan, R. D., & Davis, G. E. (2008). Cdc42- and Rac1-mediated endothelial lumen formation requires Pak2, Pak4 and Par3, and PKC-dependent signaling. *Journal of Cell Science, 121*, 989–1001.
67. Koh, W., Sachidanandam, K., Stratman, A. N., Sacharidou, A., Mayo, A. M., Murphy, E. A., et al. (2009). Formation of endothelial lumens requires a coordinated PKC{epsilon}-, Src-, Pak- and Raf-kinase-dependent signaling cascade downstream of Cdc42 activation. *Journal of Cell Science, 122*, 1812–1822.
68. Koh, W., Stratman, A. N., Sacharidou, A., & Davis, G. E. (2008). In vitro three dimensional collagen matrix models of endothelial lumen formation during vasculogenesis and angiogenesis. *Methods in Enzymology, 443*, 83–101.
69. Kwak, H. I., Mendoza, E. A., & Bayless, K. J. (2009). ADAM17 co-purifies with TIMP-3 and modulates endothelial invasion responses in three-dimensional collagen matrices. *Matrix Biology, 28*, 470–479.
70. Liu, J., Fraser, S. D., Faloon, P. W., Rollins, E. L., Vom Berg, J., Starovic-Subota, O., et al. (2007). A betaPix Pak2a signaling pathway regulates cerebral vascular stability in zebrafish. *Proceedings of the National Academy of Sciences of the United States of America, 104*, 13990–13995.
71. Liu, Y., & Senger, D. R. (2004). Matrix-specific activation of Src and rho initiates capillary morphogenesis of endothelial cells. *FASEB Journal, 18*, 457–468.
72. Lucitti, J. L., Jones, E. A., Huang, C., Chen, J., Fraser, S. E., & Dickinson, M. E. (2007). Vascular remodeling of the mouse yolk sac requires hemodynamic force. *Development, 134*, 3317–3326.
73. Macara, I. G. (2004). Par proteins: Partners in polarization. *Current Biology, 14*, R160–R162.
74. Mancuso, M. R., Davis, R., Norberg, S. M., O'Brien, S., Sennino, B., Nakahara, T., et al. (2006). Rapid vascular regrowth in tumors after reversal of VEGF inhibition. *The Journal of Clinical Investigation, 116*, 2610–2621.
75. Martin-Belmonte, F., Gassama, A., Datta, A., Yu, W., Rescher, U., Gerke, V., et al. (2007). PTEN-mediated apical segregation of phosphoinositides controls epithelial morphogenesis through Cdc42. *Cell, 128*, 383–397.
76. Miner, J. H., & Yurchenco, P. D. (2004). Laminin functions in tissue morphogenesis. *Annual Review of Cell and Developmental Biology, 20*, 255–284.
77. Morla, A., & Ruoslahti, E. (1992). A fibronectin self-assembly site involved in fibronectin matrix assembly: Reconstruction in a synthetic peptide. *The Journal of Cell Biology, 118*, 421–429.
78. Nakatsu, M. N., & Hughes, C. C. (2008). An optimized three-dimensional in vitro model for the analysis of angiogenesis. *Methods in Enzymology, 443*, 65–82.
79. Norden, P. R., Kim, D. J., Barry, D. M., Cleaver, O. B., & Davis, G. E. (2016). Cdc42 and k-Ras control endothelial tubulogenesis through apical membrane and cytoskeletal polarization: Novel stimulatory roles for GTPase effectors, the small GTPases, Rac2 and Rap1b, and inhibitory influence of Arhgap31 and Rasa1. *PLoS One, 11*, e0147758. https://doi.org/10.1371/journal.pone.0147758
80. Qi, J. H., Ebrahem, Q., Moore, N., Murphy, G., Claesson-Welsh, L., Bond, M., et al. (2003). A novel function for tissue inhibitor of metalloproteinases-3 (TIMP3): Inhibition of angiogenesis by blockage of VEGF binding to VEGF receptor-2. *Nature Medicine, 9*, 407–415.

81. Rhodes, J. M., & Simons, M. (2007). The extracellular matrix and blood vessel formation: Not just a scaffold. *Journal of Cellular and Molecular Medicine, 11*, 176–205.
82. Rupp, P. A., Czirok, A., & Little, C. D. (2003). Novel approaches for the study of vascular assembly and morphogenesis in avian embryos. *Trends in Cardiovascular Medicine, 13*, 283–288.
83. Sacharidou, A., Koh, W., Stratman, A. N., Mayo, A. M., Fisher, K. E., & Davis, G. E. (2010). Endothelial lumen signaling complexes control 3D matrix-specific tubulogenesis through interdependent Cdc42- and MT1-MMP-mediated events. *Blood, 115*(25), 5259–5269.
84. Sacharidou, A., Stratman, A. N., & Davis, G. E. (2012). Molecular mechanisms controlling vascular lumen formation in three-dimensional extracellular matrices. *Cells, Tissues, Organs, 195*, 122–143. https://doi.org/10.1159/000331410
85. San Antonio, J. D., Zoeller, J. J., Habursky, K., Turner, K., Pimtong, W., Burrows, M., et al. (2009). A key role for the integrin alpha2beta1 in experimental and developmental angiogenesis. *The American Journal of Pathology, 175*, 1338–1347.
86. Saunders, W. B., Bayless, K. J., & Davis, G. E. (2005). MMP-1 activation by serine proteases and MMP-10 induces human capillary tubular network collapse and regression in 3D collagen matrices. *Journal of Cell Science, 118*, 2325–2340.
87. Saunders, W. B., Bohnsack, B. L., Faske, J. B., Anthis, N. J., Bayless, K. J., Hirschi, K. K., et al. (2006). Coregulation of vascular tube stabilization by endothelial cell TIMP-2 and pericyte TIMP-3. *The Journal of Cell Biology, 175*, 179–191.
88. Senger, D. R., Claffey, K. P., Benes, J. E., Perruzzi, C. A., Sergiou, A. P., & Detmar, M. (1997). Angiogenesis promoted by vascular endothelial growth factor: Regulation through alpha1beta1 and alpha2beta1 integrins. *Proceedings of the National Academy of Sciences of the United States of America, 94*, 13612–13617.
89. Senger, D. R., & Davis, G. E. (2011). Angiogenesis. *Cold Spring Harbor Perspectives in Biology, 3*, a005090. https://doi.org/10.1101/cshperspect.a005090
90. Seo, D. W., Li, H., Guedez, L., Wingfield, P. T., Diaz, T., Salloum, R., et al. (2003). TIMP-2 mediated inhibition of angiogenesis: An MMP-independent mechanism. *Cell, 114*, 171–180.
91. Smith, A. O., Bowers, S. L., Stratman, A. N., & Davis, G. E. (2013). Hematopoietic stem cell cytokines and fibroblast growth factor-2 stimulate human endothelial cell-pericyte tube coassembly in 3D fibrin matrices under serum-free defined conditions. *PLoS One, 8*, e85147. https://doi.org/10.1371/journal.pone.0085147
92. Stratman, A. N., & Davis, G. E. (2012). Endothelial cell-pericyte interactions stimulate basement membrane matrix assembly: Influence on vascular tube remodeling, maturation, and stabilization. *Microscopy and Microanalysis, 18*, 68–80. https://doi.org/10.1017/S1431927611012402
93. Stratman, A. N., Davis, M. J., & Davis, G. E. (2011). VEGF and FGF prime vascular tube morphogenesis and sprouting directed by hematopoietic stem cell cytokines. *Blood, 117*, 3709–3719. https://doi.org/10.1182/blood-2010-11-316752
94. Stratman, A. N., Malotte, K. M., Mahan, R. D., Davis, M. J., & Davis, G. E. (2009). Pericyte recruitment during vasculogenic tube assembly stimulates endothelial basement membrane matrix formation. *Blood, 114*, 5091–5101.
95. Stratman, A. N., Saunders, W. B., Sacharidou, A., Koh, W., Fisher, K. E., Zawieja, D. C., et al. (2009). Endothelial cell lumen and vascular guidance tunnel formation requires MT1-MMP-dependent proteolysis in 3-dimensional collagen matrices. *Blood, 114*, 237–247.
96. Stratman, A. N., Schwindt, A. E., Malotte, K. M., & Davis, G. E. (2010). Endothelial-derived PDGF-BB and HB-EGF coordinately regulate pericyte recruitment during vasculogenic tube assembly and stabilization. *Blood, 116*, 4720–4730. https://doi.org/10.1182/blood-2010-05-286872
97. Stupack, D. G., & Cheresh, D. A. (2004). Integrins and angiogenesis. *Current Topics in Developmental Biology, 64*, 207–238.
98. Tian, Y., Lei, L., Cammarano, M., Nekrasova, T., & Minden, A. (2009). Essential role for the Pak4 protein kinase in extraembryonic tissue development and vessel formation. *Mechanisms of Development, 126*, 710–720.

99. Vogel, V. (2006). Mechanotransduction involving multimodular proteins: Converting force into biochemical signals. *Annual Review of Biophysics and Biomolecular Structure, 35*, 459–488.
100. Whelan, M. C., & Senger, D. R. (2003). Collagen I initiates endothelial cell morphogenesis by inducing actin polymerization through suppression of cyclic AMP and protein kinase A. *The Journal of Biological Chemistry, 278*, 327–334.
101. Wurtz, S. O., Schrohl, A. S., Sorensen, N. M., Lademann, U., Christensen, I. J., Mouridsen, H., et al. (2005). Tissue inhibitor of metalloproteinases-1 in breast cancer. *Endocrine-Related Cancer, 12*, 215–227.
102. Xu, K., Sacharidou, A., Fu, S., Chong, D. C., Skaug, B., Chen, Z. J., et al. (2011). Blood vessel tubulogenesis requires Rasip1 regulation of GTPase signaling. *Developmental Cell, 20*, 526–539. https://doi.org/10.1016/j.devcel.2011.02.010
103. Yaniv, K., Isogai, S., Castranova, D., Dye, L., Hitomi, J., & Weinstein, B. M. (2006). Live imaging of lymphatic development in the zebrafish. *Nature Medicine, 12*, 711–716.
104. Yu, J. A., Castranova, D., Pham, V. N., & Weinstein, B. M. (2015). Single-cell analysis of endothelial morphogenesis in vivo. *Development, 142*, 2951–2961. https://doi.org/10.1242/dev.123174
105. Yuan, L., Sacharidou, A., Stratman, A. N., Le Bras, A., Zwiers, P. J., Spokes, K., et al. (2011). RhoJ is an endothelial cell-restricted rho GTPase that mediates vascular morphogenesis and is regulated by the transcription factor ERG. *Blood, 118*, 1145–1153. https://doi.org/10.1182/blood-2010-10-315275
106. Zhong, C., Chrzanowska-Wodnicka, M., Brown, J., Shaub, A., Belkin, A. M., & Burridge, K. (1998). Rho-mediated contractility exposes a cryptic site in fibronectin and induces fibronectin matrix assembly. *The Journal of Cell Biology, 141*, 539–551.
107. Zhou, X., Rowe, R. G., Hiraoka, N., George, J. P., Wirtz, D., Mosher, D. F., et al. (2008). Fibronectin fibrillogenesis regulates three-dimensional neovessel formation. *Genes & Development, 22*, 1231–1243.
108. Zhou, Z., Apte, S. S., Soininen, R., Cao, R., Baaklini, G. Y., Rauser, R. W., et al. (2000). Impaired endochondral ossification and angiogenesis in mice deficient in membrane-type matrix metalloproteinase I. *Proceedings of the National Academy of Sciences of the United States of America, 97*, 4052–4057.
109. Zhu, W. H., Guo, X., Villaschi, S., & Francesco Nicosia, R. (2000). Regulation of vascular growth and regression by matrix metalloproteinases in the rat aorta model of angiogenesis. *Laboratory Investigation, 80*, 545–555.
110. Zovein, A. C., Luque, A., Turlo, K. A., Hofmann, J. J., Yee, K. M., Becker, M. S., et al. (2010). B1 integrin establishes endothelial cell polarity and arteriolar lumen formation via a Par3-dependent mechanism. *Developmental Cell, 18*, 39–51.

Chapter 2
Mechanical Regulation of Vascularization in Three-Dimensional Engineered Tissues

Barak Zohar, Shira Landau, and Shulamit Levenberg

2.1 Introduction

Three-dimensional (3D) tissue engineering generally involves the design of 3D polymeric scaffolds in combination with one or more cell types, to form implantable, tissue-like devices. Such engineered tissues can be used to replace autologous tissue conventionally used to repair substantial tissue damage and can serve as tissue-scale models to study normal and diseased biological processes (e.g., drug screening tests). Vascularization of engineered tissue constructs is a challenge of great significance in the field of regenerative medicine. Without a stable and perfusable blood vessel network providing oxygen and nutrients, cells cannot survive tissue dimension growth beyond several hundreds of microns, due to diffusion limitations. Several approaches have been applied to promote the vascularization of engineered implants, including pre-vascularization of implants relying on self-assembly of endothelial cells and mural cells to vessels. The mechanisms by which endothelial cells (ECs) self-assemble into vascular networks are quite diverse. Current scientific understanding generally separates these processes into vasculogenesis and angiogenesis, where vasculogenesis refers to the de novo creation of vascular networks from endothelial progenitor cells (angioblasts), as seen in the embryo's primitive vascular plexus. Angiogenesis refers to the expansion of existing vascular networks into new blood vessels, via mechanisms such as sprouting, intussusception (vessel splitting), and vessel fusion. During angiogenesis, ECs exert mechanical forces on their environment while invading, proliferating and migrating. These forces are generated by the contraction of several cytoskeletal proteins such as actin, microtubules, and actomyosin and are affected by environmental cues. Additionally, EC lining blood vessel walls are continuously exposed to mechanical

B. Zohar · S. Landau · S. Levenberg (✉)
Department of Biomedical Engineering, Technion-Israel Institute of Technology, Haifa, Israel
e-mail: shulamit@bm.technion.ac.il

S. Gerecht (ed.), *Biophysical Regulation of Vascular Differentiation and Assembly*, Biological and Medical Physics, Biomedical Engineering,
https://doi.org/10.1007/978-3-319-99319-5_2

stimuli, in the form of fluid shear stress generated by flowing blood, and tension generated by external contractile forces. Various in vitro models, consisting of ECs cultured in 3D scaffolds composed of different biomaterials, have been established to study the effect of mechanical stimuli on vascularization processes. Some of these models are designed to manipulate the mechanical properties of the 3D matrix such as matrix stiffness and boundary conditions, while others are designed to actively apply fluid shear stress and external tensile forces using designated bioreactors. This chapter will summarize the main insights gained regarding the impact of internal and external mechanical cues on the formation of vascular networks in 3D culture systems (Fig. 2.1). Internal mechanical forces refer to cell-induced forces regulated by the cellular environment, while external forces are those that are actively applied on the engineered tissue by external sources.

2.2 Internal Forces

2.2.1 Cellular Forces

Mechanical interactions between cells and the extracellular matrix (ECM) play a central role in regulation of cell division, motility, and differentiation [10, 32, 38]. Cells, including ECs, modify the mechanical and structural properties of their surrounding ECM by exerting contractile forces. Endothelial invasion and sprouting involve three-dimensional (3D) matrix deformation, as demonstrated by fluorescent particle displacement in gel [28, 49], anisotropic fibrillar structure of the ECM [30], and local ECM stiffness [25]. These matrix alterations subsequently trigger feedback responses which dictate vascular network morphogenesis. For example, endothelial sprouts exert mechanical forces that reorganize the matrix to support tubelike endothelial structures and branching point formation. It has also been shown that cell contractile forces regulate sprouting directionality. Korff et al. demonstrated that forces induced by sprouting vessels led to long-range deformation of the underlying collagen gel. Interestingly, sprouts of nearby EC spheroid followed the direction of tension-aligned fibers generated by the ECs [26]. Cell-cell mechanical communication has also been demonstrated in an experimental model in which EC sprouting correlated with substrate deformations generated by neighboring cells in a compliant polyacrylamide gel (Fig. 2.2a) [43].

2.2.2 Matrix Stiffness

The role of ECM stiffness in regulating cellular morphology, differentiation, traction force generation, focal adhesion, and cell migration dynamics is well studied [4, 10, 41, 42, 61]. Modification of the fibrin or collagen gel density has been a common approach to manipulate stiffness of 3D matrices in vitro. Studies

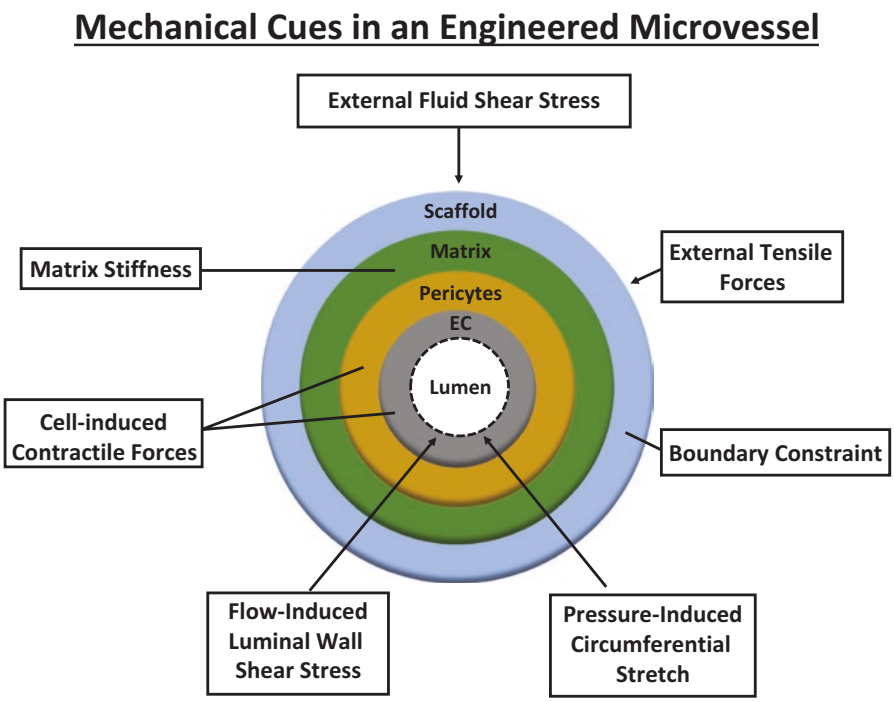

Fig. 2.1 Diagram of mechanical cues that regulate vascularization in 3D engineered tissue

demonstrate that a less dense fibrin matrix is essential for the formation of capillary-like networks and induces longer endothelial sprouts [24, 53]. Additionally, when co-cultured with supportive cells (fibroblasts) in 3D engineered construct, ECs self-assembled into more enhanced vascular networks on matrices with lower fibrin concentrations [31]. The same tendency was observed in studies utilizing collagen gels, where lower collagen density resulted in a more developed vascular network [9]. In another study, the best vascularization results were achieved with relatively intermediate collagen concentrations [48]. However, the impact of matrix stiffness per se is still questionable, since manipulation of gel density also alters chemical properties of the gel such as adhesion ligand concentrations, structure, and diffusion coefficients, all of which may directly or indirectly influence the residing cells. For example, limited diffusion of secreted growth factors was suggested as one reason for reduced sprouting in more concentrated gels [16]. Modification of collagen gel stiffness by glycation, pH adjustments, and the addition of stiffness-tunable hydrogels are some of the approaches also used today to independently study the impact of matrix stiffness on vessel networks. When adjusting gel stiffness by pH, ECs formed thicker and deeper vascular networks in rigid gels, as opposed to dense and thin networks on flexible gels [60]. Moreover, when stiffness was tuned by polyacrylamide hydrogel-coated collagen within a relevant physiological stiffness range (3–30 kPa), the expression of important pro-angiogenesis mediators (i.e., VEGFR-2,

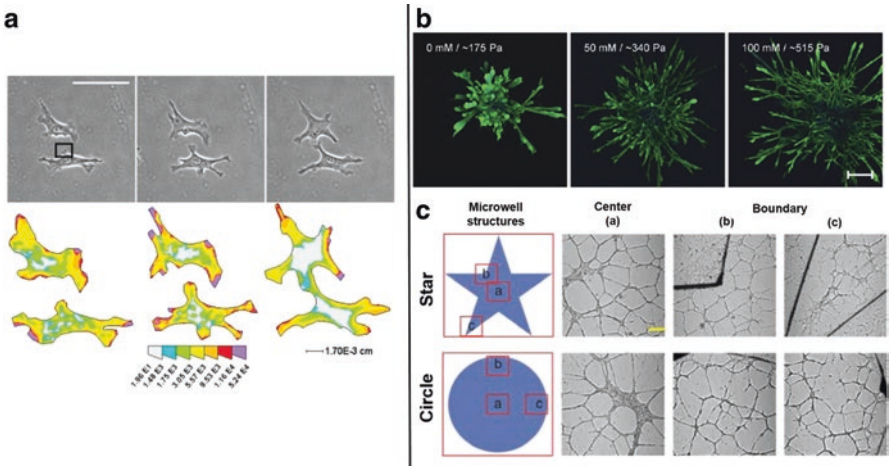

Fig. 2.2 Mechanical regulation of cell-induced forces affected by matrix stiffness and boundaries in vascular organization. (**a**) Cell-cell mechanical communication demonstrated by traction stress distribution. Phase images and corresponding traction maps of ECs coming into contact show guided communication via substrate deformations in a 5500 Pa gel conjugated with 1.0 mg/mL RGD peptide (adapted, with permission, from Reinhart-King et al. [43]). Bar, 100 μm. Color map is in units of dyn/cm^2. (**b**) Endothelial spheroids were cultured in nonenzymatically glycated collagen gels, which enabled assessment of the impact of gel stiffness on EC sprouting, independently of matrix density. Changes in the compressive modulus of the hydrogel resulted in an increase in the number and length of sprouts in the higher stiff matrix (adapted, with permission, from Mason et al. [36]). Bar, 200 μm. (**c**) The effect of mechanical boundaries on capillary-like structure formation using polydimethylsiloxane (PDMS) fences. Bright-field images of capillary-like structures on circular and star-shaped matrigels (adapted, with permission, from Sun et al. [50]). Bar, 300 μm

caveolin-1, and β-catenin) was significantly decreased on stiffer substrates [47]. Although glycated collagen culture models have shown that sprouting angiogenesis was delayed in stiff collagen gels [12], nonenzymatic glycation approach has shown altered tendency. When collagen stiffness was tuned by nonenzymatic glycation, the numbers and lengths of angiogenic sprouts were dramatically increased in a stiffer matrix (from 175 Pa to 515 Pa) (Fig. 2.2b) [36]. So despite many studies showing that vascular organization is dependent on the mechanical properties of the supporting matrix, the regulatory effect of stiffness on 3D vascular arrangement is still a source of controversy.

2.2.3 Boundary Constraint

Cells induce contractile forces that lead to the compaction of the surrounding matrix. Cells cultured in a gel with no rigid boundary (free gel) exert and sense less tension forces, compared to cells cultured in a constrained gel where the gel deformability is limited. Consequently, vascular network formation in a gel is demonstrated

to decrease when boundary limitation is high, corresponding to higher matrix stiffness conditions. In several studies, differential boundary conditions were applied by constraining the gel to predetermined boundary geometries such as a rectangle, triangle, square, star, or circle (Fig. 2.2c) [50, 52]. Sun et al. demonstrated that vascular networks situated along the boundary of the shapes were significantly denser and had a shorter mean cord length, compared with the central regions. The local strain field experienced by microvessels was predicted by computational finite element models simulating the contraction of gels constrained by various boundary conditions [50]. This boundary effect was then eliminated using a Rho-associated protein kinase inhibitor, which demonstrated the correlation with cell traction force [50]. These findings demonstrate that boundary conditions and, thus, the effective stiffness of the matrix provide an alternative means of controlling vascular organization in engineered tissues without modifying matrix chemical properties.

2.3 External Forces

2.3.1 Tensile Forces

During physiological growth, blood vessels remodel and grow in response to tensile stress and the resulting strain within the vessel wall [34]. In recent years, there have been growing attempts to include tensile stress, primarily applied by the use of bioreactors, as a mechanical stimulator when engineering blood vessels. Recent experiments show a connection between tensile stress and alignment of forming vessels. ECs grown on micro-carrier beads, cultured within a fibrin gel containing smooth muscle cells and subjected to 10% cyclic strain at 0.7 Hz, formed sprouts which aligned in parallel to the strain direction, whereas the unstrained control sprouted radially. The plasticity of this alignment was demonstrated, when the aligned strained vascularized constructs were transferred to static unstrained condition, which led to random alignment of the vessel sprouts [6]. In a similar work, researchers isolated microvessels, seeded them into a collagen gel, and applied 6% cyclic strain at 1 Hz. The forming sprouts aligned in parallel to the strain direction [27]. However, contradictory findings reported by Matsumoto et al. noted that ECs seeded on a dextran micro-carrier surrounded with fibrin gel sprouted outward, at an angle that was perpendicular to the cyclic strain [37]. Similar behavior was recorded when human pluripotent stem cell-derived vascular smooth muscle cells (vSMC) were subjected to uniaxial cyclic strain, which induced their alignment perpendicular to the stretching direction [58]. ECs seeded on collagen on top of a silicone mold and subjected to cyclic uniaxial stretch (20%, 1 Hz), also aligned perpendicular to the stretch direction and formed more vessel sprouts [59]. In a different work, ECs and fibroblasts co-cultured within Gelfoam 3D scaffolds and subjected to uniaxial cyclic stretch (10% and 1 Hz) formed vessels that aligned diagonal (30–600) to the stretching direction (Fig. 2.3a) [45]. However, ECs and fibroblasts seeded into a Gelfoam

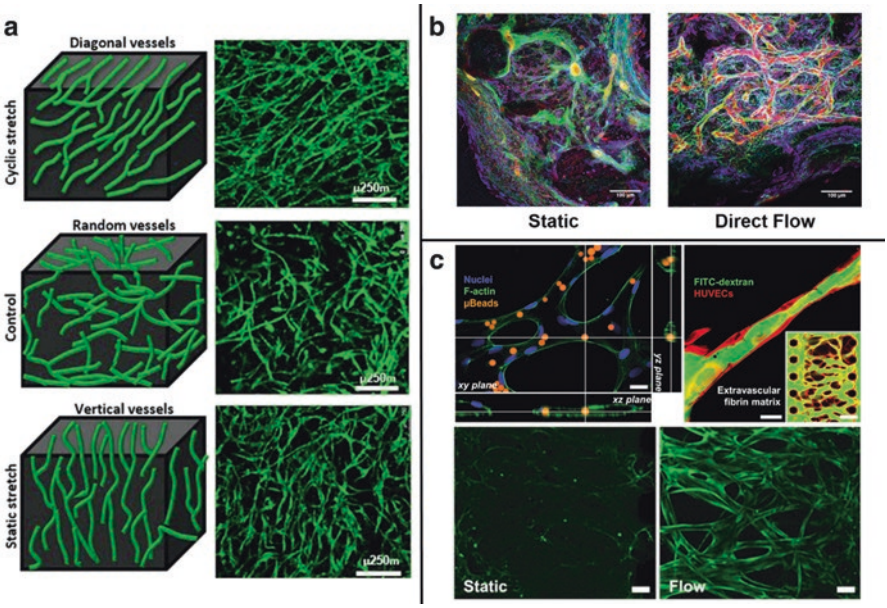

Fig. 2.3 External mechanical regulation of microvasculature by tensile forces and fluid shear stress. (**a**) The orientation of vessel-like structures upon exposure to various mechanical stretching regimens. Free-floating scaffolds (no external force) contained randomly orientated vessels, while cyclic-stretched scaffolds contained diagonal vessels and static-stretched scaffolds displayed vertically aligned vessels. Green, HUVEC-GFP cells (adapted, with permission, from Rosenfeld et al. [45]). Bar 250 μm. (**b**) Scaffold cross sections showing colocalization of collagens I and IV with EC structures. A cross section of a scaffold cultured for 7 days under static conditions and a scaffold cultured for 5 days under static conditions and then for 2 days under direct constant flow conditions (adapted, with permission, from Zohar and Blinder et al. [63]). ECs, red; collagen IV, green; and collagen I, blue. Bar, 100 μm. (**c**) A perfusable vascular network established in a microfluidic device, as demonstrated by perfusing FITC-dextran (top right) and fluorescent microbeads (top left). Endothelial cells responded to 1 h of luminal flow with an increase in nitric oxide (NO) synthesis, as demonstrated with DAF-FM DA fluorescence dye (green) (adapted, with permission, from Kim et al. [23]). Bar 50 μm

scaffold and subjected to static strain aligned parallel to the strain direction [45]. These results agree with another report of ECs and muscle cells embedded within a collagen-Matrigel 3D construct subjected to uniaxial stress [54]. In other work, Chang et al. printed and framed aligned microvessel fragments embedded within a collagen gel which was then subjected to uniaxial stress. While the pre-patterning disappeared during culture in vitro, the vasculature within the constrained constructs aligned in parallel to the stretch direction, and both maintained alignment during culture in vitro and induced invading vessels to align in the same direction post-implantation [7].

The reasons for these recorded alignments are debatable. Ingber hypothesized that local ECM thinning, caused by ECM turnover triggered by ECM modulators, increases ECM compliance, resulting in the production of tractional forces by the surrounding cells leading to local cell distortion. Consequently, increases in trans-

membrane receptor tension results in modification of cellular biochemistry, which eventually impacts cell growth and motility and overall network patterning [20]. Another work showed that tensile forces generated by ECs cause ECM alignment, leading to sprout alignment [26]. In contrast, Ceccarelli et al. claimed that vessel alignment is caused by changes in ECM stiffness (resulting from the applied strain) rather than ECM alignment [6]. Kaunas and Deguchi determined that cell alignment in response to cyclic stretch is guided by remodeling of cell adhesions and actin stress fibers, where myosin II has a major role in maintaining cellular homeostasis under mechanically stimulated environments [22].

Strain was also shown to influence cytokine secretion from stimulated vascularized constructs. Vascular endothelial growth factor (VEGF) and platelet-derived growth factor (PDGF)-ββ secretion levels increased under cyclic strain when compared to the unstimulated control group [45]. This correlates with another study that showed an increase in angiopoietin 2 (Ang-2) and PDGF-ββ secretion from ECs subjected to cyclic strain. Endothelial migration and sprout formation were both increased under cyclic strain conditions [62]. Static strain has been shown to induce vessel formation, without the need for addition of growth factors, and to stimulate muscle cells surrounding the ECs to secrete VEGF [54]. When subjecting tubular constructs composed of fibrin seeded with bovine aortic endothelial cells, to 7 days of 10% cyclic strain, the length and density of the forming sprouts were affected; stimulated constructs displayed wider, less branched sprouts compared to the unstimulated control group [14]. In addition, cyclic strain was shown to induce a short-term increase in gene expression of collagen type I, fibronectin, and elastin within human pluripotent stem cell-derived vSMCs. In the long term, uniaxial strain decreased ECM expression within mature vSMCs, whereas in less mature vSMCs, elastin upregulation was found [58]. Rho-associated kinase (ROCK) is shown to have an important role in vessel alignment and remodeling under cyclic stretch. The addition of ROCK inhibitor to a culture medium resulted in alignment suppression and a decrease in vessel sprouting. In contrast, inhibition of the receptor tyrosine kinase resulted in a decrease in vessel sprout density but had no effect on vessel alignment [59].

Stretch has also been utilized in the field of tissue engineering of large blood vessels. A special bioreactor was developed to enable application of cyclic biaxial stretch on polyglycolic acid (PGA) vessels seeded with SMCs, to mimic the stimulations in native arteries. Biaxial stretch-stimulated constructs formed elastic fibers and aligned collagen fibers, similar to those found in native arteries, with higher suture retention strength. Additionally, biaxial stretch stimulation was shown to increase the strength and compliance of the engineered blood vessels [19].

2.3.2 Fluid Shear Stress

Flow-induced shear stress is correlated with morphological changes in endothelial cells in vitro [17, 18, 39, 51] as well as with changes in gene, protein, and miRNA expression [15, 40]. In microfluidic devices [3, 13, 21, 55] and two-dimensional (2D) monolayer "flow-over" models [2, 56], flow-induced shear stress has been

shown to regulate and enhance angiogenic processes. Several groups have studied the effects of flow-induced shear stress on endothelial cells in vitro, using a parallel plate flow chamber [5, 18, 51]. This experimental setup is simple to model and provides better control over the applied shear stress. However, it does not closely mimic the 3D nature of interstitial flow, as the medium flows over the cells rather than through the scaffold. Moreover, endothelial cell response is limited as the system does not support 3D sprouting and network formation. In an alternative 3D model, consisting of 3D collagen and alginate gel plugs embedded with endothelial cells, direct flow simulation resulted in enhanced vascular morphogenesis and angiogenesis-related gene expression [29, 46]. Furthermore, in our recently published work, we demonstrated the effect of flow-induced shear stress on vascular formation and maturation in an implantable 3D engineered construct. Direct flow conditions resulted in a significant increase (>100%) in vessel network morphogenesis parameters, EC and ECM protein depth distribution, and colocalization incidence of alpha-smooth muscle actin (α-SMA) with endothelial vessel networks. These findings suggest that flow conditions promote 3D neovascularization and vascular network maturation in a 3D engineered tissue (Fig. 2.3b) [63]. In microfluidic-based platforms, luminal flow through a self-assembled microvasculature was applied to generate shear stress stimulation inside microvessels [23, 57]. The microvasculature patency was demonstrated by tracking flowing FITC-dextran and fluorescent microbeads (Fig. 2.3c) [23, 57]. The self-assembled microvessels possessed morphological and biochemical markers characteristic of natural blood vessels and exhibited strong barrier function, long-term stability, cytoskeleton rearrangements, and increased nitric oxide synthesis (Fig. 2.3c) [23].

However, the true nature of the effect of shear stress on vessel formation and behavior is still poorly understood [1]. Many molecular mechanisms and signal transduction pathways are suggested to bear shear-sensing or mechanotransductive roles. These mechanisms involve cell-matrix and cell-cell adhesion and junction molecules, membranous receptors and ion channels, the extra-membranous glycocalyx complex, and cytoskeleton proteins among others [1, 33, 44]. For example, shear stress has been shown to mediate changes in endothelial cell phenotype, by increasing RhoA (a cytoskeletal regulator) activity and promoting the formation of stress fibers [8]. Additionally, a direct connection between flow-induced shear stress and VEGF signaling during angiogenesis has been shown to be mediated by an endothelial cell-specific microRNA, called mir-126, which is regulated by the mechanosensitive zinc finger transcription factor klf2a [11, 40]. This microRNA has a pro-angiogenic function, by naturally repressing VEGF inhibitors ispred1 and pik3r2.

2.4 Conclusions and Future Perspectives

Creation of vascularized 3D engineered tissue requires a multidisciplinary approach. This involves integrating knowledge of vascular biology together with biomaterials engineering and microfluidic design, to recapitulate a microenvironment in which

cells can form mature blood vessels that can maintain tissue viability over time. The basic building blocks for blood vessel engineering are endothelial cells (ECs) and supporting cells. Both cell types can be isolated from different sources or differentiated from different pluripotent stem cells. In most of the discussed studies, ECs and supporting cells were co-cultured on different natural and synthetic biomaterials harnessed to establish a natural 3D environment supportive of vascularization processes. Both matrix stiffness and boundary constraint affect cell-induced contractile forces, which regulates cell-cell communication, vascular network structure, and directionality. External forces, in the form of fluid shear stress and tensile forces, induce vascular network formation and maturation and dictate vascular network structure and directionality. Although the effect of mechanical stimulation on vascularization is clearly demonstrated, the origin of the biological triggers remains in question. The impact of mechanical cues on vascularization can be explained by direct communication, via EC mechanotransduction sensors [1], or by indirect cues related to environmental changes such as neighbor cell responses, matrix deformation, and biochemical changes. A deeper understanding of the mechanisms through which ECs are affected by mechanical stimulation in 3D matrices may be achieved by correlating vascular morphogenesis with the levels of biosensors associated with relevant known biomechanical pathways. In addition, while the vast majority of studies focus on changes in vascular network morphology in response to mechanical cues, technical hurdles limit research on other critical functional parameters key to the success of engineered vessels, such as perfusability and barrier function. Perfusable vascular networks enable generation of both luminal shear stress and circumferential wall stress, both of which play critical roles in vascular mechanobiology [35]. Such physiologic stresses and strains exert vasoprotective actions, mediated by nitric oxide, and provide a homeostatic oxidative balance for further vascular remodeling and maturation [35]. It is very important to clarify that the developmental stage of the vascular network largely impacts endothelial cell responses to mechanical stimulation. For example, during vasculogenesis (when vascular networks are not fully established), ECs can respond to external shear stress by accelerating vascular network arrangement. This pro-angiogenic role of shear stress may be critical in cases of injury, when the tissue is undergoing a wound healing process. Conversely to anti-angiogenic role in vascular network remodeling, maturation and quiescence processes occur under homeostasis conditions regulated by luminal shear stress and circumferential wall stress.

Recently developed experimental approaches, based on evolving 3D microfabrication techniques, may open up new strategies for exploring the impact of biomechanical triggers on vascularization under more physiologically relevant conditions. Moreover, the control and repeatability of patterning vascular and perivascular cells in 3D engineered tissue will allow for a higher degree of regulation over the initial organization of vascular structures and, therefore, will enable to study cell-cell and cell-matrix mechanical interactions in more accurate and controlled systems. Such high levels of accuracy will enhance computational estimations of local mechanical cues, which can be validated by mechanical biosensor-based feedback signals. Conclusively, integration of high-precision fabrication techniques with advanced

computational models and utilization of biomechanical sensors may provide a better understanding of the means through which mechanical forces regulate the different stages of vascularization in 3D engineered tissues.

References

1. Ando, J., & Yamamoto, K. (2009). Vascular mechanobiology: Endothelial cell responses to fluid shear stress. *Circulation Journal, 73*, 1983–1992.
2. Anisi, F., Salehi-Nik, N., Amoabediny, G., Pouran, B., Haghighipour, N., & Zandieh-Doulabi, B. (2014). Applying shear stress to endothelial cells in a new perfusion chamber: Hydrodynamic analysis. *Journal of Artificial Organs, 17*, 329–336.
3. Bellan, L. M., Singh, S. P., Henderson, P. W., Porri, T. J., Craighead, H. G., & Spector, J. A. (2009). Fabrication of an artificial 3-dimensional vascular network using sacrificial sugar structures. *Soft Matter, 5*, 1354.
4. Beningo, K. A., Dembo, M., Kaverina, I., Small, J. V., & Wang, Y. L. (2001). Nascent focal adhesions are responsible for the generation of strong propulsive forces in migrating fibroblasts. *The Journal of Cell Biology, 153*, 881–888.
5. Brown, A., Burke, G., & Meenan, B. J. (2011). Modeling of shear stress experienced by endothelial cells cultured on microstructured polymer substrates in a parallel plate flow chamber. *Biotechnology and Bioengineering, 108*, 1148–1158.
6. Ceccarelli, J., Cheng, A., & Putnam, A. J. (2012). Mechanical strain controls endothelial patterning during angiogenic sprouting. *Cellular and Molecular Bioengineering, 5*, 463–473.
7. Chang, C. C., Krishnan, L., Nunes, S. S., Church, K. H., Edgar, L. T., Boland, E. D., et al. (2012). Determinants of microvascular network topologies in implanted neovasculatures. *Arteriosclerosis, Thrombosis, and Vascular Biology, 32*, 5–14.
8. De Smet, F., Segura, I., De Bock, K., Hohensinner, P. J., & Carmeliet, P. (2009). Mechanisms of vessel branching filopodia on endothelial tip cells lead the way. *Arteriosclerosis, Thrombosis, and Vascular Biology, 29*, 639–649.
9. Edgar, L. T., Underwood, C. J., Guilkey, J. E., Hoying, J. B., & Weiss, J. A. (2014). Extracellular matrix density regulates the rate of neovessel growth and branching in sprouting angiogenesis. *PLoS One, 9*, e85178.
10. Engler, A. J., Sen, S., Sweeney, H. L., & Discher, D. E. (2006). Matrix elasticity directs stem cell lineage specification. *Cell, 126*, 677–689.
11. Fish, J. E., Santoro, M. M., Morton, S. U., Yu, S., Yeh, R.-F., Wythe, J. D., et al. (2008). miR-126 regulates angiogenic signaling and vascular integrity. Dev. *Cell, 15*, 272–284.
12. Francis-Sedlak, M. E., Moya, M. L., Huang, J.-J., Lucas, S. A., Chandrasekharan, N., Larson, J. C., et al. (2010). Collagen glycation alters neovascularization in vitro and in vivo. *Microvascular Research, 80*, 3–9.
13. Galie, P. A., Nguyen, D.-H. T., Choi, C. K., Cohen, D. M., Janmey, P. A., & Chen, C. S. (2014). Fluid shear stress threshold regulates angiogenic sprouting. *Proceedings of the National Academy of Sciences of the United States of America, 111*, 7968–7973.
14. Gassman, A. A., Kuprys, T., Ucuzian, A. A., Brey, E., Matsumura, A., Pang, Y., et al. (2011). Three-dimensional 10% cyclic strain reduces bovine aortic endothelial cell angiogenic sprout length and augments tubulogenesis in tubular fibrin hydrogels. *Journal of Tissue Engineering and Regenerative Medicine, 5*, 375–383.
15. Gee, E., Milkiewicz, M., & Haas, T. L. (2010). p38 MAPK activity is stimulated by vascular endothelial growth factor receptor 2 activation and is essential for shear stress-induced angiogenesis. *Journal of Cellular Physiology, 222*, 120–126.

16. Ghajar, C. M., Chen, X., Harris, J. W., Suresh, V., Hughes, C. C. W., Jeon, N. L., et al. (2008). The effect of matrix density on the regulation of 3-D capillary morphogenesis. *Biophysical Journal, 94*, 1930–1941.
17. Helm, C.-L. E., Zisch, A., & Swartz, M. A. (2007). Engineered blood and lymphatic capillaries in 3-D VEGF-fibrin-collagen matrices with interstitial flow. *Biotechnology and Bioengineering, 96*, 167–176.
18. Hernández Vera, R., Genové, E., Alvarez, L., Borrós, S., Kamm, R., Lauffenburger, D., et al. (2009). Interstitial fluid flow intensity modulates endothelial sprouting in restricted Src-activated cell clusters during capillary morphogenesis. *Tissue Engineering. Part A, 15*, 175–185.
19. Huang, A. H., Balestrini, J. L., Udelsman, B. V., Zhou, K. C., Zhao, L., Ferruzzi, J., et al. (2016). Biaxial stretch improves elastic fiber maturation, collagen arrangement, and mechanical properties in engineered arteries. *Tissue Engineering. Part C, Methods, 22*, 524–533.
20. Ingber, D. E. (2002). Mechanical signaling and the cellular response to extracellular matrix in angiogenesis and cardiovascular physiology. *Circulation Research, 91*, 877–887.
21. Jeon, J. S., Bersini, S., Whisler, J. A., Chen, M. B., Dubini, G., Charest, J. L., et al. (2014). Generation of 3D functional microvascular networks with human mesenchymal stem cells in microfluidic systems. *Integrative Biology, 6*, 555–563.
22. Kaunas, R., & Deguchi, S. (2016). *Cyclic stretch-induced reorganization of stress fibers in endothelial cells. Vascular engineering* (pp. 99–110). Tokyo: Springer.
23. Kim, S., Lee, H., Chung, M., & Jeon, N. L. (2013). Engineering of functional, perfusable 3D microvascular networks on a chip. *Lab on a Chip, 13*, 1489–1500.
24. Kniazeva, E., & Putnam, A. J. (2009). Endothelial cell traction and ECM density influence both capillary morphogenesis and maintenance in 3-D. *American Journal of Physiology. Cell Physiology, 297*, C179–C187.
25. Kniazeva, E., Weidling, J. W., Singh, R., Botvinick, E. L., Digman, M. A., Gratton, E., et al. (2012). Quantification of local matrix deformations and mechanical properties during capillary morphogenesis in 3D. *Integrative Biology, 4*, 431–439.
26. Korff, T., & Augustin, H. G. (1999). Tensional forces in fibrillar extracellular matrices control directional capillary sprouting. *Journal of Cell Science, 112*(Pt 19), 3249–3258.
27. Krishnan, L., Underwood, C. J., Maas, S., Ellis, B. J., Kode, T. C., Hoying, J. B., et al. (2008). Effect of mechanical boundary conditions on orientation of angiogenic microvessels. *Cardiovascular Research, 78*, 324–332.
28. Krishnan, R., Klumpers, D. D., Park, C. Y., Rajendran, K., Trepat, X., van Bezu, J., et al. (2011). Substrate stiffening promotes endothelial monolayer disruption through enhanced physical forces. *American Journal of Physiology. Cell Physiology, 300*, C146–C154.
29. Lee, E. J., & Niklason, L. E. (2010). A novel flow bioreactor for in vitro microvascularization. *Tissue Engineering. Part C, Methods, 16*, 1191–1200.
30. Lee, P.-F., Yeh, A. T., & Bayless, K. J. (2009). Nonlinear optical microscopy reveals invading endothelial cells anisotropically alter three-dimensional collagen matrices. *Experimental Cell Research, 315*, 396–410.
31. Lesman, A., Koffler, J., Atlas, R., Blinder, Y. J., Kam, Z., & Levenberg, S. (2011). Engineering vessel-like networks within multicellular fibrin-based constructs. *Biomaterials, 32*, 7856–7869.
32. Lesman, A., Notbohm, J., Tirrell, D. A., & Ravichandran, G. (2014). Contractile forces regulate cell division in three-dimensional environments. *The Journal of Cell Biology, 205*, 155–162.
33. Li, Y.-S. J., Haga, J. H., & Chien, S. (2005). Molecular basis of the effects of shear stress on vascular endothelial cells. *Journal of Biomechanics, 38*, 1949–1971.
34. Liu, S. Q. (1998). Influence of tensile strain on smooth muscle cell orientation in rat blood vessels. *Journal of Biomechanical Engineering, 120*, 313–320.
35. Lu, D., & Kassab, G. S. (2011). Role of shear stress and stretch in vascular mechanobiology. *Journal of the Royal Society Interface, 8*, 1379–1385.

36. Mason, B. N., Starchenko, A., Williams, R. M., Bonassar, L. J., & Reinhart-King, C. A. (2013). Tuning three-dimensional collagen matrix stiffness independently of collagen concentration modulates endothelial cell behavior. *Acta Biomaterialia, 9*, 4635–4644.
37. Matsumoto, T., Yung, Y. C., Fischbach, C., Kong, H. J., Nakaoka, R., & Mooney, D. J. (2007). Mechanical strain regulates endothelial cell patterning in vitro. *Tissue Engineering, 13*, 207–217.
38. Munevar, S., Wang, Y., & Dembo, M. (2001). Traction force microscopy of migrating normal and H-ras transformed 3T3 fibroblasts. *Biophysical Journal, 80*, 1744–1757.
39. Ng, C. P., Helm, C.-L. E., & Swartz, M. A. (2004). Interstitial flow differentially stimulates blood and lymphatic endothelial cell morphogenesis in vitro. *Microvascular Research, 68*, 258–264.
40. Nicoli, S., Standley, C., Walker, P., Hurlstone, A., Fogarty, K. E., & Lawson, N. D. (2010). MicroRNA-mediated integration of haemodynamics and Vegf signalling during angiogenesis. *Nature, 464*, 1196–1200.
41. Pelham Jr., R. J., & Yl, W. (1997). Cell locomotion and focal adhesions are regulated by substrate flexibility. *Proceedings of the National Academy of Sciences of the United States of America, 94*, 13661–13665.
42. Reinhart-King, C. A., Dembo, M., & Hammer, D. A. (2003). Endothelial cell traction forces on RGD-derivatized polyacrylamide substrata. *Langmuir, 19*, 1573–1579.
43. Reinhart-King, C. A., Dembo, M., & Hammer, D. A. (2008). Cell-cell mechanical communication through compliant substrates. *Biophysical Journal, 95*, 6044–6051.
44. Resnick, N., Yahav, H., Shay-Salit, A., Shushy, M., Schubert, S., Zilberman, L. C. M., et al. (2003). Fluid shear stress and the vascular endothelium: For better and for worse. *Progress in Biophysics and Molecular Biology, 81*, 177–199.
45. Rosenfeld, D., Landau, S., Shandalov, Y., Raindel, N., Freiman, A., Shor, E., et al. (2016). Morphogenesis of 3D vascular networks is regulated by tensile forces. *Proceedings of the National Academy of Sciences of the United States of America, 113*, 3215–3220.
46. Rotenberg, M. Y., Ruvinov, E., Armoza, A., & Cohen, S. (2012). A multi-shear perfusion bioreactor for investigating shear stress effects in endothelial cell constructs. *Lab on a Chip, 12*, 2696–2703.
47. Santos, L., Fuhrmann, G., Juenet, M., Amdursky, N., Horejs, C.-M., Campagnolo, P., et al. (2015). Extracellular stiffness modulates the expression of functional proteins and growth factors in endothelial cells. *Advanced Healthcare Materials, 4*(14), 2056–2063.
48. Shamloo, A., & Heilshorn, S. C. (2010). Matrix density mediates polarization and lumen formation of endothelial sprouts in VEGF gradients. *Lab on a Chip, 10*, 3061–3068.
49. Steward Jr., R., Tambe, D., Hardin, C. C., Krishnan, R., & Fredberg, J. J. (2015). Fluid shear, intercellular stress, and endothelial cell alignment. *American Journal of Physiology. Cell Physiology, 308*, C657–C664.
50. Sun, J., Jamilpour, N., Wang, F.-Y., & Wong, P. K. (2014). Geometric control of capillary architecture via cell-matrix mechanical interactions. *Biomaterials, 35*, 3273–3280.
51. Ueda, A., Koga, M., Ikeda, M., Kudo, S., & Tanishita, K. (2004). Effect of shear stress on microvessel network formation of endothelial cells with in vitro three-dimensional model. *American Journal of Physiology. Heart and Circulatory Physiology, 287*, H994–H1002.
52. Underwood, C. J., Edgar, L. T., Hoying, J. B., & Weiss, J. A. (2014). Cell-generated traction forces and the resulting matrix deformation modulate microvascular alignment and growth during angiogenesis. *American Journal of Physiology. Heart and Circulatory Physiology, 307*, H152–H164.
53. Vailhé, B., Ronot, X., Tracqui, P., Usson, Y., & Tranqui, L. (1997). In vitro angiogenesis is modulated by the mechanical properties of fibrin gels and is related to αvβ3 integrin localization. *In Vitro Cellular & Developmental Biology – Animal, 33*, 763–773.
54. van der Schaft, D. W. J., van Spreeuwel, A. C. C., van Assen, H. C., & Baaijens, F. P. T. (2011). Mechanoregulation of vascularization in aligned tissue-engineered muscle: A role for vascular endothelial growth factor. *Tissue Engineering. Part A, 17*, 2857–2865.

55. Vickerman, V., & Kamm, R. D. (2012). Mechanism of a flow-gated angiogenesis switch: Early signaling events at cell--matrix and cell--cell junctions. *Integrative Biology, 4*, 863–874.
56. Walshe, T. E., dela Paz, N. G., & D'Amore, P. A. (2013). The role of shear-induced transforming growth factor-signaling in the endothelium. *Arteriosclerosis, Thrombosis, and Vascular Biology, 33*, 2608–2617.
57. Wang, X., Phan, D. T. T., Sobrino, A., George, S. C., Hughes, C. C. W., & Lee, A. P. (2016). Engineering anastomosis between living capillary networks and endothelial cell-lined microfluidic channels. *Lab on a Chip, 16*, 282–290.
58. Wanjare, M., Agarwal, N., & Gerecht, S. (2015). Biomechanical strain induces elastin and collagen production in human pluripotent stem cell-derived vascular smooth muscle cells. *American Journal of Physiology. Cell Physiology, 309*, C271–C281.
59. Wilkins, J. R., Pike, D. B., Gibson, C. C., Li, L., & Shiu, Y.-T. (2015). The interplay of cyclic stretch and vascular endothelial growth factor in regulating the initial steps for angiogenesis. *Biotechnology Progress, 31*, 248–257.
60. Yamamura, N., Sudo, R., Ikeda, M., & Tanishita, K. (2007). Effects of the mechanical properties of collagen gel on the in vitro formation of microvessel networks by endothelial cells. *Tissue Engineering, 13*, 1443–1453.
61. Yeung, T., Georges, P. C., Flanagan, L. A., Marg, B., Ortiz, M., Funaki, M., et al. (2005). Effects of substrate stiffness on cell morphology, cytoskeletal structure, and adhesion. *Cell Motility and the Cytoskeleton, 60*, 24–34.
62. Yung, Y. C., Chae, J., Buehler, M. J., Hunter, C. P., & Mooney, D. J. (2009). Cyclic tensile strain triggers a sequence of autocrine and paracrine signaling to regulate angiogenic sprouting in human vascular cells. *Proceedings of the National Academy of Sciences of the United States of America, 106*, 15279–15284.
63. Zohar, B., Blinder, Y., Mooney, D. J., & Levenberg, S. (2018). Flow-induced vascular network formation and maturation in three-dimensional engineered tissue. *ACS Biomaterials Science & Engineering, 4*(4), 1265–1271.

Chapter 3
Physiological and Pathological Vascular Aging

Patrícia R. Pitrez, Helena R. Aires, Inês Tomé, Rita Sá Ferreira, and Lino Ferreira

3.1 Introduction

It is expected that by 2030 the number of people aged 60 years and over will grow by 56% [121]. Aging is recognized as the key factor in most chronic diseases, including neurodegenerative, cerebrovascular, and cardiovascular disorders, through the accumulation of biological changes over time [84]. Thus, age-related biological changes have emerged as a serious issue, with increased socioeconomic and healthcare burdens. Several hallmarks of aging in mammals have been identified including telomere attrition, genomic instability, epigenetic modifications, loss of proteostasis, cellular senescence, mitochondrial dysfunction, altered intercellular communication, deregulated nutrient sensing, and stem cell exhaustion [55, 67, 93].

A major trigger for cellular aging and senescence is telomere shortening [3, 67]. Indeed, a cell's finite replication capacity is promoted by telomere shortening [52]. Telomeres are repeats of highly conserved nucleotide sequences that compose the chromosome ends to prevent chromosome fusion [52]. Mammalian cells do not express telomerase, the enzyme responsible for telomere replication, and because the enzyme is consumed at each cell cycle, telomeres become shorter until they cannot prevent a DNA damage response [20, 127]. Another trigger for normal aging is

P. R. Pitrez · H. R. Aires · I. Tomé
Faculty of Medicine, University of Coimbra, Coimbra, Portugal
e-mail: pitrezpatricia@uc.pt

R. S. Ferreira
Center of Neurosciences and Cell Biology, University of Coimbra, Coimbra, Portugal

L. Ferreira (✉)
Faculty of Medicine, University of Coimbra, Coimbra, Portugal

Center of Neurosciences and Cell Biology, University of Coimbra, Coimbra, Portugal
e-mail: lino@uc-biotech.pt

S. Gerecht (ed.), *Biophysical Regulation of Vascular Differentiation and Assembly*, Biological and Medical Physics, Biomedical Engineering,
https://doi.org/10.1007/978-3-319-99319-5_3

related to genomic instability. The accumulation of DNA damage over time is the result of environmental factors (e.g., chemicals, UV/IR radiation) as well as endogenous agents (e.g., DNA replication errors, reactive oxygen species). DNA damage accumulates when intrinsic mechanisms cannot eliminate these dysfunctional cells, and thus tissue and organism homeostasis become compromised [67]. However, more than being genetically predetermined, organismal lifespan is also epigenetically modified. Exposure to environmental stresses (e.g., smoking, pollution, sedentary lifestyles) during an individual's lifetime may induce epigenetic alterations that can compromise normal gene expression without altering the underlying DNA sequence [71]. These exogenous factors are major players in premature defects in mitochondrial functionality, insulin signaling, endothelial homeostasis, and redox balance, promoting early senescent features [27]. To overcome intracellular damage that accumulates with age, a quality control network, which maintains correctly folded proteins and degrades unfolded or misfolded proteins, is fundamental. This maintenance system, known as proteostasis, is supported by the heat shock family of proteins (namely, chaperones) and by the proteolytic systems ubiquitin-proteasome and lysosome-autophagy, which determine cell fate [56]. However, protein homeostasis declines with age, promoting proteotoxicity that further leads to the development of age-related proteinopathies [101]. Another trigger of normal aging is cell senescence. Cellular senescence acts as an anticancer mechanism through the activation of tumor-suppressor mechanisms in response to oncogenic stimuli, including the p53/p21 and $p16^{INK4a}$/pRB pathways [22]. However, it was recently demonstrated that eliminating senescent cells from a mice model not only increased longevity but also improved overall health, thus suggesting that senescent cells are major drivers of aging [5, 6].

This chapter reviews the physiological and pathological aging process of vessels in Hutchinson-Gilford progeria syndrome, a disease characterized by premature aging in children (focusing on the biophysical and cellular changes that occur in the vessels during aging). Many aspects observed in physiological aging are shared by pathological aging. Therefore, the use of accelerated aging models may facilitate the study of vascular aging. Finally, we review the latest efforts to create suitable in vitro models to study the process of aging in the vascular system.

3.2 Vascular Aging: General Insights

Several molecular mechanisms are implicated in vascular aging including sirtuins, telomere shortening and telomerase, progerin, klotho gene, and JunD, among others [59]. Vascular aging is characterized by collagen deposition, vascular remodeling, interstitial fibrosis, and inflammation which further leads to wall thickening, arterial stiffening, and vessel dilatation [27].

Vascular aging is evaluated in multiple ways. Vascular stiffness increases with aging and is easily monitored by pulse wave velocity [60]. High levels of C-reactive protein, an inflammatory marker, and low levels of adiponectin, an anti-atherogenic

factor, are related with atherogenesis and consequently with vascular aging [119]. Lymphocyte telomere length, easily accessed through peripheral blood, may be used as a biomarker of vessel aging since it is related with stem cell and endothelial progenitor cells (EPCs) telomere length [34]. Inflammatory markers such as the nuclear factor-kappa B (NF-$_{K}$B) and insulin growth factor-1 (IGF-1) maybe also be used as biomarkers of vascular aging. Other biomarkers are strictly linked with senescence and can reflect cell cycle arrest (e.g., p53, p21, p16^{INK4a}), absence of cellular proliferation (e.g., lack of BrdU incorporation, Ki67), activation of double-stranded brakes (e.g., H2AX, p53BP1 foci), expression of inflammatory factors (e.g., interleukin-6 and interleukin-8), cell senescence (SA-β-gal), loss of lamin B1, and activation of pathways that regulate the secretory phenotype (e.g., p-p65 or p-p38) [20, 32, 40, 95].

3.3 Physiological Vascular Aging

Vascular aging is characterized by biophysical changes. There is a fatigue of the vessels resulting from sustained mechanical stress-associated pressure caused by blood flow. The extracellular matrix (ECM) becomes stiffer, losing elasticity and, therefore, the ability to stretch [79]. In addition, endothelial cells (ECs) become dysfunctional as result of a pro-inflammatory environment and increased oxidative stress [116].

3.3.1 Altered ECM Remodeling

The vessel wall is mainly composed of an ECM which provides structural support and defines the vessel's mechanical properties. By interacting with vascular cells, the ECM is able to act as a signal transductor to modulate cell proliferation, survival, differentiation, and gene expression. The major components of the vascular ECM are collagen and elastin, complemented by other molecules including fibronectin, microfibrils, proteoglycans, and glycoproteins [136]. Different sections of the blood vessel wall have different compositions of ECM proteins [129]. In the tunica intima, ECs lined the vessel luminal surface, attaching to a basement membrane containing mainly laminin, type IV collagen, nitrogen, perlecan, types XV and VIII collagens, and fibronectin [9, 136]. Between the intima and the tunica media, arteries and veins are supported by the internal elastic lamina [31, 129]. In the tunica media, vascular smooth muscle cells (SMCs) and elastins are the major components. Elastin forms concentric fenestrated sheets, intercalated with collagen fibers and proteoglycans, which connects with SMCs [85]. Elastin is an elastic fiber produced by SMCs, presenting low tensile strength that contributes to the elasticity of the vessels and to store the recoiling energy, contributing to vessel compliancy [136]. The percentage of lamellar units present in the vessel varies with the tensile

strength that the vessel is subjected to, being higher in the larger and more proximal vessels that withstand higher wall tension [11]. Finally, tunica adventitia, the outside layer of the vessels, is rich in collagen type I and III. Collagen provides high tensile strength, which prevents wall rupture due to blood pressure. The production of the adventitia proteins is mainly done by fibroblasts [19, 136].

In aged blood vessels, the endothelium, the SMCs, and the ECM suffer structural and functional changes that lead to arterial stiffness, fibrosis, and endothelial dysfunction [88]. The ECM in the vascular wall becomes thicker and stiffer with aging, due to several factors including (1) increase of the collagen to elastin ratio, (2) impairment of the balance between ECM degradation and production, and (3) dysfunction of newly synthesized ECM [54]. Collagens and elastin are the major components of the blood vessel's ECM and the absolute and relative quantities of these proteins define the biomechanical properties of the vessels [100]. Collagen provides the tensile strength while elastin the elastic properties for the vessels [117]. Elastin represents approximately 50% of the arterial wall dry weight, and it is mainly produced by SMCs and fibroblasts, which have a low turnover rate during their life [18].

As mentioned above, through aging, changes in the composition and structure of collagen, as well as the ratio between elastin to collagen, contribute to a decrease in the total arterial compliance [118]. An increase in the content of collagen types I and III across the vessel wall [57] occurs during aging, namely, in the adventitia, causing the stiffening of the vessels [39]. In addition, increased cross-linking between collagen fibers leads to more insoluble fibers and, thus, less availability for enzymatic degradation, with an increased tensile strength [41]. The cross-linking process may be driven by enzymes, such as lysyl oxidases, which promote the formation of inter- and intramolecular cross-links [96] or by the accumulation of advanced glycation end products (AGEs) [43]. AGEs are formed by non-enzymatic glycation of proteins and lipids and their production is accelerated with aging. Collagen and elastin, present in the vessels, have a low turnover rate and become more susceptible to glycation [78, 104]. With aging, the elastin content of blood vessels decreases, thereby increasing the collagen to elastin ratio [117]. Moreover, elastin suffers structural changes, due to the repeated mechanical forces during stretches and relaxation in the cardiac cycle, as well as increased oxidative stress that concomitantly contributes to fragmentation and rupture of elastin fibers [33]. Elastin cross-linking with AGEs also contributes to an increase in fragility and fragmentation of this protein [107].

Another feature, which contributes to ECM remodeling with aging, is the imbalance between the synthesis and degradation of ECM components. Matrix metalloproteinases (MMPs) are endopeptidases capable of degrading ECM components [14]. With age, an increase in the activity of MMP-2/MMP-7/MMP-9/MMP-14 in the aortic walls of rodents, nonhuman primates, and humans has been reported [132]. Increases in MMP-2 activity in the aorta are associated with elastin fragmentation [77]. Furthermore, MMP-2 expression leads to the stimulation of transforming growth factor (TGF-β1) signaling; increased production of collagens I, II, and III by vascular SMCs; and increased secretion of fibronectin [132]. Activation of MMP-9, by pro-hypertensive factors, shear stress, pressure, and TGF-β1/SMAD

signaling, is associated with increased oxidative stress, inflammation, fibrosis, and DNA damage [91]. Altogether, changes in the expression of MMPs with aging contribute to the increased fibrosis and stiffening of the vessels.

Vascular calcification is a marker of vascular aging. It typically occurs after deposition of calcium phosphate in distinct layers of the arteries. This is an active process, similar to bone formation, which involves the differentiation of SMCs into "osteoblast-like" cells that present a secretory phenotype [66]. SMCs synthesize proteins such as alkaline phosphatase, osteopontin, osteocalcin, and collagen. Inflammation and activation of the NF-κB pathway play the main role in triggering SMCs into the osteogenic phenotype, by increasing levels of IL-6, tumor necrosis factor-alpha (TNF-α), MMP-2, MMP-9, and cathepsin S [15, 21]. The fragmentation of elastin, described above, also contributes to SMCs differentiation and the deposition of calcium [33]. The age-associated cell senescence of SMCs and their secretory phenotype, associated with activation of the NF-κB process, contribute to the differentiation of SMCs into the osteogenic phenotype [82]. Calcification in the intima, present in atherosclerosis, reduces the lumen vessel diameter and causes arterial dysfunction. In the media, calcification is concentric, with diffuse mineral deposits and promotes an increase in the arterial stiffness [66].

3.3.2 Enhanced Fibrosis

Fibrosis is defined as the formation of excessive fibrous tissue, due to increased deposition of ECM components [135]. It is an adaptive response that gradually extends to the surrounding spaces and leads to increased arterial stiffening. Aging-associated factors, such as reduced nitric oxide (NO) availability, oxidative stress, calcification, ECM remodeling, and a pro-inflammatory environment, all contribute to increased fibrosis. Pro-hypertensive factors, such as angiotensin II (Ang II), endothelin-1 (ET-1), and aldosterone, induce the activation of the signaling pathways p38 MAPK and TGF-β/SMAD, further promoting synthesis of fibrotic tissue [51, 134]. Another factor that induces fibrosis is transglutaminase (TG2), a protein that interacts with the ECM, which regulates fibroblast activity and ECM organization. The deregulation of the activity of TG2 leads to increased stiffness of the vessels [89]. Higher levels of MMP-2 and MMP-9 also contribute to the release of TGF-β1, resulting in higher ECM deposition [130].

3.3.3 Vascular Cell Dysfunction

Impairment in EC vasodilatation capacity is one of the first signs of vessel aging [106]. The main agents responsible for vasodilatation are endothelium-derived hyperpolarizing factor (EDHF), prostacyclin1 and NO [35]. EDHF contributes to endothelial vasodilatation and declines with age [26]. Prostacyclin is a cyclooxygenase

(COX)-derived vasodilator, and its contribution to endothelial vasodilatation is lost with age, in humans [105]. On the other hand, the contribution of COX-derived contractile factors, such as thromboxane A_2, increases with age [113, 125]. NO is synthesized by endothelial nitric oxide synthase (eNOS), whose activity is decreased with aging, leading to reduced availability of NO and decreased endothelial vasodilatation. This lowered availability of NO is also associated with increased reactive oxygen species (ROS) production and consequent excessive oxidative stress, by modulating the production of superoxide in human vessels [45]. Moreover, NO reacts with superoxide to produce peroxynitrite, a highly reactive specie that is cytotoxic and contributes to vascular aging [123].

One hallmark of vascular aging is EC dysfunction, triggered by chronic oxidative stress [99]. An increase in oxidative stress on aged vessels has been observed both in animal models and in humans [48, 120]. Part of this effect is mediated by ROS. An imbalance in ROS production can lead to the accumulation of damaged or misfolded proteins, DNA mutations, inflammation [122], and EC senescence [70]. The main sources of ROS that lead to oxidative stress in aged vessels are NADPH oxidases, xanthine oxidase, uncoupled NO synthase, and the mitochondrial respiratory chain [35]. NADPH oxidases are involved in the generation of superoxide and are upregulated in the presence of cardiovascular risk factors, including aging [17, 76]. Xanthine oxidase is an enzyme capable of producing ROS, and its accumulation in the aortic wall has been associated with aging [83]. The synthesis of NO by nitric oxide synthase is done by catalyzing the conversion of L-arginine to L-citrulline. For the reaction to occur, dimerization of the enzyme L-arginine and the cofactor tetrahydrobiopterin (BH_4) have to be present. Uncoupling of NO synthase happens when L-arginine and BH_4 are not present. When this occurs, it has been described that there is an increase in ROS production [112]. The mitochondria are primarily responsible for ROS production, through the respiratory chain [124]. With age, there is an accumulation of impaired mitochondria that leads to oxidative stress and contributes to vascular aging and impaired vasodilatation.

EC dysfunction triggered by inflammation is another hallmark of vascular aging [99]. In aged individuals, there is an increase of pro-inflammatory factors such as TNF-α, IL-1β, IL-6, CRP, Ang II, MMPs, calpain-1, monocyte chemoattractant protein-1 (MCP-1), interferon gamma (IFN-γ), and intercellular adhesion molecules (ICAM) [61, 131]. Upregulation of TNF-α has been described and associated with oxidative stress, endothelial dysfunction, apoptosis, and impairment of endothelium dilatation. The pro-inflammatory cytokine IL-6 is also associated with vascular diseases in aging. The inflammatory response in vascular cells is mainly mediated by the transcription factor NF-κB. When activated, it promotes the transcription of pro-inflammatory cytokines that are shown to be highly active and related with increased oxidative stress and endothelial dysfunction [1, 61].

Another hallmark of vascular aging is EC dysfunction triggered by senescence. The loss of the replicative capacity of ECs impairs the response to injury and the repair of dysfunctional endothelium [42]. The senescent phenotype in ECs can be due to replicative senescence or stress-induced premature senescence [42]. Replicative senescence occurs due to the limited potential of cell division and is

characterized by the shortening of telomere size and loss of the proliferative capacity of ECs [80]. Stress-induced premature senescence occurs after cell exposure to stressful conditions such as altered glucose levels, oxidized low-density lipoprotein, homocysteine, ceramide, Ang II, elevated blood pressure, increased ROS levels, and inflammation [115]. Senescent ECs display alterations in gene transcription and protein profile expression. Levels of transcription of IL-1α, IL-8, fibronectin, ICAM-1, p1, p53, and iNOS are shown to be upregulated, while eNOS is downregulated. Protein degradation of endothelial differentiation-related factor-1 (EDRF-1) and cyclin-dependent kinase 2 (CDK2) are increased in senescent ECs [49, 73, 80].

3.3.4 Altered Response of Vascular Cells to Flow Shear Stress

Blood flow in vessels creates a parallel friction force in the endothelium, called fluid shear stress, which influences the phenotype of ECs. ECs sense the shear stress and dynamically respond, by converting mechanical forces into intracellular signals [8]. This process is carried out by mechanotransducers such as glycocalyx, ion channels, G proteins, adhesion molecules, and the cytoskeleton [8]. The prolonged exposition to blood flow causes structural changes, including elongation of ECs in the direction of the blood flow, and the orientation of the actin cytoskeleton, microtubules, and intermediate filaments in the flow direction [62]. During aging, there is an altered response of ECs to shear stress, which can contribute to the development of atherosclerotic plaques [24]. As mentioned above, one of the main contributors for endothelial dysfunction is the reduction of NO availability due to the reduced activity of eNOS. Activation of eNOS can be carried out by fluid shear stress created by the blood flow in the endothelial layer [69]. In aged vessels, the reduced availability of NO can be associated with the lack of response of ECs to the shear stress and consequent decrease in NO production. The inflammatory process is also influenced by shear stress. During aging low levels of shear stress can promote arterial inflammation, through the induction of NK-κB expression in ECs and can contribute to the formation of atherosclerotic plaques [29]. An altered response of SMCs to shear stress also occurs in aged cells. In this case, increased aortic intraluminal pressure causes activation of ERK1/2, p38 MAPK, and JNK proteins [98].

3.4 Pathological Vascular Aging: The Example of Hutchinson-Gilford Progeria Syndrome (HGPS)

HGPS is a rare disease in which patients exhibit accelerated aging-related symptoms such as alopecia, osteoporosis, subcutaneous fat loss, lipodystrophy, and skin wrinkling [67]. Cardiovascular complications are the most devastating symptoms of this syndrome. Children develop progressive arteriosclerosis of the coronary and

cerebrovascular arteries, eventually leading to fatal myocardial infarction or stroke at a mean age of 13 years old [67]. Classical HGPS is caused by a "de novo" point mutation in the LMNA gene, leading to the production of an aberrant protein named progerin [36]. Progerin accumulates in the nuclear membrane, prompting nuclear morphology abnormalities, misregulated gene expression, loss of peripheral heterochromatin, mitochondrial dysfunction, defects in DNA repair, alternate splicing, epigenetic changes, accelerated telomere shortening, and premature senescence [44]. The same molecular mechanisms occur during normal aging, supporting the notion that HGPS mimics at least some aspects of physiological aging (Fig. 3.1). This can be partially explained by the fact that levels of progerin increase during physiological aging, although not at a same degree as in HGPS-affected cells [103].

Although not all features of physiological aging are manifested in this syndrome, from a cardiovascular standpoint, the case reports seem to be very consistent with a premature aging phenotype [7]. In fact, it has been shown that progerin accumulates mainly in the nucleus of vascular cells such as ECs, SMCs, and fibroblasts. It has also been shown that progerin is widely present in the arterial walls and intimal arteriosclerotic plaques of HGPS patients, similar to healthy aged individuals [74, 86]. This evidence partially explains the severity of the cardiovascular phenotype in HGPS children. Development of advanced fibrotic arteriosclerosis with calcification and overall thickening and stiffening of the arterial walls, as well as mild systemic inflammation levels, are some of the HGPS vascular symptoms that also typically occur in normal aging [86].

3.4.1 Altered ECM Remodeling

HGPS patients show vessel walls with marked fibrosis, having high stiffness and a decreased compliance of the vessels. Autopsies of HGPS patients reveal an accumulation of type I and type IV collagen and of proteoglycans, such as decorin and versican, as well as deposition of hyaluron in the arteriosclerotic lesions [86]. Genome-scale expression profiling of HGPS and aged-donor fibroblasts have shown altered expression of genes involved in ECM synthesis or modification [28, 68]. There is an upregulation of proteoglycan cell adhesion proteins, which are important for ECM stability and for binding other proteoglycans, hyaluron, and fibrous matrix proteins such as collagen [28, 68]. Laminin, a protein that forms essential interactions with collagen type IV and associates with cell-binding proteins, is also upregulated, thereby influencing cell attachment, morphology, and survival. A mouse model of HGPS showed increased arterial hyaluron content with age [126]. Hyaluron is an important ECM component, highly related to SMC proliferation and migration, and has been demonstrated to accumulate in early arteriosclerosis. The increased expression of fibrous proteins of the ECM, including collagen fibers, contributes to a decline in vessel elasticity [28, 68].

The ECM remodeling profile in HGPS is affected by enzyme expression. Studies have shown a specific downregulation of MMP-3 expression in HGPS cell lines and

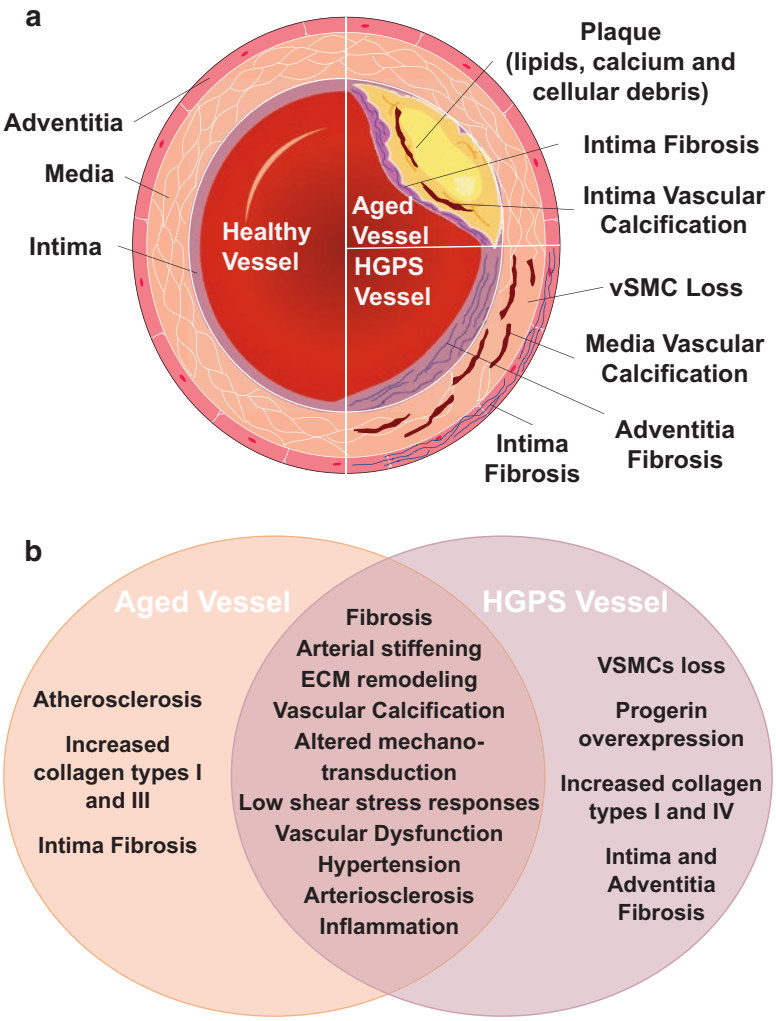

Fig. 3.1 (**a**) Schematic representation of the differences and similarities between physiological, HGPS aged, and young healthy vessel. Both aged and HGPS vessels develop marked arteriosclerotic fibrosis and calcification, with an overall thickening and stiffening of the walls. Aged vessels develop a particular type of arteriosclerotic plaques, with the accumulation of lipids, which is absent in HGPS individuals. (**b**) Similarities and differences between cellular, molecular, and biophysical components of physiological and HGPS-accelerated aging. HGPS represents a highly reliable model of vascular aging, showing similar symptoms that include vascular cell dysfunction, disruption of the ECM, and altered mechanotransduction responses

an associated donor age-dependent decline in secreted MMP-3 and MMP-2 proteins, which might contribute to the altered ECM in HGPS [50]. Differences in MMP-3 activity have also been reported in other vascular pathologies in the normal aging population [50]. Overall, there is an excess of ECM deposition, with increased

expression of ECM components and decreased expression of ECM remodeling enzymes, which leads to structural effects on tissue function and also lead to signaling imbalances.

Several pathways regulating ECM are affected in HGPS. Mutant lamin A is accountable for the inhibition of the canonical Wnt signaling pathway, which is implicated in the regulation of genes encoding ECM proteins [53]. TGF-β1/SMAD pathway has also been implicated in HGPS. This pathway can be activated through integrins, via mechanical force, contributing to increased collagen synthesis and, therefore, fibrosis [2]. Expression of TGFβ1 increases in an age-dependent manner in both HGPS and healthy cell lines. In postnatal tissues, especially those subjected to extensive mechanical stress, such as the skeletal and cardiovascular systems, the ECM assumes a structural role in maintaining tissue integrity and homeostasis [16]. In HGPS and physiological aging, there is a concomitant alteration of ECM components and pathways that regulate ECM synthesis and organization, leading to a vicious cycle of matrix remodeling that contributes to the vasculopathy of aging.

3.4.2 Arterial Stiffening and Fibrosis

Progressive development of fibrotic arteriosclerosis, associated with an abnormal ECM content, reveals a major role of the ECM in the vasculopathy of HGPS patients [111, 138]. Similar to normal aged individuals, HGPS children show typically intimal fibrotic arteriosclerotic plaques in the main cardiac arteries. These lesions have a complex morphology, including thinning of the medial layer of the vessels, subjacent to the thick arteriosclerotic plaque in the intimal region, a necrotic core, and foci of chronic inflammation. HGPS patients show evidence of marked fibrosis of the adventitial layer of large vessels, with a dense perimeter of collagen. In contrast, the same adventitial changes are not observed in normal aged individuals [23, 138]. HGPS fibroblasts have increased levels of ROS and protein oxidation, as well as decreased proteasome activity, thus contributing to cell dysfunction and altered production of ECM proteins [16]. Extensive calcification of the arteries is also frequently observed in HGPS (Fig. 3.1).

3.4.3 Vascular Cell Dysfunction

Arteriosclerosis progression and severity in HGPS vascular systems are correlated with the accumulation of vascular senescent cells [16]. Senescent ECs in arteriosclerotic patients are characterized by low EC growth potential, as well as increased DNA damage and oxidative stress [16]. Moreover, ECs with a HGPS phenotype release inflammatory molecules and express higher levels of ICAM-1, after TNF-α stimulation, than non-HGPS ECs [13]. The increase in ICAM-1 increases the adhesion of monocytes, described as the first event in the initiation of arteriosclerosis [13]. This may explain the increased inflammation and macrophage localization in

arteriosclerotic plaques of HGPS large vessels, contributing to the development of early arteriosclerosis [86]. The accumulation of both prelamin A and progerin at the nuclear envelope results in increased NF-$_K$B activation and systemic inflammation, revealing a possibility that this pathway plays a critical role in premature vascular aging [81]. It is also possible, though not yet studied, that HGPS-ECs also have an impaired NO synthesis function. Overall, EC dysfunction reduces EC contribution to arterioprotection and vascular repair.

Progressive loss of SMCs is a characteristic of HGPS patients, as well as in progeria mouse models [47]. SMCs depletion occurs mainly in arteries exposed to high flow shear stress such as the aorta and carotid [126, 138]. The loss of SMCs occurs in the media of the artery, with accumulation of matrix proteoglycan [23, 126]. The SMCs remaining in the vessels of HGPS show marked premature senescence and, it is thought, that SMC dysfunction is a major trigger of vascular calcification, another hallmark of both physiological and accelerated aging. Progerin and prelamin A accumulation in the nucleus of SMCs leads to nuclear lamina dysfunction, including impaired DNA damage response and repair. This in turn leads to the activation of senescence pathways in prelamin A-expressing SMCs, with induction of senescence-associated secretory phenotype (SASP). SASP includes inflammatory factors, extracellular matrix remodeling proteases, and proteins implicated in the regulation of SMCs calcification, such as BMP2, Runx2, osteocalcin, osteopontin, and osteoprotegerin [64]. Moreover, exposure of SMCs to calcifying medium leads to upregulation of lamin A and prelamin A expression, accompanied by an increase of pro-calcification factors and increased calcium deposition [47]. Besides the transition of SMCs to an "osteoblastic-like" phenotype, there are other factors that contribute to vascular calcification. There is enhanced formation of calcium phosphate deposits in blood vessels likely due to mitochondrial dysfunction and ATP production. Progerin-expressing SMCs showed impaired mitochondrial dysfunction and ATP production, leading to reduced synthesis of pyrophosphate (PPi), a potent inhibitor of the formation of calcium deposits. Progerin-expressing SMCs also showed upregulation of several enzymes responsible for PPi hydrolysis and of phosphate synthesis [128].

Although not yet explored, it is possible that the remodeled ECM, which involves the HGPS SMCs, has a large role in the development of vascular calcification. It has already been shown that metalloproteinases are upregulated in human arteriosclerotic plaques and that by inhibiting their activity, it is possible to reduce arterial calcification [94]. These evidences demonstrate the importance of the altered ECM in the vasculopathy of physiological and accelerated aging.

3.4.4 Altered Response of Vascular Cells to Flow Shear Stress

Cells of the cardiovascular system are exposed to various types of hemodynamic stress. Nucleus shape has been associated with adaptation to shear stress, an alteration that minimizes the total force exerted on the nuclei. Normally, when a cell is

exposed to shear stress, there are reorganization and upregulation of nuclear laminas which protect the DNA and the nucleus interior from the effects of shear stress [30, 90]. Since lamins are involved in several nuclear functions including regulation of gene expression, it is likely that alterations in the nuclear lamina response to shear stress impacts gene expression. It is also hypothesized that a cellular phenotype, activated in response to well-defined laminar shear stress, resists the development of arteriosclerotic lesions, by activating protective signaling pathways. In HGPS there is an abnormal nuclear lamina that leads to a more stiffened nucleus and failure to respond normally to shear stress [30]. Therefore, progerin-expressing cells, which do not respond normally to shear stress, contribute to the early development of arteriosclerosis in HGPS patients, evident by the fact that arteriosclerotic plaques develop preferentially in regions of elevated shear flow [90]. Moreover, it has been shown that HGPS neighboring, but unaffected cells, also have an altered response to shear stress, further contributing to the severity of the vasculopathy of HGPS [90].

Loss of SMCs in regions exposed to high fluidic shear stress, such as the aortic and carotid arteries, is strong evidence that their normal adaptation to shear stress is altered in HGPS. These altered responses are linked to changes in mechanotransduction pathways [111]. Progerin-expressing SMCs, exposed to high in vivo hemodynamic forces, have a significant reduction in the expression of mechanotransduction-related proteins such as vinculin and vimentin.

In contrast to SMCs, progerin-expressing ECs seem to be more resistant to shear stress than ECs without progerin. Indeed, an intact monolayer of vimentin-positive ECs is typically observed in progeria mouse models [111]. In aortic regions presenting SMCs loss, ECs show more than an eightfold level of vimentin expression, in comparison with ECs overlying adjacent aortic regions not depleted of SMCs. This upregulation in vimentin helps ECs withstand the same mechanical forces that are degenerative to SMCs. Furthermore, vimentin filaments in ECs associate with integrins to form cell-matrix adhesions through flow-induced focal contacts [111].

3.5 In Vitro Systems to Study Vascular Aging

Animal models are important tools to study aging, since they share common molecular mechanisms of pathophysiology with aged people, providing insight into the molecular mechanisms of aging. Therefore, a wide range of in vivo vascular aging models have been developed, such as mouse models of accelerated aging [10, 58, 72, 87, 137]. Nevertheless, vascular aging is a complex biological phenomenon in which several components are involved. Thus, it is very unlikely that an individual gene mutation in mice would recapitulate all the features of human aging. Furthermore, it is difficult to identify cellular and molecular key players to disease in whole-animal models. These limitations of vascular aging animal models lead to the development of new in vitro vascular aging models.

Two-dimensional (2D) and three-dimensional (3D) in vitro models may be used to study vascular aging. 2D models are relatively cheap and simple; however, they may not recapitulate important aspects of vascular biology [37] and in vivo predictivity [12] because cells are not exposed to normal mechanical signals, including fluid shear stress, tension, and compression. These limitations have led to increased interest in 3D models which provide more predictive data for in vivo tests [38]. Three-dimensional models may replicate both anatomical macro- and microstructures, including appropriate cell types, ECM, and suitable physiological cues [102].

Microfluidic devices offer the possibility of culturing living cells, in continuously perfused micrometer chambers, in order to model physiological functions of tissues and organs [12]. Advantages of microfluidic devices comprise (1) the possibility of incorporating physical forces, including fluid shear stress, cyclic strain, and mechanical compression, (2) the possibility of making a 3D microenvironment by using hydrogels as scaffolds, (3) the possibility of mimicking relevant tissues by incorporating human cells (cell lines, primary cells, stem cells differentiated to specific lineages as well as the differentiation process itself), and (4) controlling the distribution of chemical variables.

Cells cultured under flow conditions have different biological properties. Shear stress, which is the tangential force to the cells surface, is known to induce substantial morphological and biochemical changes in vascular cells through mechanotransduction [109]. The necessary flow rates, to reach typical shear stress forces, vary from vessel to vessel. In healthy conditions, the rate is estimated to be between 1 and 6 dyn/cm^2 in the venous system and between 10 and 70 dyn/cm^2 in the arterial system [69]. There are a variety of techniques used to achieve this, ranging from pneumatic and syringe pumps to electro-kinetics to control shear stress in microfluidic devices. Constant flow, typical of many capillaries, can be applied through gravity flow, where a height difference between inlet and outlet reservoirs is used to provide steady differential pressure [92]. However, if flow rates are extremely high, other fluid systems such as using liquid level sensing and computer-controlled valves to transmit the proper amount of media may be valuable in maintaining a certain pressure and flow rate [133]. Pulsatile flow can be achieved using an elastomeric microfluidic cell shearing chamber, interfaced with computer-controlled movement of piezoelectric pins [110]. Additional approaches to generate high shear stress in the fluidics include the incorporation of solenoid pinch valves into gravity flow to turn vessel flow on and off electronically [114], external peristaltic pumps [25], and pneumatic micropumps [108].

Microfluidic systems with progeria cells have been instrumental in the study of pathological aging [97, 111]. In one case, a microfluidic system was developed with a top fluidic channel, a middle thin polydimethylsiloxane (PDMS) membrane, and a bottom vacuum channel (Fig. 3.2a). SMCs derived from human-induced pluripotent stem cells obtained from HGPS patients (HGPS-iPSC-SMCs) were cultured on top of the membrane which was deformed by applying different amount of pressures on the bottom channel. This aged model combined biomechanical strain and flow and thus allowed for a better understanding of the inflammatory response of aged SMCs to strain, characterized by an increase in levels of inflammation markers

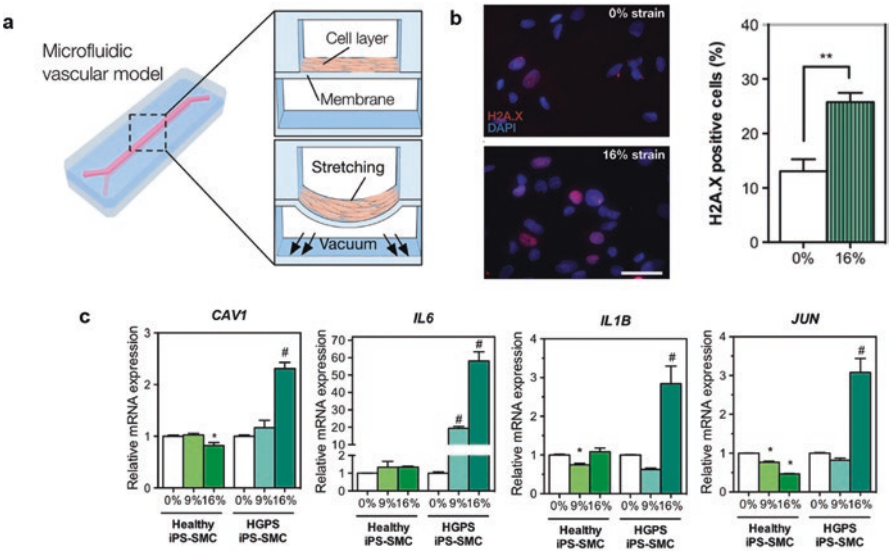

Fig. 3.2 Recapitulation of blood vessel dynamics on a chip and exacerbated response to biomechanical strain in HGPS iPS-SMCs (Copyright 2017, Small, USA, [97]). (**a**) Biomimetic microfluidic vascular model containing two overlapping channels. A cross-sectional view of the microfluidic device shows the cell layer cultured on top of the PDMS membrane and a view during vacuum stimulation regarding the downward membrane deformation. (**b**) DNA damage was evaluated in HGPS iPS-SMCs with H2A.X immunostaining and quantified (mean ± SD of $n = 3$). (**c**) Injury marker *CAV1* and inflammation markers *IL6*, *IL1B*, and *JUN* were evaluated in HGPS iPS-SMCs and healthy iPS-SMCs (*$P < 0.01$ against 0% healthy iPS-SMCs, and # indicates $P < 0.01$ against 0% HGPS iPS-SMCs; bars represent mean ± SD of $n = 5$)

as well as DNA damage (Fig. 3.2b, c) [97]. In a separate study, a microfluidic system was developed to study the response of SMCs (HGPS vs wild type) to flow shear stress [111]. The aortas were exposed to high fluidic shear stress (75 dyn/cm^2) for 30 min. Using this model, it was possible to verify that high fluidic shear stress produced a substantial decrease in vimentin of progeria aortas but not in the wildtype controls. This model showed that a decrease of this protein may contribute to development of vasculopathy in the ascending aorta in progeria syndrome. Previous models are focused mainly on aged SMCs and do not take into account the interaction with aged ECs. Co-cultures of sSMCs and ECs may be used as platforms to predict functional and pathological disease characteristics [4].

The importance of flow shear stress in aging was also addressed by a functional 3D model of HGPS that replicated an arteriole-scale tissue engineered blood vessel (TEBV) (Fig. 3.3a) [4]. HGPS-iPSC-SMCs and human cord blood-derived endothelial progenitor cells (hCB-EPCs) from a healthy donor were used. TEBVs were incorporated into a flow loop and perfused with steady laminar flow at a shear stress of 6.8 dyn/cm^2 for 1–4 weeks, for maturation and functional characterization studies. TEBVs fabricated from HGPS-iPSC-SMCs and hCB-EPCs showed reduced vasoactivity, increased medial wall thickness, increased calcification, and apoptosis

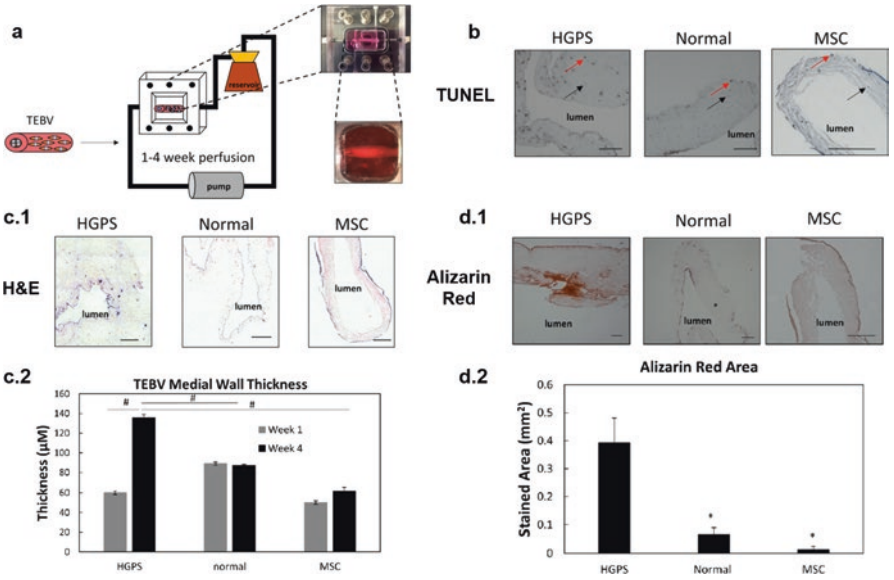

Fig. 3.3 (**a**) Schematic diagram of the procedure to produce iPSC-derived SMC TEBVs from healthy and HGPS patients (Copyright 2017, Scientific Reports, USA, [4]). SMCs were incorporated into a dense collagen gel construct and were then incorporated into a flow loop and perfused with steady laminar flow at a shear stress of 6.8 dyn/cm2 for 1–4 weeks for maturation and functional characterization studies. (**b**) Apoptosis. Histochemical analysis of MSC, normal SMC, and HGPS SMC TEBVs at week 4 with TUNEL staining. Red arrows indicate TUNEL-positive cells and black arrows indicate TUNEL-negative cells (scale bar, 200 μm). (**c**) Thickness. (**c.1**) Histochemical analysis of HGPS SMC, normal SMC, and MSC TEBVs at week 4 with H&E (Scale bar, 200 μm). (**c.2**) The average thickness of MSC, normal SMC, and HGPS SMC TEBVs at week 1 and week 4 based on H&E images. (**d**) Calcification. (**d.1**) Histochemical analysis of HGPS SMC, normal SMC, and MSC TEBVs at week 4 with Alizarin Red staining (scale bar, 200 μm). (**d.2**) Quantification of the total area positive for Alizarin Red

relative to control TEBVs (Fig. 3.3b–d) [4]. When HGPS-iPSC-SMCs were subjected to repeated pulses of electrical stimulation, they rapidly senesced [139].

3.6 Conclusions and Future Directions

This review highlights the similarities and differences in vascular aging between physiological and pathological aging, as well as the suitability of HGPS as a model of vascular aging. Some of the similarities between physiological and HGPS aging are due to the fact that progerin accumulates in vascular cells and other cells during physiological aging [75]. The derivation of iPSCs from HGPS fibroblasts has created an excellent platform to obtain cells otherwise difficult to isolate, due to the rarity of the disease [63, 139]. The use of vascular cells derived from HGPS-iPSCs may provide further insights into vascular aging [97]. Studies have demonstrated

that the accumulation of progerin in HGPS-iPSC derived SMCs led to a downregulation of DNA-dependent protein kinase catalytic subunit expression [63] and poly(ADP-ribose) polymerase 1 [138], which resulted in low cell proliferation. In addition, the use of ECs from HGPS-iPSCs showed that these cells had higher mechanosensitivity, likely due to an elevation of channel V2 expression upon mechanical stimulation [65]. It is expected that the combination of these HGPS cells in bioengineered systems will facilitate the discovery of new molecular targets. Future studies should evaluate the effect of flow shear stress in vascular cells and to determine the mechanisms behind their mechanosensitivity.

This review also highlights a set of markers and features that characterize vascular aging, both in physiological and pathological conditions. It is known that molecular aging is controlled by multiple pathways, and their impact, as well as how they intertwine, is not completely understood [59]. Although it is known that the ECM is significantly altered during aging, it remains to be determined its effect in the aging process, as well as its effects in inducing "aging" in young vascular cells. The creation of substrates with variable stiffness using recent technologies [46], as well as the identification of new ECM molecules that mediate the aging process, might facilitate the in vitro study of this process.

References

1. Adler, A. S., et al. (2007). Motif module map reveals enforcement of aging by continual NF-kappaB activity. *Genes & Development, 21*(24), 3244–3257.
2. Aliper, A. M., Csoka, A. B., Buzdin, A., Jetka, T., Roumiantsev, S., Moskalev, A., et al. (2015). Signaling pathway activation drift during aging: Hutchinson-Gilford progeria syndrome fibroblasts are comparable to normal middle-age and old-age cells. *Aging-Us, 7*(1), 26–37.
3. Armanios, M., et al. (2009). Short telomeres are sufficient to cause the degenerative defects associated with aging. *The American Journal of Human Genetics, 85*(6), 823–832.
4. Atchison, L., et al. (2017). A tissue engineered blood vessel model of Hutchinson-Gilford progeria syndrome using human iPSC-derived smooth muscle cells. *Scientific Reports, 7*(1), 8168.
5. Baker, D. J., et al. (2011). Clearance of p16Ink4a-positive senescent cells delays ageing-associated disorders. *Nature, 479*(7372), 232–236.
6. Baker, D. J., et al. (2016). Naturally occurring p16(Inks4a)-positive cells shorten healthy lifespan. *Nature, 530*(7589), 184–189.
7. Baker, P. B., Baba, N., & Boesel, C. P. (1981). Cardiovascular-abnormalities in progeria - case-report and review of the literature. *Archives of Pathology & Laboratory Medicine, 105*(7), 384–386.
8. Baratchi, S., et al. (2017). Molecular sensors of blood flow in endothelial cells. *Trends in Molecular Medicine, 23*(9), 850–868.
9. Beck Jr., L., & D'Amore, P. A. (1997). Vascular development: cellular and molecular regulation. *The FASEB Journal, 11*(5), 365–373.
10. Bergo, M. O., et al. (2002). Zmpste24 deficiency in mice causes spontaneous bone fractures, muscle weakness, and a prelamin A processing defect. *Proceedings of the National Academy of Sciences of the United States of America, 99*(20), 13049–13054.

11. Berry, C. L., Sosa-Melgarejo, J. A., & Greenwald, S. E. (1993). The relationship between wall tension, lamellar thickness, and intercellular junctions in the fetal and adult aorta: Its relevance to the pathology of dissecting aneurysm. *The Journal of Pathology, 169*(1), 15–20.
12. Bhatia, S. N., & Ingber, D. E. (2014). Microfluidic organs-on-chips. *Nature Biotechnology, 32*(8), 760–772.
13. Bonello-Palot, N., et al. (2014). Prelamin A accumulation in endothelial cells induces premature senescence and functional impairment. *Atherosclerosis, 237*(1), 45–52.
14. Bonnema, D. D., et al. (2007). Effects of age on plasma matrix metalloproteinases (MMPs) and tissue inhibitor of metalloproteinases (TIMPs). *Journal of Cardiac Failure, 13*(7), 530–540.
15. Bostrom, K. I., Rajamannan, N. M., & Towler, D. A. (2011). The regulation of valvular and vascular sclerosis by osteogenic morphogens. *Circulation Research, 109*(5), 564–577.
16. Brassard, J. A., et al. (2016). Hutchinson-Gilford progeria syndrome as a model for vascular aging. *Biogerontology, 17*(1), 129–145.
17. Briones, A. M., et al. (2005). Ageing affects nitric oxide synthase, cyclooxygenase and oxidative stress enzymes expression differently in mesenteric resistance arteries. *Autonomic & Autacoid Pharmacology, 25*(4), 155–162.
18. Brooke, B. S., Bayes-Genis, A., & Li, D. Y. (2003). New insights into elastin and vascular disease. *Trends in Cardiovascular Medicine, 13*(5), 176–181.
19. Burton, A. C. (1954). Relation of structure to function of the tissues of the wall of blood vessels. *Physiological Reviews, 34*(4), 619–642.
20. Burton, D. G., & Krizhanovsky, V. (2014). Physiological and pathological consequences of cellular senescence. *Cellular and Molecular Life Sciences, 71*(22), 4373–4386.
21. Byon, C. H., et al. (2011). Runx2-upregulated receptor activator of nuclear factor kappaB ligand in calcifying smooth muscle cells promotes migration and osteoclastic differentiation of macrophages. *Arteriosclerosis, Thrombosis, and Vascular Biology, 31*(6), 1387–1396.
22. Campisi, J. (2013). Aging, cellular senescence, and cancer. *Annual Review of Physiology, 75*(1), 685–705.
23. Capell, B. C., Collins, F. S., & Nabel, E. G. (2007). Mechanisms of cardiovascular disease in accelerated aging syndromes. *Circulation Research, 101*(1), 13–26.
24. Carallo, C., et al. (2016). Carotid endothelial shear stress reduction with aging is associated with plaque development in twelve years. *Atherosclerosis, 251*, 63–69.
25. Chau, L., Doran, M., & Cooper-White, J. (2009). A novel multishear microdevice for studying cell mechanics. *Lab on a Chip, 9*(13), 1897–1902.
26. Chennupati, R., et al. (2013). Endothelium-dependent hyperpolarization-related relaxations diminish with age in murine saphenous arteries of both sexes. *British Journal of Pharmacology, 169*(7), 1486–1499.
27. Costantino, S., Paneni, F., & Cosentino, F. (2016). Ageing, metabolism and cardiovascular disease. *The Journal of Physiology, 594*(8), 2061–2073.
28. Csoka, A. B., et al. (2004). Genome-scale expression profiling of Hutchinson-Gilford progeria syndrome reveals widespread transcriptional misregulation leading to mesodermal/mesenchymal defects and accelerated atherosclerosis. *Aging Cell, 3*(4), 235–243.
29. Cuhlmann, S., et al. (2011). Disturbed blood flow induces RelA expression via c-Jun N-terminal kinase 1 a novel mode of NF-kappa B regulation that promotes arterial inflammation. *Circulation Research, 108*(8), 950–959.
30. Dahl, K. N., et al. (2006). Distinct structural and mechanical properties of the nuclear lamina in Hutchinson-Gilford progeria syndrome. *Proceedings of the National Academy of Sciences of the United States of America, 103*(27), 10271–10276.
31. Davis, E. C. (1993). Endothelial cell connecting filaments anchor endothelial cells to the subjacent elastic lamina in the developing aortic intima of the mouse. *Cell and Tissue Research, 272*(2), 211–219.
32. Dimri, G. P., et al. (1995). A biomarker that identifies senescent human cells in culture and in aging skin in vivo. *Proceedings of the National Academy of Sciences, 92*(20), 9363–9367.

33. Duca, L., et al. (2016). Matrix ageing and vascular impacts: Focus on elastin fragmentation. *Cardiovascular Research, 110*(3), 298–308.
34. Dudinskaya, E. N., et al. (2015). Short telomere length is associated with arterial aging in patients with type 2 diabetes mellitus. *Endocrine Connections, 4*(3), 136–143.
35. El Assar, M., Angulo, J., & Rodriguez-Manas, L. (2013). Oxidative stress and vascular inflammation in aging. *Free Radical Biology & Medicine, 65*, 380–401.
36. Eriksson, M., Brown, W. T., Gordon, L. B., Glynn, M. W., Singer, J., Scott, L., et al. (2003). Recurrent de novo point mutations in lamin A cause Hutchinson-Gilford progeria syndrome. *Nature, 423*(6937), 293–298.
37. Esch, E. W., Bahinski, A., & Huh, D. (2015). Organs-on-chips at the frontiers of drug discovery. *Nature Reviews. Drug Discovery, 14*(4), 248–260.
38. Fitzgerald, K. A., et al. (2015). Life in 3D is never flat: 3D models to optimise drug delivery. *Journal of Controlled Release, 215*, 39–54.
39. Fleenor, B. S., et al. (2010). Arterial stiffening with ageing is associated with transforming growth factor-beta1-related changes in adventitial collagen: Reversal by aerobic exercise. *The Journal of Physiology, 588*(Pt 20), 3971–3982.
40. Freund, A., et al. (2012). Lamin B1 loss is a senescence-associated biomarker. *Molecular Biology of the Cell, 23*(11), 2066–2075.
41. Fujimoto, D. (1982). Aging and cross-linking in human aorta. *Biochemical and Biophysical Research Communications, 109*(4), 1264–1269.
42. Fyhrquist, F., Saijonmaa, O., & Strandberg, T. (2013). The roles of senescence and telomere shortening in cardiovascular disease. *Nature Reviews. Cardiology, 10*(5), 274–283.
43. Goldin, A., et al. (2006). Advanced glycation end products: Sparking the development of diabetic vascular injury. *Circulation, 114*(6), 597–605.
44. Gonzalo, S., Kreienkamp, R., & Askjaer, P. (2017). Hutchinson-Gilford Progeria Syndrome: A premature aging disease caused by LMNA gene mutations. *Ageing Research Reviews, 33*, 18–29.
45. Guzik, T. J., et al. (2002). Mechanisms of increased vascular superoxide production in human diabetes mellitus: Role of NAD(P)H oxidase and endothelial nitric oxide synthase. *Circulation, 105*(14), 1656–1662.
46. Hadden, W. J., et al. (2017). Stem cell migration and mechanotransduction on linear stiffness gradient hydrogels. *Proceedings of the National Academy of Sciences of the United States of America, 114*(22), 5647–5652.
47. Hamczyk, M. R., del Campo, L., & Andrés, V. (2017). Aging in the cardiovascular system: Lessons from Hutchinson-Gilford progeria syndrome. *Annual Review of Physiology, 80*, 27–48.
48. Hamilton, C. A., et al. (2001). Superoxide excess in hypertension and aging: A common cause of endothelial dysfunction. *Hypertension, 37*(2 Pt 2), 529–534.
49. Hampel, B., et al. (2006). Increased expression of extracellular proteins as a hallmark of human endothelial cell in vitro senescence. *Experimental Gerontology, 41*(5), 474–481.
50. Harten, I. A., et al. (2011). Age-dependent loss of MMP-3 in Hutchinson-Gilford progeria syndrome. *Journals of Gerontology Series a-Biological Sciences and Medical Sciences, 66*(11), 1201–1207.
51. Harvey, A., et al. (2016). Vascular fibrosis in aging and hypertension: Molecular mechanisms and clinical implications. *The Canadian Journal of Cardiology, 32*(5), 659–668.
52. Hayflick, L. (2000). The illusion of cell immortality. *British Journal of Cancer, 83*(7), 841–846.
53. Hernandez, L., et al. (2010). Functional coupling between the extracellular matrix and nuclear lamina by Wnt signaling in progeria. *Developmental Cell, 19*(3), 413–425.
54. Jacob, M. P. (2003). Extracellular matrix remodeling and matrix metalloproteinases in the vascular wall during aging and in pathological conditions. *Biomedicine & Pharmacotherapy, 57*(5–6), 195–202.
55. Jin, K. (2010). Modern biological theories of aging. *Aging and Disease, 1*(2), 72–74.

56. Kaushik, S., & Cuervo, A. M. (2015). Proteostasis and aging. *Nature Medicine, 21*(12), 1406–1415.
57. Kohn, J. C., Lampi, M. C., & Reinhart-King, C. A. (2015). Age-related vascular stiffening: Causes and consequences. *Frontiers in Genetics, 6*, 112.
58. Kuro-o, M., et al. (1997). Mutation of the mouse klotho gene leads to a syndrome resembling ageing. *Nature, 390*(6655), 45–51.
59. Laina, A., Stellos, K., & Stamatelopoulos, K. (2017). Vascular ageing: Underlying mechanisms and clinical implications. *Experimental Gerontology*. https://doi.org/10.1016/j.exger.2017.06.007
60. Laurent, S., et al. (2006). Expert consensus document on arterial stiffness: Methodological issues and clinical applications. *European Heart Journal, 27*(21), 2588–2605.
61. Lesniewski, L. A., et al. (2011). Aerobic exercise reverses arterial inflammation with aging in mice. *American Journal of Physiology. Heart and Circulatory Physiology, 301*(3), H1025–H1032.
62. Li, Y. S., Haga, J. H., & Chien, S. (2005). Molecular basis of the effects of shear stress on vascular endothelial cells. *Journal of Biomechanics, 38*(10), 1949–1971.
63. Liu, G. H., et al. (2011). Recapitulation of premature ageing with iPSCs from Hutchinson-Gilford progeria syndrome. *Nature, 472*(7342), 221–225.
64. Liu, Y., Drozdov, I., Shroff, R., Beltran, L. E., & Shanahan, C. M. (2013). Prelamin A accelerates vascular calcification via activation of the DNA damage response and senescence-associated secretory phenotype in vascular smooth muscle cells. *Circulation Research, 112*(10), e99–e109.
65. Lo, C. Y., et al. (2014). An upregulation in the expression of vanilloid transient potential channels 2 enhances hypotonicity-induced cytosolic Ca(2)(+) rise in human induced pluripotent stem cell model of Hutchinson-Gillford Progeria. *PLoS One, 9*(1), e87273.
66. London, G. M. (2013). Mechanisms of arterial calcifications and consequences for cardiovascular function. *Kidney International Supplements, 3*(5), 442–445.
67. López-Otín, C., et al. (2013). The hallmarks of aging. *Cell, 153*(6), 1194–1217.
68. Ly, D. H., et al. (2000). Mitotic misregulation and human aging. *Science, 287*(5462), 2486–2492.
69. Malek, A. M., Alper, S. L., & Izumo, S. (1999). Hemodynamic shear stress and its role in atherosclerosis. *JAMA, 282*(21), 2035–2042.
70. Malinin, N. L., West, X. Z., & Byzova, T. V. (2011). Oxidation as "the stress of life". *Aging (Albany NY), 3*(9), 906–910.
71. Maslov, A. Y., & Vijg, J. (2009). Genome instability, cancer and aging. *Biochimica et Biophysica Acta (BBA) - General Subjects, 1790*(10), 963–969.
72. Massip, L., et al. (2006). Increased insulin, triglycerides, reactive oxygen species, and cardiac fibrosis in mice with a mutation in the helicase domain of the Werner syndrome gene homologue. *Experimental Gerontology, 41*(2), 157–168.
73. Matsushita, H., et al. (2001). eNOS activity is reduced in senescent human endothelial cells: Preservation by hTERT immortalization. *Circulation Research, 89*(9), 793–798.
74. McClintock, D., Gordon, L. B., & Djabali, K. (2006). Hutchinson-Gilford progeria mutant lamin A primarily targets human vascular cells as detected by an anti-lamin A G608G antibody. *Proceedings of the National Academy of Sciences of the United States of America, 103*(7), 2154–2159.
75. McClintock, D., et al. (2007). The mutant form of lamin A that causes Hutchinson-Gilford progeria is a biomarker of cellular aging in human skin. *PLoS One, 2*(12), e1269.
76. McCrann, D. J., et al. (2009). Upregulation of Nox4 in the aging vasculature and its association with smooth muscle cell polyploidy. *Cell Cycle, 8*(6), 902–908.
77. McNulty, M., et al. (2005). Aging is associated with increased matrix metalloproteinase-2 activity in the human aorta. *American Journal of Hypertension, 18*(4 Pt 1), 504–509.
78. Meerwaldt, R., et al. (2004). Simple non-invasive assessment of advanced glycation endproduct accumulation. *Diabetologia, 47*(7), 1324–1330.

79. Meschiari, C. A., et al. (2017). The impact of aging on cardiac extracellular matrix. *Geroscience, 39*(1), 7–18.
80. Minamino, T. (2002). Endothelial cell senescence in human atherosclerosis: Role of telomere in endothelial dysfunction. *Circulation, 105*(13), 1541–1544.
81. Monaco, C., et al. (2004). Canonical pathway of nuclear factor kappa B activation selectively regulates proinflammatory and prothrombotic responses in human atherosclerosis. *Proceedings of the National Academy of Sciences of the United States of America, 101*(15), 5634–5639.
82. Nakano-Kurimoto, R., et al. (2009). Replicative senescence of vascular smooth muscle cells enhances the calcification through initiating the osteoblastic transition. *American Journal of Physiology. Heart and Circulatory Physiology, 297*(5), H1673–H1684.
83. Newaz, M. A., Yousefipour, Z., & Oyekan, A. (2006). Oxidative stress-associated vascular aging is xanthine oxidase-dependent but not NAD(P)H oxidase-dependent. *Journal of Cardiovascular Pharmacology, 48*(3), 88–94.
84. Niccoli, T., & Partridge, L. (2012). Ageing as a risk factor for disease. *Current Biology, 22*(17), R741–R752.
85. O'Connell, M. K., et al. (2008). The three-dimensional micro- and nanostructure of the aortic medial lamellar unit measured using 3D confocal and electron microscopy imaging. *Matrix Biology, 27*(3), 171–181.
86. Olive, M., et al. (2010). Cardiovascular pathology in Hutchinson-Gilford progeria: Correlation with the vascular pathology of aging. *Arteriosclerosis Thrombosis and Vascular Biology, 30*(11), 2301–U636.
87. Osorio, F. G., Navarro, C. L., Cadiñanos, J., López-Mejía, I. C., Quirós, P. M., Bartoli, C., et al. (2011). Splicing-directed therapy in a new mouse model of human accelerated aging. *Science Translational Medicine, 3*(106), 106ra107.
88. Paneni, F., et al. (2017). The aging cardiovascular system understanding it at the cellular and clinical levels. *Journal of the American College of Cardiology, 69*(15), 1952–1967.
89. Petersen-Jones, H. G., et al. (2015). Transglutaminase activity is decreased in large arteries from hypertensive rats compared with normotensive controls. *American Journal of Physiology. Heart and Circulatory Physiology, 308*(6), H592–H602.
90. Philip, J. T., & Dahl, K. N. (2008). Nuclear mechanotransduction: Response of the lamina to extracellular stress with implications in aging. *Journal of Biomechanics, 41*(15), 3164–3170.
91. Prakobwong, S., et al. (2010). Involvement of MMP-9 in peribiliary fibrosis and cholangiocarcinogenesis via Rac1-dependent DNA damage in a hamster model. *International Journal of Cancer, 127*(11), 2576–2587.
92. Price, G. M., & Tien, J. (2011). Methods for forming human microvascular tubes in vitro and measuring their macromolecular permeability. *Methods in Molecular Biology, 671*, 281–293.
93. Prinzinger, R. (2005). Programmed ageing: The theory of maximal metabolic scope. How does the biological clock tick? *EMBO Reports, 6*(Suppl 1), S14–S19.
94. Qin, X., et al. (2006). Matrix metalloproteinase inhibition attenuates aortic calcification. *Arteriosclerosis Thrombosis and Vascular Biology, 26*(7), 1510–1516.
95. Redon, C. E., et al. (2011). Recent developments in the use of γ -H2AX as a quantitative DNA double-strand break biomarker. *Aging, 3*(2), 168–174.
96. Reiser, K., McCormick, R. J., & Rucker, R. B. (1992). Enzymatic and nonenzymatic cross-linking of collagen and elastin. *The FASEB Journal, 6*(7), 2439–2449.
97. Ribas, J., Zhang, Y. S., Pitrez, P. R., Leijten, J., Miscuglio, M., Rouwkema, J., et al. (2017). Biomechanical strain exacerbates inflammation on a progeria-on-a-chip model. *Small, 13*(15). https://doi.org/10.1002/smll.201603737
98. Rice, K. M., et al. (2005). Effects of aging on pressure-induced MAPK activation in the rat aorta. *Pflügers Archiv, 450*(3), 192–199.
99. Rodriguez-Manas, L., et al. (2009). Endothelial dysfunction in aged humans is related with oxidative stress and vascular inflammation. *Aging Cell, 8*(3), 226–238.

100. Rosenbloom, J., Abrams, W. R., & Mecham, R. (1993). Extracellular matrix 4: The elastic fiber. *The FASEB Journal, 7*(13), 1208–1218.
101. Ross, C. A., & Poirier, M. A. (2004). Protein aggregation and neurodegenerative disease. *Nature Medicine, 10*(7), S10–S17.
102. Ryan, A. J., et al. (2016). Towards 3D in vitro models for the study of cardiovascular tissues and disease. *Drug Discovery Today, 21*(9), 1437–1445.
103. Scaffidi, P., & Misteli, T. (2006). Lamin A-dependent nuclear defects in human aging. *Science, 312*(5776), 1059–1063.
104. Schleicher, E. D., Wagner, E., & Nerlich, A. G. (1997). Increased accumulation of the glycoxidation product N(epsilon)-(carboxymethyl)lysine in human tissues in diabetes and aging. *The Journal of Clinical Investigation, 99*(3), 457–468.
105. Schrage, W. G., Eisenach, J. H., & Joyner, M. J. (2007). Ageing reduces nitric-oxide- and prostaglandin-mediated vasodilatation in exercising humans. *The Journal of Physiology, 579*(Pt 1), 227–236.
106. Seals, D. R., et al. (2006). Modulatory influences on ageing of the vasculature in healthy humans. *Experimental Gerontology, 41*(5), 501–507.
107. Senatus, L. M., & Schmidt, A. M. (2017). The AGE-RAGE Axis: Implications for age-associated arterial diseases. *Frontiers in Genetics, 8*, 187.
108. Shao, J., et al. (2009). Integrated microfluidic chip for endothelial cells culture and analysis exposed to a pulsatile and oscillatory shear stress. *Lab on a Chip, 9*(21), 3118–3125.
109. Shi, Z. D., & Tarbell, J. M. (2011). Fluid flow mechanotransduction in vascular smooth muscle cells and fibroblasts. *Annals of Biomedical Engineering, 39*(6), 1608–1619.
110. Song, J. W., et al. (2005). Computer-controlled microcirculatory support system for endothelial cell culture and shearing. *Analytical Chemistry, 77*(13), 3993–3999.
111. Song, M. J., et al. (2014). Shear stress-induced mechanotransduction protein deregulation and vasculopathy in a mouse model of progeria. *Stem Cell Research & Therapy, 5*(2), 41.
112. Stuehr, D., Pou, S., & Rosen, G. M. (2001). Oxygen reduction by nitric-oxide synthases. *The Journal of Biological Chemistry, 276*(18), 14533–14536.
113. Taddei, S., et al. (1997). Hypertension causes premature aging of endothelial function in humans. *Hypertension, 29*(3), 736–743.
114. Tam, J., et al. (2014). A microfluidic platform for correlative live-cell and super-resolution microscopy. *PLoS One, 9*(12), e115512.
115. Tian, X. L., & Li, Y. (2014). Endothelial cell senescence and age-related vascular diseases. *Journal of Genetics and Genomics, 41*(9), 485–495.
116. Toda, N. (2012). Age-related changes in endothelial function and blood flow regulation. *Pharmacology & Therapeutics, 133*(2), 159–176.
117. Tsamis, A., Krawiec, J. T., & Vorp, D. A. (2013). Elastin and collagen fibre microstructure of the human aorta in ageing and disease: A review. *Journal of the Royal Society Interface, 10*(83), 20121004.
118. Tsamis, A., Rachev, A., & Stergiopulos, N. (2011). A constituent-based model of age-related changes in conduit arteries. *American Journal of Physiology. Heart and Circulatory Physiology, 301*(4), H1286–H1301.
119. Tsioufis, C., et al. (2007). Low-grade inflammation and hypoadiponectinaemia have an additive detrimental effect on aortic stiffness in essential hypertensive patients. *European Heart Journal, 28*(9), 1162–1169.
120. Ungvari, Z., et al. (2011). Vascular oxidative stress in aging: A homeostatic failure due to dysregulation of NRF2-mediated antioxidant response. *American Journal of Physiology. Heart and Circulatory Physiology, 301*(2), H363–H372.
121. United Nations, D.E.S.A.P.D. (2015). *World Population Ageing 2015*.
122. Valko, M., et al. (2007). Free radicals and antioxidants in normal physiological functions and human disease. *The International Journal of Biochemistry & Cell Biology, 39*(1), 44–84.
123. van der Loo, B., et al. (2000). Enhanced peroxynitrite formation is associated with vascular aging. *The Journal of Experimental Medicine, 192*(12), 1731–1744.

124. van der Loo, B., et al. (2009). Signalling processes in endothelial ageing in relation to chronic oxidative stress and their potential therapeutic implications in humans. *Experimental Physiology, 94*(3), 305–310.
125. Vanhoutte, P. M., Feletou, M., & Taddei, S. (2005). Endothelium-dependent contractions in hypertension. *British Journal of Pharmacology, 144*(4), 449–458.
126. Varga, R., et al. (2006). Progressive vascular smooth muscle cell defects in a mouse model of Hutchinson-Gilford progeria syndrome. *Proceedings of the National Academy of Sciences of the United States of America, 103*(9), 3250–3255.
127. Victorelli, S., & Passos, J. F. (2017). Telomeres and cell senescence - size matters not. *eBioMedicine, 21*, 14–20.
128. Villa-Bellosta, R., et al. (2013). Defective extracellular pyrophosphate metabolism promotes vascular calcification in a mouse model of Hutchinson-Gilford progeria syndrome that is ameliorated on pyrophosphate treatment. *Circulation, 127*(24), 2442–2451.
129. Wagenseil, J. E., & Mecham, R. P. (2009). Vascular extracellular matrix and arterial mechanics. *Physiological Reviews, 89*(3), 957–989.
130. Wang, M., et al. (2006). Matrix metalloproteinase 2 activation of transforming growth factor-beta1 (TGF-beta1) and TGF-beta1-type II receptor signaling within the aged arterial wall. *Arteriosclerosis, Thrombosis, and Vascular Biology, 26*(7), 1503–1509.
131. Wang, M., et al. (2014). Proinflammation: The key to arterial aging. *Trends in Endocrinology and Metabolism, 25*(2), 72–79.
132. Wang, M., et al. (2015). Matrix metalloproteinases promote arterial remodeling in aging, hypertension, and atherosclerosis. *Hypertension, 65*(4), 698–703.
133. Wong, A. D., & Searson, P. C. (2014). Live-cell imaging of invasion and intravasation in an artificial microvessel platform. *Cancer Research, 74*(17), 4937–4945.
134. Wu, Z., et al. (2015). Role of p38 mitogen-activated protein kinase in vascular endothelial aging: Interaction with Arginase-II and S6K1 signaling pathway. *Aging (Albany NY), 7*(1), 70–81.
135. Wynn, T. A. (2008). Cellular and molecular mechanisms of fibrosis. *The Journal of Pathology, 214*(2), 199–210.
136. Xu, J., & Shi, G. P. (2014). Vascular wall extracellular matrix proteins and vascular diseases. *Biochimica et Biophysica Acta, 1842*(11), 2106–2119.
137. Yang, S. H., et al. (2005). Blocking protein farnesyltransferase improves nuclear blebbing in mouse fibroblasts with a targeted Hutchinson-Gilford progeria syndrome mutation. *Proceedings of the National Academy of Sciences of the United States of America, 102*(29), 10291–10296.
138. Zhang, H. Y., Xiong, Z. M., & Cao, K. (2014). Mechanisms controlling the smooth muscle cell death in progeria via down-regulation of poly(ADP-ribose) polymerase 1. *Proceedings of the National Academy of Sciences of the United States of America, 111*(22), E2261–E2270.
139. Zhang, J., et al. (2011). A human iPSC model of Hutchinson Gilford Progeria reveals vascular smooth muscle and mesenchymal stem cell defects. *Cell Stem Cell, 8*(1), 31–45.

Chapter 4
Hypoxia and Matrix Manipulation for Vascular Engineering

Michael R. Blatchley, Hasan E. Abaci, Donny Hanjaya-Putra, and Sharon Gerecht

4.1 Introduction

The permanency of multicellular organisms on Earth is stringently reliant on the ability of cells to respond and adapt to their surrounding milieu. Cells respond to a complex array of biological, biophysical, and biochemical cues to develop and regenerate functional tissues. Alterations to these properties can catastrophically result in impaired development or healing, as well as tumor development and

M. R. Blatchley
Department of Biomedical Engineering, Johns Hopkins University School of Medicine, Baltimore, MD, USA

Department of Chemical and Biomolecular Engineering, Johns Hopkins Physical Sciences–Oncology Center and Institute for NanoBioTechnology, Baltimore, MD, USA

H. E. Abaci
Department of Dermatology, Columbia University, New York, NY, USA

D. Hanjaya-Putra
Department of Aerospace and Mechanical Engineering, Notre Dame, IN, USA

S. Gerecht (✉)
Department of Biomedical Engineering, Johns Hopkins University School of Medicine, Baltimore, MD, USA

Department of Chemical and Biomolecular Engineering, Johns Hopkins Physical Sciences–Oncology Center and Institute for NanoBioTechnology, Baltimore, MD, USA

Department of Materials Science and Engineering, Johns Hopkins University, Baltimore, MD, USA

Department of Oncology, Johns Hopkins University School of Medicine, Baltimore, MD, USA
e-mail: gerecht@jhu.edu

S. Gerecht (ed.), *Biophysical Regulation of Vascular Differentiation and Assembly*, Biological and Medical Physics, Biomedical Engineering,
https://doi.org/10.1007/978-3-319-99319-5_4

metastasis. At the most basic level, two of the most critical components of the cellular microenvironment are oxygen (O_2) and the composition of the extracellular matrix (ECM).

According to the most recent findings, O_2 reached sufficient levels (estimated to be 0.2–2% O_2) for aerobic organisms to be able to survive between 2.45 and 2.2 billion years ago in the oceans [19, 154] and between 540 and 600 million years ago in Earth's atmosphere [72, 154, 194]. Ever since, O_2 has been a highly available potential source of energy for multicellular organisms to commence, survive, and multiply. Multicellular organisms require specialized systems to enable sufficient amounts of O_2 to reach their cells. For instance, insects regulate the transport of O_2 into their tissues with a special respiratory system consisting of spiracles and trachea. Around their tissues, they retain the relatively low O_2 levels (1.4 mmHg) thought to be equivalent to the atmospheric O_2 concentrations at the time of their evolution [161, 162]. In vertebrates, O_2 is carried by proteins in the blood, particularly by hemoglobin, and is transported to tissues through endothelial cells (ECs). The cells throughout the body are highly dependent on the dynamics of O_2. In humans, O_2 concentrations vary between 1 and 10% in tissues (other than the lungs) and between 5 and 13% in blood vessels [126, 155]. Therefore, the ability for cells to sense and respond to O_2 is critical, and O_2 acts as a signaling molecule for cells, regulating their metabolism, survival, cell-cell interactions, migration, and differentiation.

Besides O_2 availability, the transition from unicellular to multicellular organisms requires that cells be connected together in a way that allows them to interact with each other as parts of the same system. This interconnectedness could happen either by having junctions at the cell peripheries or by having connecting cement between the cells. Many multicellular organisms connect their cells in both ways: they use cellular junctions to allow direct signaling between cells, and they use the ECM to regulate the transport of molecules (e.g., O_2, glucose, and signaling proteins) between the cells by remodeling the components of the ECM. Thus, both cell-cell and cell-ECM interactions are significant for determining the fate of cells in tissues. Transmembrane proteins known as integrins are responsible for signaling from the ECM to the cell. Therefore, cells have different responses with respect to the composition and structure of the surrounding ECM. In particular, vascular morphogenesis is regulated by endothelial cell (EC) interactions with the ECM through integrins and is highly dependent on the ECM context [49].

In the field of vascular engineering, the effects of both O_2 tension and the ECM on blood vessel formation continue to be extensively investigated. Blood vessel formation essentially occurs by angiogenesis or vasculogenesis. Angiogenesis is the formation of blood vessels from pre-existing vasculature, orchestrated with the proliferation, migration, and assembly of ECs, as well as the remodeling of the ECM [127, 213]. Most of the ECs comprising the blood vessel walls are in a state of quiescence in physiological conditions. A stimulus is required for ECs to switch from their resting state to their navigating state, where they are activated to produce angiogenesis-promoting proteins [70]. Angiogenesis occurs in several situations, such as wound healing, arthritis, cardiovascular ischemia, and solid tumor

growth [43, 199]. In all of these situations, the tissue or vasculature is deprived of oxygen, leading to hypoxic conditions that promote angiogenesis. For vessel sprouting, the ECM surrounding the vasculature needs to be degraded so that ECs can easily navigate into the tissue and proliferate. Hypoxia is known to promote the production of ECM-degrading enzymes via secretion from activated ECs [21, 61, 65]. Thus, EC sprouting is more favorable toward hypoxic regions in the ECM through which the secretion of enzymes is upregulated by hypoxia, whereas the invasion of vessels into the ECM is not favored in the direction of sufficiently oxygenated regions.

An oxygen gradient emerges in early development, which guides cellular differentiation and morphogenesis [141]. While the O_2 uptake of early embryonic cells relies on the simple diffusion of oxygen, hypoxia starts to be observed in different regions as the embryo expands [5, 141]. The initial vascularization, vasculogenesis, starts with the differentiation of angioblasts (embryonic progenitors of ECs), which surround hemopoietic cells to form blood islands. Blood islands ultimately fuse as angioblasts differentiate into endothelial cells to form the primary capillary plexus and then undergo further tubulogenesis and vascular network formation throughout the yolk sac [156, 185, 230]. This process of vasculogenesis has been suggested to occur in hypoxic conditions [141, 156]. Hypoxia also stimulates microvascularization and the capillary network to form around the developing organs. Vasculogenesis in adult organs has been demonstrated to originate from endothelial progenitor cells (EPCs) circulating in the blood [225]. The migration of EPCs and their recruitment to the appropriate sites to induce the formation of new blood vessels depends on complex cell signaling. Circulating EPCs home to hypoxic regions along both O_2 and growth factor gradients, in particular gradients of stromal-derived factor 1 (SDF-1) [33, 51]. Investigations of tumor growth and wound healing have revealed that hypoxia occurs in both situations, inducing EPCs to migrate from the circulating blood through the ECM. Hypoxia also plays a role in the recruitment of EPCs by promoting receptor expression on the tissue that recognizes EPCs [242], as well as on the EPCs themselves [35], which is followed by their differentiation into mature ECs [32]. Moreover, vascular endothelial growth factor (VEGF), a key regulatory protein known to induce vasculogenesis and angiogenesis, was found to be upregulated in hypoxia [159]. These processes take place in the milieu of the ECM, which is mostly composed of fibronectin during early development [49, 148]. In adult tissue, on the other hand, collagen becomes abundant and controls the cellular fate.

The formation of new blood vessels through angiogenesis or vasculogenesis depends on the dynamic effects and interplay between the ECM and oxygen tension. A thorough understanding of the mechanisms involving the ECM and O_2 during angiogenesis and vasculogenesis is essential for the fundamental understanding that can be harnessed for developing vascular engineering applications. Indeed, the effects of these two factors on vascular cells are being investigated extensively. The in vitro vascularization of primary vascular cells has been studied using many different biomaterials [10, 24, 88] as three-dimensional (3D) matrix components, and

they were shown to influence various aspects of angiogenesis and vasculogenesis. Similarly, a considerable amount of work has focused on the effects of hypoxia-inducible factors (HIF1α, HIF2α, HIF3α) on the regulation of genes that induce vasculature network formation [68, 159, 241]. In addition, some researchers have also investigated the effects of hypoxia and the ECM context together [170, 177]. Success in engineering blood vessels from primary vascular cells or stem cells relies on understanding the influence of all critical parameters and controlling them in targeted directions.

The main focus of this chapter is a review and discussion of how the cells in the body respond to variations in oxygen tension and ECM components, leading to new vasculature formation.

4.2 Concepts in the Regulation of the Vasculature by Oxygen and the ECM

4.2.1 The Influence of Oxygen Tension on Vascularization

Variations in oxygen concentrations at every stage of embryogenesis and in different regions of adult tissues lead to diverse vascular responses, depending on the cell type and microenvironment. Many cell types respond differently, but also collectively, to the changes in O_2 equilibrium through specialized sensing mechanisms and effectors in order to maintain homeostasis. In this section, we will first discuss the formation and location of poorly oxygenated regions in the body, as well as the mechanisms that cells utilize to sense changes in oxygen levels. Then, we will then focus on several responses of pluripotent and vascular cells to low O_2 tensions in terms of gene regulation, differentiation, oxygen consumption, and cell survival.

4.2.1.1 The In Vivo Consequences of Oxygen Gradients

Oxygen Availability in the Body

In vertebrates, O_2 transport to the tissues relies on three main processes: the oxygenation of the blood in the alveoli in the lungs, the convectional transport of oxygen in the blood along the veins, and the diffusion of oxygen across the vessel walls followed by penetration of O_2 to the deeper tissues. There are three distinct resistances to the mass transfer of the O_2 molecule, which result in O_2 gradients throughout the body.

O_2 deprivation has been observed early in the development of mouse embryos [141]. Additionally, polarographic oxygen measurements in the human placenta have shown that O_2 levels are 1.3–3.5% in the first 8–10 weeks and reach between 7.2 and 9.5% in weeks 12–13 of pregnancy [188, 202]. Oxygen levels measured in

the gestational sac revealed even lower O_2 levels in earlier stages of embryogenesis, where O_2 is only transported by simple diffusion [115]. Diffusion, as opposed to convection, transports nutrients between cells very slowly. Before vasculogenesis begins, the maximum diameter that a spherical embryo can reach without having any anoxic cells was calculated to be 2 mm [29]. This value varies with the embryo's geometry and, most importantly, with the O_2 consumption of the animal cells. The results of in vivo imaging of various animal embryos show that the maximum diameter remains below 1 mm, which agrees with the theoretically estimated value [29, 230].

Vasculogenesis is crucial to facilitate cell proliferation and for the embryo to grow larger. In mouse embryos, vasculogenesis commences after day 7, with the differentiation of the mesoderm into angioblasts, which then assemble to form a simple circulatory system consisting of a heart, dorsal aorta, and yolk sac by day 8 [56, 107]. Afterward, spatial increases are observed in O_2 levels throughout the course of embryonic development [141]. These profound spatiotemporal O_2 level changes in the embryo can be accepted as evidence for vascular formation during embryogenesis. The large existing vasculature then sprouts and proliferates to supply O_2 and nutrients to cells located in poorly oxygenated regions. Hypoxia, considered the most critical factor controlling the angiogenesis process, works via numerous protein-signaling pathways. The mechanism determining the directionality of angiogenesis and the complex networking of endothelial capillaries around the tissues is manipulated by several other parameters, including hemodynamic forces and cytokines; this mechanism will be discussed later in the chapter [150].

Once embryonic development is complete and sufficient concentrations of O_2 and nutrients are supplied to the tissues, the oxygen gradient still persists in some tissues, providing several benefits to specific cell types. In adults, O_2 distribution ranges from 1 to 13 in normal tissues. Although the formation of blood vessels and capillary networking is complete, some tissues still lack vasculature, such as the bone marrow niche [91, 132, 175]. In such tissues, diffusion is the controlling mechanism for nutrient transport, thus resulting in a wide range of O_2 distributions from the internal hypoxic region to the external regions, which remains at physiological O_2.

The discovery of circulating EPCs in blood vessels revealed that neovascularization in adults is directed not only by angiogenesis but also by the vasculogenesis process, which depends on the renewal, mobility, recruitment, and differentiation of EPCs [12, 13, 96, 219]. The bone marrow (BM) provides a host microenvironment for a variety of cells, including hematopoietic stem cells (HSCs), mesenchymal stem cells (MSCs), and EPCs. The development of EPCs occurs in the BM, which has a unique structure that allows severe hypoxic regions to exist. Although the BM is inaccessible for noninvasive oxygen measurements, both simulation studies and qualitative measurements have demonstrated the existence of hypoxic regions. Several theoretical models have been developed in order to simulate the distribution of oxygen throughout the BM [41, 132, 133]. Chow et al. used homogeneous Kroghian models to estimate oxygen levels in the BM [41]. Their simulations suggested that both HSCs and EPCs are exposed to low O_2 tensions in the BM. There are various BM architectural organizations possible depending on parameters such

as the spatial arrangement of vasculature and the distribution of many different cell types populating the BM. Therefore, in the absence of supporting evidence from in vivo quantitative measurements, model predictions must be used to assess the effects of different parameters on the O_2 tension distribution in the BM. The model described by Kumar et al. considered three possible vessel arrangements to simulate oxygen level variations under various conditions [132]. They suggested that hypoxic, and even anoxic, regions could be found in the BM, assuming that the cells' oxygen consumption is constant and that the density of arterioles in the BM is low.

On the other hand, qualitative observations in the study by Parmar et al. demonstrated that HSCs are distributed according to oxygen availability in the BM [175]. Staining with pimonidazole and sectioning revealed the oxygen gradient throughout the BM, showing that HSCs more likely reside at the lower end of the gradient. These results are in agreement with other in vitro studies suggesting that hypoxia supports the maintenance of stemness [45, 64, 69]. Moreover, BM transplantation studies have shown that BM-derived EPCs enhance neovascularization and the formation of arteries [231, 235]. The renewal of EPCs in the BM depends on the differentiation dynamics of HSCs, which are regulated by the microenvironments (i.e., the niches) they reside in. Osteoblasts, bone cell progenitors, bind to each other and to HSCs via adhesion molecules to form the osteoblastic niche that is located far from the sinusoidal arteries. Researchers have discovered the existence of another type of niche within the BM, the vascular niche, which is located closer to the sinusoidal arteries than the osteoblastic niche. The differences in physicochemical factors within the various niches play fundamental roles in controlling the dynamics of HSC migration and differentiation. Since the vascular niche's close proximity to arteries means that it is richer in O_2 than the osteoblastic niche, Heissnig's group hypothesized that HSCs are in a quiescent state in the osteoblastic niche's severe hypoxic conditions [92]. When vasculogenesis is necessary in neighboring tissues, specific cell signaling stimulates the migration of HSCs from the osteoblastic niche to the more oxygenated vascular niche, where HSCs can switch from their quiescent state to a proliferative state. The proliferation and differentiation of HSCs reconstitute the EPC pool in the vascular niche before they enter the circulation.

Wound healing, another situation where tissue hypoxia is prevalent, consists of a series of events that includes new vasculature formation, which is regulated by varying O_2 levels. Platelets interfere with microcirculation in the wounded tissue, followed by the release of coagulation factors to reinforce the clotting process. Histamine and bradykinin, secreted by mast cells, also influence the microcirculation by enhancing vascular permeability and arteriolar vasodilation, thereby increasing the blood flow rate [11, 102]. Recruitment of leukocytes and macrophages into the damaged tissue is followed by their activation in response to several growth factors (GFs) and integrins. High rates of O_2 consumption in activated macrophages, along with perturbation of the microcirculation, lead to a further decrease in O_2 levels and result in hypoxia [204], which leads to the accumulation of HIF1α at the wound site [246]. Albina et al. [9] showed that the HIF1α mRNA of inflammatory cells peaks about 6 h after injury. On the other hand, HIF1α protein levels could be detected between 1 and 5 days after wounding. More recently, Zhang et al. [246] demon-

strated that, during the burn wound-healing process, the accumulation of HIF1α increases the number of circulating angiogenic cells, as well as smooth muscle actin-positive cells, in the wounded tissue. These hypoxic conditions—either directly or indirectly through the accumulation of HIF—stimulate angiogenesis during wound healing.

Ischemic tissues, including those affected by myocardial infarction or peripheral artery occlusion (e.g., limb ischemia), have also been a hotbed for study of the effects of low O_2 on cellular recruitment and tissue regeneration. In particular, lack of O_2 delivery to these diseased tissues results in HIF stabilization and subsequent upregulation of recruitment chemokines, perhaps most importantly SDF-1, as well as transmembrane proteins integrin β2 and ICAM-1 that facilitate adhesion of circulating cells to the damaged endothelium [33, 35, 51, 242]. Importantly, hypoxic conditions also facilitate ECM remodeling through upregulation of proteases, such as cathepsins and matrix metalloproteinases [4, 106, 226]. These factors, in concert with HIF-induced production of other pro-angiogenic factors, such as VEGF, lead to robust formation of neovasculature.

Oxygen-Sensing Mechanisms of Vascular Cells

Most cell types in the body respond to variations in O_2 tensions [233]. Gene expression, viability, metabolism, and the oxygen uptake rate of the cells change with alterations in O_2 levels, in order to maintain homeostasis. When cells experience a change in extracellular O_2 levels, they adapt to the new conditions, which may occur rapidly. Hence, O_2 sensing in cells is expected to be controlled by well-organized, highly sensitive mechanisms.

Several mechanisms have been proposed in the literature to account for O_2 sensing in cells. Although their sensitivities may differ from one another, more than one such mechanism can coexist in a cell, resulting in various cellular responses. Within the cell, the O_2 molecule mainly engages in two distinct processes: it is involved directly in biosynthesis reactions; or it participates in metabolic processes, such as the electron transport chain occurring in mitochondria. Any change in the concentration of O_2 extensively perturbs these processes and, following a sequence of events, may have a number of different effects on the cell. Therefore, O_2 sensors in cells can be mainly categorized as mitochondria-related sensors (bioenergetic) and biosynthesis-related sensors (biosynthetic)—although they can be linked to each other in some cases, making the distinction not completely clear [233].

Among the several effectors of O_2-sensing mechanisms, HIFs are the most essential in terms of the diversity of their influences. The family of HIFα subunits (HIF1α, HIF2α, and HIF3α) has been shown to be responsible for regulating expression of a large number of genes, including those coding for key regulatory proteins of angiogenesis and vasculogenesis. Although HIFα is expressed at every oxygen tension, it is rapidly ubiquitinated in normoxic conditions, resulting in its degradation. Thus, the amount of intracellular HIFα protein depends on the balance between its expression and degradation. In conditions of low O_2 availability, all HIFα proteins heterodi-

merize with HIFβ (ARNT) and form a transcriptional complex which regulates the transcription of numerous genes [159]. Stabilization of HIFα in the cell is controlled by two main O_2 sensing proteins, prolyl hydroxylase domain (PHD) and factor-inhibiting HIFα (FIH), which belong to the previously mentioned biosynthetic sensors category. Three isoforms of PHDs are present in all mammals [28]. Specific proline residues on the oxygen-dependent domain of HIFα are hydroxylated by PHDs at separate hydroxylation sites, leading to HIFα degradation. The activity of PHDs in the cytoplasm is controlled by various O_2-dependent molecular events and, directly, by the concentration of the O_2 molecule [68]. All three PHDs remain partially active in normoxia. PHD activity is expected to be very sensitive to small changes in cytoplasmic O_2 levels since K_m, the Michaelis-Menten parameter for the activation of PHDs, is approximately 230–250 μM, which is much higher than physiological oxygen concentration (approximately 60 μM) [98]. Besides, mitochondria are also involved in the PHD activation process through their consumption of O_2, regulation of reactive oxygen species (ROS), and production of nitric oxide (NO). While the stabilization of HIFα depends on PHD activity, the expression of HIFα is controlled by FIHs. Therefore, when O_2 levels are lowered, both the stabilization and transactivation of HIFα increase, resulting in several angiogenic responses that will be discussed in the following section.

NO and ROS not only contribute to the HIFα stabilization process, but they also have several direct effects on vascular cells and blood vessels. A number of studies have shown that NO induces angiogenesis, hyperpermeability, and vasodilation [73]. Moreover, NO also perturbs EC respiration through the inhibition of cytochrome c oxidase, which causes lower mitochondrial O_2 consumption [118]. Mitochondrial ROS are also increased as a consequence of electron transport chain inhibition, which then contributes to the deactivation of PHDs via oxidizing cofactor Fe (II) and helps to stabilize HIFα. ROS production, in respect to hypoxia, is proportional to the concentrations of intracellular O_2 and electron donors. Under hypoxia, the amount of O_2 required to form superoxides is decreased, whereas the concentration of the electron donors increases as a consequence of the reduction in the proximal electron transport chain. Therefore, ROS production can change in both manners, depending on the variations in these molecules' concentrations [233]. Ushia-Fukari et al. [227] showed that ROS influence the expression of surface adhesion molecules of ECs and stimulate EC proliferation and vessel permeability. Moreover, the hypoxia-induced decrease in ROS production leads to the inhibition of K^+ channels of pulmonary artery smooth muscle cells (SMCs), whereas an increase in ROS production leads to intracellular Ca^+ release from ryanodine-sensitive stores [233]. Another molecular path found between mitochondrial energy generation and K^+ channel inhibition occurs through AMP kinases. The energy of the cell is generated by the conversion of ADP to one molecule of ATP and AMP. Hence, AMP kinase becomes highly dependent on the ADP/ATP ratio, which is very sensitive to changes in cytoplasmic O_2 concentrations. AMP kinases were shown to inhibit K^+ channels through the regulation of Ca^+ release in pulmonary arterial SMCs and also to induce cellular survival in tumor cells when exposed to severe hypoxia [63, 171].

Moreover, heme oxygenases (HOs) and NADPH oxidases (NOXs) play important roles in the biosynthetic oxygen sensing of cells. NOX-2, one of the three isoforms of NOX, is used for superoxide production from molecular O_2. Hypoxic conditions can cause a decrease in NOX-2-derived ROS concentrations, due to the low K_m values (18 μM) of NOX-2; this helps Ca^+ release in pulmonary artery SMCs [239]. However, some studies also suggest that hypoxia increases NOX-2 activity, therefore causing the generation of a greater amount of ROS [233]. On the other hand, Ca^+-activated K^+ channels in glomus cells were shown to be related to the activity of HO-2, an isoform of HO which can convert heme to CO, biliverdin, and Fe(II) using O_2 and NADPH [237].

The effectiveness of an oxygen sensor can be determined by evaluating (a) its sensitivity to small changes in intracellular O_2 levels and (b) the subsequent diversity of triggered cellular responses. Taking this considerations into account, PHDs and FIHs appear to be the most critical oxygen sensors responsible for controlling HIF activity [94]. Deactivation of these two sensors leads to HIFα stabilization, initiating the regulation of hundreds of different genes. Using O_2 as a controlling parameter to engineer vascular tissues demands a clear understanding of the biochemical events that follow changes in O_2 tension, as well as the net response of the cells and how O_2 affects their collective behaviors.

4.2.1.2 Cellular Responses to Different Oxygen Concentrations

Metabolism and Oxygen Uptake Rate

Several studies have observed that the O_2 consumption of cells depends on O_2 availability [1, 26, 171, 210]. We have recently shown that the O_2 uptake rates (OURs) of EPCs and human umbilical vein endothelial cells (HUVECs) are similar, but not identical, to each other and that both decrease when O_2 availability is lowered (Fig. 4.1a) [1]. Many mechanisms have been proposed to explain the relationship between mitochondrial O_2 consumption and variations in O_2 levels. HIF1α was found to be responsible for inducing the enzymes required for glycolysis [171]. It also plays a role in activating pyruvate dehydrogenase kinase-1, which reduces the

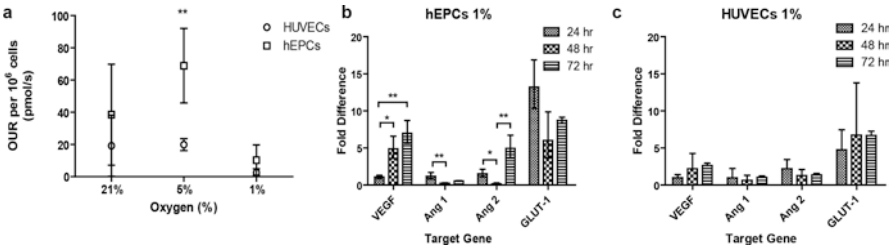

Fig. 4.1 O_2 tension regulates vascular cell responses. Comparison of EPCs and HUVECs at three different O_2 tensions in terms of (**a**) oxygen uptake rate (OUR) and (**b**, **c**) gene regulation [1]

amount of pyruvate that flows into the TCA cycle and therefore decreases aerobic respiration in mitochondria [171]. In addition, the increases in both the transcription and expression of glucose transporter protein 1 (GLUT-1) were shown to be HIF1α-dependent in hypoxic conditions [7]. In other words, deactivation of PHDs and FIHs at low O_2 levels leads to the stabilization of HIFα, which then reduces O_2 aerobic respiration by inducing pyruvate degradation while, at the same time, promoting glycolysis by increasing the expression of glucose transporter proteins. Another proposed mechanism involves the inhibition of cytochrome oxidase by NO, which is known to be regulated by shear stress and O_2 tension. NO influences mitochondrial respiration by the competitive inhibition of cytochrome oxidase with O_2 and by inhibiting electron transfer between cytochrome b and c, therefore increasing ROS production [26].

The effects of blood flow and O_2 tension are crucially important for the ECs comprising the vessel walls, since these conditions can be perturbed in many pathophysiological situations in the body. Some studies have shown mitochondrial respiration of ECs to be lower than other cell types, suggesting that most of the O_2 consumption is non-mitochondrial [78, 223]. Helmlinger et al. demonstrated that ECs consume O_2 during capillary formation, whereas they also preserve and expand the capillary structures, even under severe hypoxia (about 0.6% O_2), by upregulating VEGF expression [93]. It is not surprising that ECs possess a special type of metabolism—aerobic glycolysis in their resting state (physiological conditions) and anaerobic glycolysis in their navigating state (hypoxic conditions)—since O_2 is transported through ECs to other tissues, and thus they must possess the ability to survive and commence angiogenesis under hypoxic conditions [70].

Moreover, when ECs are exposed to excess glucose, their ATP generation shifts to glycolysis, and lactate levels, increased as a by-product of glycolysis, contribute to the inactivation of PHDs and, therefore, the stabilization of HIFα [240]. Where blood flow is perturbed, such as in ischemia and wound healing, both NO and O_2 levels are changed in blood vessels, and all of the metabolic variations discussed become more important.

Transcription of Angiogenic Genes

Manalo et al. showed in their study of ECs that 245 genes are upregulated and 325 genes are downregulated at least 1.5-fold in response to hypoxia and HIF1α. These genes are responsible for the expression of collagens, GFs, receptors, and transcription factors, all of which are significant for the processes of angiogenesis and vasculogenesis. This wide range of hypoxia-related transcription factors also indirectly affects HIF1α. The genes directly regulated by HIF1α include VEGF-A, VEGFR-1, Flt1-1, and erythropoietin (EPO). Examples of indirectly regulated genes include fibroblast growth factor (FGF), placental growth factor (PLGF), platelet-derived growth factor (PDGF), angiopoietins (ANG-1 and ANG-2), and Tie-2, the receptor of ANGs [68]. Although VEGF is the major GF that stimulates blood vessel formation, when it alone was transgenically overexpressed in mice, defective blood

vessels formed, which then led to tissue edema and inflammation [184]. On the other hand, overexpressing both VEGF and ANG-1, which is important for maintaining vascular integrity, has been shown to induce hypervascularity without imperfections in mice [218]. ANG-2 is responsible for EC apoptosis and vascular regression in the absence of VEGF, whereas, when combined with VEGF expression, it enhances angiogenic responses by destabilizing the blood vessels [100, 101]. More recently, ANG-4 was shown to function similarly to ANG-1 and to induce angiogenesis by binding the ANG receptor TIE-2, which is also upregulated by HIF1α [241]. We have recently shown that VEGF and ANG-2 genes are upregulated in hypoxic (1% O_2) cultures of EPCs and HUVECs [1], and the fold differences in upregulation levels of VEGF and ANG-2 in EPCs were shown to vary during the 3-day exposure period (Fig. 4.1b), where no significant change was observed for HUVECs (Fig. 4.1c). How hypoxia affects the regulation of these angiogenic genes depends on the cell type; for instance, VEGF is upregulated in ECs, SMCs, cardiac fibroblasts, and myocardiocytes, whereas ANG-2 is induced only in ECs [159]. Therefore, from a tissue engineering perspective, co-culturing of different cell types under controlled hypoxic conditions should be considered, since a combination of hypoxia-induced angiogenic proteins is required to obtain vascular formation without excessive permeability.

Cell Death and Survival

Hypoxia influences the proliferation and viability of many cell types [1, 69, 172, 245]. The wide spectrum of HIF1α-dependent genes also includes proapoptotic and prosurvival genes. BH3-only proapoptotic genes, a subfamily of BCL-2 that includes BNIP3, BNIP3L, NOXA, RTP801, and HGTP-P, are directly activated by HIF1α [234]. Although these genes play important roles in cellular apoptosis, a growing body of evidence suggests that hypoxia mediates cellular survival in many cell types [160, 172, 245]. Programmed cell death is, of course, a very critical step for cells and is most likely taken only after all possible survival mechanisms have been exhausted. One of these mechanisms, autophagy, is a cellular catabolic process where cytoplasmic organelles are degraded to provide ATP generation in nutrient deprivation. Hypoxia was found to induce mitochondrial autophagy via both HIF1α-dependent and HIF1α-independent pathways [172, 245]. Small interfering RNA silencing of BNIP3 and BNIP3L together suppresses autophagy to a greater extent than silencing only one of them at a time [20]. Zhang et al. have shown that mitochondrial autophagy is induced by HIF1α-dependent upregulation of BNIP3 incorporated into the constitutive expression of BECLIN-1 and ATG-5 [245]. On the other hand, the neuron-derived orphan receptor (NOR-1), which is overexpressed in ECs exposed to hypoxia, mediates cellular survival as a downstream effector of HIF1α signaling [160]. CD105, one of the EC markers also shown to play a role in cellular survival, is significantly upregulated under hypoxia [146]. In vivo studies of rats subjected to hypoxia also found the induction of mitochondrial autophagy by overexpression of BNIP3 [17]. In addition, Papandreou et al. propose

that hypoxia induces autophagy in tumor cells through AMP kinase, which is activated by hypoxia independently of HIF1α, as discussed previously in the O_2 sensing section [172].

4.2.1.3 Cell Pluripotency and Differentiation

Vasculogenesis takes place in low O_2 environments, such as the early development of the embryo, EPC regeneration in the BM, or EPC attachment and differentiation into mature ECs at neovascularization sites. All of these processes rely on pluripotent/unipotent cells differentiating into the endothelium, where O_2 tension is a crucial parameter regulating their differentiation characteristics. As already discussed, EPC regeneration in the BM depends on cellular dynamics between the osteoblastic niche (low O_2) and vascular niche (high O_2); HSCs are quiescent in the osteoblastic niche and differentiate into EPCs in the vascular niche before joining the circulation [111]. Therefore, it is important to understand the effect of O_2 tension on the differentiation of cells into EPCs/ECs as a primary step of vasculogenesis. Hypoxia enhances human embryonic stem cell (hESC) pluripotency via the upregulation of Oct-4, NANOG, and SOX-2, which are pluripotent markers [45, 64, 69, 116]. HIF2α is responsible for the overexpression of Oct-4, SOX-2, and NANOG, while HIF3α also plays a role in the process by inducing HIF2α transcription [45, 69]. Prasad et al. demonstrated that hypoxic conditions (5% O_2) prevent the spontaneous differentiation of hESCs, whereas the inhibition of Notch activation revoked this effect, suggesting that hypoxia-induced pluripotency occurs via Notch signaling [182]. On the other hand, the efficiency of the process of reprogramming mouse and human somatic cells into induced pluripotent stem cells (iPSC) was shown to be improved in 5% O_2 cultures, compared to atmospheric O_2 cultures [243]. In contrast, other studies have demonstrated that hypoxia induces the expression of early cardiac genes in spontaneously differentiating embryoid bodies (EBs) [125, 168]. In a more recent study, Lopez et al. showed that EPCs/ECs can be obtained from hESCs more efficiently when cultured in 5% O_2, compared to previous methods that induce EB formation in atmospheric O_2 [181]. Additionally, simply priming EBs in hypoxic conditions mediated suppression of pluripotent marker Oct-4 and upregulated VEGF [140]. When hPSCs are differentiated toward an endothelial lineage, hypoxia has also been shown to enhance EC differentiation through changes in the early stages (mesodermal specification) of EC lineage commitment. Interestingly this affect, which was dependent on low O_2 tension, was driven by production of ROS [135]. More in-depth investigations have uncovered the specific role of NADPH oxidase 2 (Nox2)-produced ROS in upregulating Notch signaling to facilitate differentiation toward arterial endothelial cells [119]. Another group showed a biphasic regulation of EC fate specification via a HIF1α-mediated pathway in mESCs. Hypoxia led to upregulation of the transcription factor Etv2 in the early stages of differentiation, which resulted in development of endothelial progenitor cells. Continued exposure to hypoxia led to HIF1α-induced upregulation of Notch1 signaling and formation of functional arterial endothelial cells, with

the capacity to contribute to revascularization of ischemic tissues [224]. Similarly, HIF1α also induces the differentiation of peripheral blood mononuclear cells into EPCs, and hypoxia stimulates the further differentiation of EPCs into mature ECs [8, 117].

All of these findings highlight the significance of O_2 tension as a critical parameter to control vascular differentiation of pluripotent or multipotent cells. Although some of these studies suggest contrary hypotheses, the importance of O_2 considerations in cell culture environments cannot be overstated, as O_2 tension can be manipulated to prevent spontaneous differentiation of pluripotent cells and to enhance the efficiency of the differentiation into EPCs and mature ECs.

4.2.2 Vascular Responses to ECM

In the human body, vascular cells are surrounded by diverse components of the ECM, the unique spatial and temporal distribution of which affects GF availability and matrix properties which, in turn, regulate vasculogenesis and angiogenesis. Just like oxygen tension, which varies throughout vascular development, ECM components are also uniquely distributed; for example, hyaluronic acid (HA; also known as hyaluronan) levels were found to be highest during embryogenesis and to be replaced by fibronectin and then collagen, which remains abundant throughout adulthood. In this section we will discuss ECM distribution and its effects on vascular development and maintenance. Then, we will discuss various ECM components that affect vascular morphogenesis. Lastly, we will describe strategies for manipulating the ECM using synthetic biomaterials and emerging technology.

4.2.2.1 Types of ECM Found Participating in Vascularization

The ECM surrounding blood vessels contributes significantly to their diverse functions and complexity. This ECM diversity encompasses different vascular development periods (i.e., embryonic versus adult) and specialized vessels at various locations in the body (i.e., capillary, arteriole, and venule) or tissues in the body (i.e., heart, kidney, lung, etc.). During early vascular development, the ECM provides informational cues to the vascular cells, thus regulating their differentiation, proliferation, and migration. Fibronectin and HA, which are major components of the embryonic ECM, have been shown to be vital regulators for vascularization during embryogenesis [222]. Fibronectin, a unique glycoprotein, contains cell adhesion and heparin-binding sites that synergistically modulate the activity of VEGF to enhance angiogenesis [236]. Various lineage studies have found developmental abnormalities in embryonic hearts and vessels in fibronectin-null mice, suggesting its crucial role in mediating EC interactions [14, 71]. The levels of hyaluronan, a nonsulfated linear polysaccharide, are greatest during embryogenesis and then decrease at the onset of differentiation [221], where it plays a crucial role in

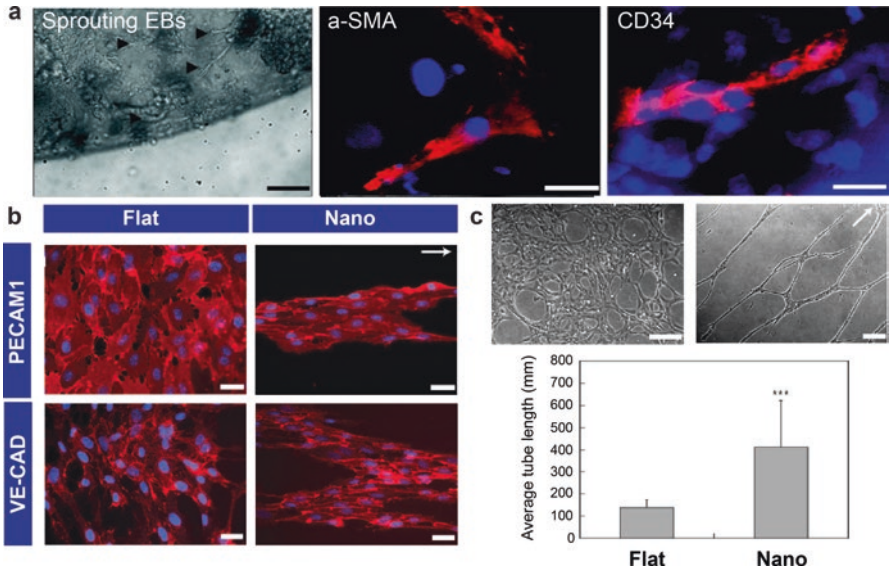

Fig. 4.2 Matrix composition and orientation affect vasculogenesis. (**a**) Hyaluronic acid microenvironment for vasculogenesis. Human ESC colonies were cultured in conditioned medium for 1 week, followed by the replacement of medium containing 50 ng/ml $VEGF_{165}$. Left: Cell sprouting was observed after 48 h of culture in medium containing VEGF (indicated by arrowheads). Middle and right: After 1 week of differentiation, sprouting elongating cells were mainly positive for alpha-smooth muscle actin (a-SMA) (middle), while some were positive for the early-stage endothelial marker CD34 (right). Scale bars—left, 100 μm; middle and right, 25 μm. Printed with permission [79]. (**b**) Nanotopography induces the formation of supercellular band structures in long-term EPC culture. EPCs cultured on flat substrates began forming confluent layers of cells after 6 days of culture. In contrast, EPCs cultured on nanotopography began to form supercellular band structures aligned in the direction of the features (as indicated by the arrow) after 6 days of culture. These morphological differences are evident through staining of PECAM-1 and VE-CAD. Scale bars are 50 μm. Printed with permission [23]. (**c**) Organized capillary tube formation in vitro. Capillary-like structures (CLSs) were induced by the addition of Matrigel after 6 days. EPCs cultured on flat substrates (upper left) formed low-density unorganized structures, while EPCs cultured on nanotopographic substrates (upper right) formed extensive networks of organized structures with (lower panel) longer average tube lengths than EPCs cultured on flat substrates (*** $p < 0.001$). The direction of the linear nanotopographic features is indicated by the arrow. Scale bars are 200 μm. Printed with permission [23]

regulating vascular development [18]. Hyaluronan and its receptor, CD44, have been shown to be essential in the formation and remodeling of blood vessels [18, 30, 62]. We have previously reported that a completely synthetic HA hydrogel can maintain the self-renewal and pluripotency of hESCs [79, 86, 87]. Interestingly, when VEGF is introduced into the culture media, this unique HA microenvironment can direct the differentiation of hESCs into vascular cells, as indicated by positive staining for α-smooth muscle actin and an early stage of the endothelial cell marker, CD34 (Fig. 4.2a). More recent studies have employed higher throughput methods to explore the effects of ECM composition on EC fate. As the ECM of the developing

embryo consists of multiple components, culturing ECs on combinatorial ECM arrays revealed optimal conditions for EC survival, in response to low O_2 and low nutrient availability [104], as well as enhancements in EC fate which were regulated by ECM composition, at least partially through upregulation of integrin β3 and its associated signaling pathway [105].

In contrast, the adult ECM consists mostly of a laminin-rich basement membrane, which maintains the integrity of the mature endothelium, and interstitial collagen I, which promotes capillary morphogenesis [50]. Although collagen I is present during development, its role becomes increasingly important in postnatal angiogenesis, after its reactive groups have been cross-linked to further stabilize the interstitial matrix [186]. EC integrins, which interact with collagens and fibrin, are key receptors in EC activation, proliferation, and tubular morphogenesis. The collagen-I-mediated activation of Src and Rho and the suppression of PKA promote the formation of prominent actin stress fibers, which mediate EC retraction and capillary morphogenesis. Moreover, the activation of Src also disrupts VE-cadherin from cell junction and cell-cell contact which, in turn, facilitates multicellular reorganization. Conversely, basement membrane laminin-1 is responsible for maintaining the mature endothelium. During the proliferative stage of morphogenesis, the laminin-rich basal lamina is degraded, exposing the tips of sprouting ECs to the underlying interstitial collagens and activating signaling pathways that drive cytoskeletal reorganization and vascular morphogenesis. This sharp difference in how ECM components affect capillary morphogenesis is responsible for controlling the delicate balance between vascular sprouting and maturation.

Once nascent vessels are formed, ECM components regulate their maturation and specialization into capillaries, arteries, and veins. Capillaries, the most abundant vessels in our body, consist of ECs surrounded by pericytes and basement membrane. Exchanges of nutrients and oxygen occur through diffusion between blood and tissue in these regions, due to the capillary's thin wall structure and large surface-area-to-volume-ratio. Maturation of the vessel wall involves the recruitment of mural cells, development of the surrounding matrix, and organ-specific specialization [113]. ECM distribution in various tissues dictates the specialization of these capillaries to support the functions of specific organs. The capillary endothelial layer is continuous in most tissues (e.g., muscle), while it is fenestrated in exocrine and endocrine glands (e.g., kidney and pancreas). Moreover, the enlarged sinusoidal capillaries of the liver, spleen, and BM are discontinuous, allowing increased exchange of hormones and metabolites between the blood and the surrounding tissues. In contrast, where the excess exchange of molecules is not desirable, such as at the blood-brain barrier and the blood-retina barrier, the interendothelial connection is further reinforced with tight junctions, such as occludin and ZO-1 [238].

Compared with capillaries, arterioles and venules have an increased coverage of mural cells and ECM components. Arterioles are completely surrounded with vascular SMCs that form a closely packed basement membrane. The walls of larger vessels are composed of three layers: the tunica intima, the tunica media, and the tunica adventitia. The EC layer of blood vessels is anchored to a basement membrane, which is the major component of the tunica intima [57]. The basement mem-

brane contains network-organizing proteins, such as collagen IV, collagen XVIII, laminin, nidogen, entactin, and the proteoglycan perlecan. The tunica media contains vascular SMCs (v-SMCs) and elastic tissue composed of elastin, fibrillins, fibulins, emilins, and microfibril-associated proteins. The tunica adventitia contains fibroblasts and elastic laminae and has its own blood supply, known as the vasa vasorum [57]. SMCs and elastic laminae contribute to the vessel tone and regulate vessel diameter and blood flow. This generic blood vessel architecture is modified with various ECM components to fulfill their individual tasks. Arteries, which function to deliver oxygenated blood, usually have a thick tunica media with numerous concentric layers of v-SMCs, whereas veins have a thick tunica adventitia layer enriched in ECM components with elastic properties, such as elastin and fibrillin.

As described, the composition of the ECM is inherently dynamic throughout development as well as vascular regeneration, positing the importance of remodeling and deposition of new ECM as these processes progress. Additionally, stability of mature vessels requires a different ECM composition than developing or regenerating vasculature. Several studies have highlighted these changes in ECM deposition and have identified regulators of these important mechanisms. Much of the work to date has established the role of perivascular cells, including pericytes and smooth muscle cells, in ECM production [232]. Crucially, ECs also produce ECM as blood vessels form. Of particular interest, endothelial progenitor populations and mature ECs produce ECM differently; EPCs produce collagen IV, fibronectin, and laminin, while mature ECs have limited ECM production in standard cell culture conditions. However, when subjected to hypoxic conditions, mature ECs adopt an ECM secretome similar to the pro-regenerative EPCs, wherein they secrete collagen IV, fibronectin, and laminin at low O_2 (1%). At moderate hypoxia (5% O_2), both cell types produce collagen I [134]. When developing engineered vasculature, these factors are critical to consider to obtain mature, long-lasting blood vessels, as ECM composition is an important parameter governing vascular stability.

4.2.2.2 Properties of the ECM that Affect Vascular Morphogenesis

Recent decades have vastly expanded our understanding of how ECM properties affect vascular assembly, primarily due to newly available, well-defined in vitro models. The most common models are cultures of ECs in gels made of different ECM components, such as collagen, fibrin, fibronectin, and Matrigel. These ECM components contain instructive physical and chemical cues that direct vascular morphogenesis, which involves several steps: (1) proteolytic degradation of basement membrane proteins by both soluble and membrane-bound matrix metalloproteinases (MMPs); (2) cell activation, proliferation, and migration; (3) vacuole and lumen assembly into a tube with tight junctions at cell-cell contacts; (4) branching and sprouting; (5) synthesis of basement membrane proteins to support the formation of capillary tube networks; and (6) tube maturation and stabilization by pericytes. These complex processes require a delicate balance between various immobilized and soluble GFs, as well as endothelial and perivascular cell

interactions. Gels made from ECM components, engineered to have properties resembling those of native tissues, have been widely explored as a tool to study the molecular regulation underlying vascular development [49] and as a scaffold to transplant vascular progenitor cells [15, 46, 164]. However, their manipulation for vascular tissue engineering has been narrowly limited by their inherent chemical and physical properties. Therefore, a great need exists to chemically modify these ECM components [40, 130] or to utilize biomaterials to form scaffolds from hydrogels, which are xeno-free and instructive for vascular tissue engineering [152]. Hydrogels are cross-linked polymer networks which can store a large amount of fluid and which have biophysical properties similar to many soft tissues [138]. Hydrogels can be engineered from natural biomaterials (including ECM components), artificial protein polymers, self-assembling peptides, and synthetic polymers to form scaffolds which mimic the native ECM. For example, dextran and chitosan, natural biomaterials with similar structures, do not possess any inherent cross-linking ability [214, 215]. However, a simple chemical modification, such as introducing double bonds into the repeating unit, allows the cross-linking of these polysaccharides to form hydrogels. Alginate is another natural material which can be physically cross-linked by adding cations (e.g., Ca^{2+} or Mg^{2+}) [80]. Another approach utilizes a purely synthetic polymer, like polyethylene glycol (PEG) or poly-[lactic-co-glycolic acid] (PLGA), whose physical and chemical properties can be easily manipulated. A simple modification can turn PEG, a cell-resistant material, into an instructive scaffold designed to promote vascularization [58, 59, 166, 176]. Furthermore, the synthetic material of choice must be biodegradable and biocompatible, and such physical properties as pore size, degradation kinetics, and matrix mechanical properties must be easily tunable to favor vascular morphogenesis. Bioactive molecules—like GFs, cell adhesion motifs such as arginine-glycine-aspartic acid (RGD), and MMP-sensitive peptides—must be presented with correct spatial and temporal distributions within the synthetic biomaterials. Next, we will discuss several strategies for manipulating the chemical and physical properties of synthetic biomaterials.

Cell Adhesion Regulates Neovascularization

In order to support vascular cells and instruct them to undergo vascular morphogenesis, synthetic biomaterials must first be able to provide cell adhesion. Instead of incorporating ECM components to make such materials bioactive, certain synthetic peptides important for vascular morphogenesis can be incorporated into these inert synthetic materials. The most common template is the integrin-binding domain of fibronectin, RGD [178], and the laminin-derived peptide IKVAV [203]. The first crucial step in vascular morphogenesis occurs when vascular cells utilize integrin receptors to sense their surrounding microenvironments. Integrins are transmembrane receptors which not only maintain cell adhesion to ECM but also control cell proliferation, migration, differentiation, and cytoskeletal organization. Since blood vessels must be able to assemble in diverse tissue environments (e.g., adult versus

embryo and muscle versus kidney), which have different distributions of ECM components (as discussed in the previous section), it is evident that both β_1 and α_v integrins can support vascular morphogenesis. For example, $\alpha_v\beta_3$ and $\alpha_2\beta_1$ integrins associate with vascular morphogenesis in collagen-rich ECM, like adult tissue, while $\alpha_5\beta_1$ and $\alpha_6\beta_1$ integrins involve fibronectin- and fibrin-rich ECM, like in embryonic tissue and healing wounds [50]. The binding of integrins onto RGD triggers several downstream signaling events mediated by Rho GTPase, particularly Rac1 and Cdc42 [49]. Extensive work by Davis and his colleagues revealed the molecular mechanism that regulates this EC morphogenesis in fibrin and collagen gels (an excellent review of their work can be found in Chap. 20 of this book). This mechanism has also been observed and controlled in synthetic (HA-based) hydrogels [89].

To further substantiate the role of cell-ECM interactions, particularly those mediated by integrin engagement, several groups have identified the importance of integrin specificity in vascular regeneration. In tumor vessels, $\alpha_v\beta_3$ is preferentially expressed, leading to formation of new, albeit disorganized, leaky vasculature [53]. In order to establish organized, mature neovessels, engagement of $\alpha_3/\alpha5\beta1$, rather than $\alpha_v\beta_3$, was necessary [147]. While RGD peptides facilitate cell adhesion in synthetic matrices, it is important to consider the non-specific integrin engagement potential of these peptides, which may influence vascular regeneration.

The number of RGD adhesion sites and the method of their presentation to the vascular cells are also crucial in affecting cell migration [82] and vascular morphogenesis [110]. Using an in vitro angiogenesis model, Folkman and Ingber were able to show that, when cultured on a moderate coating density that only partially resisted cell traction forces, ECs could retract and differentiate into branching capillary networks [67, 110]. High ECM density was saturated with RGD adhesion peptide, which allowed the ECs to spread and proliferate, while low ECM density resulted in rounded and apoptotic cells. Interestingly, in medium ECM density, with the appropriate RGD adhesion peptide, ECs collectively retracted and differentiated into branching capillary networks with hollow tubular structures. It is evident that the ECs exerted mechanical forces on the surrounding ECM to create a pathway for migration and branching in forming vascular structures [48]. Hence, both the quantity of RGD peptide and the method of presentation within the engineered synthetic biomaterials determine the initial morphogenetic events in angiogenesis.

Scaffold Degradation Regulates Vascular Morphogenesis

Scaffolds made from ECM components, like collagen and fibrin gels, contain proteolytic degradable sequences which can be degraded by the MMPs and other proteases (e.g., cathepsins) secreted by vascular cells. This cell-mediated degradation controls both structural integrity and temporal mechanical properties, which dictate the presentation of chemical and mechanical cues at various stages of angiogenesis. However, the degradation kinetics of these ECM-based scaffolds is determined by their inherent cross-linking density which, in turn, limits their manipulation for vascular tissue engineering. In contrast, synthetic biomaterials can be engineered to

have degradation profiles ranging from days to months, in order to suit the specific needs of the engineered vascularized tissue constructs [215]. The polymer backbone can be cross-linked using a nondegradable cross-linker that provides structural integrity and/or a degradable cross-linker that allows directed cell migration and vascular morphogenesis. Hydrolytic degradation by the body fluid can break down the ester bonds within the polymer backbone, allowing tissue infiltration over time [214, 215]. MMP-sensitive peptides can also be used to cross-link hydrogels, allowing cell-mediated degradation, leading to a rapid response of vascular growth. Overall, by adjusting the percentages of nondegradable and degradable cross-linkers, scaffold degradation can be tuned to allow cellular infiltration, lumen formation, and ECM synthesis and distribution.

In order for the intracellular vacuoles to coalesce into a lumen, ECs require adhesive ligands for traction [152] and utilize membrane-type-1 MMPs (MT1-MMPs) to create physical spaces which facilitate the directed migration of cells to align with neighboring cells [48, 192, 212]. Therefore, ECs can only invade this synthetic scaffold if the minimal pore size is larger than the cell diameter (e.g., a soft self-assembling peptide) [201] or if the scaffold bears an MMP-degradable sequence [153]. The Hubbell research group has pioneered this approach by incorporating an MMP-degradable sequence as a cross-linker into PEG scaffolds to promote vascular healing and therapeutic angiogenesis [196, 249]. When grafted in vivo, ECs were able to invade, remodel, and vascularize this MMP-sensitive scaffold [248, 249]. Using concepts from this work, synthetic (HA-based) biomaterials utilized spatial control of degradation through photopatterning to organize vascular morphogenesis (Fig. 4.3) [90]. Hence, incorporating MMP-degradable peptides is essential for directing vascular morphogenesis in 3D synthetic biomaterials.

Physical Orientation of the ECM

The native ECM provides an instructive template for ECs and perivascular cells to orient, interact, and organize into tubular structures. Studies have demonstrated that a stable vasculature could be achieved by co-transplantation of ECs and perivascular cells, such as MSCs or SMCs [15, 16, 128, 142, 164]. Recent studies showed that engineering a stable vascularized tissue construct requires the triculture of ECs, fibroblasts, and tissue-specific cells, such as cardiac or skeletal muscle cells [31, 142]. Perivascular cells, such as fibroblasts, stabilize the developing vascular tube through physical support, by differentiating into v-SMCs and wrapping around the nascent tube [114, 229], and chemical support, by secreting Ang-1, PDGF-BB, and tissue inhibitor of metalloproteinase-3 (TIMP-3) [95, 97]. These perivascular cells are also responsible for laying down ECM components in early embryogenesis and continue to do so throughout adulthood. Many studies using fibroblast-derived matrices have further revealed the 3D complexity of these ECM networks [206–208]. A study by Soucy and Romer showed that fibroblast-derived matrix alone is sufficient to induce HUVECs to undergo vascular morphogenesis, independent of any angiogenic factors. Further analysis of protein colocalization suggested that

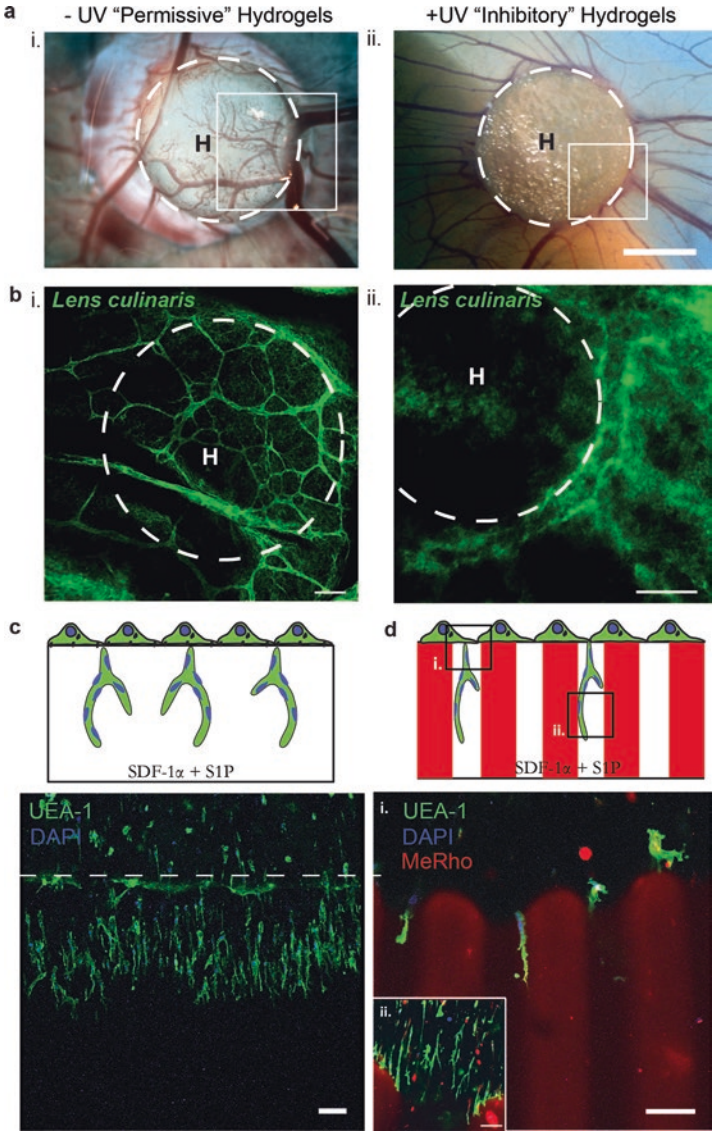

Fig. 4.3 Spatial control of vascular morphogenesis in synthetic hydrogels. (**a**, **b**) Uniform −UV (permit cell-mediated degradation) and +UV (inhibit cell-mediated degradation) hyaluronic acid (HA) hydrogels are grafted onto the CAM membrane. (**a**) LM imaging and (**b**) confocal analysis of the boxed regions in **a** shows CAM vessels penetrating into the −UV but not into the +UV hydrogels. CAM vessels are stained with Fluorescein-conjugated *Lens culinaris* lectin. Scale bars in **a**, 20 mm, and **b**, 100 μm. H = hydrogels. Dotted white lines indicate the boundaries of the hydrogels. (**c**) ECFCs are seeded on top of a uniform −UV (**c**) and 100 μm stripe photopatterned (**d**) HA hydrogels for an angiogenesis assay. After 3 days in culture, ECFCs invade and sprout into the 3D hydrogels (**c**). When photopatterned HA hydrogels are used, invasion and sprouting are observed only within the −UV regions and not within the inhibitory +UV region (**d**). Confluent monolayer of ECFCs sprouts and invades the −UV region (i) and further branches along the −UV regions (ii). The +UV regions are labeled using MeRho (*red*); ECFCs are stained with fluorescein-conjugated *UEA-I* lectin (*green*) and DAPI (*blue*). Scale bars are 100 μm. Reproduced and re-formatted with permission [90]

fibronectin with a distinct structure and organization was uniquely distributed among other secreted matrix components, such as collagen, tenascin C, versican, and decorin. Cell matrix adhesions and MT1-MMP activities were reported to orient and localize within this fibrous fibronectin, which is indicative of integrin-mediated vascular morphogenesis [190]. In fact, ECs initiate neovascularization by unfolding soluble fibronectin and depositing a pericellular network of fibrils that serve as a structural scaffolding on a mechanically ideal substratum for vessel development [247]. We have studied how such fibronectin organization influences endothelial tube formation by patterning fibronectin on cell culture surfaces to optimize vasculogenic potential and understand how microstructure influences vascular tube formation [54]. Alignment of other important ECM proteins, such as collagen, has also been shown to guide vascular regeneration by enhancing EC organization and migration [136]. Interestingly, similar effects in vascular organization are observed when tensile forces are incurred upon vascular fibrin-based constructs, where vascular network alignment was induced by application of force. Aligned microvasculature was shown to enhance vascular integration upon implantation in abdominal muscle [191]. This last study suggests a potential mechanism for organization of ECM components to guide vascular network organization through force-induced remodeling. It is likely such a mechanism is coupled with ECM degradation and secretion of new ECM components to establish a microenvironment amenable to the formation of new blood vessels.

The unique orientation, organization, and nanotopography of fibrous fibronectin represent features that can be integrated into synthetic scaffolds. Synthetic polymers, like PLGA and polycaprolactone (PCL), can be electrospun to produce various fiber sizes with micro- to nanoscale features that resemble fibrous fibronectin. We previously showed that surface nanotopography enhanced the formation of capillary-like structures (CLSs) in vitro [23]. Growing EPCs on grooves that were 600 nm wide reduced their proliferation and enhanced their migration without changing the expression of EC markers. Moreover, after 6 days of culture, the EPCs organized into superstructures along the nanogrooves, in significant contrast to the EPCs grown on planar surfaces (Fig. 4.2b). The addition of Matrigel further induced the formation of CLSs, with enhanced alignment, organization, and tube length compared to a flat surface (Fig. 4.2c). This underscores the increasingly important role of nanotopography in guiding and orienting vascular assembly. When integrated into the tissue-engineered construct—for instance, using filamentous scaffold geometry [75] and micropatterning [55, 108, 165]—the orientation and structure of the engineered vasculature can be controlled.

Regulating Matrix Mechanics

It has become increasingly evident that the biomechanical properties of the ECM, such as matrix orientation and mechanics, profoundly influence the control of vascular morphogenesis. Due to their versatility with respect to mechanical properties (e.g., cross-linking density, pore sizes, and topography), synthetic biomaterials have

powerful features that can be exploited to further direct vascularization. Changes in ECM mechanics can lead to changes in GF availability [40, 110], drive capillary morphogenesis [109], and stimulate angiogenesis in vivo [122]. By altering matrix adhesive characteristics and mechanics, Ingber and Folkman illustrated how bFGF-stimulated ECs can be switched between growth and differentiation during angiogenesis [110]. Recently, biomechanical cues from the ECM and signals from GF receptors have been implicated in regulating the balance of activity between TFII-I and GATA2 transcription factors, which govern the expression of VEGFR2 to instigate angiogenesis [158]. Matrix stiffness regulates not only the cell's response to soluble GFs but also cell morphogenesis during angiogenic sprouting. Primarily due to MMP activity, the tip of a new capillary sprout becomes thinner, locally degrading the basement membrane proteins. This region, with its high rate of ECM turnover and thin basement membrane, becomes more compliant and stretches more than the neighboring tissue. Consequently, the decrease in matrix stiffness changes the balance of forces across the cell integrin receptors, increases cell tension, and results in cytoskeletal arrangement to form branching patterns that are characteristic of all growing vascular networks [109].

The pioneering work by Deroanne et al. showed that a decrease of matrix stiffness increased capillary branching and the elongation of tubes. A reduced tension between ECs and ECM, accompanied by a profound remodeling of the actin-FAP complex, is sufficient to trigger an intracellular signaling cascade leading to tubulogenesis [52]. This observation has been further confirmed in collagen gels [52, 200], fibrin gels [211], self-assembling peptides, and HA-gelatin hydrogels.

Although ECM-based gels, such as collagen, fibrin, and Matrigel, have been widely used in angiogenesis assays, their inherent physical properties have limited their usage when studying the effects of matrix mechanics on angiogenesis. The stiffness of ECM-based gels can be increased either by increasing their concentration, which also alters their ligand and fibril density [189], or by altering the cross-linking of ECM proteins in a narrow range using a microbial transglutaminase [244]. Therefore, examining the effects of matrix stiffness alone on angiogenesis requires the use of synthetic hydrogels, the stiffness of which can be easily adjusted over a wide range of moduli without altering other chemical properties. Unlike naturally available ECM-based gels, the elasticity of which is limited to their inherent cross-linking density, synthetic HA hydrogels can be used to study a physiologically relevant range of matrix elasticity [88]. When the cross-linking density of the HA-gelatin hydrogels was further reduced, the matrix elasticity became relatively compliant, resulting in an increase of capillary branching, elongated tubes, and enlarged lumen structures [88]. On a relatively compliant matrix, EPCs can produce fewer MMPs than a stiffer matrix would require and still degrade, exert mechanical tension on, and contract the matrix to enable vascular morphogenesis. On the other hand, EPCs must produce more MMPs on a stiffer matrix, to overcome the extra mechanical barriers; even then, this local decrease in substrate stiffness cannot support vascular morphogenesis (Fig. 4.4). This model also explains the rapid appearance of large functional vessels in granulation tissue, as a response to the wound-healing mechanism [122].

In addition to the effects of matrix stiffness on postnatal vascular regeneration, matrix stiffness has been probed as an important regulator of stem cell fate. Beginning with the pioneering work of Engler et al. [60], studies examining the effects of substrate stiffness and mechanical signaling transduction pathways on stem cell fate have proven instrumental in enhancing our collective knowledge of differentiation schema. To this end, our group has shown that substrate stiffness can govern EC fate through alterations in mesodermal precursors. Similar to the enhancements in EC fate observed upon culture in low O_2 environments (Fig. 4.5a–d) [135], compliant substrates enhance mesodermal differentiation, which results in robust EC differentiation (Fig. 4.5e–i) [205].

A recent illuminating study identified stress relaxation as an important, yet understudied, regulator of mechanical signal transduction. Specifically, in alginate-based hydrogels with the same matrix stiffness and pore size, altering stress relaxation modulated MSC cell fate [34]. While studies of the effect of stress relaxation on EC fate and vascular morphogenesis have not been published, stress relaxation is an important parameter to bear in mind for biomaterial design, particularly because covalently cross-linked hydrogels do not exhibit stress relaxation behavior similar to that of the native ECM.

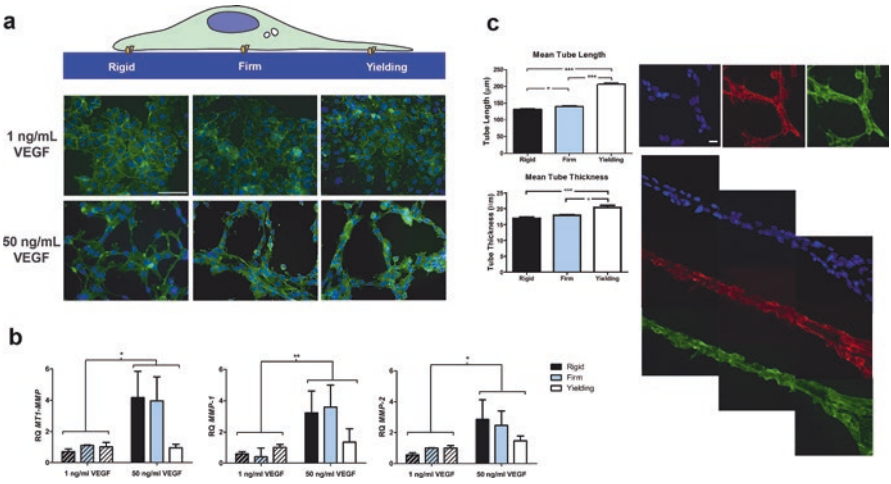

Fig. 4.4 Mechanoregulation of vascularization. (**a**) EPCs were seeded on rigid, firm, and yielding substrates for 12 h, supplemented with 1 ng/ml (low) VEGF (upper panel) and formed CLSs when supplemented with 50 ng/ml (high) VEGF (lower panel), as demonstrated by fluorescence microscopy of F-actin (green) and nuclei (blue). (**b**) Real-time RT-PCR revealed a significantly increased expression of (1) MT1-MMP, (2) MMP-1, and (3) MMP-2 in response to 50 ng/ml VEGF (high) concentration for EPCs cultured on the rigid, firm, and yielding substrates, respectively. As the matrix substrate was reduced, EPCs cultured in medium supplemented with 50 ng/ml (high) VEGF showed a decrease in expression of these MMPs. (**c**) Metamorph analysis of CLSs revealed a significant increase of mean tube length and mean tube area, as substrate stiffness decreased. Confocal analysis of nuclei (blue), VE-CAD (red), and lectin (green) further revealed that branching and hollow tubular structures formed on the yielding substrate. Significance levels were set at $*p < 0.05$, $**p < 0.01$, and $***p < 0.001$. Scale bars (**a**) 100 μm and (**c**) 20 μm. Printed with permission [88]

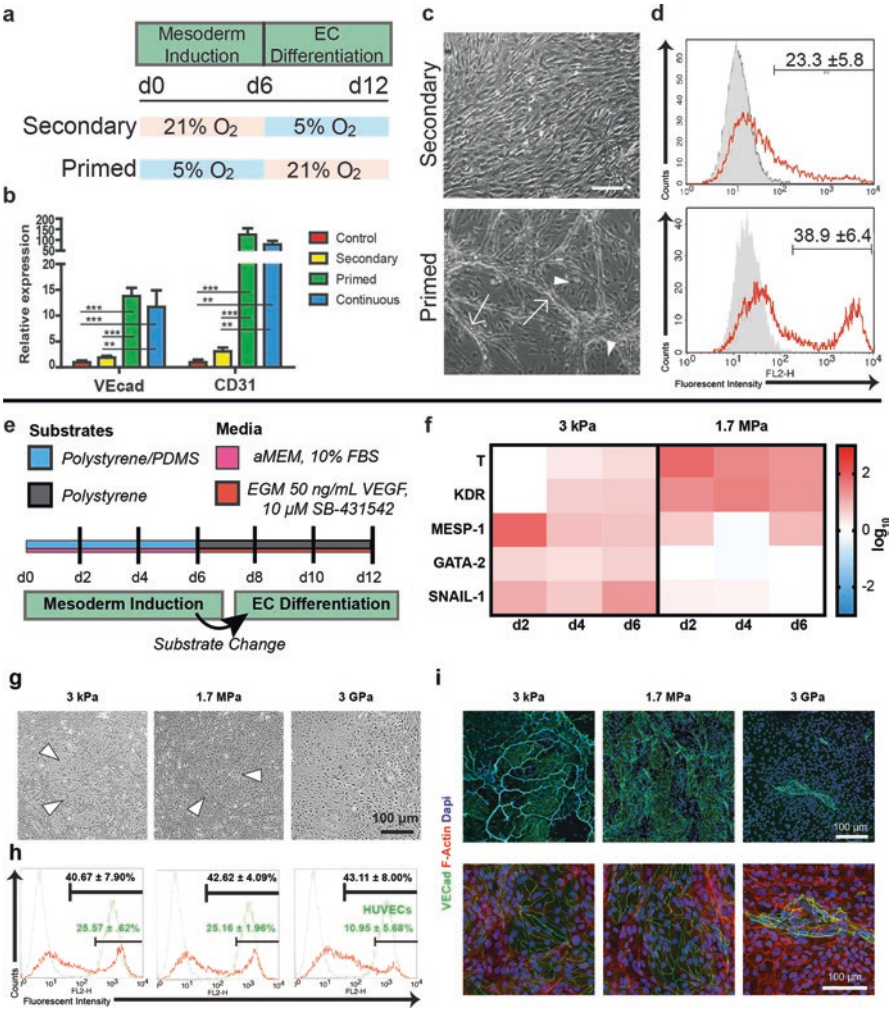

Fig. 4.5 Low O_2 and compliant substrates enhance induction of mesodermal precursor populations, thereby improving EC fate specification. (**a**) Schematic of manipulated O_2 environments studied during differentiation. (**b**) RT-PCR analysis of VEcad and CD31 expression of EVCs differentiated under the four studied oxygen conditions. Comparison of secondary and primed 5% O_2 conditions demonstrated by (**c**) light microscopy images (arrows indicate elongated cell bundles; arrowheads indicate cobblestone area-forming cells; scale bar is 100 μm) and (**d**) flow cytometry for VEcad expression. Isotype control in gray. *p<0.05; **p<0.01; ***p<0.001. (**e**) Schematic of stiffness-primed mesoderm induction followed by EC differentiation on E ~ 3 GPa substrates. a-MEM, a-minimum essential medium; FBS, fetal bovine serum; EGM, endothelial growth medium. (**f**) Gene expression of mesodermal markers for cells differentiated on soft 3-kPa substrates and stiff 1.7-MPa substrates, normalized to expression from E ~ 3 GPa surfaces. Color key is presented in log10 scale. (**g**) Bright-field images of cobblestone endothelial colonies (white arrows) on day 12 EVCs. (**h**) Day 12 EVC flow cytometry plots of VECad expression in red, with corresponding HUVEC VECad expression in green. Black font, VECad+ cells; green font, highly expressing VECad+ cells. Data are presented as means ± SEM. (**i**) Representative immunofluorescence images of VECad expression on day 12 EVCs: low-magnification (top) and high-magnification (bottom) images are shown (green, VECad; red, phalloidin; blue, nuclei). Reproduced and re-formatted with permission [135, 205]

These studies underline the importance of engineering a tissue construct with a matrix stiffness amenable to promote in vivo vascularization. However, investigating how matrix stiffness may affect in vivo vascularization remains challenging due to the complexity of the system, which involves matrix remodeling, host capillary ingrowth, as well as anastomosis of the vascular construct and contributions from other cell types. For example, in vivo vascular ingrowth into Matrigel scaffolds was found to be optimal at intermediate matrix stiffness, in sharp contrast to the observed in vitro ingrowth [158]. Elegant work by Yoder's research group also found that increasing the collagen concentration yielded stiffer scaffolds, which in turn promoted host capillary ingrowth in vivo. Compared to stiffer scaffolds, softer scaffolds might have experienced excessive in vivo remodeling and failed to retain the vascular constructs. Moreover, in vitro angiogenesis studies have found that ECM-based gels produce a much narrower range of stiffness [46, 158] than synthetic hydrogels [88, 158]. Future investigations are needed to evaluate vascularization by both the host capillary and the engineered vascular construct over a wider range of physiologically relevant matrix elasticities. Despite the differences in scaffold composition (ECM-based gels versus synthetic hydrogels), culture conditions (in vitro versus in vivo), assay type (2D versus 3D), and ranges of matrix stiffness, all of these studies highlight the relevance of engineering scaffolds with mechanical elasticity suited to the specific needs of tissue vascularization.

4.2.3 The Effects of Oxygen Availability and the ECM

In this section, we will consider O_2 tension and the ECM as two interdependent factors determining the efficiency of vasculature formation. We will review currently available O_2 measurement techniques and challenges, along with the mathematical modeling approaches used to overcome some of these challenges in describing O_2 gradients in 3D environments. Then, we will discuss cellular adaptations and responses to O_2 availability in 3D ECM constructs and the possible outcomes of variations in O_2 distribution in 3D cultures of vascular cells.

4.2.3.1 Varying Oxygen Tensions in the ECM of Tissue and Matrix Scaffolds: Measuring and Modeling

Oxygen Measurement Techniques and Challenges

Manipulation of oxygen, in order to direct pluripotent or vascular cells to form blood vessels, requires knowing the precise O_2 tension that the cells are exposed to under varying conditions. Many different O_2 measurement techniques have been used in vitro and in vivo. The accuracy of these measurements is fundamental to confidently describe the cellular responses under various O_2 availabilities, as well as to controlling the O_2 tension in order to direct angiogenesis and vasculogenesis. An

O_2 measurement method needs several properties to be considered superior, including accuracy, sensitivity, repeatability, rapidity, and noninvasiveness. Although some methods are used more commonly in a broader range of applications, no "gold standard" exists for all applications, since the method chosen usually depends on the purpose of the measurement. In vivo O_2 measurement methods can be divided into two main categories: (1) direct measurements, where the concentration or the partial pressure of O_2 is directly measured, and (2) indirect measurements, where levels of O_2-indicative molecules (e.g., hemoglobin, cytochrome) are detected and correlated to relative O_2 concentrations.

The most common direct measurements are electrodes, phosphorescent probes, electron paramagnetic resonance (EPR) oximetry, and nuclear magnetic resonance (NMR). Some of the indirect measurement methods involve monitoring of hemoglobin/myoglobin, mitochondrial cytochromes, and NADH/FADH [209]. Springett's paper thoroughly reviews the benefits and limitations of the most recent methods [209].

In addition, in vitro studies have applied these currently available methods to monitor O_2 levels quantitatively, such as by measuring O_2 tensions at the cellular level in 2D monolayer cell cultures or O_2 gradients in 3D gels or scaffolds. Two major methods used to measure O_2 levels during in vitro cultures are polarographic and fluorescence quenching techniques. The latter has been shown to surpass the polarographic technique, which consumes O_2 during the measurements [197]. When an implemented measurement technique, like the polarographic technique, consumes O_2, it more likely generates even greater inaccuracies and leads to incorrect conclusions in low O_2 environments, as occurred in studies investigating the effect of hypoxia in 3D scaffolds [36, 120, 145]. Fluorescence quenching technology is available both for invasive applications, using an electrode probe with a very thin (approximately 5 μm) tip, and for noninvasive applications, using a sensor patch composed of a ruthenium-based metal complex that can be excited by an external fluorescent light source.

Modeling Oxygen Transport in Tissues

The limitations of these measurement techniques, caused mostly by the difficulties in measuring spatial O_2 concentrations in tissues or scaffolds, raise a need for predictive mathematical models. Transport of O_2 in vivo is controlled by several parameters, including blood flow rate, degree of vascularization in the tissue, physiological distance of the cells from the microvasculature, and, depending on cell type, the cells' rate of O_2 consumption. These factors affect O_2 distribution in the tissue, and some can also have an impact on O_2 transport in 3D in vitro cultures of pluripotent or vascular cells. Additional factors that in vitro studies should consider are the geometry of the scaffold, the available surface area for O_2 transport from the environment to the system, and controlled dissolved O_2 levels in the culture media.

In general, fundamental mathematical models estimating O_2 distribution in 3D constructs can be classified into: (1) static models, where O_2 is only transported via diffusion, and (2) dynamic models, where convectional transport of O_2 is also incor-

porated using perfusion systems, such as microfluidic devices, or microcirculation in the tissues.

Static Models

In tissues cultivated under static conditions within 3D scaffolds, using different types of biomaterials, spatial O_2 concentration can be defined with a one-dimensional (1D), unsteady-state species continuity equation:

$$\frac{\partial Co_2}{\partial t} = Do_2 \frac{\partial C^2 o_2}{\partial z^2} - R \tag{4.1}$$

where Co_2 is the spatial O_2 concentration in the scaffold changing with time (t) and axial position (z), D_{O2} is the diffusion coefficient of O_2 in the scaffold material, and R is the oxygen consumption rate of cells. This form of the transport equation has been used in many studies attempting to predict the O_2 gradients in 3D scaffolds [27, 76, 137]. The equation implies that O_2 changes both with time and depth, while being consumed by the cells as it diffuses from the environment into the scaffold. Boundary conditions, which are critical for O_2 distribution, depend on the O_2 equilibrium between the environment (media/air) and the boundaries of the scaffold. Therefore, for a 3D scaffold with a depth of L and open boundaries from both sides, the boundary conditions can be given as:

$$\text{At } z = 0 \text{ and } z = L,\ C_{O2} = S.P_{O2} \tag{4.2}$$

Thus, the solubility (S) of O_2 in the scaffold material is one of the determining parameters of O_2 distribution. Although the diffusion coefficient can also be considered a critical factor in relatively stiff scaffolds of the sort usually used for cartilage and cardiomyocyte tissues [27], it has been shown to be less significant for the natural hydrogel scaffolds commonly used for vascular tissues, such as collagen and HA. For instance, the diffusion coefficient of O_2 in collagen gels was found to be 99% of that in water [83]. Therefore, modeling studies usually assumed that it has the same O_2 diffusion coefficient as water or cell media (3.3×10^{-5} cm^2/s at 37 °C) [157]. The consumption rate of O_2 (R) given in Eq. (4.1) is a function of both C_{O2} and ρ_{cell} and is governed by the Michaelis-Menten equation, which states that the O_2 uptake rate of each cell increases with O_2 availability, reaching a maximum at a point, V_{max}:

$$R = \rho_{cell} \frac{V_{max} C_{O2}}{K_m + C_{O2}} \tag{4.3}$$

where K_m is the O_2 concentration at which the O_2 uptake rate is half of its maximum value and ρ_{cell} is the cell density as a function of time and position. Different groups have reported the V_{max} and K_m parameters of many vascular cell types at various cell seeding densities [78, 163]. For example, the V_{max} and K_m of HUVECs, at a density

of 1×10^6 cells/ml, are found to be 22.05 ± 1.92 (pmol s^{-1} 10^{-6} cells) and 0.55 ± 0.02 (μM), respectively [78]. It should be noted that these parameters are estimated as to mitochondrial consumption of O_2. However, as already discussed, ECs also consume O_2 for ROS production, and the theoretical models should also take this additional O_2 consumption into account by, for example, including a linear correlation in the O_2 consumption rate equation (Eq. (4.3)). Besides, all estimations of the V_{max} and K_m parameters for the O_2 consumption of different cell types are carried out in 2D cultures. The literature currently lacks studies investigating whether or not, depending on the composition of the extracellular matrix, encapsulating cells in 3D gels changes their consumption of O_2.

Vascular cells proliferate, die, migrate, and assemble during 3D cultivation, which affects their spatial and temporal density and, therefore, O_2 distribution. Models developed for 3D cultures of cardiomyocytes take into account the cellular proliferation and changes in the dimensions of the cells during nutrient transport in scaffolds [76, 77]. However, we need more detailed models, which consider how capillary formation affects O_2 transport, to achieve more reliable estimations of spatial O_2 concentration. Tube formation and the networking of ECs in 3D gels have been simulated by more complicated numerical models [47, 139], although the effects of O_2 concentrations on tube formation dynamics still need to be incorporated.

Dynamic and In Vivo Models

The models used for static cultures in 3D scaffolds can also be used to describe O_2 distributions in vivo when combined with a fluid perfusion model that considers the convectional O_2 transfer to the tissues. The velocity profile of a fluid in capillaries or in an engineered microchannel system can be calculated using the simplified Navier-Stokes equation with cylindrical coordinates given for a laminar, one-dimensional, steady-state, and fully developed flow of an incompressible fluid:

$$\frac{dP}{dz} = \mu\left[\frac{1}{r}\frac{d}{dr}\left(r\frac{dV_z}{dr}\right)\right] \tag{4.4}$$

where P is the total pressure in the fluid changing in an axial direction, μ is the viscosity of the fluid, and V_z is the axial velocity of the fluid changing in a radial direction. After estimating the blood velocity profile, the species continuity equation, which involves both diffusional and convectional transfers of O_2, can be used to obtain the O_2 distribution inside the capillary or microchannel:

$$V_z\frac{\partial C_{O2}}{\partial z} = D_{O2}^{\text{Blood}}\left[\frac{1}{r}\frac{\partial}{\partial r}\left(r\frac{\partial C_{O2}}{\partial r}\right)+\frac{\partial^2 C_{O2}}{\partial r}\right] \tag{4.5}$$

The technical difficulties of making quantitative O_2 measurements in BM have led many researchers to develop mathematical models to describe BM O_2 distribu-

tion [41, 131, 133]. Additional parameters that need to be considered in vivo are the vascularization of the tissue and the transport of O_2 via hemoglobin proteins, making the concentration of hemoglobin another essential factor for determining the oxygenation of the tissue. Studies take these additional factors into account using the following equation:

$$D_{O2}^{j}\left[\nabla^2 C_{O2}^{j}\right] = V_z \frac{\partial}{\partial z}\left[C_{O2}^{j} + N\varphi_{O2}\right] \tag{4.6}$$

The superscript j denotes each sinusoid/arteriole around the BM. N is the O_2 carrying capacity of the blood and is the concentration of O_2 bound to hemoglobin, which depends on the plasma O_2 concentrations [180]. Finally, spatial and temporal C_{O2} in tissue can be estimated in a similar manner to the in vitro models, using Eq. (4.1) incorporated with the continuity of fluxes assumption at the ECM-vessel interface as a boundary condition.

4.2.3.2 Targeted Cellular Responses to O_2 Availability in Matrix Hydrogels

Engineering vascular tissues in a 3D ECM is well-orchestrated process combining proliferation, apoptosis, migration, activation, and assembly of vascular or precursor cells inside the construct. As discussed in the previous section, the composition of the biomaterial used to encapsulate the cells is critical for cellular fate and vessel formation. In addition to the effects of the chemical and physical properties of the ECM material on blood vessel formation, temporal and spatial levels of O_2 and other nutrients are also crucial for various targeted cellular responses. A number of studies have investigated the effects of matrix content and stiffness on angiogenesis/vasculogenesis [109], and many others have proposed using different types of biosynthetic materials to develop more precise blood vessels [10, 152]. However, only a few studies have highlighted how O_2 gradients occurring in the matrix contribute to the angiogenic process [93, 170, 177]. The availability of O_2 and other nutrients decreases at the center of the gel compared to the periphery, especially in engineered vascular tissues, which require a high cell seeding density for sufficient vascular tissue generation or repair. Hence, cells that reside along various layers of the matrix respond differently to the nonuniform distribution of O_2 and nutrients. For primary vascular cells to form blood vessels, they require survival, activation, and the induction of angiogenesis by GFs, cell signaling, and regression. All of these responses, necessary for blood vessel formation, are controlled by ECM properties, as well as by O_2 availability. Therefore, the influences of both the ECM and dissolved O_2 distribution should be considered simultaneously.

Cell assembly and tube formation in the ECM require a sufficient cell density. Deprived of O_2 and nutrients, vascular cells can undergo apoptosis or necrosis [21]. These two cellular death mechanisms should be distinguished; apoptosis contributes to the process of angiogenesis at any O_2 tension, whereas necrosis usually

results in the collapsing and deformation of tubes [195]. The critical issues to consider to prevent cellular necrosis during 3D vascular cell cultures are the permeability of the ECM material to O_2 and glucose, the cell seeding density, and the thickness of the gel. Thus, cell seeding density is constrained by an upper limit, above which the cells undergo necrosis due to nutrient deprivation, and a lower limit, below which the cells cannot assemble sufficiently to form tube-like structures. Both limits depend on the equilibrium O_2 levels in the environment.

Cells may also die as a result of apoptosis after their encapsulation in the gel. Interestingly, some groups have demonstrated that programmed cellular death is necessary for angiogenesis/vasculogenesis [195]. Segura et al., having studied tube formation of ECs in both 2D Matrigel and 3D collagen, concluded that a considerable number of cells undergo apoptosis at the initial stages of cultivation and that, once angiogenesis is induced and tube formation has started, no further apoptosis occurs throughout the process. Inhibition of proapoptotic proteins has been shown to correlate with defective tube formations, suggesting that apoptosis is important for avoiding imperfections during blood vessel growth. Hypoxia, as already discussed, induces angiogenic responses and also regulates proapoptotic gene expressions. Thus, spatial variations in O_2 levels may alter the apoptotic responses in the gel and therefore regulate vascular tube morphogenesis.

MMPs are promoted by integrin-ligand interactions between cells and the ECM, leading to the degradation of the ECM and facilitating the migration of the cells [81]. It is hypothesized that ECM fragmentation, orchestrated by the secretion of MMPs, can mediate caspase activity through the rebinding of ECM protein fragments to unligated integrins, namely, death receptors [38]. Therefore, the survival of ECs depends on the balance between cell survival promoters, such as FAK, Src, and Raf, and cellular apoptosis promoters, such as caspase 8 and caspase 3. Hypoxia may again play a critical role here, affecting both sides of the equilibrium, by upregulating MMPs and VEGF at the same time [21, 93]. Hypoxia, accompanied by nonuniform distribution of O_2 throughout the gel, can result in spatial differences of cellular viability, which may subsequently disrupt vascular networking.

Overall, blood vessel growth requires remodeling of the ECM, which is based on two distinct mechanisms: (1) degradation of the ECM by secreted proteases, and (2) production of new ECM to support the invading vasculature. Many studies have shown that hypoxia can regulate the degradation, maintenance, and synthesis of the ECM [61, 179]. ECM degradation is important for cellular migration into and blood vessel invasion of tissue. MMPs, as mentioned above, are a major family of proteinases that participate in the degradation of the ECM during angiogenesis. In particular, MMP-2 and MMP-9, both members of the gelatinase subgroup of MMPs, have been shown to contribute to the process of angiogenesis [85]. MMP-2 secreted by the cells is activated through membrane MT1-MMPs where the activation can be avoided in the presence of tissue inhibitor of MMP-2 (TIMP-2) at high levels [99]. Furthermore, hypoxia was shown to influence the expression of MMP-2, as well as of MT1-MMP and TIMP-2, in ECs [21]. Lahat's group demonstrated the upregulation of MMP-2 expression in hypoxic (0.3% O_2) cultures of HUVECs, whereas MT1-MMP and TIMP-2 are downregulated, enhancing migration and tube formation [21].

ECM degradation is accompanied by ECM production and the secretion of cells. Once the quiescent state of the ECs composing the blood vessel walls is perturbed and angiogenesis is induced, ECs start to proliferate and invade the neighboring ECM by using proteinases. At the same time, they start to remodel the existing ECM by synthesizing new ECM. In healing wounds, ECs produce transitional ECM proteins, including fibrinogen and fibronectin, and temporarily deposit them in the ECM in order to provide available ligands during vessel growth [38]. Moreover, ECs also produce such matricellular proteins as tenascin C and SPARC in the ECM to mediate angiogenesis [38]. Clearly, the new ECM synthesis of cells is crucial for angiogenesis, and hypoxia, through HIF1α, has been shown to regulate the expressions of many different types of ECM proteins [167]. For example, many in vivo and in vitro studies have shown that hypoxia enhanced the synthesis of collagen, the most abundant protein in mammalian tissues [22, 103, 217].

Moreover, proliferation of the cells during angiogenesis/vasculogenesis in 3D scaffolds is regulated by basic fibroblast growth factor (bFGF) and VEGF, which are known to be hypoxia-dependent proteins [177]. In most studies of the vascularization of 3D scaffolds, both GFs are broadly used as soluble factors that supplement cell growth medium to induce proliferation and migration [127, 193]. In addition, Shen et al. demonstrated that immobilization of VEGF into a 3D collagen scaffold promotes EC viability, proliferation, and vascularization [198]. VEGF has been shown to promote blood vessel formation, not only by inducing cellular proliferation and migration but also by directly regulating elongation and capillary networking in 3D ECM constructs deprived of O_2 and nutrients [93]. Helminger et al. used a sandwich system to seed HUVECs inside a collagen gel [93]. The transfer of O_2 and nutrients was accomplished with only simple diffusion through the edges of the collagen, so that O_2 and nutrient levels decreased toward the center. They found that, in a short time period (about nine hours), VEGF intensity increased in the interior regions deprived of O_2, which correlates well with cell elongation and branching. VEGF promoted capillary networking independently of proliferation, highlighting the role of autocrine VEGF in the reorganization of vascular networks in hypoxic regions of solid tumors. Another study focusing on quantitative measurements of O_2 gradients in 3D collagen also showed that increased VEGF concentrations correlated well to decreasing O_2 levels throughout the 3D constructs during a ten day period of cultivation [36].

A few studies considering the induction of angiogenesis by hypoxia in 3D scaffolds have emphasized that lowering the O_2 tension in 3D gels improved cellular branching and tube formation of ECs [170, 177]. As made abundantly clear throughout this chapter, both O_2 and matrix mechanics act as potent upstream regulators of a variety of signaling pathways that contribute significantly to the regulation of vascular differentiation as well as morphogenesis. To better understand these processes, engineers and biologists together have built an impressive library of materials and assays to examine an array of signaling cascades guiding the formation of blood vessels. There are several interesting platforms that can be used to study the effect of hypoxia and O_2 gradients on cellular function, including hydrogels (Fig. 4.6) [143, 144, 173, 187] and microfabrication or microfluidic devices [2,

3, 6, 37, 74, 169]. Stiffness gradients can also be controlled to study ranges of viscoelasticity and their effect on cell fate, migration, and other parameters [84]. Finally, O_2 and matrix mechanics can be independently controlled in the same system using gelatin- and dextran-based hydrogels. These polymers can be both enzymatically cross-linked by an O_2-consuming reaction to create hypoxic conditions and cross-linked by a secondary non-O_2-consuming reaction, to create a stiffer microenvironment without appreciably affecting microenvironmental O_2 [25].

A growing body of publications have both investigated the influence of the ECM composition on angiogenesis/vasculogenesis and suggested the crucial roles of hypoxia in blood vessel formation. In addition, the evidence discussed above is sufficient to suggest that the ECM composition and O_2 tension are coupled factors that need to be taken into account concurrently when developing and repairing vascular tissues in 3D microenvironments.

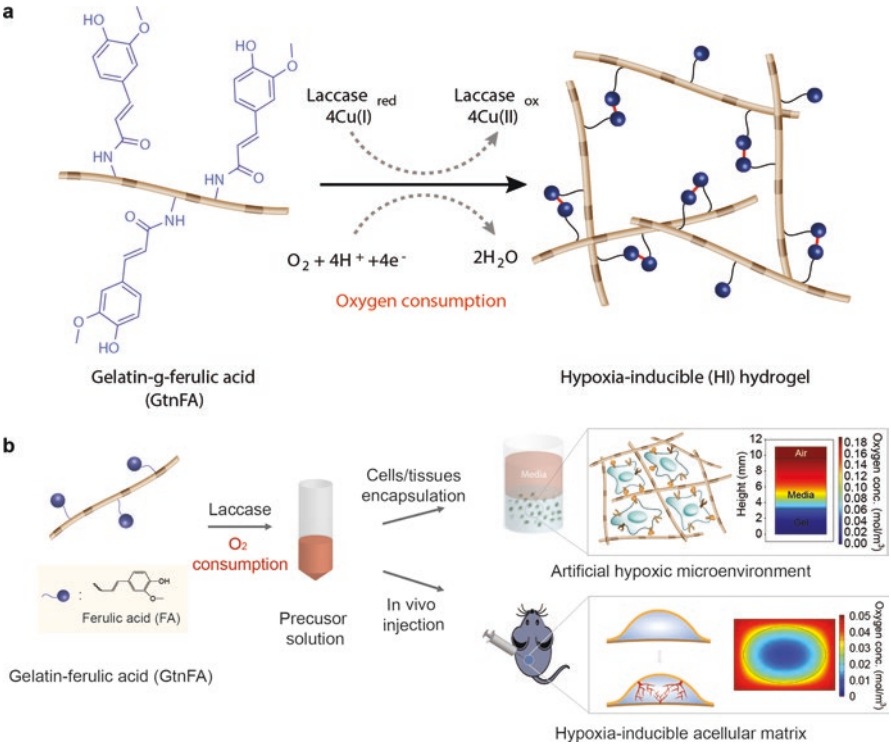

Fig. 4.6 O_2 controllable hydrogels can be used to study the effects of hypoxic gradients both in vitro and in vivo. (**a**) Synthesis of Gtn–FA, which can form a hydrogel network via a laccase-mediated cross-linking reaction with O_2 consumption. (**b**) The Gtn–FA precursor solution can be mixed with either cells or tissues to provide artificial hypoxic microenvironments with O_2 gradients (see inserted computer simulation of O_2 tension and gradients). The precursor solution can also be directly injected into the animal as a hypoxia-inducible acellular matrix that induces temporal hypoxia and an O_2 gradient in the body (see inserted computer simulation of oxygen tension and gradients). Reproduced and re-formatted with permission [144]

4.3 Future Directions

Understanding the simultaneous effects of the ECM and O_2 tension on the processes of angiogenesis/vasculogenesis will enable researchers to control these two factors and thereby manipulate cellular responses in desired directions. Recent developments in many different fields of research, such as smart biomaterials and microfluidics, have made it possible to design and construct novel in vitro microenvironments for cells. Smart biomaterials have been developed that can dynamically respond to external stimuli, such as light [79], pH [174], temperature [216], and cytokines [124]; these materials can truly mimic the complexity of a native ECM environment. The ability to control the physical and chemical properties of the gels at different spaces and times will provide better control over different stages of angiogenesis. Light-sensitive hydrogels can be used to create biomaterials with distinct cross-linking densities to promote and inhibit cell spreading and migration [121], which in turn can be used to pattern complex vascular networks. Since vascular morphogenesis is sensitive to tissue stiffness [52], orientation [23], and polarity [42, 149], researchers could also induce vascular assembly into a tube by creating elasticity, GFs, adhesion peptide, and oxygen gradients along the 3D scaffold [144, 151, 228]. The development of photodegradable hydrogels, as well as the control of cell-mediated degradation in synthetic hydrogels, whose mechanical and chemical properties are controllable during the timescale of cellular development [123], has enabled control of vascular assembly [89, 90]. On the other hand, creating smart biomaterials that can shrink, swell, or degrade in response to oxygen tension would also be desirable to prevent the formation of anoxic regions inside the gels. More precise temporal control of O_2 gradients inside the constructs could also be beneficial to explain various phenomena taking place in the body, such as EPC regeneration in the BM and embryonic development, where the O_2 gradient plays a critical role in differentiation and migration dynamics.

Figure 4.7 illustrates two proposed approaches for controlling oxygen distribution and ECM properties. One proposal for regulating O_2 gradients inside the gel would be to incorporate microfluidic technology [66, 129, 163, 220]. Although this approach provides better O_2 control over 3D microenvironments, the problem of spatial variations in O_2 levels throughout the gel, due to the cells' O_2 consumption, must still be addressed. Advancements in microfluidic technology could enable spatial O_2 control over 3D microenvironments; for instance, the gel could be prepared around a microtube, which would supply O_2 by flushing growth media containing a desired amount of O_2 (Fig. 4.7a). Hence, different O_2 gradients could be generated via the manipulation of O_2 concentrations in the outside environment and inside the microtube.

Another method for controlling and improving O_2 transport in the gel would be to microencapsulate O_2 carrier liquids, such as perfluorocarbons (PFCs). Due to their high capacity to dissolve O_2, PFCs have been used as a blood replacement to improve O_2 delivery to tissues [112, 183]. Based on the high oxygen-carrying capacity of PFCs, Radisic et al. [183] developed a PFC-perfused system to supply sufficient

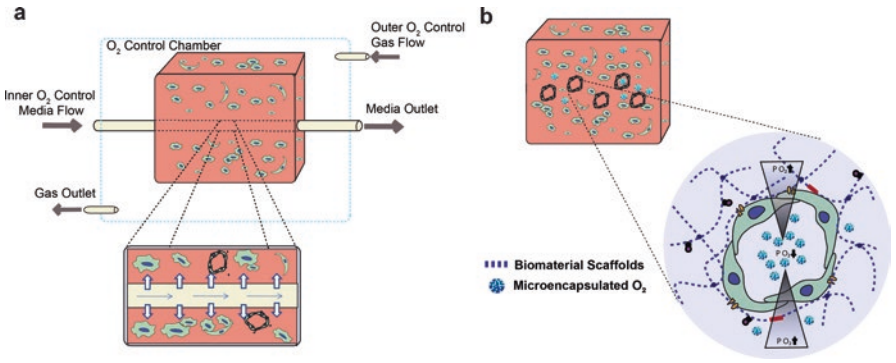

Fig. 4.7 Controlling ECM and O_2 in vitro by (**a**) 3D gel prepared around a microtube supplying O_2 (insert: white arrows indicate oxygen transport; blue arrows indicate the direction of airflow) and (**b**) microencapsulated O_2 carriers, such as PFCs, embedded within 3D gel. Drawing not to scale

levels of oxygen to 3D cardiomyocyte cultures. A study by Chin et al. [39] made a similar attempt, developing hydrogel-PFC composite scaffolds to improve oxygenation throughout the gel. In a similar manner, taking advantage of the high O_2 solubility of PFCs, controlled release of O_2 in 3D microenvironments could be improved via microencapsulation of PFCs (Fig. 4.7b). Polymeric microspheres loaded with O_2 have also been shown to be effective in enhancing cell viability in anoxic microenvironments [44].

The continued development of novel biomaterial technologies, which enable the study of human cells in highly biomimetic settings in vitro, will continue to guide discovery of cell behavior and vascular morphogenesis. These powerful systems, coupled with continued innovation throughout all areas of biotechnology, including gene editing and stem cell technology, have positioned the field of vascular tissue engineering in a fascinating arena, where new therapeutic targets and more robust vascularized constructs continue to be discovered and translated to the clinic. Combining expertise in biology, materials science, engineering, and medicine will continue to inform our understanding of the complex cell-cell and cell-matrix interactions that drive tissue formation and regeneration.

Acknowledgments We would like to acknowledge funding from various agencies that supported our studies throughout the years, primarily the American Heart Association, the Maryland Stem Cell Research Fund, the National Science Foundation, and the National Institutes of Health.

References

1. Abaci, H. E., Truitt, R., Luong, E., Drazer, G., & Gerecht, S. (2010). Adaptation to oxygen deprivation in cultures of human pluripotent stem cells, endothelial progenitor cells, and umbilical vein endothelial cells. *American Journal of Physiology. Cell Physiology, 298*(6), C1527–C1537.

2. Abaci, H. E., Devendra, R., Smith, Q., Gerecht, S., & Drazer, G. (2012). Design and development of microbioreactors for long-term cell culture in controlled oxygen microenvironments. *Biomedical Microdevices, 14*(1), 145–152.
3. Abaci, H. E., Shen, Y. I., Tan, S., & Gerecht, S. (2014). Recapitulating physiological and pathological shear stress and oxygen to model vasculature in health and disease. *Scientific Reports, 4*, 9.
4. Abbott, J. D., Huang, Y., Liu, D., Hickey, R., Krause, D. S., & Giordano, F. J. (2004). Stromal cell-derived factor-1 alpha plays a critical role in stem cell recruitment to the heart after myocardial infarction but is not sufficient to induce homing in the absence of injury. *Circulation, 110*(21), 3300–3305.
5. Adelman, D. M., Maltepe, E., & Simon, M. C. (1999). Multilineage embryonic hematopoiesis requires hypoxic ARNT activity. *Genes & Development, 13*(19), 2478–2483.
6. Adler, M., Polinkovsky, M., Gutierrez, E., & Groisman, A. (2010). Generation of oxygen gradients with arbitrary shapes in a microfluidic device. *Lab on a Chip, 10*(3), 388–391.
7. Airley, R., Loncaster, J., Davidson, S., Bromley, M., Roberts, S., Patterson, A., et al. (2001). Glucose transporter glut-1 expression correlates with tumor hypoxia and predicts metastasis-free survival in advanced carcinoma of the cervix. *Clinical Cancer Research, 7*(4), 928–934.
8. Akita, T., Murohara, T., Ikeda, H., Sasaki, K., Shimada, T., Egami, K., et al. (2003). Hypoxic preconditioning augments efficacy of human endothelial progenitor cells for therapeutic neovascularization. *Laboratory Investigation, 83*(1), 65–73.
9. Albina, J. E., Mastrofrancesco, B., Vessella, J. A., Louis, C. A., Henry Jr., W. L., & Reichner, J. S. (2001). HIF-1 expression in healing wounds: HIF-1alpha induction in primary inflammatory cells by TNF-alpha. *American Journal of Physiology. Cell Physiology, 281*(6), C1971–C1977.
10. Almany, L., & Seliktar, D. (2005). Biosynthetic hydrogel scaffolds made from fibrinogen and polyethylene glycol for 3D cell cultures. *Biomaterials, 26*(15), 2467–2477.
11. Artuc, M., Hermes, B., Steckelings, U. M., Grutzkau, A., & Henz, B. M. (1999). Mast cells and their mediators in cutaneous wound healing--active participants or innocent bystanders? *Experimental Dermatology, 8*(1), 1–16.
12. Asahara, T., & Kawamoto, A. (2004). Endothelial progenitor cells for postnatal vasculogenesis. *American Journal of Physiology. Cell Physiology, 287*(3), C572–C579.
13. Asahara, T., Masuda, H., Takahashi, T., Kalka, C., Pastore, C., Silver, M., et al. (1999). Bone marrow origin of endothelial progenitor cells responsible for postnatal vasculogenesis in physiological and pathological neovascularization. *Circulation Research, 85*(3), 221–228.
14. Astrof, S., Crowley, D., & Hynes, R. O. (2007). Multiple cardiovascular defects caused by the absence of alternatively spliced segments of fibronectin. *Developmental Biology, 311*(1), 11–24.
15. Au, P., Tam, J., Fukumura, D., & Jain, R. K. (2008). Bone marrow derived mesenchymal stem cells facilitate engineering of long-lasting functional vasculature. *Blood, 111*(9), 4551–4558.
16. Au, P., Daheron, L. M., Duda, D. G., Cohen, K. S., Tyrrell, J. A., Lanning, R. M., et al. (2008). Differential in vivo potential of endothelial progenitor cells from human umbilical cord blood and adult peripheral blood to form functional long-lasting vessels. *Blood, 111*(3), 1302–1305.
17. Band, M., Joel, A., Hernandez, A., & Avivi, A. (2009). Hypoxia-induced BNIP3 expression and mitophagy: In vivo comparison of the rat and the hypoxia-tolerant mole rat, spalax ehrenbergi. *FASEB Journal, 23*(7), 2327–2335.
18. Banerjee, S. D., & Toole, B. P. (1992). Hyaluronan-binding protein in endothelial cell morphogenesis. *Journal of Cell Biology, 119*(3), 643–652.
19. Bekker, A., Holland, H. D., Wang, P. L., Rumble 3rd, D., Stein, H. J., Hannah, J. L., et al. (2004). Dating the rise of atmospheric oxygen. *Nature, 427*(6970), 117–120.
20. Bellot, G., Garcia-Medina, R., Gounon, P., Chiche, J., Roux, D., Pouyssegur, J., et al. (2009). Hypoxia-induced autophagy is mediated through hypoxia-inducible factor induction of BNIP3 and BNIP3L via their BH3 domains. *Molecular and Cellular Biology, 29*(10), 2570–2581.

21. Ben-Yosef, Y., Miller, A., Shapiro, S., & Lahat, N. (2005). Hypoxia of endothelial cells leads to MMP-2-dependent survival and death. *American Journal of Physiology. Cell Physiology, 289*(5), C1321–C1331.
22. Berg, J. T., Breen, E. C., Fu, Z., Mathieu-Costello, O., & West, J. B. (1998). Alveolar hypoxia increases gene expression of extracellular matrix proteins and platelet-derived growth factor-B in lung parenchyma. *American Journal of Respiratory and Critical Care Medicine, 158*(6), 1920–1928.
23. Bettinger, C. J., Zhang, Z., Gerecht, S., Borenstein, J., & Langer, R. (2008). Enhancement of in vitro capillary tube formation by substrate nanotopography. *Advanced Materials, 20*, 99–103.
24. Bianchi, F., Rosi, M., Vozzi, G., Emanueli, C., Madeddu, P., & Ahluwalia, A. (2007). Microfabrication of fractal polymeric structures for capillary morphogenesis: Applications in therapeutic angiogenesis and in the engineering of vascularized tissue. *Journal of Biomedical Materials Research. Part B, Applied Biomaterials, 81*(2), 462–468.
25. Blatchley, M., Park, K. M., & Gerecht, S. (2015). Designer hydrogels for precision control of oxygen tension and mechanical properties. *Journal of Materials Chemistry B, 3*(40), 7939–7949.
26. Boveris, A., Costa, L. E., Poderoso, J. J., Carreras, M. C., & Cadenas, E. (2000). Regulation of mitochondrial respiration by oxygen and nitric oxide. *Annals of the New York Academy of Sciences, 899*, 121–135.
27. Brown, D. A., MacLellan, W. R., Laks, H., Dunn, J. C., Wu, B. M., & Beygui, R. E. (2007). Analysis of oxygen transport in a diffusion-limited model of engineered heart tissue. *Biotechnology and Bioengineering, 97*(4), 962–975.
28. Bruick, R. K., & McKnight, S. L. (2001). A conserved family of prolyl-4-hydroxylases that modify HIF. *Science, 294*(5545), 1337–1340.
29. Burggren, W. W. (2004). What is the purpose of the embryonic heart beat? Or how facts can ultimately prevail over physiological dogma. *Physiological and Biochemical Zoology, 77*(3), 333–345.
30. Camenisch, T. D., Spicer, A. P., Brehm-Gibson, T., Biesterfeldt, J., Augustine, M. L., Calabro Jr., A., et al. (2000). Disruption of hyaluronan synthase-2 abrogates normal cardiac morphogenesis and hyaluronan-mediated transformation of epithelium to mesenchyme. *Journal of Clinical Investigation, 106*(3), 349–360.
31. Caspi, O., Lesman, A., Basevitch, Y., Gepstein, A., Arbel, G., Habib, I. H., et al. (2007). Tissue engineering of vascularized cardiac muscle from human embryonic stem cells. *Circulation Research, 100*, 263.
32. Ceradini, D. J., & Gurtner, G. C. (2005). Homing to hypoxia: HIF-1 as a mediator of progenitor cell recruitment to injured tissue. *Trends in Cardiovascular Medicine, 15*(2), 57–63.
33. Ceradini, D. J., Kulkarni, A. R., Callaghan, M. J., Tepper, O. M., Bastidas, N., Kleinman, M. E., et al. (2004). Progenitor cell trafficking is regulated by hypoxic gradients through HIF-1 induction of SDF-1. *Nature Medicine, 10*(8), 858–864.
34. Chaudhuri, O., Gu, L., Klumpers, D., Darnell, M., Bencherif, S. A., Weaver, J. C., et al. (2016). Hydrogels with tunable stress relaxation regulate stem cell fate and activity. *Nature Materials, 15*(3), 326.
35. Chavakis, E., Aicher, A., Heeschen, C., Sasaki, K. I., Kaiser, R., El Makhfi, N., et al. (2005). Role of beta 2-integrins for homing and neovascularization capacity of endothelial progenitor cells. *Journal of Experimental Medicine, 201*(1), 63–72.
36. Cheema, U., Brown, R. A., Alp, B., & MacRobert, A. J. (2008). Spatially defined oxygen gradients and vascular endothelial growth factor expression in an engineered 3D cell model. *Cellular and Molecular Life Sciences, 65*(1), 177–186.
37. Chen, Y. A., King, A. D., Shih, H. C., Peng, C. C., Wu, C. Y., Liao, W. H., et al. (2011). Generation of oxygen gradients in microfluidic devices for cell culture using spatially confined chemical reactions. *Lab on a Chip, 11*(21), 3626–3633.
38. Cheresh, D. A., & Stupack, D. G. (2008). Regulation of angiogenesis: Apoptotic cues from the ECM. *Oncogene, 27*(48), 6285–6298.

39. Chin, K., Khattak, S. F., Bhatia, S. R., & Roberts, S. C. (2008). Hydrogel-perfluorocarbon composite scaffold promotes oxygen transport to immobilized cells. *Biotechnology Progress, 24*(2), 358–366.
40. Chiu, L. L. Y., & Radisic, M. (2010). Scaffolds with covalently immobilized VEGF and angiopoietin-1 for vascularization of engineered tissues. *Biomaterials, 31*(2), 226–241.
41. Chow, D. C., Wenning, L. A., Miller, W. M., & Papoutsakis, E. T. (2001). Modeling pO(2) distributions in the bone marrow hematopoietic compartment. I. Krogh's model. *Biophysical Journal, 81*(2), 675–684.
42. Chung, S., & Andrew, D. J. (2008). The formation of epithelial tubes. *Journal of Cell Science, 121*(21), 3501–3504.
43. Colville-Nash, P. R., & Scott, D. L. (1992). Angiogenesis and rheumatoid arthritis: Pathogenic and therapeutic implications. *Annals of the Rheumatic Diseases, 51*(7), 919–925.
44. Cook, C. A., Hahn, K. C., Morrissette-McAlmon, J. B. F., & Grayson, W. L. (2015). Oxygen delivery from hyperbarically loaded microtanks extends cell viability in anoxic environments. *Biomaterials, 52*, 376–384.
45. Covello, K. L., Kehler, J., Yu, H., Gordan, J. D., Arsham, A. M., Hu, C. J., et al. (2006). HIF-2alpha regulates Oct-4: Effects of hypoxia on stem cell function, embryonic development, and tumor growth. *Genes & Development, 20*(5), 557–570.
46. Critser, P. J., Kreger, S. T., Voytik-Harbin, S. L., & Yoder, M. C. (2010). Collagen matrix physical properties modulate endothelial colony forming cell-derived vessels in vivo. *Microvascular Research, 80*, 23–30.
47. Daphne, M. (2003). A mechanochemical model of angiogenesis and vasculogenesis. *Modelisation mathematique et analyse numerique, 37*(4), 581–599.
48. Davis, G. E., & Camarillo, C. W. (1995). Regulation of endothelial cell morphogenesis by integrins, mechanical forces, and matrix guidance pathways. *Experimental Cell Research, 216*(1), 113–123.
49. Davis, G. E., Koh, W., & Stratman, A. N. (2007). Mechanisms controlling human endothelial lumen formation and tube assembly in three-dimensional extracellular matrices. *Birth Defects Research. Part C, Embryo Today, 81*(4), 270–285.
50. Davis, G. E., & Senger, D. R. (2008). Extracellular matrix mediates a molecular balance between vascular morphogenesis and regression. *Current Opinion in Hematology, 15*(3), 197–203.
51. De Falco, E., Porcelli, D., Torella, A. R., Straino, S., Iachininoto, M. G., Orlandi, A., et al. (2004). SDF-1 involvement in endothelial phenotype and ischemia-induced recruitment of bone marrow progenitor cells. *Blood, 104*(12), 3472–3482.
52. Deroanne, C. F., Lapiere, C. M., & Nusgens, B. V. (2001). In vitro tubulogenesis of endothelial cells by relaxation of the coupling extracellular matrix-cytoskeleton. *Cardiovascular Research, 49*(3), 647–658.
53. Desgrosellier, J. S., & Cheresh, D. A. (2010). Integrins in cancer: Biological implications and therapeutic opportunities. *Nature Reviews Cancer, 10*(1), 9–22.
54. Dickinson, L. E., Moura, M. E., & Gerecht, S. (2010). Guiding endothelial progenitor cell tube formation using patterned fibronectin surfaces. *Soft Matter, 6*(20), 5109–5119.
55. Dickinson, L. E., Ho, C. C., Wang, G. M., Stebe, K. J., & Gerecht, S. (2010). Functional surfaces for high-resolution analysis of cancer cell interactions on exogenous hyaluronic acid. *Biomaterials, 31*(20), 5472–5478.
56. Drake, C. J., & Fleming, P. A. (2000). Vasculogenesis in the day 6.5 to 9.5 mouse embryo. *Blood, 95*(5), 1671–1679.
57. Eble, J. A., & Niland, S. (2009). The extracellular matrix of blood vessels. *Current Pharmaceutical Design, 15*, 1385–1400.
58. Ehrbar, M., Djonov, V. G., Schnell, C., Tschanz, S. A., Martiny-Baron, G., Schenk, U., et al. (2004). Cell-demanded liberation of VEGF121 from fibrin implants induces local and controlled blood vessel growth. *Circulation Research, 94*(8), 1124–1132.

59. Ehrbar, M., Metters, A., Zammaretti, P., Hubbell, J. A., & Zisch, A. H. (2005). Endothelial cell proliferation and progenitor maturation by fibrin-bound VEGF variants with differential susceptibilities to local cellular activity. *Journal of Controlled Release, 101*(1-3), 93–109.
60. Engler, A. J., Sen, S., Sweeney, H. L., & Discher, D. E. (2006). Matrix elasticity directs stem cell lineage specification. *Cell, 126*(4), 677–689.
61. Erler, J. T., Bennewith, K. L., Cox, T. R., Lang, G., Bird, D., Koong, A., et al. (2009). Hypoxia-induced lysyl oxidase is a critical mediator of bone marrow cell recruitment to form the premetastatic niche. *Cancer Cell, 15*(1), 35–44.
62. Evanko, S. P., Parks, W. T., & Wight, T. N. (2004). Intracellular hyaluronan in arterial smooth muscle cells: Association with microtubules, RHAMM, and the mitotic spindle. *The Journal of Histochemistry and Cytochemistry, 52*(12), 1525–1535.
63. Evans, A. M., Mustard, K. J., Wyatt, C. N., Peers, C., Dipp, M., Kumar, P., et al. (2005). Does AMP-activated protein kinase couple inhibition of mitochondrial oxidative phosphorylation by hypoxia to calcium signaling in O2-sensing cells? *The Journal of Biological Chemistry, 280*(50), 41504–41511.
64. Ezashi, T., Das, P., & Roberts, R. M. (2005). Low O2 tensions and the prevention of differentiation of hES cells. *Proceedings of the National Academy of Sciences of the United States of America, 102*(13), 4783–4788.
65. Fahling, M., Perlewitz, A., Doller, A., & Thiele, B. J. (2004). Regulation of collagen prolyl 4-hydroxylase and matrix metalloproteinases in fibrosarcoma cells by hypoxia. *Comparative Biochemistry and Physiology, Part C: Toxicology & Pharmacology, 139*(1-3), 119–126.
66. Figallo, E., Cannizzaro, C., Gerecht, S., Burdick, J. A., Langer, R., Elvassore, N., et al. (2007). Micro-bioreactor array for controlling cellular microenvironments. *Lab on a Chip, 7*(6), 710–719.
67. Folkman, J., Haudenschild, C. C., & Zetter, B. R. (1979). Long-term culture of capillary endothelial cells. *Proceedings of the National Academy of Sciences of the United States of America, 76*(10), 5217–5221.
68. Fong, G. H. (2009). Regulation of angiogenesis by oxygen sensing mechanisms. *Journal of Molecular Medicine, 87*(6), 549–560.
69. Forristal, C. E., Wright, K. L., Hanley, N. A., Oreffo, R. O., & Houghton, F. D. (2010). Hypoxia inducible factors regulate pluripotency and proliferation in human embryonic stem cells cultured at reduced oxygen tensions. *Reproduction, 139*(1), 85–97.
70. Fraisl, P., Mazzone, M., Schmidt, T., & Carmeliet, P. (2009). Regulation of angiogenesis by oxygen and metabolism. *Developmental Cell, 16*(2), 167–179.
71. Francis, S. E., Goh, K. L., Hodivala-Dilke, K., Bader, B. L., Stark, M., Davidson, D., et al. (2002). Central roles of alpha5beta1 integrin and fibronectin in vascular development in mouse embryos and embryoid bodies. *Arteriosclerosis, Thrombosis, and Vascular Biology, 22*(6), 927–933.
72. Frei, R., Gaucher, C., Poulton, S. W., & Canfield, D. E. (2009). Fluctuations in Precambrian atmospheric oxygenation recorded by chromium isotopes. *Nature, 461*(7261), 250–253.
73. Fukumura, D., Kashiwagi, S., & Jain, R. K. (2006). The role of nitric oxide in tumour progression. *Nature Reviews. Cancer, 6*(7), 521–534.
74. Funamoto, K., Zervantonakis, I. K., Liu, Y. C., Ochs, C. J., Kim, C., & Kamm, R. D. (2012). A novel microfluidic platform for high-resolution imaging of a three-dimensional cell culture under a controlled hypoxic environment. *Lab on a Chip, 12*(22), 4855–4863.
75. Gafni, Y., Zilberman, Y., Ophir, Z., Abramovitch, R., Jaffe, M., Gazit, Z., et al. (2006). Design of a filamentous polymeric scaffold for in vivo guided angiogenesis. *Tissue Engineering, 12*(11), 3021–3034.
76. Galban, C. J., & Locke, B. R. (1999). Effects of spatial variation of cells and nutrient and product concentrations coupled with product inhibition on cell growth in a polymer scaffold. *Biotechnology and Bioengineering, 64*(6), 633–643.
77. Galban, C. J., & Locke, B. R. (1999). Analysis of cell growth kinetics and substrate diffusion in a polymer scaffold. *Biotechnology and Bioengineering, 65*(2), 121–132.

78. Garedew, A., Kammerer, U., & Singer, D. (2009). Respiratory response of malignant and placental cells to changes in oxygen concentration. *Respiratory Physiology & Neurobiology, 165*(2-3), 154–160.
79. Gerecht, S., Burdick, J. A., Ferreira, L. S., Townsend, S. A., Langer, R., & Vunjak-Novakovic, G. (2007). Hyaluronic acid hydrogel for controlled self-renewal and differentiation of human embryonic stem cells. *Proceedings of the National Academy of Sciences of the United States of America, 104*(27), 11298–11303.
80. Gerecht-Nir, S., Cohen, S., Ziskind, A., & Itskovitz-Eldor, J. (2004). Three-dimensional porous alginate scaffolds provide a conducive environment for generation of well-vascularized embryoid bodies from human embryonic stem cells. *Biotechnology and Bioengineering, 88*(3), 313–320.
81. Giannelli, G., Falk-Marzillier, J., Schiraldi, O., Stetler-Stevenson, W. G., & Quaranta, V. (1997). Induction of cell migration by matrix metalloprotease-2 cleavage of laminin-5. *Science, 277*(5323), 225–228.
82. Gobin, A. S., & West, J. L. (2002). Cell migration through defined, synthetic extracellular matrix analogues. *The FASEB Journal, 16*, 751–753.
83. Guaccio, A., Borselli, C., Oliviero, O., & Netti, P. A. (2008). Oxygen consumption of chondrocytes in agarose and collagen gels: A comparative analysis. *Biomaterials, 29*(10), 1484–1493.
84. Hadden, W. J., Young, J. L., Holle, A. W., McFetridge, M. L., Kim, D. Y., Wijesinghe, P., et al. (2017). Stem cell migration and mechanotransduction on linear stiffness gradient hydrogels. *Proceedings of the National Academy of Sciences of the United States of America, 114*(22), 5647–5652.
85. Hagemann, T., Robinson, S. C., Schulz, M., Trumper, L., Balkwill, F. R., & Binder, C. (2004). Enhanced invasiveness of breast cancer cell lines upon co-cultivation with macrophages is due to TNF-alpha dependent up-regulation of matrix metalloproteases. *Carcinogenesis, 25*(8), 1543–1549.
86. Hanjaya-Putra, D., & Gerecht, S. (2009). Vascular engineering using human embryonic stem cells. *Biotechnology Progress, 25*(1), 2–9.
87. Hanjaya-Putra, D., & Gerecht, S. (2009). Mending the failing heart with a vascularized cardiac patch. *Cell Stem Cell, 5*(6), 575–576.
88. Hanjaya-Putra, D., Yee, J., Ceci, D., Truitt, R., Yee, D., & Gerecht, S. (2009). Vascular endothelial growth factor and substrate mechanics regulate in vitro tubulogenesis of endothelial progenitor cells. *Journal of Cellular and Molecular Medicine, 14*(10), 2436–2447.
89. Hanjaya-Putra, D., Bose, V., Shen, Y. I., Yee, J., Khetan, S., Fox-Talbot, K., et al. (2011). Controlled activation of morphogenesis to generate a functional human microvasculature in a synthetic matrix. *Blood, 118*(3), 804–815.
90. Hanjaya-Putra, D., Wong, K. T., Hirotsu, K., Khetan, S., Burdick, J. A., & Gerecht, S. (2012). Spatial control of cell-mediated degradation to regulate vasculogenesis and angiogenesis in hyaluronan hydrogels. *Biomaterials, 33*(26), 6123–6131.
91. Harrison, J. S., Rameshwar, P., Chang, V., & Bandari, P. (2002). Oxygen saturation in the bone marrow of healthy volunteers. *Blood, 99*(1), 394.
92. Heissig, B., Hattori, K., Dias, S., Friedrich, M., Ferris, B., Hackett, N. R., et al. (2002). Recruitment of stem and progenitor cells from the bone marrow niche requires MMP-9 mediated release of kit-ligand. *Cell, 109*(5), 625–637.
93. Helmlinger, G., Endo, M., Ferrara, N., Hlatky, L., & Jain, R. K. (2000). Formation of endothelial cell networks. *Nature, 405*(6783), 139–141.
94. Hirota, K., & Semenza, G. L. (2005). Regulation of hypoxia-inducible factor 1 by prolyl and asparaginyl hydroxylases. *Biochemical and Biophysical Research Communications, 338*(1), 610–616.
95. Hirschi, K. K., & D'Amore, P. A. (1996). Pericytes in the microvasculature. *Cardiovascular Research, 32*(4), 687–698.
96. Hirschi, K. K., Ingram, D. A., & Yoder, M. C. (2008). Assessing identity, phenotype, and fate of endothelial progenitor cells. *Arteriosclerosis, Thrombosis, and Vascular Biology, 28*(9), 1584–1595.

97. Hirschi, K. K., Rohovsky, S. A., & D'Amore, P. A. (1998). PDGF, TGF-Î², and heterotypic cell-cell interactions mediate endothelial cell-induced recruitment of 10T1/2 cells and their differentiation to a smooth muscle fate. *Journal of Cell Biology, 141*(3), 805–814.
98. Hirsila, M., Koivunen, P., Gunzler, V., Kivirikko, K. I., & Myllyharju, J. (2003). Characterization of the human prolyl 4-hydroxylases that modify the hypoxia-inducible factor. *The Journal of Biological Chemistry, 278*(33), 30772–30780.
99. Hofmann, U. B., Westphal, J. R., Van Kraats, A. A., Ruiter, D. J., & Van Muijen, G. N. (2000). Expression of integrin alpha(v)beta(3) correlates with activation of membrane-type matrix metalloproteinase-1 (MT1-MMP) and matrix metalloproteinase-2 (MMP-2) in human melanoma cells in vitro and in vivo. *International Journal of Cancer, 87*(1), 12–19.
100. Holash, J., Wiegand, S. J., & Yancopoulos, G. D. (1999). New model of tumor angiogenesis: Dynamic balance between vessel regression and growth mediated by angiopoietins and VEGF. *Oncogene, 18*(38), 5356–5362.
101. Holash, J., Maisonpierre, P. C., Compton, D., Boland, P., Alexander, C. R., Zagzag, D., et al. (1999). Vessel cooption, regression, and growth in tumors mediated by angiopoietins and VEGF. *Science, 284*(5422), 1994–1998.
102. Hopf, H. W., & Rollins, M. D. (2007). Wounds: An overview of the role of oxygen. *Antioxidants & Redox Signaling, 9*(8), 1183–1192.
103. Horino, Y., Takahashi, S., Miura, T., & Takahashi, Y. (2002). Prolonged hypoxia accelerates the posttranscriptional process of collagen synthesis in cultured fibroblasts. *Life Sciences, 71*(26), 3031–3045.
104. Hou, L. Q., CoIler, J., Natu, V., Hastie, T. J., & Huang, N. F. (2016). Combinatorial extracellular matrix microenvironments promote survival and phenotype of human induced pluripotent stem cell-derived endothelial cells in hypoxia. *Acta Biomaterialia, 44*, 188–199.
105. Hou, L. Q., Kim, J. J., Wanjare, M., Patlolla, B., Coller, J., Natu, V., et al. (2017). Combinatorial extracellular matrix microenvironments for probing endothelial differentiation of human pluripotent stem cells. *Scientific Reports, 7*, 12.
106. Huang, P. H., Chen, Y. H., Wang, C. H., Chen, J. S., Tsai, H. Y., Lin, F. Y., et al. (2009). Matrix metalloproteinase-9 is essential for ischemia-induced neovascularization by modulating bone marrow-derived endothelial progenitor cells. *Arteriosclerosis, Thrombosis, and Vascular Biology, 29*(8), 1179–1U58.
107. Huber, T. L., Kouskoff, V., Fehling, H. J., Palis, J., & Keller, G. (2004). Haemangioblast commitment is initiated in the primitive streak of the mouse embryo. *Nature, 432*(7017), 625–630.
108. Igarashi, S., Tanaka, J., & Kobayashi, H. (2007). Micro-patterned nanofibrous biomaterials. *Journal of Nanoscience and Nanotechnology, 7*(3), 814–817.
109. Ingber, D. E. (2002). Mechanical signaling and the cellular response to extracellular matrix in angiogenesis and cardiovascular physiology. *Circulation Research, 91*(10), 877–887.
110. Ingber, D. E., & Folkman, J. (1989). Mechanochemical switching between growth and differentiation during fibroblast growth factor-stimulated angiogenesis in vitro: Role of extracellular matrix. *Journal of Cell Biology, 109*(1), 317–330.
111. Iwasaki, H. (2009). The Niche regulation of hematopoietic stem cells. In *Regulatory networks in stem cells* (pp. 165–175). New York: Humana Press.
112. Iyer, R. K., Radisic, M., Cannizzaro, C., & Vunjak-Novakovic, G. (2007). Synthetic oxygen carriers in cardiac tissue engineering. *Artificial Cells, Blood Substitutes, and Immobilization Biotechnology, 35*(1), 135–148.
113. Jain, R. K. (2003). Molecular regulation of vessel maturation. *Nature Medicine, 9*(6), 685–693.
114. Jain, R. K., Au, P., Tam, J., Duda, D. G., & Fukumura, D. (2005). Engineering vascularized tissue. *Nature Biotechnology, 23*(7), 821–823.
115. Jauniaux, E., Gulbis, B., & Burton, G. J. (2003). The human first trimester gestational sac limits rather than facilitates oxygen transfer to the foetus--a review. *Placenta, 24*(Suppl A), S86–S93.
116. Ji, L., Liu, Y. X., Yang, C., Yue, W., Shi, S. S., Bai, C. X., et al. (2009). Self-renewal and pluripotency is maintained in human embryonic stem cells by co-culture with human fetal liver

stromal cells expressing hypoxia inducible factor 1alpha. *Journal of Cellular Physiology, 221*(1), 54–66.
117. Jiang, M., Wang, B., Wang, C., He, B., Fan, H., Guo, T. B., et al. (2008). Angiogenesis by transplantation of HIF-1 alpha modified EPCs into ischemic limbs. *Journal of Cellular Biochemistry, 103*(1), 321–334.
118. Jones 3rd, C. I., Han, Z., Presley, T., Varadharaj, S., Zweier, J. L., Ilangovan, G., et al. (2008). Endothelial cell respiration is affected by the oxygen tension during shear exposure: Role of mitochondrial peroxynitrite. *American Journal of Physiology. Cell Physiology, 295*(1), C180–C191.
119. Kang, X. L., Wei, X. X., Wang, X. H., Jiang, L., Niu, C., Zhang, J. Y., et al. (2016). Nox2 contributes to the arterial endothelial specification of mouse induced pluripotent stem cells by upregulating notch signaling. *Scientific Reports, 6*, 13.
120. Kellner, K., Liebsch, G., Klimant, I., Wolfbeis, O. S., Blunk, T., Schulz, M. B., et al. (2002). Determination of oxygen gradients in engineered tissue using a fluorescent sensor. *Biotechnology and Bioengineering, 80*(1), 73–83.
121. Khetan, S., Chung, C., & Burdick, J. A. (2009). Tuning hydrogel properties for applications in tissue engineering. *Conference Proceedings: Annual International Conference of the IEEE Engineering in Medicine and Biology Society, 1*, 2094–2096.
122. Kilarski, W. W., Samolov, B., Petersson, L., Kvanta, A., & Gerwins, P. (2009). Biomechanical regulation of blood vessel growth during tissue vascularization. *Nature Medicine, 15*(6), 657–664.
123. Kloxin, A. M., Kasko, A. M., Salinas, C. N., & Anseth, K. S. (2009). Photodegradable hydrogels for dynamic tuning of physical and chemical properties. *Science, 324*(5923), 59–63.
124. Klumb, L. A., & Horbett, T. A. (1992). Design of insulin delivery devices based on glucose sensitive membranes. *Journal of Controlled Release, 18*(1), 59–80.
125. Koay, E. J., & Athanasiou, K. A. (2008). Hypoxic chondrogenic differentiation of human embryonic stem cells enhances cartilage protein synthesis and biomechanical functionality. *Osteoarthritis and Cartilage, 16*(12), 1450–1456.
126. Koh, M. Y., & Powis, G. (2012). Passing the baton: The HIF switch. *Trends in Biochemical Sciences, 37*(9), 364–372.
127. Koh, W., Stratman, A. N., Sacharidou, A., & Davis, G. E. (2008). In vitro three dimensional collagen matrix models of endothelial lumen formation during vasculogenesis and angiogenesis. *Methods in Enzymology, 443*, 83–101.
128. Koike, N., et al. (2004). Tissue engineering: Creation of long-lasting blood vessels. *Nature, 428*, 138.
129. Korin, N., Bransky, A., Dinnar, U., & Levenberg, S. (2009). Periodic "flow-stop" perfusion microchannel bioreactors for mammalian and human embryonic stem cell long-term culture. *Biomedical Microdevices, 11*(1), 87–94.
130. Kreger, S. T., & Voytik-Harbin, S. L. (2009). Hyaluronan concentration within a 3D collagen matrix modulates matrix viscoelasticity, but not fibroblast response. *Matrix Biology, 28*(6), 336–346.
131. Kumar, R., Stepanek, F., & Mantalaris, A. (2003). *A conceptual model for oxygen transport in the human marrow*. Modelling and Control in Biomedical Systems 2003 (Including Biological Systems). pp. 365–370.
132. Kumar, R., Stepanek, F., & Mantalaris, A. (2004). An oxygen transport model for human bone marrow microcirculation. *Food and Bioproducts Processing, 82*(C2), 105–116.
133. Kumar, R., Panoskaltsis, N., Stepanek, F., & Mantalaris, A. (2008). Coupled oxygen-carbon dioxide transport model for the human bone marrow. *Food and Bioproducts Processing, 86*(C3), 211–219.
134. Kusuma, S., Zhao, S., & Gerecht, S. (2012). The extracellular matrix is a novel attribute of endothelial progenitors and of hypoxic mature endothelial cells. *FASEB Journal, 26*(12), 4925–4936.
135. Kusuma, S., Peijnenburg, E., Patel, P., & Gerecht, S. (2014). Low oxygen tension enhances endothelial fate of human pluripotent stem cells. *Arteriosclerosis, Thrombosis, and Vascular Biology, 34*(4), 913–920.

136. Lai, E. S., Huang, N. F., Cooke, J. P., & Fuller, G. G. (2012). Aligned nanofibrillar collagen regulates endothelial organization and migration. *Regenerative Medicine, 7*(5), 649–661.
137. Landman, K. A., & Cai, A. Q. (2007). Cell proliferation and oxygen diffusion in a vascularising scaffold. *Bulletin of Mathematical Biology, 69*(7), 2405–2428.
138. Langer, R., & Tirrell, D. A. (2004). Designing materials for biology and medicine. *Nature, 428*(6982), 487–492.
139. Lanza, V. A., Ambrosi, D., & Preziosi, L. (2006). Exogenous control of vascular network formation in vitro: A mathematical model. *Networks and Heterogeneous Media, 1*(4), 621–638.
140. Lee, S. W., Jeong, H. K., Lee, J. Y., Yang, J., Lee, E. J., Kim, S. Y., et al. (2012). Hypoxic priming of mESCs accelerates vascular-lineage differentiation through HIF1-mediated inverse regulation of Oct4 and VEGF. *EMBO Molecular Medicine, 4*(9), 924–938.
141. Lee, Y. M., Jeong, C. H., Koo, S. Y., Son, M. J., Song, H. S., Bae, S. K., et al. (2001). Determination of hypoxic region by hypoxia marker in developing mouse embryos in vivo: A possible signal for vessel development. *Developmental Dynamics, 220*(2), 175–186.
142. Levenberg, S., Rouwkema, J., Macdonald, M., Garfein, E. S., Kohane, D. S., Darland, D. C., et al. (2005). Engineering vascularized skeletal muscle tissue. *Nature Biotechnology, 23*(7), 879–884.
143. Lewis, D. M., Park, K. M., Tang, V., Xu, Y., Pak, K., Eisinger-Mathason, T. S. K., et al. (2016). Intratumoral oxygen gradients mediate sarcoma cell invasion. *Proceedings of the National Academy of Sciences, 113*, 9292–9297.
144. Lewis, D. M., Blatchley, M. R., Park, K. M., & Gerecht, S. (2017). O-2-controllable hydrogels for studying cellular responses to hypoxic gradients in three dimensions in vitro and in vivo. *Nature Protocols, 12*(8), 1620–1638.
145. Lewis, M. C., Macarthur, B. D., Malda, J., Pettet, G., & Please, C. P. (2005). Heterogeneous proliferation within engineered cartilaginous tissue: The role of oxygen tension. *Biotechnology and Bioengineering, 91*(5), 607–615.
146. Li, C., Issa, R., Kumar, P., Hampson, I. N., Lopez-Novoa, J. M., Bernabeu, C., et al. (2003). CD105 prevents apoptosis in hypoxic endothelial cells. *Journal of Cell Science, 116*(Pt 13), 2677–2685.
147. Li, S. R., Nih, L. R., Bachman, H., Fei, P., Li, Y. L., Nam, E., et al. (2017). Hydrogels with precisely controlled integrin activation dictate vascular patterning and permeability. *Nature Materials, 16*(9), 953.
148. Limper, A. H., & Roman, J. (1992). Fibronectin. A versatile matrix protein with roles in thoracic development, repair and infection. *Chest, 101*(6), 1663–1673.
149. Lubarsky, B., & Krasnow, M. A. (2003). Tube morphogenesis: Making and shaping biological tubes. *Cell, 112*(1), 19–28.
150. Lucitti, J. L., Jones, E. A., Huang, C., Chen, J., Fraser, S. E., & Dickinson, M. E. (2007). Vascular remodeling of the mouse yolk sac requires hemodynamic force. *Development, 134*(18), 3317–3326.
151. Lutolf, M. P. (2009). Biomaterials: Spotlight on hydrogels. *Nature Materials, 8*(6), 451–453.
152. Lutolf, M. P., & Hubbell, J. A. (2005). Synthetic biomaterials as instructive extracellular microenvironments for morphogenesis in tissue engineering. *Nature Biotechnology, 23*(1), 47–55.
153. Lutolf, M. P., Lauer-Fields, J. L., Schmoekel, H. G., Metters, A. T., Weber, F. E., Fields, G. B., et al. (2003). Synthetic matrix metalloproteinase-sensitive hydrogels for the conduction of tissue regeneration: Engineering cell-invasion characteristics. *Proceedings of the National Academy of Sciences of the United States of America, 100*(9), 5413–5418.
154. Lyons, T. W., Reinhard, C. T., & Planavsky, N. J. (2014). The rise of oxygen in Earth's early ocean and atmosphere. *Nature, 506*(7488), 307–315.
155. Ma, T., Grayson, W. L., Frohlich, M., & Vunjak-Novakovic, G. (2009). Hypoxia and stem cell-based engineering of mesenchymal tissues. *Biotechnology Progress, 25*(1), 32–42.
156. Maltepe, E., & Simon, M. C. (1998). Oxygen, genes, and development: An analysis of the role of hypoxic gene regulation during murine vascular development. *Journal of Molecular Medicine, 76*(6), 391–401.

157. Mamchaoui, K., & Saumon, G. (2000). A method for measuring the oxygen consumption of intact cell monolayers. *American Journal of Physiology. Lung Cellular and Molecular Physiology, 278*(4), L858–L863.
158. Mammoto, A., Connor, K. M., Mammoto, T., Yung, C. W., Huh, D., Aderman, C. M., et al. (2009). A mechanosensitive transcriptional mechanism that controls angiogenesis. *Nature, 457*(7233), 1103–1108.
159. Manalo, D. J., Rowan, A., Lavoie, T., Natarajan, L., Kelly, B. D., Ye, S. Q., et al. (2005). Transcriptional regulation of vascular endothelial cell responses to hypoxia by HIF-1. *Blood, 105*(2), 659–669.
160. Martorell, L., Gentile, M., Rius, J., Rodriguez, C., Crespo, J., Badimon, L., et al. (2009). The hypoxia-inducible factor 1/NOR-1 axis regulates the survival response of endothelial cells to hypoxia. *Molecular and Cellular Biology, 29*(21), 5828–5842.
161. Massabuau, J. C. (2001). From low arterial- to low tissue-oxygenation strategy. An evolutionary theory. *Respiration Physiology, 128*(3), 249–261.
162. Massabuau, J. C. (2003). Primitive, and protective, our cellular oxygenation status? *Mechanisms of Ageing and Development, 124*(8-9), 857–863.
163. Mehta, G., Mehta, K., Sud, D., Song, J. W., Bersano-Begey, T., Futai, N., et al. (2007). Quantitative measurement and control of oxygen levels in microfluidic poly(dimethylsiloxane) bioreactors during cell culture. *Biomedical Microdevices, 9*(2), 123–134.
164. Melero-Martin, J. M., De Obaldia, M. E., Kang, S. Y., Khan, Z. A., Yuan, L., Oettgen, P., et al. (2008). Engineering robust and functional vascular networks in vivo with human adult and cord blood-derived progenitor cells. *Circulation Research, 103*(2), 194–202.
165. Moon, J. J., Hahn, M. S., Kim, I., Nsiah, B. A., & West, J. L. (2009). Micropatterning of poly(ethylene glycol) diacrylate hydrogels with biomolecules to regulate and guide endothelial morphogenesis. *Tissue Engineering Part A, 15*(3), 579–585.
166. Moon, J. J., Saik, J. E., Poché, R. A., Leslie-Barbick, J. E., Lee, S.-H., Smith, A. A., et al. (2010). Biomimetic hydrogels with pro-angiogenic properties. *Biomaterials, 31*(14), 3840–3847.
167. Myllyharju, J., & Schipani, E. (2010). Extracellular matrix genes as hypoxia-inducible targets. *Cell and Tissue Research, 339*(1), 19–29.
168. Niebruegge, S., Bauwens, C. L., Peerani, R., Thavandiran, N., Masse, S., Sevaptisidis, E., et al. (2009). Generation of human embryonic stem cell-derived mesoderm and cardiac cells using size-specified aggregates in an oxygen-controlled bioreactor. *Biotechnology and Bioengineering, 102*(2), 493–507.
169. Oppegard, S. C., Blake, A. J., Williams, J. C., & Eddington, D. T. (2010). Precise control over the oxygen conditions within the Boyden chamber using a microfabricated insert. *Lab on a Chip, 10*(18), 2366–2373.
170. Ottino, P., Finley, J., Rojo, E., Ottlecz, A., Lambrou, G. N., Bazan, H. E., et al. (2004). Hypoxia activates matrix metalloproteinase expression and the VEGF system in monkey choroid-retinal endothelial cells: Involvement of cytosolic phospholipase A2 activity. *Molecular Vision, 10*, 341–350.
171. Papandreou, I., Cairns, R. A., Fontana, L., Lim, A. L., & Denko, N. C. (2006). HIF-1 mediates adaptation to hypoxia by actively downregulating mitochondrial oxygen consumption. *Cell Metabolism, 3*(3), 187–197.
172. Papandreou, I., Lim, A. L., Laderoute, K., & Denko, N. C. (2008). Hypoxia signals autophagy in tumor cells via AMPK activity, independent of HIF-1, BNIP3, and BNIP3L. *Cell Death and Differentiation, 15*(10), 1572–1581.
173. Park, K. M., & Gerecht, S. (2014). Hypoxia-inducible hydrogels. *Nature Communications, 5*, 12.
174. Park, T. G., & Hoffman, A. S. (1992). Synthesis and characterization of pH- and or temperature-sensitive hydrogels. *Journal of Applied Polymer Science, 46*(4), 659–671.
175. Parmar, K., Mauch, P., Vergilio, J. A., Sackstein, R., & Down, J. D. (2007). Distribution of hematopoietic stem cells in the bone marrow according to regional hypoxia. *Proceedings of the National Academy of Sciences of the United States of America, 104*(13), 5431–5436.

176. Phelps, E. A., Landazuri, N., Thule, P. M., Taylor, W. R., & Garcia, A. J. (2009). Bioartificial matrices for therapeutic vascularization. *Proceedings of the National Academy of Sciences, 107*(8), 3323–3328.
177. Phillips, P. G., Birnby, L. M., & Narendran, A. (1995). Hypoxia induces capillary network formation in cultured bovine pulmonary microvessel endothelial cells. *The American Journal of Physiology, 268*(5 Pt 1), L789–L800.
178. Pierschbacher, M. D., & Ruoslahti, E. (1984). Cell attachment activity of fibronectin can be duplicated by small synthetic fragments of the molecule. *Nature, 309*(5963), 30–33.
179. Pollard, P. J., Loenarz, C., Mole, D. R., McDonough, M. A., Gleadle, J. M., Schofield, C. J., et al. (2008). Regulation of Jumonji-domain-containing histone demethylases by hypoxia-inducible factor (HIF)-1alpha. *The Biochemical Journal, 416*(3), 387–394.
180. Popel, A. S. (1989). Theory of oxygen transport to tissue. *Critical Reviews in Biomedical Engineering, 17*(3), 257–321.
181. Prado-Lopez, S., Conesa, A., Arminan, A., Martinez-Losa, M., Escobedo-Lucea, C., Gandia, C., et al. (2010). Hypoxia promotes efficient differentiation of human embryonic stem cells to functional endothelium. *Stem Cells, 28*, 407–418.
182. Prasad, S. M., Czepiel, M., Cetinkaya, C., Smigielska, K., Weli, S. C., Lysdahl, H., et al. (2009). Continuous hypoxic culturing maintains activation of Notch and allows long-term propagation of human embryonic stem cells without spontaneous differentiation. *Cell Proliferation, 42*(1), 63–74.
183. Radisic, M., Deen, W., Langer, R., & Vunjak-Novakovic, G. (2005). Mathematical model of oxygen distribution in engineered cardiac tissue with parallel channel array perfused with culture medium containing oxygen carriers. *American Journal of Physiology. Heart and Circulatory Physiology, 288*(3), H1278–H1289.
184. Risau, W. (1997). Mechanisms of angiogenesis. *Nature, 386*(6626), 671–674.
185. Risau, W., & Flamme, I. (1995). Vasculogenesis. *Annual Review of Cell and Developmental Biology, 11*, 73–91.
186. Robins, S. P. (2007). Biochemistry and functional significance of collagen cross-linking. *Biochemical Society Transactions, 35*(5), 849–852.
187. Rodenhizer, D., Gaude, E., Cojocari, D., Mahadevan, R., Frezza, C., Wouters, B. G., et al. (2016). A three-dimensional engineered tumour for spatial snapshot analysis of cell metabolism and phenotype in hypoxic gradients. *Nature Materials, 15*(2), 227.
188. Rodesch, F., Simon, P., Donner, C., & Jauniaux, E. (1992). Oxygen measurements in endometrial and trophoblastic tissues during early pregnancy. *Obstetrics and Gynecology, 80*(2), 283–285.
189. Roeder, B. A., Kokini, K., Sturgis, J. E., Robinson, J. P., & Voytik-Harbin, S. L. (2002). Tensile mechanical properties of three-dimensional type I collagen extracellular matrices with varied microstructure. *Journal of Biomechanical Engineering, 124*(2), 214–222.
190. Romer, L. H., Birukov, K. G., & Garcia, J. G. (2006). Focal adhesions: Paradigm for a signaling nexus. *Circulation Research, 98*(5), 606–616.
191. Rosenfeld, D., Landau, S., Shandalov, Y., Raindel, N., Freiman, A., Shor, E., et al. (2016). Morphogenesis of 3D vascular networks is regulated by tensile forces. *Proceedings of the National Academy of Sciences of the United States of America, 113*(12), 3215–3220.
192. Sage, E. H., & Vernon, R. B. (1994). Regulation of angiogenesis by extracellular matrix: The growth and the glue. *Journal of Hypertension, 12*(suppl. 10), S145–S152.
193. Saunders, W. B., Bayless, K. J., & Davis, G. E. (2005). MMP-1 activation by serine proteases and MMP-10 induces human capillary tubular network collapse and regression in 3D collagen matrices. *Journal of Cell Science, 118*(Pt 10), 2325–2340.
194. Scott, C., Lyons, T. W., Bekker, A., Shen, Y., Poulton, S. W., Chu, X., et al. (2008). Tracing the stepwise oxygenation of the Proterozoic ocean. *Nature, 452*(7186), 456–459.
195. Segura, I., Serrano, A., De Buitrago, G. G., Gonzalez, M. A., Abad, J. L., Claveria, C., et al. (2002). Inhibition of programmed cell death impairs in vitro vascular-like structure formation and reduces in vivo angiogenesis. *The FASEB Journal, 16*(8), 833–841.

196. Seliktar, D., Zisch, A. H., Lutolf, M. P., Wrana, J. L., & Hubbel, J. A. (2004). MMP-2 sensitive, VEGF-bearing bioactive hydrogels for promotion of vascular healing. *Journal of Biomedical Materials Research - Part A, 68*(4), 704–716.
197. Shaw, A. D., Li, Z., Thomas, Z., & Stevens, C. W. (2002). Assessment of tissue oxygen tension: Comparison of dynamic fluorescence quenching and polarographic electrode technique. *Critical Care, 6*(1), 76–80.
198. Shen, Y. H., Shoichet, M. S., & Radisic, M. (2008). Vascular endothelial growth factor immobilized in collagen scaffold promotes penetration and proliferation of endothelial cells. *Acta Biomaterialia, 4*(3), 477–489.
199. Shweiki, D., Neeman, M., Itin, A., & Keshet, E. (1995). Induction of vascular endothelial growth factor expression by hypoxia and by glucose deficiency in multicell spheroids: Implications for tumor angiogenesis. *Proceedings of the National Academy of Sciences of the United States of America, 92*(3), 768–772.
200. Sieminski, A. L., Hebbel, R. P., & Gooch, K. J. (2004). The relative magnitudes of endothelial force generation and matrix stiffness modulate capillary morphogenesis in vitro. *Experimental Cell Research, 297*(2), 574–584.
201. Sieminski, A. L., Was, A. S., Kim, G., Gong, H., & Kamm, R. D. (2007). The stiffness of three-dimensional ionic self-assembling peptide gels affects the extent of capillary-like network formation. *Cell Biochemistry and Biophysics, 49*(2), 73–83.
202. Siggaard-Andersen, O., & Huch, R. (1995). The oxygen status of fetal blood. *Acta Anaesthesiologica Scandinavica. Supplementum, 107*, 129–135.
203. Silva, G. A., Czeisler, C., Niece, K. L., Beniash, E., Harrington, D. A., Kessler, J. A., et al. (2004). Selective differentiation of neural progenitor cells by high-epitope density nanofibers. *Science, 303*(5662), 1352–1355.
204. Silver, I. A. (1984). Cellular microenvironment in healing and non-healing wounds. In T. K. Hunt (Ed.), *Soft and hard tissue repair* (pp. 50–66). New York: Praeger.
205. Smith, Q., Chan, X. Y., Carmo, A. M., Trempel, M., Saunders, M., & Gerecht, S. (2017). Compliant substratum guides endothelial commitment from human pluripotent stem cells. *Science Advances, 3*(5), 9.
206. Sorrell, J. M., Baber, M. A., & Caplan, A. I. (2007). A self-assembled fibroblast-endothelial cell co-culture system that supports in vitro vasculogenesis by both human umbilical vein endothelial cells and human dermal microvascular endothelial cells. *Cells, Tissues, Organs, 186*(3), 157–168.
207. Sottile, J., & Hocking, D. C. (2002). Fibronectin polymerization regulates the composition and stability of extracellular matrix fibrils and cell-matrix adhesions. *Molecular Biology of the Cell, 13*(10), 3546–3559.
208. Soucy, P. A., & Romer, L. H. (2009). Endothelial cell adhesion, signaling, and morphogenesis in fibroblast-derived matrix. *Matrix Biology, 28*(5), 273–283.
209. Springett, R., & Swartz, H. M. (2007). Measurements of oxygen in vivo: Overview and perspectives on methods to measure oxygen within cells and tissues. *Antioxidants & Redox Signaling, 9*(8), 1295–1301.
210. Steinlechner-Maran, R., Eberl, T., Kunc, M., Margreiter, R., & Gnaiger, E. (1996). Oxygen dependence of respiration in coupled and uncoupled endothelial cells. *The American Journal of Physiology, 271*(6 Pt 1), C2053–C2061.
211. Stephanou, A., Meskaoui, G., Vailhe, B., & Tracqui, P. (2007). The rigidity in fibrin gels as a contributing factor to the dynamics of in vitro vascular cord formation. *Microvascular Research, 73*(3), 182–190.
212. Stratman, A. N., Saunders, W. B., Sacharidou, A., Koh, W., Fisher, K. E., Zawieja, D. C., et al. (2009). Endothelial cell lumen and vascular guidance tunnel formation requires MT1-MMP-dependent proteolysis in 3-dimensional collagen matrices. *Blood, 114*(2), 237–247.
213. Stupack, D. G., & Cheresh, D. A. (2002). ECM remodeling regulates angiogenesis: Endothelial integrins look for new ligands. *Science's STKE, 2002*(119), pe7.

214. Sun, G., & Chu, C.-C. (2006). Synthesis, characterization of biodegradable dextran-allyl isocyanate-ethylamine/polyethylene glycol-diacrylate hydrogels and their in vitro release of albumin. *Carbohydrate Polymers, 65*(3), 273–287.
215. Sun, G., Shen, Y.-I., Ho, C. C., Kusuma, S., & Gerecht, S. (2009). Functional groups affect physical and biological properties of dextran-based hydrogels. *Journal of Biomedical Materials Research Part A, 93*(3), 1080–1090.
216. Sun, G. M., Zhang, X. Z., & Chu, C. C. (2007). Formulation and characterization of chitosan-based hydrogel films having both temperature and pH sensitivity. *Journal of Materials Science. Materials in Medicine, 18*(8), 1563–1577.
217. Tajima, R., Kawaguchi, N., Horino, Y., Takahashi, Y., Toriyama, K., Inou, K., et al. (2001). Hypoxic enhancement of type IV collagen secretion accelerates adipose conversion of 3T3-L1 fibroblasts. *Biochimica et Biophysica Acta, 1540*(3), 179–187.
218. Thurston, G., Suri, C., Smith, K., McClain, J., Sato, T. N., Yancopoulos, G. D., et al. (1999). Leakage-resistant blood vessels in mice transgenically overexpressing angiopoietin-1. *Science, 286*(5449), 2511–2514.
219. Timmermans, F., Plum, J., Yoder, M. C., Ingram, D. A., Vandekerckhove, B., & Case, J. (2009). Endothelial progenitor cells: Identity defined? *Journal of Cellular and Molecular Medicine, 13*(1), 87–102.
220. Toh, Y. C., Zhang, C., Zhang, J., Khong, Y. M., Chang, S., Samper, V. D., et al. (2007). A novel 3D mammalian cell perfusion-culture system in microfluidic channels. *Lab on a Chip, 7*(3), 302–309.
221. Toole, B. P. (2001). Hyaluronan in morphogenesis. *Seminars in Cell & Developmental Biology, 12*(2), 79–87.
222. Toole, B. P. (2004). Hyaluronan: From extracellular glue to pericellular cue. *Nature Reviews. Cancer, 4*(7), 528–539.
223. Tsai, A. G., Johnson, P. C., & Intaglietta, M. (2003). Oxygen gradients in the microcirculation. *Physiological Reviews, 83*(3), 933–963.
224. Tsang, K. M., Hyun, J. S., Cheng, K. T., Vargas, M., Mehta, D., Ushio-Fukai, M., et al. (2017). Embryonic stem cell differentiation to functional arterial endothelial cells through sequential activation of ETV2 and NOTCH1 signaling by HIF1 alpha. *Stem Cell Reports, 9*(3), 796–806.
225. Urbich, C., & Dimmeler, S. (2004). Endothelial progenitor cells: Characterization and role in vascular biology. *Circulation Research, 95*(4), 343–353.
226. Urbich, C., Heeschen, C., Aicher, A., Sasaki, K., Bruhl, T., Farhadi, M. R., et al. (2005). Cathepsin L is required for endothelial progenitor cell-induced neovascularization. *Nature Medicine, 11*(2), 206–213.
227. Ushio-Fukai, M., & Nakamura, Y. (2008). Reactive oxygen species and angiogenesis: NADPH oxidase as target for cancer therapy. *Cancer Letters, 266*(1), 37–52.
228. Vega, S. L., Kwon, M. Y., Song, K. H., Wang, C., Mauck, R. L., Han, L., et al. (2018). Combinatorial hydrogels with biochemical gradients for screening 3D cellular microenvironments. *Nature Communications, 9*, 10.
229. Vo, E., Hanjaya-Putra, D., Zha, Y., Kusuma, S., & Gerecht, S. (2010). Smooth-muscle-like cells derived from human embryonic stem cells support and augment cord-like structures in vitro. *Stem Cell Reviews, 6*, 237–247.
230. Walls, J. R., Coultas, L., Rossant, J., & Henkelman, R. M. (2008). Three-dimensional analysis of vascular development in the mouse embryo. *PLoS One, 3*(8), e2853.
231. Walter, D. H., Rittig, K., Bahlmann, F. H., Kirchmair, R., Silver, M., Murayama, T., et al. (2002). Statin therapy accelerates reendothelialization: A novel effect involving mobilization and incorporation of bone marrow-derived endothelial progenitor cells. *Circulation, 105*(25), 3017–3024.
232. Wanjare, M., Kusuma, S., & Gerecht, S. (2014). Defining differences among perivascular cells derived from human pluripotent stem cells. *Stem Cell Reports, 2*(5), 561–575.
233. Ward, J. P. (2008). Oxygen sensors in context. *Biochimica et Biophysica Acta, 1777*(1), 1–14.

234. Webster, K. A. (2006). Puma joins the battery of BH3-only proteins that promote death and infarction during myocardial ischemia. *American Journal of Physiology. Heart and Circulatory Physiology, 291*(1), H20–H22.
235. Werner, N., Junk, S., Laufs, U., Link, A., Walenta, K., Bohm, M., et al. (2003). Intravenous transfusion of endothelial progenitor cells reduces neointima formation after vascular injury. *Circulation Research, 93*(2), e17–e24.
236. Wijelath, E. S., Rahman, S., Namekata, M., Murray, J., Nishimura, T., Mostafavi-Pour, Z., et al. (2006). Heparin-II domain of fibronectin is a vascular endothelial growth factor-binding domain: Enhancement of VEGF biological activity by a singular growth factor/matrix protein synergism. *Circulation Research, 99*(8), 853–860.
237. Williams, S. E., Wootton, P., Mason, H. S., Bould, J., Iles, D. E., Riccardi, D., et al. (2004). Hemoxygenase-2 is an oxygen sensor for a calcium-sensitive potassium channel. *Science, 306*(5704), 2093–2097.
238. Wolburg, H., & Lippoldt, A. (2002). Tight junctions of the blood-brain barrier: Development, composition and regulation. *Vascular Pharmacology, 38*(6), 323–337.
239. Wolin, M. S., Ahmad, M., & Gupte, S. A. (2005). Oxidant and redox signaling in vascular oxygen sensing mechanisms: Basic concepts, current controversies, and potential importance of cytosolic NADPH. *American Journal of Physiology. Lung Cellular and Molecular Physiology, 289*(2), L159–L173.
240. Xu, W., Koeck, T., Lara, A. R., Neumann, D., DiFilippo, F. P., Koo, M., et al. (2007). Alterations of cellular bioenergetics in pulmonary artery endothelial cells. *Proceedings of the National Academy of Sciences of the United States of America, 104*(4), 1342–1347.
241. Yamakawa, M., Liu, L. X., Date, T., Belanger, A. J., Vincent, K. A., Akita, G. Y., et al. (2003). Hypoxia-inducible factor-1 mediates activation of cultured vascular endothelial cells by inducing multiple angiogenic factors. *Circulation Research, 93*(7), 664–673.
242. Yoon, C. H., Hur, J., Oh, I. Y., Park, K. W., Kim, T. Y., Shin, J. H., et al. (2006). Intercellular adhesion molecule-1 is upregulated in ischemic muscle, which mediates trafficking of endothelial progenitor cells. *Arteriosclerosis, Thrombosis, and Vascular Biology, 26*(5), 1066–1072.
243. Yoshida, Y., Takahashi, K., Okita, K., Ichisaka, T., & Yamanaka, S. (2009). Hypoxia enhances the generation of induced pluripotent stem cells. *Cell Stem Cell, 5*(3), 237–241.
244. Yung, C. W., Wu, L. Q., Tullman, J. A., Payne, G. F., Bentley, W. E., & Barbari, T. A. (2007). Transglutaminase crosslinked gelatin as a tissue engineering scaffold. *Journal of Biomedical Materials Research Part A, 83A*(4), 1039–1046.
245. Zhang, H., Bosch-Marce, M., Shimoda, L. A., Tan, Y. S., Baek, J. H., Wesley, J. B., et al. (2008). Mitochondrial autophagy is an HIF-1-dependent adaptive metabolic response to hypoxia. *The Journal of Biological Chemistry, 283*(16), 10892–10903.
246. Zhang, X., Liu, L., Wei, X., Tan, Y. S., Tong, L., Chang Bs, R., et al. (2010). Impaired angiogenesis and mobilization of circulating angiogenic cells in HIF-1alpha heterozygous-null mice after burn wounding. *Wound Repair and Regeneration, 18*, 193–201.
247. Zhou, X., Rowe, R. G., Hiraoka, N., George, J. P., Wirtz, D., Mosher, D. F., et al. (2008). Fibronectin fibrillogenesis regulates three-dimensional neovessel formation. *Genes and Development, 22*(9), 1231–1243.
248. Zisch, A. H., Lutolf, M. P., & Hubbell, J. A. (2003). Biopolymeric delivery matrices for angiogenic growth factors. *Cardiovascular Pathology, 12*(6), 295–310.
249. Zisch, A. H., Lutolf, M. P., Ehrbar, M., Raeber, G. P., Rizzi, S. C., Davies, N., et al. (2003). Cell-demanded release of VEGF from synthetic, biointeractive cell ingrowth matrices for vascularized tissue growth. *The FASEB Journal, 17*(15), 2260–2262.

Chapter 5
3D Printing Technology for Vascularization

Enoch Yeung, Pooja Yesantharao, Chin Siang Ong, and Narutoshi Hibino

5.1 Introduction

The paradigm shift from therapeutic to regenerative medicine over the past few decades has prompted the advancement of technologies that can be used to treat organ failure. Since the first organ transplant surgery in the 1950s, a kidney transplant between identical twins [21], regenerative medicine techniques have been used to restore tissue function and repair diseased organs. Within the realm of regenerative medicine, "tissue engineering is an interdisciplinary field that applies the principles of engineering and the life sciences toward the development of biological substitutes that restore, maintain, or improve tissue function" (quote from [31]). The goal of tissue engineering is to produce constructs with the capacity for long-term survival. Thus, ensuring a robust capillary supply to these tissue constructs is of paramount importance. However, most tissue-engineered fabrication techniques that require manual processing procedures are limited by the inconsistency in the microstructure construction. Due to such limitations in the precise control of the material behavior and internal structure of the construction, these techniques were unable to reach the ultimate goal of fabricating persistently viable engineered tissue. However, newer 3D printing technologies allow for precise and delicate manipulation of printed materials and the printing trajectory, leading to refined printed grafts.

3D engineered constructs enable cell adhesion, growth, and regeneration. Ideally speaking, the scaffold, which forms the porous structure of the constructs, starts degrading after implantation of the vascular constructs. This allows for the growth and proliferation of the printed cells, thereby promoting new tissue formation and restoration of tissue function [43]. The microstructure parameters of the printed

E. Yeung · P. Yesantharao · C. S. Ong · N. Hibino (✉)
Division of Cardiac Surgery, Johns Hopkins Hospital, Baltimore, MD, USA
e-mail: nhibino1@jhmi.edu

S. Gerecht (ed.), *Biophysical Regulation of Vascular Differentiation and Assembly*, Biological and Medical Physics, Biomedical Engineering,
https://doi.org/10.1007/978-3-319-99319-5_5

grafts, including pore dimension and distribution, play an important role in the active cell regeneration process in terms of nutrient/oxygen exchange and metabolite waste removal. Furthermore, 3D printed tissue and vascular constructs can be tailor-made to patient-specific organ tissue morphologies using various image mapping techniques like X-ray, magnetic resonance imaging (MRI), or computed tomography (CT) [19]. The extreme precision and delicate cell/biomaterial handling algorithms used in 3D bioprinting allow for microvascular construction with native-like cellular signaling.

In this chapter we will discuss different 3D printing approaches, including inkjet, extrusion, laser and scaffold-free methods, and their current applications in fabrication of microvascular network (diameter <1 mm) and vascular graft (diameter ≥1 mm).

5.2 Methodology

In each method section, the discussion of the application is divided into microvascular channel creation and vascular graft creation, with tables corresponding to each. Table 5.1 is for microvascular channel creation, and Table 5.2 is vascular graft creation.

5.2.1 Inkjet-Based Printing

5.2.1.1 Principle (Fig. 5.1)

Inkjet printing technology was developed in the 1950s. In 2D printing, materials are first loaded as liquids into a nozzled chamber. During printing, the materials are pushed out from a syringe-like device, forming a stream of droplets due to Plateau-Rayleigh instability. The droplets are then charged by an electrode and deflected by an electric field to print at a desired position on the substrate. In 3D inkjet printing, the same principles are applied. The printing materials, which can include a hydrogel scaffold, living cells, or a mixture of both, are precisely deposited as droplets [19]. Different types of driving energy technologies have been described, including thermal, piezoelectric, and electrostatic modalities. In thermal inkjet systems, rapid heat energy provides the driving pressure for the bioink droplets, whereas in piezoelectric systems, polycrystalline ceramics promote the conversion of electric energy to mechanical energy, to allow for particle deposition. The nozzle is critical for droplet loading in inkjet systems. However, the shear forces exerted by the nozzle on the printed droplets can impact cell viability and the chemical properties of the bioink. This necessitated the development of a droplet-on-demand system, introduced to minimize such damages, using a micro-valve to precisely deliver the bioink [7].

Table 5.1 Overview samples of biofabrication of vascular tissue using 3D printing technology-microvascular network creation

Printing technique		Materials	Cells	Sacrificial materials/supportive materials	Years	References
IB	Electrostatic	Alginate			2008	[40]
IB	Electrostatic	Alginate			2008	[38]
IB	Thermal	Fibrin	HMVECs		2009	[4]
IB	DOD	Mouse collagen type 1	HUVECs	Gelatin	2012	[55]
IB	DOD	Mouse collagen type 1	HUVECs	Gelatin	2014	[32]
IB	DOD	Mouse collagen type 1	HUVECs	Gelatin	2014	[33]
EB	Direct	Alginate	RHECs		2009	[27]
EB	Direct	Alginate	Mouse fibroblast		2015	[15]
EB	Direct	GelMA/alginate	HUVECs		2016	[3]
EB	Direct	GelMA/PEGTA/ alginate	HUVECs, hMSC		2016	[24]
EB	Direct	GelMA/alginate	HUVECs, CM		2016	[54]
EB	Indirect	Hydrogel		Pluronic F127	2011	[51]
EB	Indirect	GelMA	HNDF, HUVECs	Pluronic F127	2014	[28]
EB	Indirect	Gelatin	HNDF, HUVECs, hMSC		2016	[29]
LB		Alginate/glycerol	Rabbit carcinoma cell B16, HUVECs		2010	[18]
LB		Matrigel	HUVECs, HUVSMC		2010	[50]
LB	DLP	GelMA/GM-HA	HUVEC, mouse fibroblast (C3H/10T1/2 cells)		2017	[56]
SF			HUVSMCs/HSFs/PASMCs	Agarose	2009	[41]

Table 5.2 Overview samples of biofabrication of vascular tissue using 3D printing technology-vascular graft creation

Printing technique		Materials	Cells	Sacrificial materials/ supportive materials	Diameter/dimension of the constructs (mm)	Year	References
IB	Thermal	Alginate	Rat smooth muscle cell		2	2005	[26]
IB		Agarose hydrogel	hMSC, human MG-63 cells		~5	2013	[11]
IB		Agarose hydrogel	Human MG-63 cells		~6	2013	[2]
EB	Direct	Polyurethane/ alginate	ADSC		5	2013	[52]
EB	Direct	PGA, PCLC			12	2017	[14]
LB	DLP	EGT/UDA/HEA			~1	2011	[1]
LB	SL	PTHF-DA	HDF		~2	2012	[36]
LB	DLP	PPF			1	2016	[35]
SF			PACs/HACs/HMFs HUVEC/ mouse myoblasts C2C12	Agarose	~3	2006	[25]
SF			Mouse fibroblast	Alginate	~3	2012	[53]
SF			HASMCs/HUVECs	Agarose	~5	2014	[48]
SF			MEFs	Agarose	~9	2015	[30]
SF			HUVEC/HASMC/HNDFB		1.5	2015	[23]

EB extrusion based, *LB* laser based, *IB* inkjet based, *SF* scaffold-free, *DOD* droplet on demand, *DLP* digital light processing, *SL* stereolithography, *EGTG* ethylene glycol bisthioglycolate, *UDA* Genomer 4215, *HEA* hydroxyethylacrylate, *PTHF-DA* polytetrahydrofuran-diacrylates, *PPF* poly(propylene fumarate), *ADSC* adipose-derived stem cell, *hMSC* human mesenchymal stem cells, *HUVECS* human umbilical vein endothelial cells, *HUVSMC* human umbilical vein smooth muscle cells, *HDF* human dermal fibroblast, *HMVEC* human microvascular endothelial cells, *RHEC* rat heart endothelial cells, human MG-63 cells, an osteosarcoma-derived cell line, *PACs* pig articular chondrocytes, *HACs* human articular chondrocytes, *HMFs* human myofibroblasts, *HSF* human skin fibroblasts, *PASMCs* porcine aortic smooth muscle cells, *MEFs* mouse embryonic fibroblast, *HASMC* human aortic smooth muscle cells, *HNDFB* human normal dermal fibroblasts

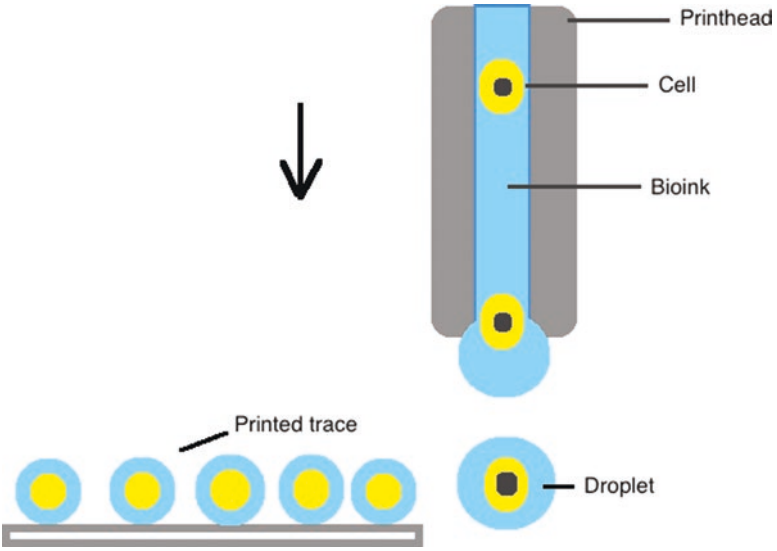

Fig. 5.1 A schematic of inkjet-based bioprinting. Droplets of a cell with bioink are formed from the reservoir to be deposited on a collection plate

5.2.1.2 Application

Microvascular Network Creation (Table 5.1)

Nishiyama et al. printed vascular constructs following the same method described above, using a custom inkjet bioprinter with a position detection accuracy of less than a few micrometers [39]. This experiment demonstrated a technique for bioprinting a 3D structure using a laminating method, which involves the sequential deposition of materials. They used a viscosity enhancer to consolidate and fortify the constructs. The group further investigated the use of such technology to fabricate smaller-scale tubular constructs (200 um in diameter, compared to the original 1 mm diameter tubes), using a small-sized nozzle head, to downsize the printed hydrogel droplets from 40 um to 25 um [40]. These smaller-sized tubular structures signified the potential for the use of this technology in vascular tissue engineering.

Cui et al. used bioink in a modified HP Deskjet 600 thermal printer to print microvascular constructs. Human microvascular endothelial cells (HMVECs) in a fibrin hydrogel were concurrently deposited into a thrombin substrate [4]. In 3 weeks, printed microvasculature lined by HMVEC was observed in the scaffold. Similarly, Zhao et al. developed a perfusable vascular channel using rat collagen type 1, human umbilical vein endothelial cells (HUVECs), and gelatin, to construct a vascular network [55]. Mesoscopic fluorescence molecular tomography (MFMT) demonstrated that the endothelial cells, which lined in the inner layer of the branching vascular networks, were evenly distributed and showed signs of migration in the luminal surface. Further, this experiment also provided a visualization of fluid flow

in these channels. This printed construct was used to further evaluate the efficacy of biofabricating vascular networks.

Multi-scale vascular network fabrication was further demonstrated by Lee et al. using a combination of materials including rat collagen type 1, HUVECs, and gelatin [32]. This multi-scale vascular network consisted of a single vascular channel with smaller-sized, branching vascular sprouts. HUVEC viability was improved when the bioink was formulated with higher cell concentrations and when the HUVECs were placed in a flow culture after printing, which involved perfusing the printed vascular tissue with medium. There was no significant difference in the permeability of the unlined and the cell-lined vascular constructs. A larger vascular network with a capillary system was constructed by Lee et al. using a similar principle [33]. The group created two vascular channels with numerous smaller, branching, interconnected channels. Fibrin, HUVEC, and normal human lung fibroblast (NHIF) were incubated in the spaces between the channels. Two weeks after printing, this study demonstrated the formation of a mature capillary network with HUVEC integration into the microvasculature, thus illustrating the potential for using 3D printing techniques to construct sophisticated vascular networks on a capillary-sized scale.

Vascular Graft Creation (Table 5.2)

Tubular structure fabrication using 3D inkjet printing was first introduced by Kesari et al. in the Boland laboratory [26]. The group used a modified HP697c inkjet printer to fabricate cylindrical structures, 2 mm in diameter, using alginate and rat smooth muscle cells (SMCs). The SMCs were added in a layer-by-layer manner with manual cell suspension, where the SMCs were pipetted into the hydrogel construct during the process of alginate deposition. Printed cell viability and alignment were demonstrated using this methodology. Furthermore, the printed vascular constructs demonstrated vasoreactive ability when tested using vasoconstriction agonist endothelin-1 (ET-1) solution. This study is a noted milestone in the 3D inkjet printing of vascular tissue.

Larger vascular constructs for use in regenerative medicine and organ transplantation have also been investigated. Challenges in printing large-scale constructs include ensuring adequate physical support of the large structures, as well as ensuring the long-term viability of the printed cells due to the increased distance over which nutrients and metabolites must be transferred within these larger constructs. Campos et al. fabricated large vascular constructs (diameter ~5 mm), which were immersed in a solution of high-density hydrophobic fluorocarbon, to enhance the physical properties of the vascular constructs [11]. Cell growth and the rate of extracellular matrix secretion were both increased in the fluorocarbon solution submersed constructs. Moreover, the contact angle of the droplet in these constructs was shown to be significantly higher, indicating that a higher printing precision and resolution were obtained using this technique. Blaeser et al. used this same submersion method to fabricate a cell-laden arterial bifurcated vasculature of 5 mm

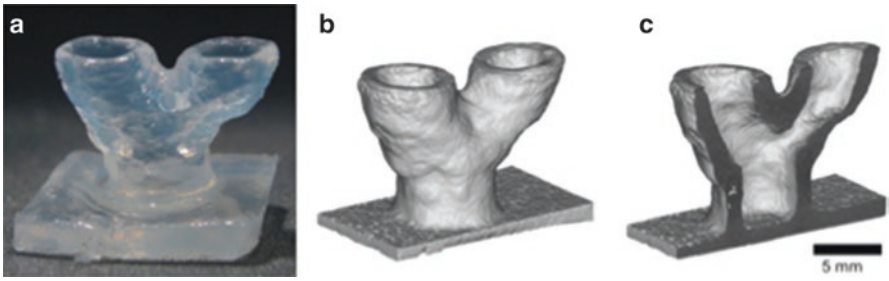

Fig. 5.2 (**a**) Photograph of the bifurcation model. (**b**, **c**) CT images of the vascular construct in full and in sectional view (scale bar, 5 mm). Blaeser, A., et al., Biofabrication under fluorocarbon: a novel freeform fabrication technique to generate high aspect ratio tissue-engineered constructs. Biores Open Access, 2013. **2**(5): p. 374-84 [2, 14]

outer diameter and 3 cm in length [2] (Fig. 5.2). Though necrotic centers were observed 7 days after fabrication, the cell viability of the printed construct was reported to be higher than 90%. This highlights the feasibility of printing large-scale vascular constructs with branching components, a discovery with huge implications to address unmet needs in cardiovascular surgery.

5.2.2 Extrusion-Based Printing (Direct/Indirect)

5.2.2.1 Principle (Fig. 5.3)

The basic principle of extrusion bioprinting is to extrude bioinks from a reservoir in a predetermined manner. The heated printer head extrudes materials in filament form to create a three-dimensional structure. The construction of the graft is achieved through a layer-by-layer deposition of bioink, followed by a cross-linking reaction. It is the most popular 3D printing technique and has been used in numerous tissue regeneration studies, for both hard and soft tissues [12, 45, 49].

The extrusion machine setup includes a driving system (mechanical or pneumatic), a dispensing system, and a three-axis robotic platform. Continuous pressure exerted on the bioink delivers a continuous line of printed material. Extrusion-based bioprinting techniques, used to fabricate vascular constructs, can be divided into direct and indirect methods. In the direct method, the vascular construct is printed directly from the deposition of bioink. The indirect method involves the use of sacrificial materials, such as alginate, gelatin, and agarose, to build molds for bioink deposition that are removed once the printed vascular construct is fabricated [46].

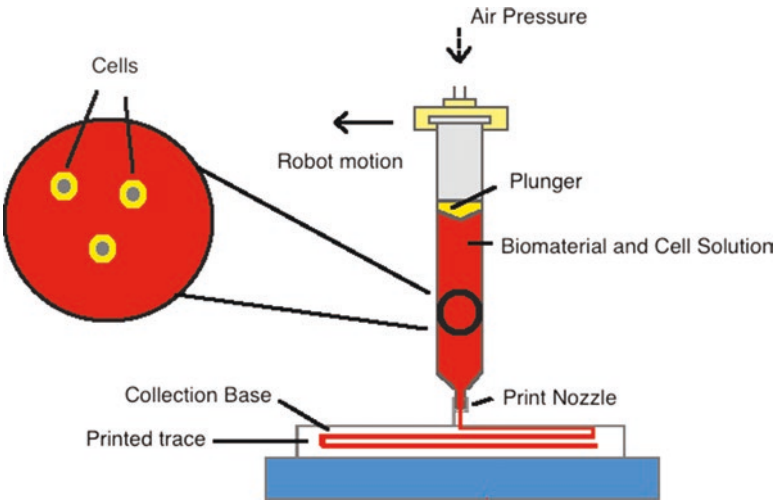

Fig. 5.3 A schematic of the extrusion-based bioprinting. A cell/bioink is forced from a syringe reservoir and deposited as a printing trace on the collection plate

5.2.2.2 Application

Microvascular Network Creation (Table 5.1)

Khalil et al. used a pneumatic nozzle system with an aqueous alginate solution and rat heart endothelial cells (RHECs), to print a microvascular network [27]. The group demonstrated a high live/dead RHEC cell ratio in the printed vascular scaffold, even 14 days after printing. Furthermore, the mechanical properties of the printed scaffold were unchanged over 3 weeks post-printing. In order to evaluate the capillary system construction, a built-in microchannel system within the vascular constructs was developed by Gao et al. [15]. A coaxial nozzle system, with an inner flow of calcium chloride and outer flow of alginate solution, was used. These microchannels formed the interface between calcium chloride and sodium alginate solutions, where the cross-linkage took place. The group described the creation of parallel microchannels alternating in two different sizes of channel, using the additional ungelled sodium alginate for hollow filament deposition. The ungelled sodium alginate was deposited on the outer surface of each individual channel, so as to form a parallel network. Then hollow channels, in between the regular channels, were created by removal of the ungelled printed alginate. The group also demonstrated improved cell viability using vascular constructs with microchannels, versus those without microchannels, when the sodium alginate scaffolds were co-printed with mouse fibroblasts.

The microvascular system was further investigated by Colosi et al. [3] using a coaxial nozzle extrusion system to print a microfluidic channel composed of low

viscosity bioink, to allow for cell migration within the vascular construct [3]. This study used GelMA (gelatin methacrylate) and alginate bioinks laden with HUVECs. GelMA is a collagen in the photopolymerizable methacrylate (MA) family, which is cross-linked after printing using UV radiation. HUVEC growth and alignment in the vascular channel was successfully demonstrated. The group reported synchronous beating of cardiomyocytes, after secondary seeding of cardiomyocytes into the constructs, thereby demonstrating the potential for use of the construct as a platform for further tissue engineering applications.

Jia et al. demonstrated the ability to print various shapes and sizes (inner diameter 400–1000 um) of perfusable vascular network structures [24]. The group used a coaxial nozzle system to print bioink composed of gelatin methacryloyl (GelMA), poly(ethylene glycol)-tetra-acrylate (PEGTA), and sodium alginate. PEGTA is a branched, tetravalent chemical structure derivative of poly(ethylene glycol) (PEG). In this study, the PETGA increased the physical strength of the construct by increasing cross-links with GelMA. The encapsulation of HUVECs and human mesenchymal stem cells (hMSCs) into the bioink was used to evaluate the cytocompatibility of this printing methodology. Surface modification with ethylenediaminetetraacetic acid (EDTA) solution was done after bioprinting, to enhance cell migration and proliferation. The group reported optimal cell density as well as highly organized cell migration patterns. This study was significant in that it demonstrated the capacity to print well-organized vascular networks that could be adequately perfused. Zhang et al. evaluated the cardiac tissue remodeling by seeding cardiomyocytes into the organized vascular scaffold [54]. The group used HUVEC-encapsulated bioink to print vascular tissue scaffolds, which were then seeded with neonatal rat cardiomyocytes, to create an endothelialized microvascular structure. Bioink composed of GelMA, alginate, and endothelial cells was used to construct the microfibrous scaffold. Cardiomyocytes were then seeded into the interstitial spaces, in the multiple layers of the highly organized vascular network. The mechanical properties of these constructs were affected by the distance between layers of the scaffold. The degree of HUVEC dispersion within the scaffold resembled the pattern of native blood vessels. Synchronous beating of cardiomyocytes in the endothelialized microenvironment was noted within 3 days, after seeding. Perfusion of the construct under a bioreactor improved the viability of cardiomyocytes. The team also explored the endothelialized myocardial model in response to doxorubicin, a common oncological drug. The HUVECs and cardiomyocytes showed a dose-dependent response to the drug, demonstrating the potential utility of the printed vascular construct for pharmacologic testing.

Indirect extrusion 3D bioprinting techniques have allowed researchers to create complicated networks of materials in predetermined geometries, by manipulating the design of the sacrificial materials. Microvasculature networks with small caliber diameters have been developed and investigated by several research groups. Wu et al. used aqueous Pluronic F127, a copolymer with two hydrophilic poly(ethylene oxide) (PEO) parts and one hydrophobic poly(propylene oxide) (PPO), in a PEO-PPO-PEO arrangement, acting as the sacrificial material in a hydrogel matrix to construct various sized vascular channels [51]. They examined the mechanical

properties of the printed structures in vitro. Similarly, Kolesky et al. described the use of Pluronic F127 and GelMA laden with human neonatal dermal fibroblasts (HNDFs), to print vascular networks [28]. In that experiment, the microvascular channel was formed similar to the strategy employed by Wu et al. [51]. After the evacuation of Pluronic F127, the GelMA was photopolymerized before HUVECs were seeded into the channels. The group showed high cell viability of HNDFs and HUVECs, 1 week after printing.

Kolesky et al. described the use of "vascular ink," which contained Pluronic F127 and thrombin mixtures, and "cell ink," which contained fibrinogen and gelatin mixtures, in the construction of a thick vascular network (>10 mm) [29]. The group demonstrated the perfusability of the vascular constructs in a complex microenvironment. The vascular channels, which were lined by HUVECs, were incorporated into a human mesenchymal cell (hMSC) printed network. After 6 weeks, the group described the osteogenic differentiation of the hMSCs. This experiment demonstrated the development of thick vascular network using 3D printing technology.

Vascular Graft Creation (Table 5.2)

Various fabrication technologies have been investigated, to improve oxygen and nutrients delivery in printed vascular grafts. Wang et al. developed a novel bioink delivery system to fabricate vascular tissue (diameter 3–5 mm) with a strong outer layer coated with synthetic polymer, to provide mechanical protection for the inner core [52]. The inner core was coated with a cell-laden hydrogel, to provide an organized microenvironment that would support cellular metabolism. In the experiment, a double nozzle system was used to deposit the polyurethane and adipose-derived stem cell (ADSC) bioink. The thickness of the outer layer had a huge impact on the geometry of the construct, the formation of the interface between the two layers, and the viability of the printed cells. This study optimized these parameters to create robust vascular constructs and drew attention to the evaluation of perfusion ability of printed vascular channels.

Besides the in vitro vascular graft engineering studies described here, a preclinical study was conducted by Fukunishi et al. [14]. The group performed a thoracic inferior vena cava (IVC) interposition graft implantation surgery in vivo, using a 3D printed graft composed of polyglycolic acid (PGA) and poly(L-lactide-co-ε-caprolactone) (PLCL) scaffolds. The study involved a 6-month follow-up period. No significant difference in mechanical properties was noted between the tissue-engineered vascular graft and the native IVC. The extracellular content of the TEVG, examined at 6-month time points, demonstrated that elastic and collagen levels were comparable to native IVC. This study validated the feasibility of 3D printing patient-specific vascular constructs to treat vascular disease. Further animal studies are warranted for the development of clinically relevant and patient-specific 3D printed vascular constructs.

5.2.3 *Laser-Based 3D Printing*

5.2.3.1 Principle (Fig. 5.4)

Laser-based 3D printing can be divided into two main approaches: laser-guided direct writing (LGDW) and laser-induced forward transfer (LIFT) [44]. Laser 3D printing technologies involve the use of a high-powered pulsatile laser source; a "print ribbon," which is a sacrificial layer consisting of laser-absorbing biocompatible materials; the bioink; and a receiving substrate.

In laser 3D bioprinting techniques, the bioink is coated onto a print ribbon. Pulses of laser energy are used to print the cells, by volatilizing the bioink on the print ribbon and transferring the cells from the ribbon to the receiving substrate [22]. The advantages of this printing modality include high post-printing cell viability, compatibility with a wide range of bioinks, and printing precision at the cellular level [34]. However, the laser 3D printing setup is more expensive and requires more sophisticated machinery than other printing modalities.

5.2.3.2 Applications

Microvascular Network Creation (Table 5.1)

Guillotin et al. investigated the feasibility of using laser bioprinting to print high-resolution cellular structures, using the rabbit carcinoma cell line B16 and HUVECs [18]. They demonstrated the successful use of laser-induced forward transfer (LIFT), for high-resolution cell printing with excellent precision in controlling

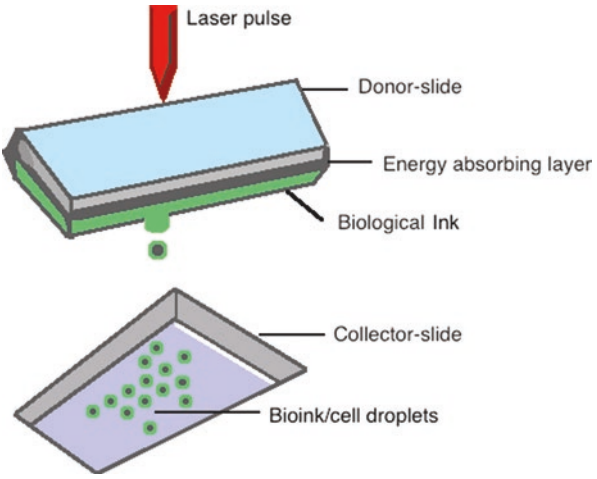

Fig. 5.4 A schematic of laser-based bioprinting. A pressure bubble generated by the laser pulse pushes the cell/bioink onto the collector slide

spatial arrangements of the printed cells. They also reported a high viability in the printed HUVECs containing microchannels. Using similar laser bioprinting techniques, Wu et al. developed a branched vascular microenvironment (~50–100 um in caliber) with HUVECs and human umbilical vein smooth muscle cells (HUVSMCs) [50]. The group first printed a structure with HUVECs, which was incubated for a day before the scaffold was removed. HUVSMCs were then printed on top of this structure, creating a combined microvasculature environment. In this study, the development of self-formed network lumens was dependent on the laser-printed lumen, demonstrating the potential for using 3D laser bioprinting to make a stable vasculature network. Though the exact ratio of HUVECs and HUVSMCs was not quantified, proliferation and differentiation patterns in the vascular construct demonstrated that there was high printed cell viability and robust cell-cell interactions.

More recently, a microscale capillary-like vascular network was developed by Zhu et al. using LGDW printing with a bioink composed of HUVECs and mouse fibroblasts encapsulated in GelMA and GM-HA [56]. Cell viability of the printed vascular tissues was over 85%, and pericyte phenotype induction by the mouse fibroblasts facilitated endothelial network formation by the HUVECs. To investigate endothelial network formation in vivo and anastomosis formation with the host vessels, the vascularized capillary network was implanted subcutaneously into a mouse model. The capillary network was observed to be dense 2 weeks after the surgery, and successful anastomoses between the printed vascular network and the host vasculature were demonstrated. This study demonstrated the potential for complex vascular biofabrication using laser 3D printing technology.

Vascular Graft Creation (Table 5.2)

3D laser bioprinting has also been used to fabricate larger-caliber vascular tissues. For instance, Baudis et al. used digital light photopolymerization (DLP) techniques to construct large-scale vascular tissue [1]. They developed a bioink formulation composed of photoelastomers made from cross-linked monoacrylate (MA) and dicarylate (DA), dithiol-based chain transfer agent (CTA), and a reactive diluent, designed to optimize the mechanical properties and geometry of the printed vascular constructs. The printed vessels were demonstrated to have mechanical properties comparable to native blood vessels. The DLP technique, which involved irradiation of a photosensitive resin, allowed for fabrication of vascular constructs with very precise dimensions (~1 mm in caliber). The photosensitive resin enabled the formation of a reversible crosslink in the printed tissue. These cross-links conferred mechanical properties that mimic those of the native porcine coronary artery, in terms of suture tear resistance, tensile strength, and fracture strain.

The use of photosensitive resin was further investigated by Wolfdietrich Meyer et al. for the fabrication of bifurcated large-diameter, native-like tubular systems (diameter ~2 mm) [36]. The study employed a series of photosensitive oligomer-

polytetrahydrofuran-diacrylate (PTHF-DA) groups with different end groups—with two laser printing technologies, stereolithography processing (SL) and multiphoton polymerization (MMP). The polymeric coil structure of the PTHF-DA was thought to contribute to the physical properties of the printed construct (including melting and crystallization points) as well as to the branched shape of the final construct. The team further tested the structure for the shape memory effect (SME). The fabricated polymer, which was reshaped by several winding springs, showed an excellent SME by returning to its original shape. This property has important implications in the application of printed vascular tissue to clinical settings.

Laser bioprinted large-scale vessels were also investigated in vivo. Melchiorri et al. implanted laser-printed vascular grafts in mice [35]. The group used biodegradable poly(propylene fumarate) (PPF) to fabricate vasculature with DLP technology. The mechanical properties of the printed grafts were evaluated prior to the implantation surgery. At the 6-month follow-up period, the patency of the graft in vivo was 100%, and the degradation of the graft mass was noted. However, maintaining structural and mechanical support for the tissue construct has yet been met due to the demand of adequate neotissue formation. Vascular remodeling in the interface between the grafted and native vessels was observed, and neovessel formation was mainly noted on the inner surface of the lumens. This experiment provided an insight into the application of laser-printed vascular constructs and the potential for vascular remodeling in vivo.

5.2.4 Scaffold-Free 3D Printing

5.2.4.1 Principle

Scaffolds have traditionally been used as supportive infrastructures for 3D printed tissues. Though scaffold-based 3D printing modalities have been successfully used to print native-like tissue constructs, the scaffolds themselves pose concerns. These include biocompatibility, immunogenicity, degradation rate, cytotoxicity of the degradation products, and altered properties of printed tissues due to residual polymers [6]. Neotissue formation requires the microenvironment to provide sufficient physical support and nutritional supply to allow for continuous cell growth and uninterrupted cell-cell signal transduction, all of which are impacted by the presence of scaffolding. Given the limitations of scaffold-based printing technologies, scaffold-free 3D printing techniques have been developed. These methods use cell-only bioink to increase the concentration of printed cells. Inkjet (or droplet-based) and extrusion-based 3D printing approaches have all been used with cell-only bioink to fabricate scaffold-free constructs. Cell-free bioink can be formulated in two ways—as either a cell pellet or as cell aggregates. In scaffold-free bioprinting, the cellular bioink is printed in a supporting cast, in which the maturation of the tissue structure takes place [7, 42].

5.2.4.2 Application

Microvascular Network Creation (Table 5.1)

Norotte et al. described a novel technique in fabricating small-diameter multilayer tubular vascular grafts (diameter ~900 um) using HUVSMCs, human skin fibroblasts (HSFs), and porcine aortic smooth muscle cells (PASMCs) [41]. The team employed scaffold-free 3D printing technology to produce a cylindrical agarose support mold. Spheroids prepared from the co-culture of mixed cells were printed into the mold to allow fusion and maturation of the tissue. The team was also able to print a double-layer vascular tubular structure using the same technique. However, it was noted that tissues printed using these techniques matured faster and had suboptimal porous geometries.

Vascular Graft Creation (Table 5.2)

Kelm et al. first attempted a two-step scaffold-free fabrication process to create vascular tissue [25]. The first step of this process involved microtissue fabrication using human myofibroblasts (HMFs), pig articular chondrocytes (PACs), and human articular chondrocytes (HACs). The second step involved the amalgamation of mouse myoblasts and HUVECs, in a cylindrical agarose cast, to produce a microtissue tubular structure (diameter ~3 mm). The microtissue was then implanted in the chorioallantoic membrane (CAM) of a chicken embryo for evaluation of vascularization potential in vivo. The printed tissues demonstrated successful angiogenic potential in vivo.

Tan et al. printed a larger vascular construct model (~5 mm diameter) using a scaffold-free approach and evaluated the cell-cell interaction between living cells in the construct [48]. The team used a robotic microdroplet system, to construct a hydrogel mold into which spheroids created from co-culture of human aortic smooth muscle cells (hSMCs) and human umbilical vein endothelial cells (HUVECs) were printed. They found that collagen type 1, which was extensively secreted from the printed cells, was essential to spheroid adhesion and maturation of the vascular construct.

Xu et al. investigated the fabrication of different shapes of tubular structures [53]. The group created zigzag 2–3 mm caliber tubular structures using a scaffold-free bioink containing mouse fibroblasts. The fabrication process, which involved inkjet 3D printing technology with alternating speeds of the print head, made use of the overhang of each sequential layer of bioink (a distance about 20 um) to create a slightly curved shape in the printed tube. The printed constructs had high cell viability of over 80%. This study demonstrated the capacity of 3D printing to fabricate vascular constructs with complex geometries that better mimic native human vasculature.

Taking the fabrication of scaffold-free vascular constructs a step further, Kucukgul et al. proposed a method for patient-specific scaffold-free 3D printing of

macrovascular tissue in a porcine abdominal aortic model [30]. The team optimized their 3D printing algorithm to consider the precise geometries of the aorta. A tubular construct was printed, in a self-support model with mouse embryonic fibroblasts (MEFs), using this proposed algorithm.

More recently, Itoh et al. tested a scaffold-free 3D printed vascular graft in vivo, using an aortic graft interposition surgery in a rat model [23]. In this study, the vascular graft was printed using HUVECs, human aortic smooth muscle cells (HASMCs), and human normal dermal fibroblasts (HNDFBs). The graft underwent remodeling in vivo, demonstrating enlargement of the lumen. The biocompatibility of the graft was demonstrated by the significantly larger amount of extracellular matrix that was secreted in the scaffold-free graft, when compared to a scaffold-based graft.

5.3 Discussion

There are various 3D bioprinting modalities, each with particular strengths and weaknesses, depending on the type of vascular construct that is desired. Inkjet printing is very cost-effective and provides medium to high resolution of printed constructs. However, the cell density of bioinks that can be successfully printed and the capacity to construct complex, precise 3D structures are limited due to the droplet-based technology, despite controlled positioning of the print head improving the precision of droplet deposition [22]. Furthermore, even with the development of "droplet-on-demand technology", the nozzle used in inkjet printing may have detrimental effects on cell survival due to the thermal and physical stress exerted on the bioink [5, 16].

Extrusion-based printing is also cost-effective and provides the versatility of using bioinks that consist of cells encapsulated in hydrogel prior to printing. This technology produces constructs with good mechanical properties because it allows for printing with high viscosity and high cell density materials. Another advantage of extrusion printing is the ability to form solid 3D structures using filament form deposition of the hydrogel. However, printed cell viability is lower than that of the other modalities [37]. Also, the even spacing of cells within the hydrogel cannot be guaranteed using this technique, which could compromise the cell-to-cell contact. Additionally, the printing resolution of extrusion printing is limited, compared to other 3D printing methods [13].

Laser-based 3D printing also allows for printing with high cell density bioink and provides excellent resolution due to the nozzle-free approach. However, there are disadvantages associated with this technique, including its high cost and long printing times. Furthermore, the long-term cytotoxicity effects, from the irradiation of the high-power laser, are yet to be determined [17].

The scaffold-free approach to 3D bioprinting also carries the advantage of being able to print bioinks with high cell densities and for creating constructs that preserve and promote cell-cell interactions. However, the structural integrity and mechanical

behavior of the printed vascular constructs still need to be optimized. Another drawback of the scaffold-free approach is the difficulty of producing large-scale vascular tissues [42].

The biomaterials used in the 3D printing process have a critical impact on the quality of the fabricated vascular tissue. Generally speaking, an ideal bioprinting material would provide structural integrity with adequate mechanical strength after printing, promote engraftment with host tissue while avoiding immunogenicity, and facilitate cell proliferation, aggregation, and differentiation. The physical characteristics of the bioink, such as viscosity, mechanical strength, pore size, etc., must be considered when deciding which type of 3D printing technology to employ, given the limitations of the various technologies as previously described. Additionally, the pore size of the bioink must also be considered, given its impact on extracellular matrix deposition, which in turn determines cellular adhesion and organization. Cellular organization within the printed hydrogel has a tremendous influence on cell-cell signaling and plays a key role in the nutritional transfer critical for cellular metabolism. In fact, post-print cell viability is shown to be correlated to pore size by Domingos et al. [9]. Lastly, cytocompatibility of the bioink, with the host tissue and the immunogenicity of the printed material, must also be considered when evaluating the long-term success of the printed tissues. Studies investigating the 3D printing of vascular tissue have demonstrated high cell viability, but the degradation rate of the 3D printed vascular scaffolds, when engrafted in vivo, indicates that immunogenicity of these constructs must be further evaluated.

Self-assembly of cell aggregates (spheroids) in the scaffold-free printing approach has shown great promise and is an important milestone in scaffold-free 3D bioprinting. Currently, different approaches to speed up the cellular assembly in spheroid formation are under investigation. Additionally, maturogenic factors, which are biochemical molecules, are shown to improve the cohesive properties of spheroids by Hadju et al. [20]. The use of magnetized bioinks to print physiologically robust spheroids with enhanced cell-cell communication has also been demonstrated [10, 43]. Lastly, the lockyball technique has been demonstrated to improve the regenerative capacity of scaffold-free vascular tissue constructs, by using a microscaffold with hooks, to reduce mechanical stress on printed spheroids [8].

Regarding the application to fabrication of vascular tissue, 3D printing methodology has the potential for use in the large-scale production of microvascular networks. The highly controllable deposition of bioink during printing allows for the production of a wide range of sizes and types of vascular networks. However, there is still much research needed in order to print biomimetic vascular tissue constructs that are optimized for use in clinical applications.

An emerging application of 3D printing technology in vascular engineering is the creation of patient-specific TEVGs. It caters to the patient's native vascular anatomy and potentially allows for more optimized hemodynamics after surgery. This would reduce unnecessary power loss and cardiac workload and thereby delay the onset of heart failure, especially in young patients with congenital heart disease. Advances in imaging techniques and the virtual surgical planning strategy, described by Siallagan et al., have also allowed for the construction and precise implantation

of patient-specific vascular grafts. Computational analysis has improved not only the physical parameters of printed grafts but has also helped in estimating flow dynamics of the graft in vivo [47]. Those advancements have been indispensable to the clinical application of the 3D printing constructs.

5.4 Conclusion

This chapter presents several 3D printing methodologies, including inkjet, extrusion, laser, and scaffold-free techniques, and their current applications in vascular tissue fabrication. The ultimate clinical goal of 3D printing technologies is to improve patient outcomes using 3D printed constructs. Despite the breakthroughs and progress in 3D bioprinting and vascular tissue engineering, there are still many technical and biological limitations that must be overcome. Further optimization and innovation are needed in terms of the printing process, tissue regeneration, and the biomaterials used. Multidisciplinary research will play a key role in addressing these challenges and realizing the translation of 3D printing technology to clinical practice.

References

1. Baudis, S., Nehl, F., Ligon, S. C., Nigisch, A., Bergmeister, H., Bernhard, D., et al. (2011). Elastomeric degradable biomaterials by photopolymerization-based CAD-CAM for vascular tissue engineering. *Biomedical Materials, 6*(5), 055003.
2. Blaeser, A., et al. (2013). Biofabrication under fluorocarbon: A novel freeform fabrication technique to generate high aspect ratio tissue-engineered constructs. *Bioresearch Open Access, 2*(5), 374–384.
3. Colosi, C., et al. (2016). Microfluidic bioprinting of heterogeneous 3D tissue constructs using low-viscosity bioink. *Advanced Materials, 28*(4), 677–684.
4. Cui, X., & Boland, T. (2009). Human microvasculature fabrication using thermal inkjet printing technology. *Biomaterials, 30*(31), 6221–6227.
5. Cui, X., et al. (2012). Thermal inkjet printing in tissue engineering and regenerative medicine. *Recent Patents on Drug Delivery & Formulation, 6*(2), 149–155.
6. Dahl, S. L., et al. (2007). Mechanical properties and compositions of tissue engineered and native arteries. *Annals of Biomedical Engineering, 35*(3), 348–355.
7. Datta, P., Ayan, B., & Ozbolat, I. T. (2017). Bioprinting for vascular and vascularized tissue biofabrication. *Acta Biomaterialia, 51*, 1–20.
8. Dernowsek, J. A., et al. (2016). Tissue spheroids encaged into microscaffolds with internal structure to increase cell viability. *Procedia CIRP, 49*, 174–177.
9. Domingos, M., et al. (2013). The first systematic analysis of 3D rapid prototyped poly(ε-caprolactone) scaffolds manufactured through BioCell printing: The effect of pore size and geometry on compressive mechanical behaviour and in vitro hMSC viability. *Biofabrication, 5*(4), 045004.
10. Du, V., et al. (2015). Magnetic engineering of stable rod-shaped stem cell aggregates: Circumventing the pitfall of self-bending. *Integrative Biology (Cambridge), 7*(2), 170–177.

11. Duarte Campos, D. F., et al. (2013). Three-dimensional printing of stem cell-laden hydrogels submerged in a hydrophobic high-density fluid. *Biofabrication, 5*(1), 015003.
12. Duarte Campos, D. F., et al. (2015). The stiffness and structure of three-dimensional printed hydrogels direct the differentiation of mesenchymal stromal cells toward adipogenic and osteogenic lineages. *Tissue Engineering Part A, 21*(3–4), 740–756.
13. Ferris, C. J., et al. (2013). Biofabrication: An overview of the approaches used for printing of living cells. *Applied Microbiology and Biotechnology, 97*(10), 4243–4258.
14. Fukunishi, T., et al. (2017). Preclinical study of patient-specific cell-free nanofiber tissue-engineered vascular grafts using 3-dimensional printing in a sheep model. *The Journal of Thoracic and Cardiovascular Surgery, 153*(4), 924–932.
15. Gao, Q., et al. (2015). Coaxial nozzle-assisted 3D bioprinting with built-in microchannels for nutrients delivery. *Biomaterials, 61*, 203–215.
16. Gudapati, H., Dey, M., & Ozbolat, I. (2016). A comprehensive review on droplet-based bioprinting: Past, present and future. *Biomaterials, 102*, 20–42.
17. Guillemot, F., et al. (2011). Laser-assisted bioprinting to deal with tissue complexity in regenerative medicine. *MRS Bulletin, 36*(12), 1015–1019.
18. Guillotin, B., et al. (2010). Laser assisted bioprinting of engineered tissue with high cell density and microscale organization. *Biomaterials, 31*(28), 7250–7256.
19. Guo, Y., et al. (2017). Inkjet and inkjet-based 3D printing: Connecting fluid properties and printing performance. *Rapid Prototyping Journal, 23*(3), 562–576.
20. Hajdu, Z., et al. (2010). Tissue spheroid fusion-based in vitro screening assays for analysis of tissue maturation. *Journal of Tissue Engineering and Regenerative Medicine, 4*(8), 659–664.
21. Harrison, J. H., Merrill, J. P., & Murray, J. E. (1956). Renal homotransplantation in identical twins. *Surgical Forum, 6*, 432–436.
22. Irvine, S. A., & Venkatraman, S. S. (2016). Bioprinting and differentiation of stem cells. *Molecules, 21*(9), E1188.
23. Itoh, M., et al. (2015). Scaffold-free tubular tissues created by a bio-3D printer undergo remodeling and endothelialization when implanted in rat Aortae. *PLoS One, 10*(9), e0136681.
24. Jia, W., et al. (2016). Direct 3D bioprinting of perfusable vascular constructs using a blend bioink. *Biomaterials, 106*, 58–68.
25. Kelm, J. M., et al. (2006). Design of custom-shaped vascularized tissues using microtissue spheroids as minimal building units. *Tissue Engineering, 12*(8), 2151–2160.
26. Kesari, P., Xu, T., & Boland, T. (2004). Layer-by-layer printing of cells and its application to tissue engineering. *MRS Proceedings, 845*, AA4.5.
27. Khalil, S., & Sun, W. (2009). Bioprinting endothelial cells with alginate for 3D tissue constructs. *Journal of Biomechanical Engineering, 131*(11), 111002.
28. Kolesky, D. B., et al. (2014). 3D bioprinting of vascularized, heterogeneous cell-laden tissue constructs. *Advanced Materials, 26*(19), 3124–3130.
29. Kolesky, D. B., et al. (2016). Three-dimensional bioprinting of thick vascularized tissues. *Proceedings of the National Academy of Sciences of the United States of America, 113*(12), 3179–3184.
30. Kucukgul, C., et al. (2015). 3D bioprinting of biomimetic aortic vascular constructs with self-supporting cells. *Biotechnology and Bioengineering, 112*(4), 811–821.
31. Langer, R., & Vacanti, J. P. (1993). Tissue engineering. *Science, 260*(5110), 920–926.
32. Lee, V. K., et al. (2014). Creating perfused functional vascular channels using 3D bio-printing technology. *Biomaterials, 35*(28), 8092–8102.
33. Lee, V. K., et al. (2014). Generation of multi-scale vascular network system within 3D hydrogel using 3D bio-printing technology. *Cellular and Molecular Bioengineering, 7*(3), 460–472.
34. Lee, V. K., et al. (2015). 3D bioprinting and 3D imaging for stem cell engineering. In K. Turksen (Ed.), *Bioprinting in regenerative medicine* (pp. 33–66). Cham: Springer.
35. Melchiorri, A. J., et al. (2016). 3D-printed biodegradable polymeric vascular grafts. *Advanced Healthcare Materials, 5*(3), 319–325.
36. Meyer, W., et al. (2012). Soft polymers for building up small and smallest blood supplying systems by stereolithography. *Journal of Functional Biomaterials, 3*(2), 257–268.

37. Murphy, S. V., & Atala, A. (2014). 3D bioprinting of tissues and organs. *Nature Biotechnology, 32*(8), 773–785.
38. Nakamura, M., Nishiyama, Y., & Henmi, C. 2008. 3D micro-fabrication by inkjet 3D biofabrication for 3D tissue engineering. In *2008 International Symposium on Micro-Nano Mechatronics and Human Science*.
39. Nishiyama, Y., et al. (2008). Ink jet three-dimensional digital fabrication for biological tissue manufacturing: Analysis of alginate microgel beads produced by ink jet droplets for three dimensional tissue fabrication. *Journal of Imaging Science and Technology, 52*(6), 60201-1–60201-6.
40. Nishiyama, Y., et al. (2008). Development of a three-dimensional bioprinter: construction of cell supporting structures using hydrogel and state-of-the-art inkjet technology. *Journal of Biomechanical Engineering, 131*(3), 035001–035001-6.
41. Norotte, C., et al. (2009). Scaffold-free vascular tissue engineering using bioprinting. *Biomaterials, 30*(30), 5910–5917.
42. Ozbolat, I. T. (2015). Scaffold-based or scaffold-free bioprinting: Competing or complementing approaches? *Journal of Nanotechnology in Engineering and Medicine, 6*(2), 024701–024701-6.
43. Ozbolat, I. T. (2017). *3D bioprinting: Fundamentals, principles and applications*. New York: Elsevier.
44. Ozbolat, I. T., Moncal, K. K., & Gudapati, H. (2017). Evaluation of bioprinter technologies. *Additive Manufacturing, 13*(Suppl C), 179–200.
45. Poldervaart, M. T., et al. (2013). Sustained release of BMP-2 in bioprinted alginate for osteogenicity in mice and rats. *PLoS One, 8*(8), e72610.
46. Richards, D., et al. (2017). 3D bioprinting for vascularized tissue fabrication. *Annals of Biomedical Engineering, 45*(1), 132–147.
47. Siallagan, D., et al. (2017). Virtual surgical planning, flow simulation, and 3-dimensional electrospinning of patient-specific grafts to optimize Fontan hemodynamics. *The Journal of Thoracic and Cardiovascular Surgery, 155*(4), 1734–1742.
48. Tan, Y., et al. (2014). 3D printing facilitated scaffold-free tissue unit fabrication. *Biofabrication, 6*(2), 024111.
49. Wang, X., et al. (2016). 3D bioprinting technologies for hard tissue and organ engineering. *Materials (Basel), 9*(10), 802.
50. Wu, P. K., & Ringeisen, B. R. (2010). Development of human umbilical vein endothelial cell (HUVEC) and human umbilical vein smooth muscle cell (HUVSMC) branch/stem structures on hydrogel layers via biological laser printing (BioLP). *Biofabrication, 2*(1), 014111.
51. Wu, W., DeConinck, A., & Lewis, J. A. (2011). Omnidirectional printing of 3D microvascular networks. *Advanced Materials, 23*(24), H178–H183.
52. Xiaohong, W., Kai, H., & Weiming, Z. (2013). Optimizing the fabrication processes for manufacturing a hybrid hierarchical polyurethane–cell/hydrogel construct. *Journal of Bioactive and Compatible Polymers, 28*(4), 303–319.
53. Xu, C., et al. (2012). Scaffold-free inkjet printing of three-dimensional zigzag cellular tubes. *Biotechnology and Bioengineering, 109*(12), 3152–3160.
54. Zhang, Y. S., et al. (2016). Bioprinting 3D microfibrous scaffolds for engineering endothelialized myocardium and heart-on-a-chip. *Biomaterials, 110*, 45–59.
55. Zhao, L., et al. (2012). The integration of 3-D cell printing and mesoscopic fluorescence molecular tomography of vascular constructs within thick hydrogel scaffolds. *Biomaterials, 33*(21), 5325–5332.
56. Zhu, W., et al. (2017). Direct 3D bioprinting of prevascularized tissue constructs with complex microarchitecture. *Biomaterials, 124*, 106–115.

Chapter 6
Strategies for Tissue Engineering Vascularized Cardiac Patches to Treat Myocardial Infarctions

Justin Morrissette-McAlmon, Robert N. Hawthorne, Shawna Snyder, and Warren L. Grayson

6.1 Introduction

Myocardial infarction (MI) affects more than 1.3 million Americans each year [7]. MI, caused by thrombotic occlusion of coronary arteries, often results in heart failure, cardiac rupture, and death due to the limited regenerative capacity of human myocardium [127]. A lack of blood flow to the myocardium during MI results in necrosis of cardiac myocytes, which leads to the subsequent release of their intracellular contents, activating resident macrophages, and initiating an inflammatory cascade [31, 32]. This inflammatory cascade further damages cardiac myocytes and leads to destruction of the extracellular matrix (ECM). Recent advances, which

J. Morrissette-McAlmon · R. N. Hawthorne
Translational Tissue Engineering Center, Johns Hopkins University School of Medicine, Baltimore, MD, USA

Department of Biomedical Engineering, Johns Hopkins University School of Medicine, Baltimore, MD, USA

S. Snyder
Department of Art as Applied to Medicine, Johns Hopkins University School of Medicine, Baltimore, MD, USA

W. L. Grayson (✉)
Translational Tissue Engineering Center, Johns Hopkins University School of Medicine, Baltimore, MD, USA

Department of Biomedical Engineering, Johns Hopkins University School of Medicine, Baltimore, MD, USA

Department of Material Sciences and Engineering, Johns Hopkins University School of Engineering, Baltimore, MD, USA

Institute for NanoBioTechnology (INBT), Johns Hopkins University School of Engineering, Baltimore, MD, USA
e-mail: wgrayson@jhmi.edu

S. Gerecht (ed.), *Biophysical Regulation of Vascular Differentiation and Assembly*, Biological and Medical Physics, Biomedical Engineering,
https://doi.org/10.1007/978-3-319-99319-5_6

include stem cell transplantation, thrombolytic therapy, and stenting of coronary arteries, have improved myocardial salvage, but therapies that directly induce regeneration of the ventricular wall and improvement in functionality are lacking.

Cardiovascular tissue engineering has the potential to ameliorate the damage resulting from the limited endogenous repair mechanisms of the heart following MI [45]. Currently, there are no methods that completely repair the damaged myocardium post injury. Tissue engineering approaches aim to regenerate the myocardium by mimicking the tissue structure and cell composition. The native makeup of the myocardium includes a host of cells that are critical for survival, maturation, and repair. These cell types include cardiomyocytes, fibroblasts, endothelial cells, vascular smooth muscle cells, and macrophages [103] (Fig. 6.1). The myocardium is a highly metabolic, vascularized tissue characterized by having three endothelial cells to every one cardiomyocyte and an intercapillary distance of 15–50 μm [62]. Tissue engineering of the myocardium requires the development of adequate interconnected capillary networks that have the ability to anastomose quickly with the host vasculature, to maintain cell viability. Engineered pre-vasculature could expedite integration of the graft with host tissue and enhance regeneration. Vascular structures require perivascular cells, for angiogenic growth factor release and stabilization. Thus, multiple cell types are required to form functional vasculature as well as a syncytium of cardiomyocytes.

Through tissue engineering, there have been several strategies developed to enhance cardiac regeneration. These strategies include the injection of cells within hydrogels, or preassembly of epicardial patches with cells, natural and synthetic materials, and growth factors. Tissue engineering strategies aim to recapitulate key structural elements of the myocardium.

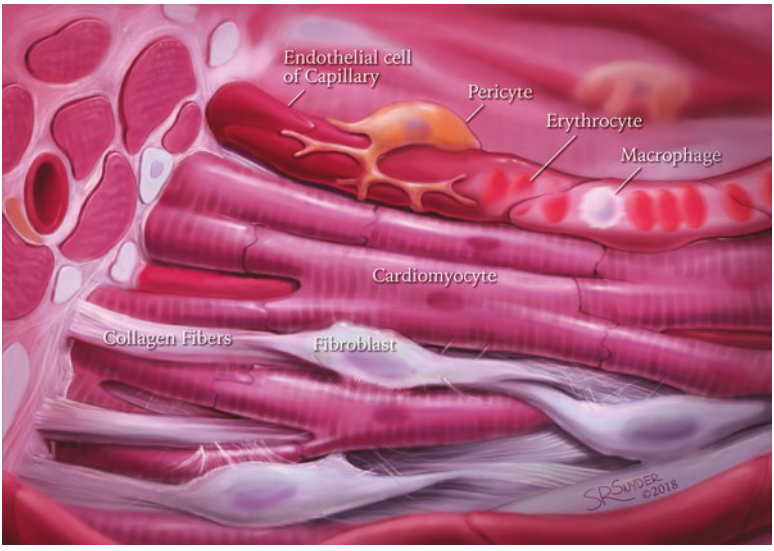

Fig. 6.1 Schematic illustrating structure and composition of the native myocardium

6.2 Tissue-Engineered Cardiac Patches

Cardiac patches are designed to be placed epicardially where they integrate with the healthy tissue surrounding the infarcted region, shunting the electrical signals over the scar tissue and contributing to the contractile function of the heart (Fig. 6.2). In vivo studies of engineered cardiac patches primarily rely on two types of assessments: functional characterization and tissue-level analysis. Functional studies include measurements of cardiovascular output, such as ventricular ejection fraction, and end-systolic and end-diastolic volumes, all of which can be measured in living specimens using echocardiography. Also included under the functional umbrella is the organ-level electrophysiology of the heart which can be assessed by electrocardiogram, in live specimens, and by whole-heart optical mapping postmortem [103]. Tissue-level investigations of in vivo experiments involve assessing cell survival and morphology as well as tissue organization. For example, a surgically implanted engineered cardiac patch might be assessed for anastomosis of host vasculature with engrafted vasculature or for migration of cells between graft and host. Histology and immunohistochemistry are crucial tools for these measurements as they can be used to differentiate cell types and sources and can help characterize the composition and organization of the extracellular matrix.

There are also several in vitro assessments performed on engineered cardiac tissues for which optimization is believed to correspond to improved clinical outcomes. Electrophysiological measurements are frequently treated as the gold

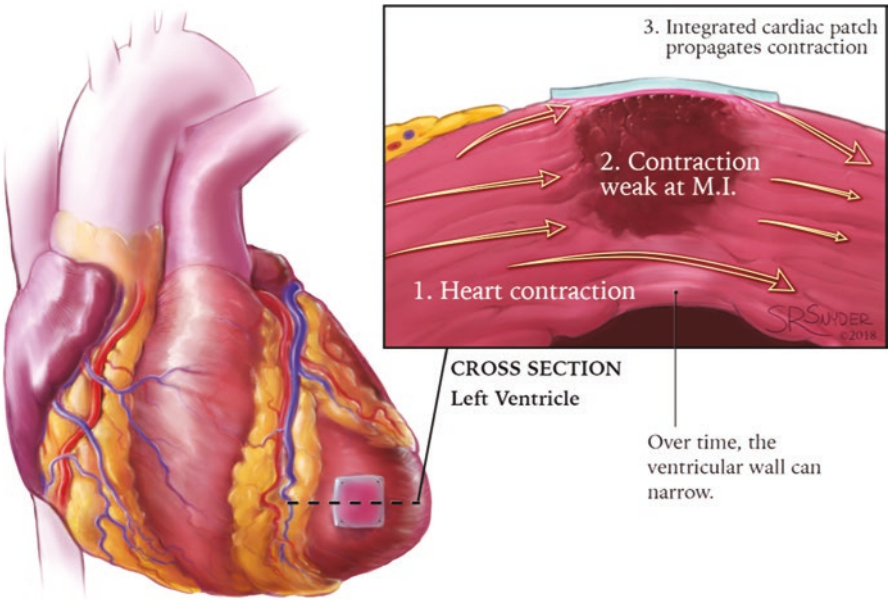

Fig. 6.2 Schematic demonstrating the theoretical application of a myocardial patch placed over an infarct to aid in restoration of lost contractility

standard to evaluate engineered cardiac tissues, with conduction velocities and action potential shapes seen in mature adult tissues established as ideal. These measurements also allow engineers to evaluate uniformity across the tissue and to gauge the maturity of stem cell-derived cardiomyocytes. However, full electrophysiological characterization of these tissues requires extensive facilities and expertise, and, as a result, much of the literature relies on stimulated contractile force measurements. Sometimes referred to in the literature as "twitch force," this assessment is frequently used as a measure of tissue development. Increased force is believed to correlate with improved tissue maturity and clinical outcomes. Cell and tissue-level analyses are also frequently performed on engineered tissue in vitro, as cellular morphology and tissue organization are important determinants of tissue function.

6.3 Cell Sources

Approaches to engineer cardiac grafts employ the combination of multiple cell types, typically including cardiomyocytes (electrically excitable cells), endothelial cells (vessel development), and fibroblasts/mural cells (vasculature stabilization). Each of these phenotypes may be derived from various sources (see Table 6.1).

6.3.1 Cardiomyocytes

Most commonly, cardiac tissue engineering strategies are studied using neonatal rat ventricular cardiomyocytes (NRVCMs). NRVCMs are isolated from newborn (day 0–3) rat hearts that have been minced and digested with trypsin and collagenase. To enrich the cardiomyocyte population, cells are usually plated into flasks and incubated for short periods, to allow for the selective adherence of fibroblasts in order to purify the NRVCM population. NRVCMs retain the ability to contract ex vivo, undergo a rapid dedifferentiation-redifferentiation cycle, and can be easily plated into monolayers. NRVCMs are widely used to study morphological, electrophysiological, and biochemical characteristics of cardiomyocytes. Despite their advantages, NRVCMs have the main disadvantage of being rodent-derived. Electrophysiologically, NRVCMs have little to no plateau phase when cultured in vitro. In addition, NRVCMs differ in their excitation-coupling, with a lack of T-tubule systems relative to adult myocytes, and their ability to maintain cytosolic Ca^{2+} signaling independent of the sarcoplasmic reticulum calcium release [56]. And while the adult rat myocardium has conduction velocities of 69 ± 6 cm/s in the longitudinal direction and 19 ± 5 cm/s in the transverse direction, there is yet to be a report of tissue-engineered grafts achieving these values [92]. These cells are also not able to be cultured for extended periods of time, especially in monolayers [26].

While healthy human cardiomyocytes isolated from adult hearts cannot be obtained ethically, the use of pluripotent stem cells has provided an avenue to obtain

Table 6.1 Tri-culture studies used for engineering vascularized cardiac grafts

	Cells	Culture conditions	Cardiac characterization	Vascular characterization	Ref.
NRVCM	*NRVCM* • 80,000–160,000 cells/disk • Percentage: 40–80% *D4T endothelial cells* • 8000–24,000 cells/disk Percentage: 4–13% *Cardiac fibroblasts* • 28,000–48,000 cells/disk • Percentage: 16–47%	• Matrigel-coated PEG disks size: 0.32 cm^2 • Microchannels: 100–200 μm diam × 3–4 mm • PEG disk were coated with Matrigel • Supporting cells cultured for 2 days before addition of NRVCMs • Cell tracking: Day 1 and day 4	*Advantages*: • Excitation threshold: Statistically similar in the 65:17:18 group (4 V/cm) and NRVCM control (3.2 V/cm) • Maximum captured rate: Statistically similar in tri-culture groups and NRVCM only control (value) *Limitations*: • Cardiomyocytes were clustered into cell aggregates	*Advantages*: • Positive staining for CD31/PECAM-1 • 31% EC yielded statistically higher percentage of positive staining for CD31 compared to 47% and 16% *Limitations*: • Network development cannot be	[50, 51]
	NRVCM • 1,140,000 cells • Percentage: 57% *Neonatal cardiac fibroblasts* • 580,000 cells • Percentage: 29% *Rat aortic endothelial cells* • 280,000 cells • Percentage: 14%	• Microtemplated PMMA with PC molds for fibrin hydrogels • Fibrin hydrogels were rehydrated through sterile PBS • 2 mm diameter biopsy punch was used to establish scaffold • 200 mg/ml fibrinogen • Tri-culture cellular mixture was pipetted into fibrin hydrogel • Constructs were cultured for 8 days	*Advantages*: • Cardiomyocytes survived in the scaffolds over time • Positive staining for Desmin for cardiomyocytes • Revealed maintenance of stiffness of fibrin hydrogels in the presence of factor XIII and Aprotinin *Limitations*: • No functional characterization of the cardiomyocytes	*Advantages*: • Vessel formation occurred in pore channels of the scaffold • RECA-1 positive staining colocalized within pore channels • Vessels appeared to form lumens *Limitations*: • Vessels density not robust • Vessel quantity not characterized	[117]
	NRVCM • 500,000 cells • Percentage: 77–90% *hASCs* • 50,000–100,000 cells • Percentage: 9–16% *HUVECs* • 5000–50,000 cells • Percentage: 1–8%	• Monolayer culture on plastic coverslips: 2 cm^2 • Coated with fibronectin • NRVCM cells cultured 2 days before addition of supporting cell types • Cells were optically mapped on days 5–8	*Advantages*: • Electrophysiological properties are similar to NRVCM only group (Max Captured rate ~ 7 Hz) • Assessed the impact of hASCs and hDFs when co-cultured with cardiomyocytes • Found the percentage of stromal cells that did not impede electrophysiological outputs. *Limitations*: • Cultured on monolayer • Cardiomyocyte source is not clinically translatable to humans • Maturation of cardiomyocytes in the presence of supporting cell types not evaluated	*Advantages*: • Dense vessel networks were created in the presence of all three cell types at 500:50:25 ratio *Limitations*: • Cord-like structures • No 3D vessels with lumens • Vasculature is not organized relative to cardiomyocytes	[82]

(continued)

Table 6.1 (continued)

	Cells	Culture conditions	Cardiac characterization	Vascular characterization	Ref.
hESC-CM	*hESC-CM* • 400,000 cells • Percentage: 33–40% *Embryonic mouse fibroblasts* • 200,000–400,000 cells • Percentage: 20–33% *hESC-EC or HUVECs* • 400,000 cells • Percentage: 33–40%	• 50% PLLA: 50% PLGA size: 9 mm^3 (3 mm × 3 mm × 1 mm) • Pore size: 212–600 μm 93% porosity • Cultured for 2 weeks • 8–10 μL culture media: Growth factor reduced Matrigel mix (1:1) • Simultaneously seeded	*Advantages*: • Spontaneous beating occurred at day 4 • Ca^{2+} impulse propagation in line with contraction • Contractility is responsive to cardiac drugs like isoproterenol and carbamylcholine • Increased proliferation of cardiomyocytes in the presence of endothelial cells *Limitations*: • Alignment of cardiomyocytes were not characterized • Electrophysiological properties not characterized (i.e. conduction velocity and maximum captured rate)	*Advantages*: • No significant difference with between 1:1 and 1:2 (FB:EC) • Tri-culture resulted in 5.12 lumen density while endothelial was 1.57 • Implanted in vivo and becomes functional with host vasculature *Limitations*: • Did not organize into blood vessels without fibroblasts • Mainly compact clusters	[13, 64]
	hESC-CM • 2,000,000 cells • Percentage: 40% *Mouse embryonic fibroblasts (MEF) or NHDF* • 2,000,000 cells • Percentage: 40% *hESC-EC or HUVECs* • 1,000,000 cells • Percentage: 20%	• Spheroid/cell clusters • Cultured in low attachment plates • Cultured for 3 days and 8 days • Placed in vivo in a skeletal muscle defect and nude rat hearts	*Advantages*: • Human cardiac tissues patches contracted and could be paced up to 2–3 Hz • Increased collagen content in the tri-culture • Increased force of contraction ~8 mN/mm^2 compared to 2 mN/mm^2 • Increased normalized force in the presence of all three cell types • Increased force in tri-culture with increased differential strain *Limitations*: • Unorganized structure • Lack of mechanical integrity	*Advantages*: • Vessel structures increased in HuEB media as compared to RPMI B27 • Increased CD31 staining compared to cardiomyocyte only control • Anastomosis with host vasculature in vivo *Limitations*: • Vessel length not assessed in vitro before implantation	[111]

hESC-CM	*hESC-CM /NRVCM* • 32 million cells • Percentage: 80% *hMSC* • Four million cells • Percentage: 10% *HUVECs* • Four million cells • Percentage: 10%	• POMaC base of scaffold • 5 mm length • 3.1 mm width • 150–300 μm thickness • Fibrin hydrogel for seeding cells (33 mg/mL fibrinogen and 25 U/mL thrombin)	*Advantages*: • Synchronous contractions occurred as early as day 4 • Conduction velocity was near 4.8 cm/s in vascularized samples without conduction block • Responsive to epinephrine • Cultured with perfusion in bioreactor • Tunable mechanical properties based off of design • Lactate dehydrogenase decreased with perfusion *Limitations*: • Not uniformly aligned although anisotropic design • Electromechanical stimulation needed to improve electrophysiology	*Advantages*: • Endothelial cells coated the lumen structure in the parenchymal space • Connection of vasculature throughout scaffold • 3D microvasculature observed • Connected to the femoral vessels in vivo *Limitations*: • Vasculature is not interspersed through cardiomyocytes which is not similar to the native myocardium	[138]
	hESC-CM • Not provided *hMSC* • Not provided *HUVECs* • 375,000 cells	• Decellularized spinach leaf • Coated with 10 μg/mL fibronectin for cell attachment • Grown for 14 days	*Advantages*: • Cardiomyocytes have the ability to attach to the surface of the leaf with ECM protein coating • Spontaneous beating at day 5 • Calcium activity was maintained for 21 days on spinach leaf *Limitations*: • Cardiomyocytes clustered across the spinach leaf rather than making a syncytium • Decreased contractility over time • Contractility strain on TCPS was higher than spinach substrates • Structural integrity for in vivo implantation	*Advantages*: • HUVECs perfused into decellularized plant vasculature to obtain develop vasculature *Limitations*: • Vasculature is not interspersed through leaf while cardiomyocytes which is not similar to the native myocardium	[37]

(continued)

Table 6.1 (continued)

	Cells	Culture conditions	Cardiac characterization	Vascular characterization	Ref.
hiPSC-CM	*hiPSC-CM* • Two million cells • Percentage: 33% *hiPSC-SMC* • Two million cells • Percentage: 33% *hiPSC-EC* • Two million cells • Percentage: 33%	• Fibrin hydrogel loaded with IGF-1 for cell survival • Directly injected cells into hydrogel on the myocardium • Cells are differentiated into three lineages (CM, SMC, and EC) and injected directly into hydrogel without in vitro culture	*Advantages*: • Improved functionality in vivo with triculture and patch present and reduced CM apoptosis of myocytes • Increased ejection fraction • Decreased infarct size • Cell survival was greatest in tri-culture cells + patch group *Limitations*: • Cardiac electrophysiology not characterized prior to in vivo implantation	*Advantages*: • Tri-culture promoted survival and proliferation of cardiomyocytes • Engineered vasculature promotes host vasculature angiogenic response *Limitations*: • Vasculature was not characterized before implantation into the infarcted myocardium	[134]
	hiPSC-ECM • One million cells • Percentage: 76% *hMSC* • 400,000 cells (w/ hiPSC-ECM) • 300,000 cells (w/hCMVECs) • Percentage: 23%/38% *hCMVECs* • 500,000 cells • Percentage: 63%	• 3D collagen cell carrier • hMSC/hCMVECs culture for 7 days under vascular conditions • hMSC/hiPSC-ECMs cultured for 7–14 days on top pre vascularized cultures	*Advantages*: • Positive staining for cardiac MHC across the construct • Rhythmic contractions • Calcium flux monitored across system `*Limitations*: • Cardiomyocyte orientation not controlled • Electrophysiological parameters not examined	*Advantages*: • CD31 positive cord-like structures established • Pericyte-like cell stained positive for SMA • Sequential seeding of vasculature cells • Positive staining for AcLDL and vWF in the tri-culture system *Limitations*: • Vasculature is reduced in the presence of all three cell types	[122]
	hiPSC-CM • 14,850–23,100 cells • Percentage: 45–70% *hCF* • 0 to 13,200 cells • Percentage: 0–40% *HUVECs* • 4950–9900 cells • Percentage: 15–30%	• 3D bioprinting (0.32 cm^3) • Single layer of cell aggregates (cardiospheres) that were 450–550 μm in diameter • Printed on needle Array • Cardiac patch was matured for 72 h with needle array in place • Cardiospheres beat after 2 days and fused after removal of needle array • Cardiospheres were implanted onto myocardium and secured with tissue glue in vivo	*Advantages*: • Electrophysiological parameters quantified • Ventricular-like action potentials • Developed gap junctions (Cx-43) to propagate signal as a syncytium • Low levels of cell death from TUNEL assay • Conduction velocity near 4.6 cm/s *Limitations*: • Conduction velocity decreased with increased fibroblast percentage	*Advantages*: • CD31 staining throughout the cardiosphere • Nascent vasculature development in vivo *Limitations*: • Vasculature not quantified • Presence of 3D lumens not investigate or represented	[85]
	hiPSC-CM • 4 M/mL • Percentage: 65% *hPC* • 0.36 M/mL • Percentage: 6% *BOEC* • 1.82 M/mL cells • Percentage: 29%	• Fibrin hydrogel • 8.4 mm × 5 mm • 4 mg/mL fibrinogen • 120 μL total volume • Bilayer patch was created by coating with fibrinogen and 10 U/mL thrombin • Grown for 14 days	*Advantages*: • Bilayer patch resulted in increased CM density compared to control (237 vs 35 CM/mm^2) • CM only patches underwent more apoptosis than bilayer (75.4% vs 37.5%) • Bilayer patch output was 2.17 nN/input CM vs 0.3 nN/input CM *Limitations*: • Electrophysiological properties not analyzed • Alignment of cardiomyocyte	*Advantages*: • ~34 lumens/mm^2 • ~65 vessels/mm^2 in vivo • ~67% perfused fraction of vasculature *Limitations*: • Vasculature developed independently of cardiomyocyte culture which is not similar to the native myocardium	[101]

viable human cardiomyocytes. Human embryonic stem cells have been used to differentiate stem cells into functional human cardiomyocytes. hESC-CMs have well-documented electrophysiological properties, contract rhythmically, and are responsive to cardiac compounds. Similar to NRVCMs, hESC-CMs can be genetically manipulated but have the advantage of being maintained in vitro for longer periods. These cells can also be engrafted into the human myocardium [98]. While these cells are advantageous for studying human cardiomyocytes, there are ethical and regulatory concerns related to the accessibility to embryos as well the immune response that arises with transplantation [74]. Additionally, hESCs have been shown to have genetic instability, and specifically, cardiomyocytes are immature in their development. Finally, due to the pluripotent state of the stem cells, they have the potential to form teratomas when transplanted in vivo. To rectify these problems, recent work has established that purifying the culture and removing undifferentiated stem cells should reduce the probability of uncontrolled cell proliferation.

Human-induced pluripotent stem cells (hiPSCs) have similar characteristics to hESCs and have the advantage that they can be used autologously. The hiPSC-derived cardiomyocytes (hiPSC-CMs) circumvent ethical concerns associated with hESCs, but there is variability among cell lines derived from different patients. While these cell types are capable of spontaneously contracting, their functional and structural immaturity needs to be addressed. For example, hiPSC-CMs are polygonal in shape and mononucleated (while the adult myocytes are larger, rod-like, and binucleated), and they exhibit fetal-like sarcomeric organization, ion channel expression, force generation, and action potential shape. Sarcomeres in hiPSC-CMs are shorter and more disorganized than in the adult myocyte [133]. The hiPSC-CMs also have reduced contractile machinery, as compared to the adult myocyte, and have not undergone isotype switch to a stiffer form of titin. Similar to neonatal rat cardiomyocytes, these cells exhibit immature calcium-handling properties and no T-tubule formation [123]. Finally, gap junction proteins are located around the cardiomyocytes, rather than located at the intercalated disk space in pluripotent stem cells, which yields slower conduction velocities compared to the native human adult heart [133]. In spite of these limitations, hiPSC-derived cardiomyocytes (hiPSC-CMs) are a suitable cell source for drug screens and disease modeling, based on their electrophysiological characteristics.

6.3.2 Endothelial Cells

Several sources of endothelial cells have been used for vessel development. These include human umbilical vein endothelial cells (HUVECs), endothelial colony-forming cells (ECFCs) (also termed blood outgrowth endothelial cells (BOECs) or endothelial progenitor cells (EPCs)), human embryonic stem cell-derived endothelial cells (hESC-ECs), and human-induced pluripotent stem cell-derived endothelial cells (hiPSC-ECs). HUVECs display a mature phenotype and have been shown to

develop cord-like structures in monolayers and vascularized lumens in 3D microenvironments that can anastomose with host vasculature in vivo.

ECFCs are critical in wound healing/ischemic environments and are found circulating in peripheral blood. These endothelial progenitor cells are advantageous for patient-specific therapies and have the ability to mature and anastomose with host vasculature. While patient-specific, these cells are in limited supply circulating in the peripheral blood, they are initially slow growing, and it takes many passages to acquire enough cells to perform experiments or use for therapies.

More recently, hESC-EC and hiPSC-EC have been used to make vascular structures in vitro and can anastomose with host vasculature in vivo. hESC-ECs and hiPSC-ECs have the ability to make lumens in 3D cultures (i.e., hydrogels) and are responsive to vascular endothelial growth factor (VEGF) and basic fibroblast growth factor (bFGF) signaling [58, 59]. While phenotypically similar to both mature and immature endothelial cells, some studies indicate that though hESC-ECs and hiPSC-ECs may be less responsive to shear stress [135], they retain the ability to be differentiated into arterial and venous endothelial cells [139].

6.3.3 Fibroblast(-Like) Cells

Developing stable, perfusable vascular networks that can anastomose with host vasculature, to deliver nutrients, increases the capacity to enhance the viability of engineered grafts. Vascular stabilization occurs through the activity of mural cells, i.e., pericytes or smooth muscle cells. Several mesenchymal phenotypes (characterized as being positive for surface markers CD73, CD90, and CD105) have been used to perform this function [3]. In particular, fibroblasts from the skin, lung, and bladder have been widely used, though their perivascular characteristics vary with the anatomical site of isolation. Dermal fibroblasts are the most translatable due to the ease of obtaining them from the skin and their potential to rapidly proliferate and to express limited perivascular potential. Chen et al. demonstrated vessel development using normal human lung fibroblasts in co-culture with HUVECs or EPCs. Vessel development was monitored over 7 days, in the presence of low (0.2 million cells/mL) or high (two million cells/mL) concentrations of fibroblasts. The higher concentration of normal lung fibroblasts co-cultured with HUVECs or EPCs resulted in longer vessels, compared to the lower concentration of fibroblasts [15]. Costa-Almeida et al. compared the vessel development of human dermal fibroblasts coupled with HUVECs or blood outgrowth endothelial cells (BOECs). Studies were completed at 2:1 ratio of EC-FB. Cells were co-cultured for up to 21 days. By day 21, the co-culture of BOECs and NHDF resulted in ~32 capillary-like structures/mm^2, while HUVEC and NHDF co-cultures developed ~30 capillary-like structures/mm^2. The average length of the capillary-like structures decreased from day 14 to day 21 in both groups [21].

Cardiac fibroblasts are specifically derived from the myocardium through biopsy. This, however, causes damage to the myocardium. Cardiac fibroblasts contribute to

the myocardial structure and can potentially aid in signal transduction between cardiomyocytes. They can be found in the wound healing environment post injury and provide paracrine signaling [88, 91]. Cardiac fibroblasts have perivascular potential and serve as a suitable source of cardiomyocyte co-culture. Twardowski et al. focused on the role of vascular development with cardiac fibroblasts coupled with endothelial cells. The study specifically looked at using rat aortic endothelial cells (rAEC) coupled with neonatal cardiac fibroblasts (nCF) in fibrin hydrogels. As a positive control for pericyte-like cells, rat bone marrow-derived mesenchymal stem cells (BM-MSCs) were used to compare vessel assembly. Seeding support cells and endothelial cells at 1:1 ratio, this study demonstrated that nCF-rAEC developed longer sprouting networks compared to when endothelial cells were co-cultured with BM-MSCs [120].

As indicated above, BM-MSCs can potentially serve as pericyte-like cells/mural cells and stabilize vascular structures. While these cells have many potential benefits, there is high morbidity associated with their extraction, and cell yields are relatively low. In contrast, adipose-derived stem/stromal cells (ASCs) can be procured in high numbers from a minimally invasive liposuction procedure. In addition to acting as mural cells, ASCs secrete an abundance of proangiogenic growth factors. ASCs are also capable of modulating inflammatory responses, reducing apoptosis, preventing fibrosis, and stimulating endogenous repair and neovascularization and can withstand temporary ischemia [49, 90, 124]. ASCs have also been shown to electrically couple with neonatal rat cardiomyocytes by forming gap junctions, which would indicate that these cells have the potential to behave as cardiac fibroblasts [18]. There are no studies to date that demonstrate the potential of hASCs to behave as both cardiac fibroblasts and perivascular cells, within the same cultures.

Merfeld-Clauss et al. have monitored vessel assembly of hASCs coupled with cord-blood endothelial colony-forming cells (cbECFCs). In the monolayer culture, there was dense vessel network assembly which appeared to regress over time. When cbECFCs were cultured with coronary artery smooth muscle cells (SMCs), aortic SMCs, normal human dermal fibroblasts, or human ASCs, the hASCs had statistically higher tube lengths [76]. In a 2015 report, this group reported that Activin A expression directed hASC differentiation down the smooth muscle lineage, when in direct contact with cbECFCs [77]. Hutton et al. found that heterogeneous hASCs contained a small amount of endothelial cells with the ability to expand and form vessel networks. These cells, cultured in high-density (20,000 cells/cm^2) monolayer, resulted in the development of CD31+ vessel structures [47]. This study was followed up with 3D vascular development in fibrin hydrogels [48]. Freiman et al. developed vessel networks with co-cultures of hASCs or normal human dermal fibroblasts and human adipose-derived microvascular endothelial cells (HAMECs) or HUVECs. It was found that the co-culture of hASCs and HAMECs resulted in the greatest increase in vessel length by day 7 and maintained the vessel length up until day 14 [34].

6.4 Multicellular Strategies

Several strategies have been used to develop vascularized contractile grafts that recapitulate key characteristics of the native myocardium. A common feature of these approaches is the culture of the three essential cell types: (1) contractile, electrically excitable cardiomyocytes; (2) endothelial cells, to self-assemble into vascular networks; and (3) fibroblasts-like cells, to stabilize cardiac and vascular function (see Table 6.2). The first such reported tri-culture system utilized hESC-CMs, hESC-ECs, or HUVECs and mouse embryonic fibroblasts (mFBs) combined in a cell ratio of 1:1:1 (hCM-mFB-hEC) and seeded into 1:1 mixed poly-L-lactic acid (PLLA)/polylactic-glycolic acid (PLGA) scaffolds via Matrigel [13, 63] (Fig. 6.3). This study demonstrated that vascular structures were stabilized in the presence of fibroblasts and developed increased lumens and vessel density. Without the presence of fibroblasts, vessel structures were limited in development. In this tri-culture system, cardiomyocytes displayed chronotropic responses to compounds like isoproterenol and carbamylcholine [13, 63]. While this approach was a landmark in the development of vascularized cardiac tissues, there was limited quantitative characterization of cardiomyocyte interconnectivity or electrophysiology.

Fibrin hydrogels have also been used extensively as a scaffold for cardiac grafts [101, 117, 134]. Ye et al. co-cultured cardiomyocytes, smooth muscle cells, and endothelial cells, all derived from hiPSCs at a ratio of 1:1:1. These cells were directly injected into the infarct or directly injected into a fibrin hydrogel loaded with insulin-like growth factor (IGF). Groups that were tested included direct cell injection, fibrin patch only, and hEC plus hSMC encapsulated within the fibrin hydrogel. After 4 weeks of in vivo implantation, the cardiac patch resulted in increased ejection fraction which was near that of the sham rat. In addition, the injection of all three cell types into fibrin hydrogels resulted in the smallest infarct size compared to MI with no treatment and patch only groups after 4 weeks. The tri-culture group injected into the fibrin hydrogel had the greatest thickening fraction comparable to that of the sham. In this study, cells were not cultivated in hydrogels before injection; therefore, characterization of the cardiomyocyte contractility or vessel development was not completed in vitro before implantation. Schaefer et al. co-cultured hiPSC-CMs, human pericytes, and human blood outgrowth endothelial cells (BOEC). In this study, the presence of vasculature structures improved the force of contraction over time and increased the presence of the mature form of cardiac troponin (cTnI) compared to the immature form (ssTnI) normally observed in immature tissues. There was nearly 1 mN of force generated in these constructs by day 14. When the patch was implanted in vivo, the vasculature anastomosed with the host vasculature and also integrated with cardiomyocytes. There were nearly 150 vessels/mm^2 in the tri-culture system. One limitation of these approaches is that hydrogel systems are isotropic, with cells growing in several directions. The native myocardium is anisotropic. In addition, hydrogels do not allow for the highest level of homotypic cell-cell connections among cardiomyocytes, when multiple cell types are encapsulated.

Scaffold and hydrogel studies typically require all cells to be seeded simultaneously. Subsequent studies demonstrate advantages associated with a sequential

Table 6.2 Summary of cell types used for tri-culture systems

		Advantages	Limitations	Ref.
Cardiomyocytes	NRVCMs	• Contract ex vivo • Relatively easy to form in monolayers • Well documented electrophysiological properties • Reproducibility of phenotype • Easily accessible	• Rodent specific • No direct clinical translatability • Little to no plateau phase • Immature calcium handling • Limited t-tubule formation • Isolation techniques vary	[56, 26]
	hESC-CMs	• Contractile • Well documented electrophysiological properties • Derived from human embryos • Mimics human cell characteristics • Can be sorted by markers like VCAM-1	• Ethics • Teratoma formation • Accessibility • Immunogenicity • Genetic instability • Fetal like in morphology and electrophysiology	[39, 113]
	hiPSC-CMs	• Contractile upon differentiation • Obtained from reprogrammed somatic cells with factors (Oct4, Sox2, Klf4, and c-Myc1 or Oct4, Nanog, Sox2, and Lin28) • Have the potential to provide unlimited numbers of cardiomyocytes • Mimics human cell characteristic • Model monogenic diseases • Can be sorted to increase purity • Autologous/patient specific with less immunogenicity	• Reprogramming techniques vary • Scale up • Inter line variability • Cell purity • Relatively immature • Fetal like sarcomere organization • Fetal like force generation • Fetal like Ion Channel expression • Mononucleated • Polygonal in cell shape • Mixed phenotypes • Epigenetic memory	[103, 133, 52]

(continued)

Table 6.2 (continued)

		Advantages	Limitations	Ref.
Endothelial Cells	Primary endothelial cells (HUVECs)	• Mature like endothelial cells from large vessels • Easily expanded • Positive for markers CD31, CD54, CD62e, vWF, and AcLDL • Responsive to exogenous growth factors (i.e. VEGF, FGF2) • Ability to anastomose with host vasculature in vivo	• Allogenic • Typically are pooled from multiple donors • Sensitive to cell density during expansion • Sensitive to hypoxia	[90, 25, 73, 87, 130]
	hECFCs/ BOECs/ EPCs	• Progenitor cells • Found in circulation • CD31, CD34, CD105, CD144, CD146, vWF, eNOS, VEGFR2 positive • Autologous/patient specific • Ability to anastomose with host vasculature • Found in sites of ischemia and wound healing • Paracrine support for myocytes • Express Connexin 43 (Cx-43) and Cx-45 • Integrate with resident vasculature • Can be used for many passages in vitro	• Low in number in peripheral blood • Require many expansions • Slow growing initially	[90, 22, 30]
	hESC-ECs	• Can form tubes like structures in vitro with sorted pure population • Can anastomose with host vasculature in vivo • CD31 positive	• Ethics • Immunogenicity • Teratocarcinoma formation • Differentiation protocol varies causing potential instability in passages post differentiation • Requires selection for EC specific cells	[17, 46, 66]
	hiPSC-ECs	• Autologous/patient specific • Can be disease specific • Can form tubes like structures in vitro with sorted pure population • Can anastomose with host vasculature in vivo • Have the ability to develop large numbers of endothelial cells quickly	• Various differentiation protocols • Interline variability due to reprogramming methods. Differentiation protocol varies causing high heterogeneity in the derived ECs • Requires flow sorting/magnetic sorting for EC specific cells	[59, 58, 69, 105]

Fibroblast-like cells	Fibroblast	• Patient specific • Easily accessible • Multipotent • Perivascular potential • Can act as pericyte-like cell when coupled with endothelial cells	• Limited perivascular potential • Characteristics vary based off of site of isolation • May alter electrophysiological properties of CMs	[3, 15, 10, 65]
	Cardiac fibroblasts	• Cardiac specific • Major cellular component of the native myocardium • Maintain cardiac structure and function • Found in wound healing post infarction • Promoted sprouting of endothelial cells in co-culture	• Causes damage to myocardium upon isolation • Has experimentally slowed conduction in co-culture with cardiomyoctes in vitro	[88, 120, 51, 6, 35, 109]
	BM-MSC	• Immunomodulatory • CD73, CD90, and CD105 positive • Pericyte-like cell • Multipotent • Autologous/patient specific • Stabilize vasculature • Secrete VEGF, bFGF, Ang-1 and EGF when co-cultured with ECs	• Painful isolation • Limited cell numbers • Can potentially differentiate down the osteogenic lineage in the myocardium • May alter electrophysiological properties of CMs	[124, 49, 90]
	hASC	• Pro-angiogenic • High perivascular potential • Differentiate down the smooth muscle lineage when co-cultured with ECs • Relatively easy isolation • Immunomodulatory • May develop gap junctions when coupled cardiomyocytes	• Limited mechanistic information on effects when coupled with cardiomyocytes	[76, 77, 47, 48, 34]
	Pericytes	• Promote vascular stabilization • Secrete pro-angiogenic growth factors • When coupled with cardiomyocytes in vivo have shown improvement post MI in ejection fraction and fractional shortening	• Difficult to isolate • Not an abundant cell source • Limited data on the CM electrophysiology when coupled	[62]

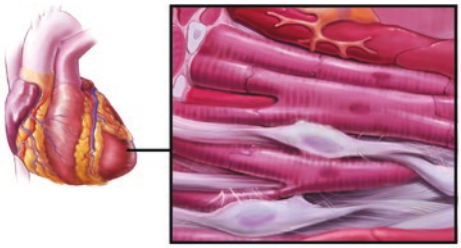

Native Heart Properties

Structured collagen network that guides cardiomyocyte alignment.

Highly vascularized with supporting cell types such as pericytes.

Scaffold Materials		Culture Procedures	
Type	Description	Type	Description
PLLA/PLGA	Cells seeded onto 3D printed bioscaffold	Sequential Seeding	Cells of tri-culture seeded in separate groups over a period of time.
Hydrogels	Cells suspended in tunable microscaffold	Spatial Separation	Cells of tri-culture seeded on different areas of bioscaffold.
Aggregation Spheroids	Cell clusters of tri-culture cell types		

Fig. 6.3 Strategies for the development of vascularized cardiac tissue grafts for infarct repair

seeding strategy, whereby cardiomyocytes are cultured for a period of time before supporting cells were added (Fig. 6.3). In one such study, cells were seeded onto micropatterned polyethylene glycol (PEG) hydrogels coated with Matrigel™, to enhance cell attachment and the development of cardiac organoids [50]. NRVCMs were seeded with D4T endothelial cells and neonatal cardiac fibroblasts at three different CM-FB-EC ratios (40:13:47; 60:9:31; and 80:4:16). Cells were seeded simultaneously or sequentially. In sequential seeding, the cell ratios were maintained, and D4T ECs and nCFs were seeded 2 days prior to the addition of cardiomyocytes and evaluated for electrophysiological and contractile changes relative to NRVCM-only cultures. Simultaneously seeded tri-cultures resulted in increased excitation threshold to 6 V/cm, compared to ~3 V/cm in NRVCM-only controls, and decreased maximum capture rates from ~4.2 to 3 Hz. Upon sequential seeding however, the conditions containing the highest percentage of cardiomyocytes coupled with supporting cell types resulted in an excitation threshold closest to the NRVCM-only control of about 3–4 V/cm, with statistically unchanged maximum capture rates. The data demonstrated that the greatest presence of CD31/PECAM-1 positively stained cells was found in the simultaneously seeded cultures, but electrophysiological and functional parameters were sacrificed, relative to the sequentially seeded cultures. Although the

cells were positive for CD31, the development of cord-like structures was not uniformly seen throughout the constructs. Recent studies have also investigated the impact of using hASCs in lieu of human dermal fibroblasts, together with NRVCMs and HUVECs. ASCs have been found to be beneficial in ischemic settings like myocardial infarction. Studies that have injected hASCs into rats and pigs have found paracrine secretion of multiple growth factors. Echocardiograms revealed a decrease in infarct size, an increase in wall thickness, a decrease in end-systolic and end-diastolic volumes, an increase in left ventricle ejection fraction, and a left ventricle fractional shortening [102]. Therefore, within a monolayer in vitro system, NRVCM-hASC and hASC-HUVEC co-cultures were first used to determine the appropriate tri-culture ratios. In the tri-culture system, an NRVCM-hASC-HUVEC ratio of 10:2:1 resulted in vessel development of 70 mm per 3240 mm^2 with an average of 454 junctions. The electrophysiological properties were reported as 20 ± 2 cm/s; APD_{80} and APD_{30} of 122 ± 5 ms and 59 ± 4 ms, respectively; and maximum capture rate of 7.4 ± 0.6 Hz [82]. From these studies, it could be seen that sequential seeding allowed cardiomyocytes to develop cell-cell connections and allow for improved electrophysiological outcomes for cardiomyocytes. Although this allowed for the development of close cell-cell connections, the cultures were 2D in nature.

Zhang et al. developed the AngioChip that enabled the formation of 3D tissues with spatial and temporal control while seeding different cell populations (Fig. 6.3). AngioChips were made from the micropatterned biodegradable elastomer poly(octamethylene maleate (anhydride) citrate) (POMaC), and cells were encapsulated into collagen hydrogels. The tri-culture system was developed from NRVCMs or hESC-CMs, hMSCs, and HUVECs. Uniquely, these devices allowed for the development of channels to accommodate medium perfusion and to provide adequate nutrient transfer to cardiomyocytes. After optical mapping the resulting conduction velocity was 4.8 cm/s. In this system the channels were coated with vascular cells to develop a channel for nutrient perfusion and ideal integration when implanted in vivo. The AngioChip was surgically implanted and demonstrated "artery-to-artery" anastomosis with host vasculature [138]. Employing similar principles for spatial control, Gershlak et al. developed a decellularized spinach leaf system, which served as an attractive biomaterial for cardiac tissue engineering. The native venous architecture of the leaves provided intrinsic vasculature networks. The spinach leaf was reseeded with a tri-culture system consisting of hESC-CMs, hMSCs, and HUVECs. After 10 days of culture, the tri-culture system resulted in 10% contractile strain. Contractile strength peaked at day 7 and was maintained until day 17. After day 17, there was a decrease in contractile strength. The endothelial cells (HUVECs) were reseeded, through the cannula, and appeared to line the spinach leaf to form vessel like structures within the inherent plant structure [37].

Another promising strategy used cell clusters rather than individual cell suspensions (Fig. 6.3). Stevens et al. developed spheroid/cell cluster tri-culture systems which were seeded with hESC-CMs, hDF, and HUVECs. In this system, there was increased force of contraction over time, as well as increased force-length relationships in the presence of all three cell types. In addition, these clusters developed a similar percentage of contraction in the patches as the control group, up to 3 Hz

pacing. The vessel characterization showed increased CD31 staining, compared to cardiomyocyte-only control, and anastomosis with host vasculature when implanted in vivo [111]. Ong et al. developed a 3D printed tri-culture system in which cells are the matrix. This tri-culture consisted of hiPSC-CMs, hCFs, and HUVECs. The electrophysiological properties consisted of ventricular-like action potentials and conduction velocity near 4.6 cm/s, which appeared to decrease with increased fibroblast percentage. CD31 staining was found in the histology inside the cell cluster, but vessel density was not calculated. When the scaffold was implanted in vivo, there was nascent vasculature development [85].

6.5 Biomaterials

Biomaterials are designed to provide structural support, alignment cues, and bioactive signaling to enhance cardiomyocyte function and maximize contractile and electrophysiological properties. In addition, incorporation of proangiogenic cues facilitates the development of dense vasculature [125]. Biomaterial choices for the development of vascularized cardiac grafts range from natural to synthetic biopolymers. For example, PLLA/PLGA (in a 1:1 ratio) has been used to create a sponge-like, biocompatible scaffold. PLGA has a high degradation rate, while PLLA provides mechanical support to the 3D structure [67]. Alternatively, PEG and POMaC, which degrades easily through hydrolysis, are the materials to which hydrogels containing cells will be cultured [50, 51, 79]. These polymers were coated with Matrigel™ or a combination of Matrigel™ and collagen.

Hydrogels are an attractive material because they are generally made from natural materials and can be modified to tune their properties, encapsulate cells, and serve as an adhesive to maintain cells in the desired location. The native myocardium is composed mostly of collagen leading to the hypothesis that collagen gels would facilitate a similar extracellular matrix composition. While hydrogels are attractive sources for providing a scaffold for development, there are drawbacks. These include limited mechanical integrity, reduced flexibility in seeding procedures, and isotropy [42]. Various processing strategies have been employed to minimize these limitations. Despite collagen being a major extracellular matrix protein, of the native myocardium, many multicellular approaches utilize fibrin as a scaffold. Fibrin is composed of fibrinogen and cross-linked with thrombin. Fibrin has the ability to recruit vasculature because it is proangiogenic [15]. Fibrin is often used in cardiac patch systems because it has many attractive features and naturally occurs at wound sites [70, 131]. Among fibrin's benefits are its ability to promote angiogenesis, cell survival, and extracellular matrix secretion [117]. This matrix secretion, in combination with the natural strain stiffening of fibrin, mimics the mechanics of the cardiac microenvironment [9, 100]. To provide mechanical integrity and facilitate the development of alignment and tension for cardiomyocyte contractility, researchers have developed casting methods like posts for fibrin hydrogels

[96, 116, 128]. Recently, fibrin was electrospun into microfibers. Electrospun microfibers offer the added advantage of tunable mechanical properties and alignment cues, which is critical for myocardial tissue [140]. Other groups initiated a bilayer scaffold approach, which includes culturing cardiomyocyte gels and vascular gels both independently and in combination for therapy [101].

Decellularized matrices are also attractive for the development of tissues because they utilize nature's platform. Most recently, the Gaudette group developed vascularized cardiac tissue on a decellularized spinach leaf. The spinach leaf was specifically used because it possesses an intrinsic network that could be used for the development of dense vessel networks alongside contractile cardiomyocytes [37]. Other groups have decellularized rat, porcine, and human myocardium and reseeded them with cardiomyocytes and endothelial cells [86]. Currently, the drawbacks to decellularized matrix are the reseeding efficiency and that the detergents used to decellularize can alter the stiffness of the matrix.

6.6 Biophysical Cues

Cellular behavior is strongly influenced by the properties of the cells' microenvironment. Hence, tissue engineering strategies aim to tightly regulate the biochemical, mechanical, and electrical cues experienced by cells, to influence cell- and tissue-level behaviors. However, the ideal microenvironment for cardiac development is not necessarily conducive to angiogenesis and vice versa. This discord presents a challenge in the engineering of tissues with both mature cardiac function and functional vasculature and necessitates a firm understanding of how environmental factors contribute to each process.

6.6.1 Biochemical Cues

Embryological studies have proven that cardiac development relies heavily on the biochemical makeup of its surroundings, as small variations in localization, timing, or concentration of certain signaling molecules can result in hugely consequential cardiac defects. The earliest stage of cardiogenesis, the formation of cardiac progenitor cells, relies on nodal, a cytokine in the TGF-β family [11]. Wnt/β-catenin and bone morphogenic protein (BMP) signaling also play critical roles in early differentiation by facilitating the proliferation of cardiac progenitors, although evidence suggests that both factors can exert an inhibitory effect on terminal cardiac differentiation [60, 61, 83, 137]. These embryological revelations have yielded a variety of approaches to promote myocardial differentiation in pluripotent cells, the most efficient of which rely on modulating Wnt, BMP, and fibroblast growth factor (FGF) signaling, with small molecule regimens [68]. In a widely cited report,

Burridge and colleagues found that L-ascorbic acid 2-phosphate and recombinant human albumin, along with transient exposure to CHIR99021 (a glycogen synthase kinase 3 inhibitor) and IWR-1 (an inhibitor of Wnt/β-catenin signaling), are sufficient to induce cardiac differentiation in 11 hiPSC lines [12].

Dozens of factors have been identified as promoting angiogenesis, enacting their effects via a variety of mechanisms. Among the most relevant and researched, in the context of vascularized cardiac tissues, are vascular endothelial growth factor (VEGF), platelet-derived growth factor subunit B (PDGF-B), and angiopoietin-1 (Ang-1). In tri-culture experiments combining hESC-derived cardiomyocytes with endothelial cells and fibroblasts, Caspi et al. showed that the tri-cultures developed much more significant vasculature and also showed increased expression of VEGF, PDGF-B, and Ang-1 [13]. The importance of these factors was further confirmed when Hao and colleagues reported increased vascular development, in the infarcted myocardium of mice, in response to hydrogel-delivered VEGF-A and PDGF-BB [41]. In addition to traditionally recognized proangiogenic factors, some hormones and cytokines with unrelated primary functions have been shown to improve vasculature in engineered cardiac tissues; specifically, insulin-like growth factor 1 (IGF-1) and stromal cell-derived factor 1 (SDF-1) in combination with VEGF increased the vascular development in an engineered cardiac patch [24]. This effect was at least partially mediated by SDF-1's ability to attract CD34-positive hematopoietic progenitor cells.

The functional mechanisms of cytokines and hormones are often complex and influenced by the method of delivery. Alberti and colleagues concluded that these effects can drastically alter stem cell fate, by showing that immobilizing leukemia inhibitory factor in a gelatin matrix significantly improved its ability to maintain pluripotency in hESCs [1]. Similarly striking effects were observed in studies of biochemical control of vascularization. Early experiments revealed that heparin-mediated binding of VEGF to a collagen matrix promoted endothelial cell proliferation [110] and that immobilizing VEGF promoted penetration of endothelial cells into collagen matrices [104]. Chiu and Radisic subsequently demonstrated that endothelial cells formed significantly more vasculature on scaffolds with covalently immobilized VEGF and Ang-1 than scaffolds treated with soluble factor [16]. In that experiment the authors utilized 1-ethyl-3-[3-dimethylaminopropyl]carbodiimide hydrochloride (EDC) and N-hydroxysulfosuccinimide (sulfo-NHS) to covalently bind VEGF and Ang-1 to the collagen substrate. Factor immobilization using sulfonated alginate matrices has proven a very effective tool for promoting vasculature in complex tissue environments with many cell types, including cardiac tissue. FGF presented in this manner produced twice the blood vessel density as soluble FGF, when implanted subcutaneously in mice, and matrix-bound hepatocyte growth factor (HGF) similarly increased vascular density by nearly twofold, over all controls in mouse hind limb ischemia model [33, 99]. Despite these advances, the utility of presenting pro-cardiac molecules in this manner has not been rigorously evaluated. For the most part, experiments using multiple cell types have administered these molecules either before they are used in the patch or by including them as soluble factors in the media.

6.6.2 *Effect of Substrate Stiffness, Guidance, and Alignment Cues*

Of the many characteristics of the extracellular matrix, mechanical stiffness has been identified as particularly important to cellular differentiation and behavior. The role of matrix stiffness in supporting cardiomyocytes is poorly understood, and a wide range of elasticities has been reported as optimal for their culture. In one of the earliest studies on this topic, Jacot et al. reported that NRVCMs grown on 10 kPa polyacrylamide (PA) displayed improved markers of functional maturity, such as contractile force generation and sarcoplasmic calcium stores [53]. Similarly, Engler and colleagues found that embryonic cardiomyocytes isolated from rats and seeded on collagen-coated polyacrylamide matrices displayed much greater functional maturity on matrices with elastic moduli in the range of normal rat myocardium (~11 kPa), as opposed to stiffer matrices falling in the range of infarcted myocardium (~34 kPa) [28]. However, shortly thereafter, it was reported that NRVCMs cultured on very soft, 3 kPa PA scaffolds developed more electrophysiologically mature phenotypes but that other measures of functional maturity, such as cellular elongation and contractile force generation, were optimized on stiffer 50 kPa scaffolds [8]. The question of optimal substrate stiffness is further complicated by evidence that cardiomyocytes require different levels of substrate stiffness at different stages of differentiation. In 2010, Young and Engler found that a hyaluronic acid matrix, engineered to stiffen over time, increased expression of maturity markers in NRVCMs nearly threefold over standard scaffolds [136]. Another recent report suggested that CMs derived from iPSCs display improved initial differentiation, on protein-coated tissue culture plastic (elastic modulus ~2 GPa), but that they developed more mature beating behavior and contractile function on 20 kPa PA scaffolds [43].

Stiffness is also an important consideration in vascularization, as evidenced by experiments showing that angiogenesis in hydrogels seeded with HUVECs is strongly affected by the elastic modulus of the hydrogel. In a key report, Sieminski and colleagues showed that the softer collagen gels (Young's modulus = 6 kPa) developed more robust vascular networks than the stiffer gels (10 kPa) they tested [107]. This report also suggested that the relative magnitudes of the matrix stiffness, and the force of endothelial cell traction, regulate angiogenesis. They found that human blood outgrowth endothelial cells (HBOEC), which exert more traction force than HUVECs, formed thin, branched vasculature with thick walls in floating 10 kPa gels, while HUVECs formed vasculature with thin walls and larger lumens. However, if the stiffness was decreased to 6 kPa, both cell types formed narrow, thick-walled structures, while, if the apparent stiffness was increased by mechanically restraining the gel, both cell types formed thin-walled vasculature with large lumens.

Determining the ideal elasticity for vascularization of cardiac tissues is further complicated by inconsistencies in the literature. Wide varieties of matrix materials have been utilized, but it is very possible that optimal stiffness is different for each

material. Also, stiffness is measured and reported differently throughout the literature, with some authors reporting elastic modulus and others choosing to measure storage or complex moduli; these are related but they can be substantively different, in the context of viscoelastic materials. Despite these irregularities, it is likely that substrates optimized for endothelial proliferation and angiogenesis are much softer than those optimized for cardiomyocyte maturation, as the reported stiffnesses of angiogenic substrates ranged from under 100 Pa to about 6 kPa [2, 95, 107], while cardiomyocyte differentiation and maturation are reported to thrive in matrices with elastic moduli in the range of 10–50 kPa and have been shown to be actively suppressed on very soft (1–3 kPa) substrates [43, 71].

6.6.3 Alignment

Anisotropy and cellular alignment are prominent characteristics of cardiac physiology, and the alignment of cardiomyocytes is critical to normal electrophysiological and contractile behavior. In comparing cultures of NRVCMs grown on a flat surface with random orientation to cultures grown on a grooved substrate with increased alignment, Chung et al. found that the aligned cultures exhibited increased conduction velocities [19]. Alignment of 3D NRVCM cultures was also shown to increase the stimulated force of contraction [9]. Reproducing this organization has been a major goal of the tissue engineering field, and cardiomyocyte alignment is frequently used as a measurement of tissue maturity and predictor of functional capacity.

This anisotropy is not limited to cardiomyocytes as it is also present in the vasculature of native myocardium, where blood vessels are highly aligned in near-parallel organization [54, 94]. There have been efforts to recapitulate this vessel-level alignment to maximize biosimilarity, because, in theory, microvascular alignment could improve nutrient delivery and promote the survival of cardiomyocytes in the construct. An experiment in which pre-vascularized cardiac patches, formed with either randomly oriented or uniaxially aligned vasculature, were grafted onto infarcted myocardium in mice showed improved lumenal density and network length among the aligned samples in vitro. It also showed that their in vivo effects were indistinguishable, as they displayed similar total and perfused luminal densities, as well as similar improvements in scar tissue formation and functional outcomes [96]. These results raised questions regarding the importance of vascular alignment to the function of engineered cardiac tissues. In another set of experiments, researchers combined separately generated layers of aligned microvessels and aligned cardiomyocytes. They found that the combined patch exhibited much greater force of contraction in vivo and significantly reduced scar formation in mouse myocardial infarction models. Patches containing CMs only did not [101]. Without controlling for a patch with randomly oriented vasculature, the importance of alignment is impossible to assess.

6.6.4 Electrical and Mechanical Stimulation

Electrical and mechanical stimulation applied in culture can have a significant impact on the maturation of CMs and the development of vasculature in tissue-engineered constructs. In the development of engineered cardiac tissues that recapitulate the behavior of native myocardium, the ability to control the cellular environment and apply external stimuli is very important. Therefore, significant investment has been made in developing devices capable of reliably applying electrical and mechanical stimulation to these tissues and investigating optimal stimulation for cardiac development and angiogenesis.

6.6.5 Electrical Stimulation

Electrical forces play a key role in cardiac development, as spontaneous electrical activity begins in what will become the sinoatrial node as early as 20 days after fertilization [44]. Electrical stimulation has proven a useful tool in cardiac tissue engineering. Radisic and colleagues showed that applying electrical pulses at 1 Hz to cardiomyocyte-laden hydrogels resulted in improved CM alignment, a 50% increase in maximum capture rate, a threefold increase in gap junctions, and a fourfold increase in the fractional change in the surface area of the construct induced by each beat, suggesting increases in electrical coupling, electromechanical coupling, and force of contraction [93]. It has since been demonstrated that a ±2.5 V biphasic pulse, applied at 1 Hz, can drive progenitor cells toward cardiomyocyte lineages. This is evidenced by increases in cell length and alignment, along with increased expression of GATA-4, Cx43, and troponin T apparent after only 1 day of stimulation [89]. It has also been suggested that "electrical conditioning" can help establish automaticity in CMs, since the cultures electrically paced for 7 days displayed autonomous beating at the stimulated rate, even after the stimulus has been removed [27].

Electrical activity certainly has some effect on vasculature, as sympathetic nervous signaling is an important regulator of vascular tone. Sub-millisecond, 250 V electrical pulses applied at 10 Hz have been shown to cause vascular contraction in less than 10 s and reduces blood loss in models of acute traumatic injury [75]. However, the effects of electrical stimulation on endothelial cells and angiogenesis are more poorly understood. Various kinds of electrical stimulation have been shown to increase angiogenesis in a wide array of settings, including diabetic ischemia and neural progenitor cell treatment for ischemic stroke [5, 36]. These effects are believed to be primarily mediated by upregulation of VEGF in other cell types, as opposed to acting directly on endothelial cells [40], though there is some evidence that direct current electrical stimulation can upregulate VEGF receptors on endothelial cells, essentially priming them for biochemical stimulation [4, 141].

Experiments using electrical stimulation to promote angiogenesis generally utilize constant electrical fields, as opposed to experiments focusing on cardiomyocyte development which usually use regular electrical pulses. Thus far, investigations of cardiomyocyte-endothelial cell co-cultures have opted either to forego electrical stimulation or to use periodic electrical stimulation regimens created for CMs, even though the effects of periodic electrical stimulation on endothelial cells and angiogenesis are largely unknown. More directed investigation would be critical to understanding how electrical stimulation of engineered tissues can be optimized, for both CM maturation and for vascular development.

In the design of bioreactors with electrical stimulation capabilities, the application of field pulses to a 3D culture is relatively easy to adapt from 2D systems. A common configuration for such devices involves using two parallel electrodes to generate an electric field across a substrate [84, 89, 112, 115]. Tandon and colleagues, for example, developed a system that uses carbon rods to induce an electric field across a chamber that can support monolayers, three-dimensional cardiac tissue constructs, and micropatterned cellular substrates [115]. In subsequent studies, 1 Hz stimulation applied using this setup was shown to improve CM elongation and alignment, increase conduction velocity, and strengthen the tissue-level force of contraction [92]. This strategy has proven successful even with more complicated systems like the Biowire platform, a cell culture system that utilizes both architectural and electrical signaling to generate more mature cardiomyocytes [84]. The system consists of a collagen matrix, embedded with cardiomyocytes and supporting cell types, surrounding a single surgical suture, all within a template PDMS channel. This platform has since been expanded to also allow for perfusion of the biowire system during culture, facilitating an array of pharmacologic experiments.

6.6.6 Mechanical Stimulation

Myocardial development depends on a complex series of mechanical forces acting in concert to promote cardiomyocyte maturation, organization, and electrophysiological function. Animal studies provide strong evidence for the importance of mechanical stimulation, as they show that altering hemodynamic pressure and contractility in the fetal heart had dramatic effects on myocardial function [55, 80, 114]. It has since been established that imposing static or cyclic strain onto an engineered tissue has the ability to induce cardiomyocyte hypertrophy, promote maturity in stem cell-derived CMs, and improve myocardial organization [119, 132]. Cyclic strain is now understood as particularly important to CM development. Gwak and colleagues showed that applying 10% strain at 1 Hz to rat ESC-CMs upregulated cardiomyocyte-specific genes and resulted in a more mature microstructure, with Z-line formation and more organized myofibrillar bundles [39]. Another study found that the frequency of strain applications might have important differential effects on gene expression. Using ESC-CMs, they found that 10% strain applied at 3 Hz for 3 days resulted in a twofold increase in α-cardiac actin expression,

compared to unstretched controls, while 1 Hz and 2 Hz stimulation did not produce statistically significant changes [106].

Mechanical forces also play a powerful role in regulating endothelial cell behavior and vascularization. In vitro and in vivo studies have confirmed that the shear stress caused by blood flow strongly affects the phenotype of vascular endothelial cells [118]. However, in engineered cardiac tissues, where there is generally no blood flow during in vitro culture, the field has relied on tissue-level strain instead. Like cardiomyocytes, endothelial cells in engineered scaffolds have been shown to respond positively to uniaxial static strain, displaying improved angiogenesis and vascular alignment [23, 57]. However, the effect of cyclic strain on angiogenesis is more controversial. Some early reports suggested that cyclic uniaxial strain can actually disrupt endothelial networks and result in more random vascular organization [129]. Other studies present evidence that cyclic strain promotes endothelial cell and vascular alignment parallel to the strain [14, 38, 57, 108], and others have suggested that the strain induced by surrounding cell contraction is sufficient to induce that effect [121]. Again, the frequency of this strain is an important factor, as experiments using human coronary artery endothelial cells show that a minimum threshold frequency of 0.1 Hz is required to elicit an alignment effect and that the alignment develops more robustly and on a shorter time scale when the strain was applied at 1 Hz [38].

Experiments culturing endothelial cells and cardiomyocytes together, along with a variety of vascular support cell types (detailed above), have thus far been conducted using either cyclic strain conditions or no induced strain at all. These co-culture and tri-culture experiments have produced significant advancements in generating vascularized cardiac tissue. Very little work, however, has been done to evaluate whether using these conditions is optimal for promoting both cardiomyocyte development and endothelial cell survival and vascular network formation. It is very possible that conditions chosen to promote cardiomyocyte maturation are impeding angiogenesis in the tissues. Careful optimization of mechanical stimulation will be important in the continued development of these systems.

6.6.7 Combined Electrical and Mechanical Stimulation

Applying strain conditions and electrical stimulation together has proven a particular engineering challenge, and several bioreactors have been designed with the aim of incorporating these stimuli into hydrogel cultures [20, 72, 78, 81, 126]. These devices take advantage of the full diversity of mechanical strain modalities detailed above and have been configured to apply uniaxial and circumferential strain [20, 29, 72, 81, 126]. Across these devices, though, the vast majority generate electrical stimulation using the parallel electrode setup. A notable exception is the bioreactor reported by Cook and colleagues, which applies electrical impulses via the integration of a direct contact in the clamping mechanism that secures the tissue in place [20]. The characteristics that vary widely between these devices, including substrate

material compatibility, sterility requirements, incubator compatibility, and the integration of sensors, must all be considered in selecting the appropriate system for a particular application.

6.7 Conclusions

Multicellular systems have been developed to mimic the native myocardium and prolong survival of cardiac grafts when implanted in vivo. Several strategies utilizing simultaneous seeding, sequential seeding, and the combination of vascularized and cardiac constructs have been explored to achieve fully vascularized, contractile grafts. While a complete human system will be critical to the clinical translation of this technology, there are important questions surrounding the maturation of pluripotent stem cell-derived cardiomyocytes that must be addressed. Several techniques are under investigation, to improve the maturation of those cells and the overall organization and functionality of engineering cardiac grafts, including electrical stimulation, mechanical stimulation, and a combination of electromechanical stimulation. Recent developments have greatly improved the physiological relevance and translational potential of engineered cardiac patches, but further applications will hinge on the incorporation of dense, functional vasculature and co-alignment of cardiomyocytes.

References

1. Alberti, K., Davey, R. E., Onishi, K., George, S., Salchert, K., Seib, F. P., et al. (2008). Functional immobilization of signaling proteins enables control of stem cell fate. *Nature Methods, 5*(7), 645–650. https://doi.org/10.1038/nmeth.1222
2. Allen, P., Melero-Martin, J., & Bischoff, J. (2011). Type I collagen, fibrin and PuraMatrix matrices provide permissive environments for human endothelial and mesenchymal progenitor cells to form neovascular networks. *Journal of Tissue Engineering and Regenerative Medicine, 5*(4), 1–18. https://doi.org/10.1002/term.389
3. Alt, E., Yan, Y., Gehmert, S., Song, Y. H., Altman, A., Gehmert, S., et al. (2011). Fibroblasts share mesenchymal phenotypes with stem cells, but lack their differentiation and colony-forming potential. *Biology of the Cell, 103*(4), 197–208. https://doi.org/10.1042/BC20100117
4. Bai, H., Forrester, J. V., & Zhao, M. (2015). DC electric stimulation upregulates angiogenic factors in endothelial cells through activation of VEGF receptors. *Cytokine, 55*(1), 110–115. https://doi.org/10.1016/j.cyto.2011.03.003
5. Baker, L. L., Chambers, R., DeMuth, S. K., & Villar, F. (1997). Effects of electrical stimulation on wound healing in patients with diabetic ulcers. *Diabetes Care, 20*, 405–412.
6. Baum, J., & Duffy, H. S. (2011). Fibroblasts and myofibroblasts: What are we talking about? *Journal of Cardiovascular Pharmacology, 57*(4), 376–379. https://doi.org/10.1097/FJC.0b013e3182116e39
7. Benjamin, E. J., Blaha, M. J., Chiuve, S. E., Cushman, M., Das, S. R., Deo, R., et al. (2017). Heart disease and stroke statistics-2017 update: A report from the American Heart Association. *Circulation, 135*, e146. https://doi.org/10.1161/CIR.0000000000000485

8. Bhana, B., Iyer, R. K., Chen, W. L. K., Zhao, R., Sider, K. L., Likhitpanichkul, M., et al. (2010). Influence of substrate stiffness on the phenotype of heart cells. *Biotechnology and Bioengineering, 105*(6), 1148–1160. https://doi.org/10.1002/bit.22647
9. Black, L. D., Meyers, J. D., Weinbaum, J. S., Shvelidze, Y. A., & Tranquillo, R. T. (2009). Cell-induced alignment augments twitch force in fibrin gel-based engineered myocardium via gap junction modification. *Tissue Engineering. Part A, 15*(10), 3099–3108. https://doi.org/10.1089/ten.TEA.2008.0502
10. Blasi, A., Martino, C., Balducci, L., Saldarelli, M., Soleti, A., Navone, S. E., et al. (2011). Dermal fibroblasts display similar phenotypic and differentiation capacity to fat-derived mesenchymal stem cells, but differ in anti-inflammatory and angiogenic potential. *Vascular Cell, 3*(1), 5. https://doi.org/10.1186/2045-824X-3-5
11. Brennan, J., Lu, C. C., Norris, D. P., Rodriguez, T. A., Beddington, R. S., & Robertson, E. J. (2001). Nodal signaling in the epiblast patterns the early mouse embryo. *Nature, 411*(6840), 965–969.
12. Burridge, P. W., Matsa, E., Shukla, P., Lin, Z. C., Churko, J. M., Ebert, A. D., et al. (2014). Chemically defined and small molecule-based generation of human cardiomyocytes. *Nature Methods, 11*(8), 855–860. https://doi.org/10.1038/nmeth.2999
13. Caspi, O., Lesman, A., Basevitch, Y., Gepstein, A., Arbel, G., Habib, I. H., et al. (2007). Tissue engineering of vascularized cardiac muscle from human embryonic stem cells. *Circulation Research, 100*, 263–272. https://doi.org/10.1161/01.RES.0000257776.05673.ff
14. Ceccarelli, J., Cheng, A., & Putnam, A. J. (2012). Mechanical strain controls endothelial patterning during angiogenic sprouting. *Cellular and Molecular Bioengineering, 5*(4), 463–473. https://doi.org/10.1007/s12195-012-0242-y
15. Chen, X., Aledia, A. S., Popson, S. A., Him, L., Hughes, C. C. W., & George, S. C. (2010). Rapid anastomosis of endothelial progenitor cell-derived vessels with host vasculature is promoted by a high density of cotransplanted fibroblasts. *Tissue Engineering. Part A, 16*(2), 585–594. https://doi.org/10.1089/ten.tea.2009.0491
16. Chiu, L. L. Y., & Radisic, M. (2010). Scaffolds with covalently immobilized VEGF and Angiopoietin-1 for vascularization of engineered tissues. *Biomaterials, 31*(2), 226–241. https://doi.org/10.1016/j.biomaterials.2009.09.039
17. Cho, S.-W., Yang, F., Son, S. M., Park, H. J., Green, J. J., Bogatyrev, S., et al. (2012). Therapeutic angiogenesis using genetically engineered human endothelial cells. *Journal of Controlled Release, 160*(3), 515–524. https://doi.org/10.1016/j.jconrel.2012.03.006
18. Choi, Y. S., Dusting, G. J., Stubbs, S., Arunothayaraj, S., Han, X. L., Collas, P., et al. (2010). Differentiation of human adipose-derived stem cells into beating cardiomyocytes. *Journal of Cellular and Molecular Medicine, 14*(4), 878–889. https://doi.org/10.1111/j.1582-4934.2010.01009.x
19. Chung, C. Y., Bien, H., & Entcheva, E. (2007). The role of cardiac tissue alignment in modulating electrical function. *Journal of Cardiovascular Electrophysiology, 18*(12), 1323–1329. https://doi.org/10.1111/j.1540-8167.2007.00959.x
20. Cook, C. A., Huri, P. Y., Ginn, B. P., Gilbert-Honick, J., Somers, S. M., Temple, J. P., et al. (2016). Characterization of a novel bioreactor system for 3D cellular mechanobiology studies. *Biotechnology and Bioengineering, 113*(8), 1825–1837. https://doi.org/10.1002/bit.25946
21. Costa-Almeida, R., Gomez-Lazaro, M., Ramalho, C., Granja, P. L., Soares, R., & Guerreiro, S. G. (2015). Fibroblast-endothelial partners for vascularization strategies in tissue engineering. *Tissue Engineering. Part A, 21*(5-6), 1055–1065. https://doi.org/10.1089/ten.tea.2014.0443
22. Critser, P. J., & Yoder, M. C. (2010). Endothelial colony-forming cell role in neoangiogenesis and tissue repair. *Current Opinion in Organ Transplantation, 15*, 68. https://doi.org/10.1097/MOT.0b013e32833454b5
23. van der Schaft, D. W. J., van Spreeuwel, A. C. C., van Assen, H. C., & Baaijens, F. P. T. (2011). Mechanoregulation of vascularization in aligned tissue-engineered muscle: A role for vascular endothelial growth factor. *Tissue Engineering. Part A, 17*(21-22), 2857–2865. https://doi.org/10.1089/ten.tea.2011.0214

24. Dvir, T., Kedem, A., Ruvinov, E., Levy, O., Freeman, I., Landa, N., et al. (2009). Prevascularization of cardiac patch on the omentum improves its therapeutic outcome. *Proceedings of the National Academy of Sciences, 106*(35), 14990–14995. https://doi.org/10.1073/pnas.0812242106
25. Eckermann, C. W., Lehle, K., Schmid, S. A., Wheatley, D. N., & Kunz-Schughart, L. A. (2011). Characterization and modulation of fibroblast/endothelial cell co-cultures for the in vitro preformation of three-dimensional tubular networks. *Cell Biology International, 35*(11), 1097–1110. https://doi.org/10.1042/CBI20100718
26. Ehler, E., Moore-Morris, T., & Lange, S. (2013). Isolation and culture of neonatal mouse cardiomyocytes. *Journal of Visualized Experiments, 79*, 1–10. https://doi.org/10.3791/50154
27. Eng, G., Lee, B. W., Protas, L., Gagliardi, M., Brown, K., Kass, R. S., et al. (2016). Autonomous beating rate adaptation in human stem cell-derived cardiomyocytes. *Nature Communications, 7*, 10312. https://doi.org/10.1038/ncomms10312
28. Engler, A. J., Carag-Krieger, C., Johnson, C. P., Raab, M., Tang, H. Y., Speicher, D. W., et al. (2008). Embryonic cardiomyocytes beat best on a matrix with heart-like elasticity: Scar-like rigidity inhibits beating. *Journal of Cell Science, 121*(22), 3794–3802. https://doi.org/10.1242/jcs.029678
29. Feng, Z., Matsumoto, T., Nomura, Y., & Nakamura, T. (2005). An electro-tensile bioreactor for 3-D culturing of cardiomyocytes. *IEEE Engineering in Medicine and Biology Magazine, 24*(4), 73–79. https://doi.org/10.1109/MEMB.2005.1463399
30. Forrester, J. S., White, A. J., Matsushita, S., Chakravarty, T., & Makkar, R. R. (2009). New paradigms of myocardial regeneration post-infarction. Tissue preservation, cell environment, and pluripotent cell sources. *JACC. Cardiovascular Interventions, 2*(1), 1–8. https://doi.org/10.1016/j.jcin.2008.10.010
31. Frangogiannis, N. G. (2015). The inflammatory response in myocardial injury, repair and remodeling. *Nature Reviews Cardiology, 11*(5), 255–265. https://doi.org/10.1038/nrcardio.2014.28
32. Frantz, S., Bauersachs, J., & Ertl, G. (2009). Post-infarct remodelling: Contribution of wound healing and inflammation. *Cardiovascular Research, 81*(3), 474–481. https://doi.org/10.1093/cvr/cvn292
33. Freeman, I., Kedem, A., & Cohen, S. (2008). The effect of sulfation of alginate hydrogels on the specific binding and controlled release of heparin-binding proteins. *Biomaterials, 29*(22), 3260–3268. https://doi.org/10.1016/j.biomaterials.2008.04.025
34. Freiman, A., Shandalov, Y., Rozenfeld, D., Shor, E., Segal, S., Ben-David, D., et al. (2016). Adipose-derived endothelial and mesenchymal stem cells enhance vascular network formation on three-dimensional constructs in vitro. *Stem Cell Research & Therapy, 7*(1), 5. https://doi.org/10.1186/s13287-015-0251-6
35. Gaudesius, G., Miragoli, M., Thomas, S. P., & Rohr, S. (2003). Coupling of cardiac electrical activity over extended distances by fibroblasts of cardiac origin. *Circulation Research, 93*(5), 421–428. https://doi.org/10.1161/01.RES.0000089258.40661.0C
36. George, P. M., Bliss, T. M., Hua, T., Lee, A., Oh, B., Levinson, A., et al. (2017). Electrical preconditioning of stem cells with a conductive polymer scaffold enhances stroke recovery. *Biomaterials, 142*, 31–40. https://doi.org/10.1016/j.biomaterials.2017.07.020
37. Gershlak, J. R., Hernandez, S., Fontana, G., Perreault, L. R., Hansen, K. J., Larson, S. A., et al. (2017). Crossing kingdoms: Using decellularized plants as perfusable tissue engineering scaffolds. *Biomaterials, 125*, 13–22. https://doi.org/10.1016/j.biomaterials.2017.02.011
38. Greiner, A. M., Biela, S. A., Chen, H., Spatz, J. P., & Kemkemer, R. (2015). Featured article: Temporal responses of human endothelial and smooth muscle cells exposed to uniaxial cyclic tensile strain. *Experimental Biology and Medicine, 240*(10), 1298–1309. https://doi.org/10.1177/1535370215570191
39. Gwak, S. J., Bhang, S. H., Kim, I. K., Kim, S. S., Cho, S. W., Jeon, O., et al. (2008). The effect of cyclic strain on embryonic stem cell-derived cardiomyocytes. *Biomaterials, 29*(7), 844–856. https://doi.org/10.1016/j.biomaterials.2007.10.050

40. Hang, J., Kong, L., Gu, J. W., & Adair, T. (1995). VEGF gene expression is upregulated in electrically stimulated rat skeletal muscle. *The American Journal of Physiology, 269*(5), 1827–1831. https://doi.org/10.1152/ajpheart.1995.269.5.H1827
41. Hao, X., Silva, E. A., Månsson-Broberg, A., Grinnemo, K. H., Siddiqui, A. J., Dellgren, G., et al. (2007). Angiogenic effects of sequential release of VEGF-A165 and PDGF-BB with alginate hydrogels after myocardial infarction. *Cardiovascular Research, 75*(1), 178–185. https://doi.org/10.1016/j.cardiores.2007.03.028
42. Hasan, A., Khattab, A., Islam, M. A., Hweij, K. A., Zeitouny, J., Waters, R., et al. (2015). Injectable hydrogels for cardiac tissue repair after myocardial infarction. *Advancement of Science, 2*(11), 1–18. https://doi.org/10.1002/advs.201500122
43. Hirata, M., & Yamaoka, T. (2017). Effect of stem cell niche elasticity/ECM protein on the self-beating cardiomyocyte differentiation of induced pluripotent stem (iPS) cells at different stages. *Acta Biomaterialia, 65*, 44–52. https://doi.org/10.1016/j.actbio.2017.10.032
44. Hirota, A., Fujii, S., & Kamino, K. (1979). Optical monitoring of spontaneous electrical activity of 8-somite embryonic chick heart. *The Japanese Journal of Physiology, 29*(5), 635–639. https://doi.org/10.2170/jjphysiol.29.635
45. Hirt, M. N., Hansen, A., & Eschenhagen, T. (2014). Cardiac tissue engineering : State of the art. *Circulation Research, 114*(2), 354–367. https://doi.org/10.1161/CIRCRESAHA.114.300522
46. Huang, N. F., Niiyama, H., Peter, C., De, A., Natkunam, Y., Fleissner, F., et al. (2010). Embryonic stem cell-derived endothelial cells engraft into the ischemic hindlimb and restore perfusion. *Arteriosclerosis, Thrombosis, and Vascular Biology, 30*(5), 984–991. https://doi.org/10.1161/ATVBAHA.110.202796
47. Hutton, D. L., Logsdon, E. A., Moore, E. M., Mac Gabhann, F., Gimble, J. M., & Grayson, W. L. (2012). Vascular morphogenesis of adipose-derived stem cells is mediated by heterotypic cell-cell interactions. *Tissue Engineering. Part A, 18*(15-16), 1729–1740. https://doi.org/10.1089/ten.TEA.2011.0599
48. Hutton, D. L., Moore, E. M., Gimble, J. M., & Grayson, W. L. (2013). Platelet-derived growth factor and spatiotemporal cues induce development of vascularized bone tissue by adipose-derived stem cells. *Tissue Engineering. Part A, 19*(17-18), 2076–2086. https://doi.org/10.1089/ten.TEA.2012.0752
49. Ikegame, Y., Yamashita, K., Hayashi, S.-I., Mizuno, H., Tawada, M., You, F., et al. (2011). Comparison of mesenchymal stem cells from adipose tissue and bone marrow for ischemic stroke therapy. *Cytotherapy, 13*(6), 675–685. https://doi.org/10.3109/14653249.2010.549122
50. Iyer, R. K., Chiu, L. L. Y., & Radisic, M. (2009). Microfabricated poly(ethylene glycol) templates enable rapid screening of triculture conditions for cardiac tissue engineering. *Journal of Biomedical Materials Research. Part A, 89*(3), 616–631. https://doi.org/10.1002/jbm.a.32014
51. Iyer, R. K., Chui, J., & Radisic, M. (2009). Spatiotemporal tracking of cells in tissue-engineered cardiac organoids. *Journal of Tissue Engineering and Regenerative Medicine, 3*(3), 196–207. https://doi.org/10.1002/term.153
52. Jackman, C. P., Shadrin, I. Y., Carlson, A. L., & Bursac, N. (2015). Human cardiac tissue engineering: From pluripotent stem cells to heart repair. *Current Opinion in Chemical Engineering, 7*, 57–64. https://doi.org/10.1016/j.coche.2014.11.004
53. Jacot, J. G., McCulloch, A. D., & Omens, J. H. (2008). Substrate stiffness affects the functional maturation of neonatal rat ventricular myocytes. *Biophysical Journal, 95*(7), 3479–3487. https://doi.org/10.1529/biophysj.107.124545
54. Kajiya, F., & Goto, M. (1999). Integrative physiology of coronary microcirculation. *The Japanese Journal of Physiology, 49*(3), 229–241. https://doi.org/10.2170/jjphysiol.49.229
55. Kira, Y., Nakaoka, T., Hashimoto, E., Okabe, F., Asano, S., & Sekine, I. (1994). Effect of long-term cyclic mechanical load on protein synthesis and morphological changes in cultured myocardial cells from neonatal rat. *Cardiovascular Drugs and Therapy, 8*, 251–262.
56. Korhonen, T., Hänninen, S. L., & Tavi, P. (2009). Model of excitation-contraction coupling of rat neonatal ventricular myocytes. *Biophysical Journal, 96*(3), 1189–1209. https://doi.org/10.1016/j.bpj.2008.10.026

57. Krishnan, L., Underwood, C. J., Maas, S., Ellis, B. J., Kode, T. C., Hoying, J. B., et al. (2008). Effect of mechanical boundary conditions on orientation of angiogenic microvessels. *Cardiovascular Research, 78*(2), 324–332. https://doi.org/10.1093/cvr/cvn055
58. Kurokawa, Y. K., Yin, R. T., Shang, M. R., Shirure, V. S., Moya, M. L., & George, S. C. (2017). Human induced pluripotent stem cell-derived endothelial cells for three-dimensional microphysiological systems. *Tissue Engineering. Part C, Methods, 23*(8), 474–484. https://doi.org/10.1089/ten.tec.2017.0133
59. Kusuma, S., Shen, Y.-I., Hanjaya-Putra, D., Mali, P., Cheng, L., & Gerecht, S. (2013). Self-organized vascular networks from human pluripotent stem cells in a synthetic matrix. *Proceedings of the National Academy of Sciences, 110*(31), 12601–12606. https://doi.org/10.1073/pnas.1306562110
60. Kwon, C., Arnold, J., Hsiao, E. C., Taketo, M. M., Conklin, B. R., & Srivastava, D. (2007). Canonical Wnt signaling is a positive regulator of mammalian cardiac progenitors. *Proceedings of the National Academy of Sciences of the United States of America, 104*(26), 10894–10899. https://doi.org/10.1073/pnas.0704044104
61. Kwon, C., Qian, L., Cheng, P., Nigam, V., Arnold, J., & Srivastava, D. (2009). A regulatory pathway involving Notch1/β-catenin/Isl1 determines cardiac progenitor cell fate. *Nature Cell Biology, 11*(8), 951–957. https://doi.org/10.1038/ncb1906.A
62. Lesman, A., Gepstein, L., & Levenberg, S. (2010). Vascularization shaping the heart. *Annals of the New York Academy of Sciences, 1188*, 46–51. https://doi.org/10.1111/j.1749-6632.2009.05082.x
63. Lesman, A., Gepstein, L., & Levenberg, S. (2014). Cell tri-culture for cardiac vascularization. *Methods in Molecular Biology, 1181*, 131–137. https://doi.org/10.1007/978-1-4939-1047-2_12
64. Lesman, A., Habib, M., Caspi, O., Gepstein, A., Arbel, G., Levenberg, S., et al. (2010). Transplantation of a tissue-engineered human vascularized cardiac muscle. *Tissue Engineering. Part A, 16*(1), 115–125. https://doi.org/10.1089/ten.TEA.2009.0130
65. Lesman, A., Koffler, J., Atlas, R., Blinder, Y. J., Kam, Z., & Levenberg, S. (2011). Engineering vessel-like networks within multicellular fibrin-based constructs. *Biomaterials, 32*(31), 7856–7869. https://doi.org/10.1016/j.biomaterials.2011.07.003
66. Levenberg, S., Golub, J. S., Amit, M., Itskovitz-Eldor, J., & Langer, R. (2002). Endothelial cells derived from human embryonic stem cells. *Proceedings of the National Academy of Sciences of the United States of America, 99*(7), 4391–4396. https://doi.org/10.1073/pnas.032074999
67. Levenberg, S., Rouwkema, J., Macdonald, M., Garfein, E. S., Kohane, D. S., Darland, D. C., et al. (2005). Engineering vascularized skeletal muscle tissue. *Nature Biotechnology, 23*(7), 879–884. https://doi.org/10.1038/nbt1109
68. Lewandowski, J., Kolanowski, T. J., & Kurpisz, M. (2017). Techniques for the induction of human pluripotent stem cell differentiation towards cardiomyocytes. *Journal of Tissue Engineering and Regenerative Medicine, 11*(5), 1658–1674. https://doi.org/10.1002/term.2117
69. Lian, X., Bao, X., Al-Ahmad, A., Liu, J., Wu, Y., Dong, W., et al. (2014). Efficient differentiation of human pluripotent stem cells to endothelial progenitors via small-molecule activation of WNT signaling. *Stem Cell Reports, 3*(5), 804–816. https://doi.org/10.1016/j.stemcr.2014.09.005
70. Liau, B., Christoforou, N., Leong, K. W., & Bursac, N. (2011). Pluripotent stem cell-derived cardiac tissue patch with advanced structure and function. *Biomaterials, 32*(35), 9180–9187. https://doi.org/10.1016/j.biomaterials.2011.08.050
71. Lin, Y.-L., Chen, C.-P., Lo, C.-M., & Wang, H.-S. (2016). Stiffness-controlled three-dimensional collagen scaffolds for differentiation of human Wharton's jelly mesenchymal stem cells into cardiac progenitor cells. *Journal of Biomedial Materials Research Part A, 104*(9), 2234–2242. https://doi.org/10.1002/jbm.a.35762
72. Lu, L., Mende, M., Yang, X., Körber, H. F., Schnittler, H. J., Weinert, S., et al. (2013). Design and validation of a bioreactor for simulating the cardiac niche: A system incorporating cyclic stretch, electrical stimulation and constant perfusion. *Tissue Engineering. Part A, 19*, 403. https://doi.org/10.1089/ten.TEA.2012.0135

73. Lu, Y., Yu, T., Liang, H., Wang, J., Xie, J., Shao, J., et al. (2014). Nitric oxide inhibits heteroadhesion of cancer cells to endothelial cells: Restraining circulating tumor cells from initiating metastatic cascade. *Scientific Reports, 4*, 1–9. https://doi.org/10.1038/srep04344
74. Lundy, S. D., Zhu, W., Regnier, M., & Laflamme, M. A. (2013). Structural and functional maturation of cardiomyocytes derived from human pluripotent stem cells. *Stem Cells and Development, 22*(14), 1991. https://doi.org/10.1089/scd.2012.0490
75. Mandel, Y., Manivanh, R., Dalal, R., Huie, P., Wang, J., Brinton, M., et al. (2013). Vasoconstriction by electrical stimulation: New approach to control of non-compressible hemorrhage. *Scientific Reports, 3*, 1–7. https://doi.org/10.1038/srep02111
76. Merfeld-Clauss, S., Gollahalli, N., March, K. L., & Traktuev, D. O. (2010). Adipose tissue progenitor cells directly interact with endothelial cells to induce vascular network formation. *Tissue Engineering. Part A, 16*(9), 2953–2966. https://doi.org/10.1089/ten.tea.2009.0635
77. Merfeld-Clauss, S., Lupov, I. P., Lu, H., Feng, D., Compton-Craig, P., March, K. L., et al. (2014). Adipose stromal cells differentiate along a smooth muscle lineage pathway upon endothelial cell contact via induction of activin A. *Circulation Research, 115*(9), 800–809. https://doi.org/10.1161/CIRCRESAHA.115.304026
78. Miklas, J. W., Nunes, S. S., Sofla, A., Reis, L. A., Pahnke, A., Xiao, Y., et al. (2014). Bioreactor for modulation of cardiac microtissue phenotype by combined static stretch and electrical stimulation. *Biofabrication, 6*(2), 1–27. https://doi.org/10.1088/1758-5082/6/2/024113
79. Montgomery, M., Ahadian, S., Davenport Huyer, L., Lo Rito, M., Civitarese, R. A., Vanderlaan, R. D., et al. (2017). Flexible shape-memory scaffold for minimally invasive delivery of functional tissues. *Nature Materials, 16*(10), 1038. https://doi.org/10.1038/nmat4956
80. Montgomery, M., Jiao, Y., Phillips, S., Singh, G., Xu, J., Balsara, R., et al. (1998). Alterations in sheep fetal right ventricular tissue with induced hemodynamic pressure overload. *Basic Research in Cardiology, 93*(3), 192–200.
81. Morgan, K. Y., & Black, L. D. (2014). Mimicking isovolumic contraction with combined electromechanical stimulation improves the development of engineered cardiac constructs. *Tissue Engineering. Part A, 20*(11-12), 1654–1667. https://doi.org/10.1089/ten.tea.2013.0355
82. Morrissette-Mcalmon, J., Blazeski, A., Somers, S., Kostecki, G., Tung, L., & Grayson, W. L. (2018). Adipose-derived perivascular mesenchymal stromal/stem cells promote functional vascular tissue engineering for cardiac regenerative purposes. *Journal of Tissue Engineering and Regenerative Medicine, 12*, e962. https://doi.org/10.1002/term.2418
83. Naito, A. T., Shiojima, I., Akazawa, H., Hidaka, K., Morisaki, T., Kikuchi, A., et al. (2006). Developmental stage-specific biphasic roles of Wnt/beta-catenin signaling in cardiomyogenesis and hematopoiesis. *Proceedings of the National Academy of Sciences, 103*(52), 19812–19817. https://doi.org/10.1073/pnas.0605768103
84. Nunes, S. S., Miklas, J. W., Liu, J., Aschar-Sobbi, R., Xiao, Y., Zhang, B., et al. (2013). Biowire: A platform for maturation of human pluripotent stem cell-derived cardiomyocytes. *Nature Methods, 10*(8), 781–787. https://doi.org/10.1038/nmeth.2524
85. Ong, C. S., Fukunishi, T., Zhang, H., Huang, C. Y., Nashed, A., Blazeski, A., et al. (2017). Biomaterial-free three-dimensional bioprinting of cardiac tissue using human induced pluripotent stem cell derived cardiomyocytes. *Scientific Reports, 7*(1), 2–12. https://doi.org/10.1038/s41598-017-05018-4
86. Ott, H. C., Matthiesen, T. S., Goh, S.-K., Black, L. D., Kren, S. M., Netoff, T. I., et al. (2008). Perfusion-decellularized matrix: Using nature's platform to engineer a bioartificial heart. *Nature Medicine, 14*(2), 213–221. https://doi.org/10.1038/nm1684
87. Park, H.-J., Zhang, Y., Georgescu, S. P., Johnson, K. L., Kong, D., & Galper, J. B. (2006). Human umbilical vein endothelial cells and human dermal microvascular endothelial cells offer new insights into the relationship between lipid metabolism and angiogenesis. *Stem Cell Reviews, 2*(2), 93–101. https://doi.org/10.1007/s12015-006-0015-x
88. Pedrotty, D. M., Klinger, R. Y., Kirkton, R. D., & Bursac, N. (2009). Cardiac fibroblast paracrine factors alter impulse conduction and ion channel expression of neonatal rat cardiomyocytes. *Cardiovascular Research, 83*(4), 688–697. https://doi.org/10.1093/cvr/cvp164

89. Pietronave, S., Zamperone, A., Oltolina, F., Colangelo, D., Follenzi, A., Novelli, E., et al. (2014). Monophasic and biphasic electrical stimulation induces a precardiac differentiation in progenitor cells isolated from human heart. *Stem Cells and Development, 23*(8), 888–898. https://doi.org/10.1089/scd.2013.0375
90. Pill, K., Hofmann, S., Redl, H., & Holnthoner, W. (2015). Vascularization mediated by mesenchymal stem cells from bone marrow and adipose tissue: A comparison. *Cell Regeneration, 4*(1), 1–10. https://doi.org/10.1186/s13619-015-0025-8
91. Porter, K. E., & Turner, N. A. (2009). Cardiac fibroblasts: At the heart of myocardial remodeling. *Pharmacology & Therapeutics, 123*(2), 255–278. https://doi.org/10.1016/j.pharmthera.2009.05.002
92. Radisic, M., Fast, V. G., Sharifov, O. F., Iyer, R. K., Park, H., & Vunjak-Novakovic, G. (2009). Optical mapping of impulse propagation in engineered cardiac tissue. *Tissue Engineering. Part A, 15*(4), 851–860. https://doi.org/10.1089/ten.tea.2008.0223
93. Radisic, M., Park, H., Shing, H., Consi, T., Schoen, F. J., Langer, R., et al. (2004). Functional assembly of engineered myocardium by electrical stimulation of cardiac myocytes cultured on scaffolds. *Proceedings of the National Academy of Sciences, 101*(52), 18129–18134. https://doi.org/10.1073/pnas.0407817101
94. Rakusan, K., Flanagan, M. F., Geva, T., Southern, J., & Van Praagh, R. (1992). Morphometry of human coronary capillaries during normal growth and the effect of age in left ventricular pressure-overload hypertrophy. *Circulation, 86*(1), 38–46. https://doi.org/10.1161/01.CIR.86.1.38
95. Rao, R. R., Peterson, A. W., Ceccarelli, J., Putnam, A. J., & Stegemann, J. P. (2012). Matrix composition regulates three-dimensional network formation by endothelial cells and mesenchymal stem cells in collagen/fibrin materials. *Angiogenesis, 15*(2), 253–264. https://doi.org/10.1007/s10456-012-9257-1
96. Riemenschneider, S. B., Mattia, D. J., Wendel, J. S., Schaefer, J. A., Ye, L., Guzman, P. A., et al. (2016). Inosculation and perfusion of pre-vascularized tissue patches containing aligned human microvessels after myocardial infarction. *Biomaterials, 36*(5), 1011–1014. https://doi.org/10.1016/j.biomaterials.2016.04.031
97. Riemenschneider, S. B., Mattia, D. J., Wendel, J. S., Schaefer, J. A., Ye, L., Guzman, P. A., et al. (2016). Inosculation and perfusion of pre-vascularized tissue patches containing aligned human microvessels after myocardial infarction. *Biomaterials, 97*, 51–61. https://doi.org/10.1016/j.biomaterials.2016.04.031
98. Robertson, C., Tran, D., & George, S. (2013). Concise review: Maturation phases of human pluripotent stem cell-derived cardiomyocytes. *Stem Cells, 31*(5), 1–17. https://doi.org/10.1002/stem.1331
99. Ruvinov, E., Leor, J., & Cohen, S. S. (2010). The effects of controlled HGF delivery from an affinity-binding alginate biomaterial on angiogenesis and blood perfusion in a hindlimb ischemia model. *Biomaterials, 31*(16), 4573–4582. https://doi.org/10.1016/j.biomaterials.2010.02.026
100. Schaaf, S., Eder, A., Vollert, I., Stöhr, A., Hansen, A., & Eschenhagen, T. (2014). Generation of strip-format fibrin-based engineered heart tissue (EHT). *Methods in Molecular Biology, 1181*, 121–129. https://doi.org/10.1007/978-1-4939-1047-2_11
101. Schaefer, J. A., Guzman, P. A., Riemenschneider, S. B., Kamp, T. J., & Tranquillo, R. T. (2018). A cardiac patch from aligned microvessel and cardiomyocyte patches. *Journal of Tissue Engineering and Regenerative Medicine, 12*, 546. https://doi.org/10.1002/term.2568
102. Schenke-Layland, Y. K., Strem, B. M., Deemedio, M. T., Hedrick, M. H., Roos, K. P., et al. (2010). Adipose tissue-derived cells improve cardiac function following myocardial infarction. *The Journal of Surgical Research, 153*(2), 217–223. https://doi.org/10.1016/j.jss.2008.03.019
103. Shadrin, I. Y., Allen, B. W., Qian, Y., Jackman, C. P., Carlson, A. L., Juhas, M. E., et al. (2017). Cardiopatch platform enables maturation and scale-up of human pluripotent stem cell-derived engineered heart tissues. *Nature Communications, 8*(1), 1825. https://doi.org/10.1038/s41467-017-01946-x

104. Shen, Y. H., Shoichet, M. S., & Radisic, M. (2008). Vascular endothelial growth factor immobilized in collagen scaffold promotes penetration and proliferation of endothelial cells. *Acta Biomaterialia, 4*(3), 477–489. https://doi.org/10.1016/j.actbio.2007.12.011
105. Shen, Y. I., Cho, H., Papa, A. E., Burke, J. A., Chan, X. Y., Duh, E. J., et al. (2016). Engineered human vascularized constructs accelerate diabetic wound healing. *Biomaterials, 102*, 107–119. https://doi.org/10.1016/j.biomaterials.2016.06.009
106. Shimko, V. F., & Claycomb, W. C. (2008). Effect of mechanical loading on three-dimensional cultures of embryonic stem cell-derived cardiomyocytes. *Tissue Engineering. Part A, 14*(1), 49–58. https://doi.org/10.1089/ten.a.2007.0092
107. Sieminski, A. L., Hebbel, R. P., & Gooch, K. J. (2004). The relative magnitudes of endothelial force generation and matrix stiffness modulate capillary morphogenesis in vitro. *Experimental Cell Research, 297*(2), 574–584. https://doi.org/10.1016/j.yexcr.2004.03.035
108. Sinha, R., Le Gac, S., Verdonschot, N., Van Den Berg, A., Koopman, B., & Rouwkema, J. (2016). Endothelial cell alignment as a result of anisotropic strain and flow induced shear stress combinations. *Scientific Reports, 6*, 29510. https://doi.org/10.1038/srep29510
109. Souders, C. A., Bowers, S. L. K., & Baudino, T. A. (2009). Cardiac fibroblast: The renaissance cell. *Circulation Research, 105*(12), 1164–1176. https://doi.org/10.1161/CIRCRESAHA.109.209809
110. Steffens, G. C. M., Yao, C., Prével, P., Markowicz, M., Schenck, P., Noah, E. M., et al. (2004). Modulation of angiogenic potential of collagen matrices by covalent incorporation of heparin and loading with vascular endothelial growth factor. *Tissue Engineering, 10*(9-10), 1502–1509. https://doi.org/10.1089/ten.2004.10.1502
111. Stevens, K. R., Kreutziger, K. L., Dupras, S. K., Korte, F. S., Regnier, M., Muskheli, V., et al. (2009). Physiological function and transplantation of scaffold-free and vascularized human. *Proceedings of the National Academy of Sciences of the United States of America, 106*(39), 16568.
112. Sun, X., & Nunes, S. S.. (2017). Maturation of human stem cell-derived cardiomyocytes in biowires using electrical stimulation. *Journal of Visualized Experiments*, (123), 1–8. doi:https://doi.org/10.3791/55373.
113. Sun, X., & Nunes, S. S. (2017). Bioengineering approaches to mature human pluripotent stem cell-derived cardiomyocytes. *Frontiers in Cell and Development Biology, 5*, 19. https://doi.org/10.3389/fcell.2017.00019
114. Taber, L. A. (1998). Mechanical aspects of cardiac development. *Progress in Biophysics and Molecular Biology, 69*, 237–255.
115. Tandon, N., Cannizzaro, C., Chao, P.-H. G., Maidhof, R., Marsano, A., Au, H. T., et al. (2009). Electrical stimulation systems for cardiac tissue engineering. *Nature Protocols, 4*(2), 155–173. https://doi.org/10.1038/nprot.2008.183
116. Thompson, S. A., Copeland, C. R., Reich, D. H., & Tung, L. (2011). Mechanical coupling between myofibroblasts and cardiomyocytes slows electric conduction in fibrotic cell monolayers. *Circulation, 123*(19), 2083–2093. https://doi.org/10.1161/CIRCULATIONAHA.110.015057
117. Thomson, K. S., Korte, F. S., Giachelli, C. M., Ratner, B. D., Regnier, M., & Scatena, M. (2013). Prevascularized microtemplated fibrin scaffolds for cardiac tissue engineering applications. *Tissue Engineering. Part A, 19*(7-8), 967–977. https://doi.org/10.1089/ten.tea.2012.0286
118. Topper, J. N., & Gimbrone Jr., M. A. (1999). Blood flow and vascular gene expression: Fluid shear stress as a modulator of endothelial phenotype. *Molecular Medicine Today, 5*(1), 40–46. https://doi.org/10.1016/S1357-4310(98)01372-0
119. Tulloch, N. L., Muskheli, V., Razumova, M. V., Korte, F. S., Regnier, M., Hauch, K. D., et al. (2011). Growth of engineered human myocardium with mechanical loading and vascular Coculture. *Circulation Research, 109*, 47–59. https://doi.org/10.1161/CIRCRESAHA.110.237206

120. Twardowski, R. L., & Black, L. D. (2014). Cardiac fibroblasts support endothelial cell proliferation and sprout formation but not the development of multicellular sprouts in a fibrin gel co-culture model. *Annals of Biomedical Engineering, 42*(5), 1074–1084. https://doi.org/10.1007/s10439-014-0971-2
121. Underwood, C. J., Edgar, L. T., Hoying, J. B., & Weiss, J. A. (2014). Cell-generated traction forces and the resulting matrix deformation modulate microvascular alignment and growth during angiogenesis. *American Journal of Physiology. Heart and Circulatory Physiology, 307*(2), H152–H164. https://doi.org/10.1152/ajpheart.00995.2013
122. Valarmathi, M. T., Fuseler, J. W., Davis, J. M., & Price, R. L. (2017). A novel human tissue-engineered 3-D functional vascularized cardiac muscle construct. *Frontiers in Cell and Development Biology, 5*, 1–24. https://doi.org/10.3389/fcell.2017.00002
123. Veerman, C. C., Kosmidis, G., Mummery, C. L., Casini, S., Verkerk, A. O., & Bellin, M. (2015). Immaturity of human stem-cell-derived cardiomyocytes in culture: Fatal flaw or soluble problem? *Stem Cells and Development, 24*(9), 1035–1052. https://doi.org/10.1089/scd.2014.0533
124. Verseijden, F., Posthumus-van Sluijs, S. J., Pavljasevic, P., Hofer, S. O. P., van Osch, G. J. V. M., & Farrell, E. (2010). Adult human bone marrow- and adipose tissue-derived stromal cells support the formation of prevascular-like structures from endothelial cells in vitro. *Tissue Engineering. Part A, 16*(1), 101–114. https://doi.org/10.1089/ten.TEA.2009.0106
125. Vunjak-Novakovic, G., Tandon, N., Godier, A., Maidhof, R., Marsano, A., Martens, T. P., et al. (2010). Challenges in cardiac tissue engineering. *Tissue Engineering Part B: Reviews, 16*(2), 169.
126. Wang, B., Wang, G., To, F., Butler, J. R., Claude, A., McLaughlin, R. M., et al. (2013). Myocardial scaffold-based cardiac tissue engineering: Application of coordinated mechanical and electrical stimulations. *Langmuir, 29*(35), 11109–11117. https://doi.org/10.1021/la401702w
127. Weinberger, F., Mannhardt, I., & Eschenhagen, T. (2017). Engineering cardiac muscle tissue: A maturating field of research. *Circulation Research, 120*(9), 1487–1500. https://doi.org/10.1161/CIRCRESAHA.117.310738
128. Wendel, J. S., Ye, L., Tao, R., Zhang, J., Zhang, J., Kamp, T. J., et al. (2015). Functional effects of a tissue-engineered cardiac patch from human induced pluripotent stem cell-derived cardiomyocytes in a rat infarct model. *Stem Cells Translational Medicine, 4*(11), 1324–1332. https://doi.org/10.5966/sctm.2015-0044
129. Wilson, C. J., Kasper, G., Schütz, M. A., & Duda, G. N. (2009). Cyclic strain disrupts endothelial network formation on Matrigel. *Microvascular Research, 78*(3), 358–363. https://doi.org/10.1016/j.mvr.2009.08.002
130. Wu, P. K., & Ringeisen, B. R. (2010). Development of human umbilical vein endothelial cell (HUVEC) and human umbilical vein smooth muscle cell (HUVSMC) branch/stem structures on hydrogel layers via biological laser printing (BioLP). *Biofabrication, 2*(1), 014111. https://doi.org/10.1088/1758-5082/2/1/014111
131. Xiong, Q., Hill, K. L., Li, Q., Suntharalingam, P., Mansoor, A., Wang, X., et al. (2011). A fibrin patch-based enhanced delivery of human embryonic stem cell-derived vascular cell transplantation in a porcine model of postinfarction left ventricular remodeling. *Stem Cells, 29*(2), 367–375. https://doi.org/10.1002/stem.580
132. Yamazaki, T., Komuro, I., & Yazaki, Y. (1995). Molecular mechanisms of cardiac cellular hypertrophy by mechanical stress. *Journal of Molecular and Cellular Cardiology, 27*, 133–140.
133. Yang, X., Pabon, L., & Murry, C. E. (2014). Engineering adolescence: Maturation of human pluripotent stem cell-derived cardiomyocytes. *Circulation Research, 114*(3), 511–523. https://doi.org/10.1161/CIRCRESAHA.114.300558
134. Ye, L., Chang, Y.-H., Xiong, Q., Zhang, P., Zhang, L., Somasundaram, P., et al. (2014). Cardiac repair in a porcine model of acute myocardial infarction with human induced pluripotent stem cell-derived cardiovascular cell populations. *Cell Stem Cell, 15*(6), 750–761. https://doi.org/10.1016/j.stem.2014.11.009

135. Yoder, M. C. (2015). Differentiation of pluripotent stem cells into endothelial cells. *Current Opinion in Hematology, 22*(3), 252–257. https://doi.org/10.1097/MOH.0000000000000140
136. Young, J. L., & Engler, A. J. (2011). Hydrogels with time-dependent material properties enhance cardiomyocyte differentiation in vitro. *Biomaterials, 32*(4), 1002–1009. https://doi.org/10.1016/j.biomaterials.2010.10.020
137. Yuasa, S., Itabashi, Y., Koshimizu, U., Tanaka, T., Sugimura, K., Kinoshita, M., et al. (2005). Transient inhibition of BMP signaling by Noggin induces cardiomyocyte differentiation of mouse embryonic stem cells. *Nature Biotechnology, 23*(5), 607–611. https://doi.org/10.1038/nbt1093
138. Zhang, B., Montgomery, M., Chamberlain, M. D., Ogawa, S., Korolj, A., Pahnke, A., et al. (2016). Biodegradable scaffold with built-in vasculature for organ-on-a-chip engineering and direct surgical anastomosis. *Nature Materials, 15*(6), 669–678. https://doi.org/10.1038/nmat4570
139. Zhang, J., Chu, L.-F., Hou, Z., Schwartz, M. P., Hacker, T., Vickerman, V., et al. (2017). Functional characterization of human pluripotent stem cell-derived arterial endothelial cells. *Proceedings of the National Academy of Sciences, 114*, E6072. https://doi.org/10.1073/pnas.1702295114
140. Zhang, S., Liu, X., Barreto-Ortiz, S. F., Yu, Y., Ginn, B. P., DeSantis, N. A., et al. (2014). Creating polymer hydrogel microfibres with internal alignment via electrical and mechanical stretching. *Biomaterials, 35*(10), 3243–3251. https://doi.org/10.1016/j.biomaterials.2013.12.081
141. Zhao, M., Bai, H., Wang, E., Forrester, J. V., & McCaig, C. D. (2004). Electrical stimulation directly induces pre-angiogenic responses in vascular endothelial cells by signaling through VEGF receptors. *Journal of Cell Science, 117*(3), 397–405. https://doi.org/10.1242/jcs.00868

Chapter 7
Pro-Angiogenic Regenerative Therapies for the Damaged Brain: A Tissue Engineering Approach

Lina R. Nih, Stanley T. Carmichael, and Tatiana Segura

7.1 Introduction

According to the American Heart Association, 15 million people suffer ischemic stroke worldwide each year [5]. Of these, five million die and five million are permanently disabled. These sobering statistics demonstrate stroke's global impact and emphasize the importance of deepening our understanding in order to design efficient treatments. To date, the overwhelming majority of brain repair research focuses on developing therapies that promote tissue repair through neuronal replacement with neuronal-derived progenitor cell transplantation or pro-neuronal drugs administration [23]. However, extensive and unsuccessful clinical trials show that this approach does not lead to long-term development of all brain cell types or the establishment of functional interactions between the different networks. Both experimental and clinical studies have reported that angiogenesis and neurogenesis in the ischemic brain work in tandem [26] and that enhanced vessel formation and restored perfusion after stroke reduces the severity of damage [31], promotes tissue repair [24], and significantly extends survival of stroke patients [20]. Therefore, developing pro-angiogenic regenerative therapies offers tremendous potential in stroke treatment. Preclinical studies using provascular growth factor and progenitor cells show promising results in enhancing revascularization and tissue repair after stroke. The therapeutic outcome, however, is often limited by poor survival of

L. R. Nih (✉) · S. T. Carmichael
Department of Neurology, David Geffen School of Medicine,
University of California, Los Angeles, CA, USA
e-mail: lnih@ucla.edu; Scarmichael@mednet.ucla.edu

T. Segura (✉)
Department of Biomedical Engineering, Neurology, Dermatology, Pratt School of Engineering, Duke University, Durham, NC, USA
e-mail: tatiana.segura@duke.edu

S. Gerecht (ed.), *Biophysical Regulation of Vascular Differentiation and Assembly*, Biological and Medical Physics, Biomedical Engineering,
https://doi.org/10.1007/978-3-319-99319-5_7

transplanted cells, uncontrolled cell differentiation, non-sustained delivery of growth factors, and ineffective engraftment with the host tissue. A tissue engineering approach provides an alternative for treating the damaged brain, as it provides multifunctional solutions to overcome the limitations of conventional approaches. In this chapter, we focus on the limitations of current pro-angiogenic therapies using vascular growth factors and some recent advances using engineered biomaterials and drug delivery systems for brain tissue repair.

7.2 The Neurovascular Damage after Stroke

The neuron has traditionally been viewed as the centerpiece of the mammalian central nervous system (CNS) because of its fundamental role in neurotransmission. Thus, the classical approach of neurorepair was solely based on neuroprotection and neuron cell replacement. Over the past decade, remarkable advances have been made in understanding the mechanisms of neurorepair, such as neurogenesis (formation of new neurons), angiogenesis (formation of new blood vessels), gliogenesis (formation of new glial cells), and re-myelinization, among other processes. These discoveries changed the classical view of brain repair, providing greater understanding of the brain as a whole and supporting the hypothesis that saving neurons alone may not be sufficient [8]. This concept of a "neurovascular unit" defines tissue remodeling as a highly dynamic process between vascular, neuronal, and glial cells. After stroke, these cells respond to injury in a coordinated and synergistic manner, releasing molecular signals and trophic factors that mutually influence each other to create a pro-repair environment where tissue regeneration and neurological recovery may take place [32]. In recent years, the promotion of vascular growth and remodeling in the injured brain is increasingly recognized as a particularly promising approach to treat brain illnesses [9]. This approach has brought confidence that stimulating the growth of new vessels both in and around the ischemic site may stabilize brain perfusion and promote tissue repair through neuronal survival, plasticity, and functional recovery [13, 14, 18].

7.3 Spatiotemporal Dynamic of Brain Angiogenesis

At the core of an ischemic incident, the severe energy and glucose loss induces a rapid neuronal death, leaving behind a necrotic site within minutes after the stroke onset. However, the surrounding area, called penumbra, has a mild-to-moderate vascular compromise, where the energy deficit is less severe and collateral vessels maintain a certain degree of blood flow (Fig. 7.1).

This area may be rescued if blood flow is restored [10]. Increasing evidence, in both human stroke patients and animal experimental models, suggests that angiogenesis occurs in those penumbra areas [28]. Indeed, an increasing body of evidence

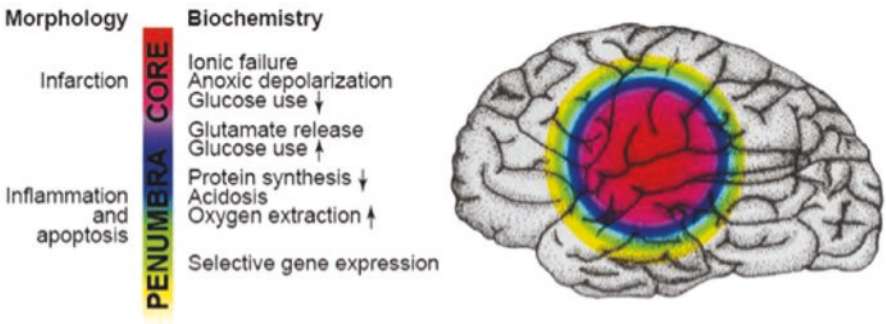

Fig. 7.1 Schematic of the human brain with the core of the ischemic core and the penumbra. Figure reprinted from [10] with the permission from Elsevier

suggests that newly formed vessels in the periphery of the injured site mediate recovery via the activation of endogenous mechanisms of plasticity [7]. In particular, it was shown that angiogenesis and neurogenesis not only work in tandem but are also causally linked. The daily administration of an angiogenesis inhibitor, in a mouse model of ischemic stroke, is associated with a significant reduction of proliferation, migration, and differentiation of endogenous neural progenitors which impairs their functional recovery [24, 26]. In addition, aggregate data supports a "cleanup hypothesis," whereby the newly formed vessels in the penumbra serve to facilitate macrophage infiltration and clear up necrotic debris [22, 37].

7.4 Role of VEGF in Endogenous Angiogenesis

In both experimental and clinical studies, enhanced vessel formation and restored perfusion in the ischemic border correlate with improved long-term recovery and longer survival times [20]. Older patients, who tend to do worse after stroke, often show reduced new vessel formation in the penumbra [2, 12, 34]. Similarly, patients who develop dementia after stroke have reduced blood flow in cortical regions adjacent to the stroke [30]. Pro-repair factors correlated with brain angiogenesis have also been extensively assessed in experimental stroke models. One major endogenous signal, vascular endothelial growth factor (VEGF) is found in both neurons and astrocytes after cerebral ischemia [1, 39]. A positive correlation was found between the severity of damages and the concentration of VEGF in stroke patients [31]. Likewise, postmortem studies reveal an increased expression of the pro-angiogenic factor and its receptor VEGFR-2, both at mRNA and protein levels in the penumbra [17]. In addition, studies have shown that a deficit in VEGF distribution is associated with disorganized and impaired vessel formation, suggesting that ECM-binding VEGF isoforms provide essential stimulatory cues to initiate vessel branching [29].

7.5 Current VEGF-Based Therapeutic Approach

Interestingly, studies with therapeutic VEGF application revealed quite different effects, depending on the timing of administration and the route of growth factor delivery. The systemic or intracerebral administration of VEGF, within the first 48 h after stroke onset, was associated with an increased blood-brain barrier opening and subsequent edema and promoted the formation of disorganized and immature vasculature [39]. Likewise, the early administration of an antagonist for endogenous VEGF reduced the ischemia−/reperfusion-related brain edema and injury [35]. Similarly, infusing VEGF into the lateral ventricles stimulated angiogenesis and decreased infarct volume in rodent models of cerebral ischemia [33]. In transgenic mice overexpressing human VEGF 165, brain microvessel density was significantly increased, compared to wild-type before and after ischemia [36]. In addition, VEGF is associated with a reduced infarct volume when topically applied on the surface of the reperfusion site in a transient model of cerebral ischemia [15]. A completely different picture resulted from studies where VEGF was administered repeatedly [33], in delayed delivery (after day 3) [16] or when the growth factor was encapsulated in a hydrogel [11]. These studies consistently found improvement in neurological deficits following VEGF therapy, along with a reduction in ischemic injury, brain edema, and blood-brain barrier permeability for serum proteins, with an overall better effect when administered locally rather than systemically [21]. This suggests that maintaining elevated tissue levels of VEGF in the stroke site, for prolonged periods of time along with controllable spatial distribution, dosage, and duration of exposure, satisfies many of the characteristics of an ideal delivery system, by overcoming the main limitations of poor penetration across the blood-brain barrier, the clinically unviable option of repeated local injections, and the short VEGF half-life time.

7.6 Tissue Engineering Approach to Promote Brain Angiogenesis

Recent advances in our understanding of the central nervous system and the development of sophisticated biomaterials have significantly changed the landscape for developing strategies to repair the damaged brain. Tissue engineering approaches now offer the potential to design biomaterials tailored for particular applications such as hydrogels to fill out the stroke site, where necrotic tissue gives place to an empty compartmentalized cavity. These biomaterials offer a physical support for cell infiltration in a highly inflamed and damaged tissue, and present the ability to protect and enhance the beneficial effect of provascular growth factors, known to have a short half-life time and severe side effects due to its ability to promote vascular permeability [39]. Developing engineered pro-repair approaches is a scientific challenge on many levels, since (1) therapeutic agents must remain alive/active

during and after brain transplantation, (2) the success of a therapy is widely dependent on the interaction between the transplanted/injected material and the host tissue, (3) the material degradation rate and composition must be finely tuned to allow tissue growth, and (4) the success of a pro-repair therapy relies on the simultaneous activation of axonal sprouting, vascular growth, neurogenesis, and modulation of the injury-induced inflammation, each presenting unique biological challenges.

In recent years, several experimental studies developed injectable hydrogels and growth factor delivery systems to promote poststroke angiogenesis through VEGF administration. A 2010 study from Emerich D.F. et al. describes the effect of an injectable VEGF-loaded alginate-based hydrogel on poststroke functional recovery [11]. Behavioral testing shows that the performance of rats, receiving VEGF gels in the striatum 15 min prior to stroke, was significantly improved relative to a blank gel with or without VEGF. This study strengthens previous evidence that VEGF exerts neuroprotective properties when upregulated prior to injury.

Zhang et al. attempt to restore tissue integrity in a rat model of brain damage by implanting a porous polydimethylsiloxane-tetraethoxysilane (PDMS-TEOS) hybrid with or without VEGF [38]. Despite a low infiltration of vessels in the injected materials, the VEGF-loaded gel was associated with a significant increase of proliferating endothelial cells within the implanted material (Fig. 7.2). However, the use of a non-injectable material does not meet the clinical need for a minimally invasive therapy.

A similar approach was used by Ju et al. with a hyaluronic acid (HA)-based hydrogel mixed with poly(lactic-co-glycolic) acid (PLGA) microspheres containing VEGF and angiopoietin-1 [19]. The authors report that the implantation of the HA-PLGA composite in the cortical lesion significantly increased blood vessel density and reduced inflammation in the peri-infarct. Although this material demonstrated potential for promoting angiogenesis, the HA-PLGA composite's non-injectability reduces its potential for clinical translation. Interestingly, an injection of the same VEGF-releasing PLGA particles in the stroke cavity was associated with poor vascular effect, suggesting that the presence of a matrix-derived scaffold is required to provide a structural support to growing vessels [6]. Recently, Oshikawa

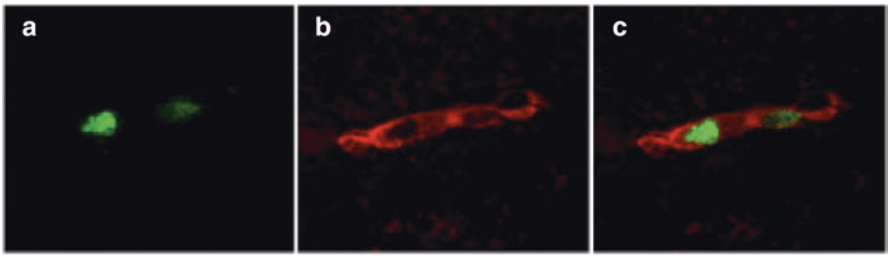

Fig. 7.2 Transplantation of a porous PDMS-TEOS material with VEGF in a rat model of cortical brain damage. Double immunofluorescence study showing proliferating cells (**a**) endothelial cells (**b**) and a merge image of both stainings (**c**) within the implanted material. Figure reprinted from [38] with the permission from Elsevier

et al. developed an implantable porous laminin-based sponge material that immobilizes histidine-tagged VEGF via affinity interactions [27]. The authors report that the laminin-VEGF transplantation into the injured cortex significantly increased vessel density in and around the transplant, compared with laminin gel with and without soluble VEGF. However, this non-injectable material is invasive and would require further modification to be clinically translatable.

In order to fill the need for an injectable scaffold that provides both structural support and delivers multiple provascular factors in a sustained manner, we developed a delivery system where VEGF is encapsulated in protease-specific, cleavable peptides, in which degradation rate controls the VEGF release in the brain [40]. We showed that the combination of VEGF nanocapsules and HA hydrogel with fibronectin-derived RGD peptide can be injected directly into the stroke cavity, which promotes greater vessel formation and pericyte recruitment, in and around the lesion site, compared with empty HA and HA + soluble VEGF (Fig. 7.3).

Recently, we showed that displaying VEGF in a clustered conformation by immobilizing covalently the growth factor on nanoparticles of heparin and controlling the discrete distribution on the particle's surface modulates vascular sprouting and endothelial proliferation in vitro [4]. In addition, the severe inflammatory response after stroke is widely regarded as the cause that impedes axonal growth in the damaged central nervous system [3]. Thus, we hypothesized that the brain administration of a dual-function engineered biomaterial with both immunomodulatory and angiogenic properties, directly to the stroke cavity, can promote tissue formation de novo by modulating poststroke inflammatory response and vessel growth. For this, male adult mice were subjected to an ischemic stroke and injected with a hyaluronic acid-based hydrogel containing heparin nanoparticles and different clusterization densities of bound VEGF onto heparin particle's surface [25]. We found that the highly clustered VEGF lead to the highest degree of vascular growth in and around the stroke site (Fig. 7.4). Moreover, the addition of naked heparin particles generates a vascularized network of regenerated functional axonal connections that leads to recovery and reduces the poststroke inflammation. These results are lost with the absence or reduction of bound VEGF where only the immunomodulator effect is observed and with the absence or reduction of heparin particles where angiogenesis is no longer associated with axonal sprouting.

7.7 Conclusion

The use of pro-angiogenic materials, for focal and controlled delivery of vascular growth factors to the brain, is an emerging discipline in the field of brain repair. Although these materials have demonstrated potential in activating endogenous endothelial cells in and around the damaged tissue, their ability to form vascular structure de novo in the injected site is limited. Future work in this area needs to

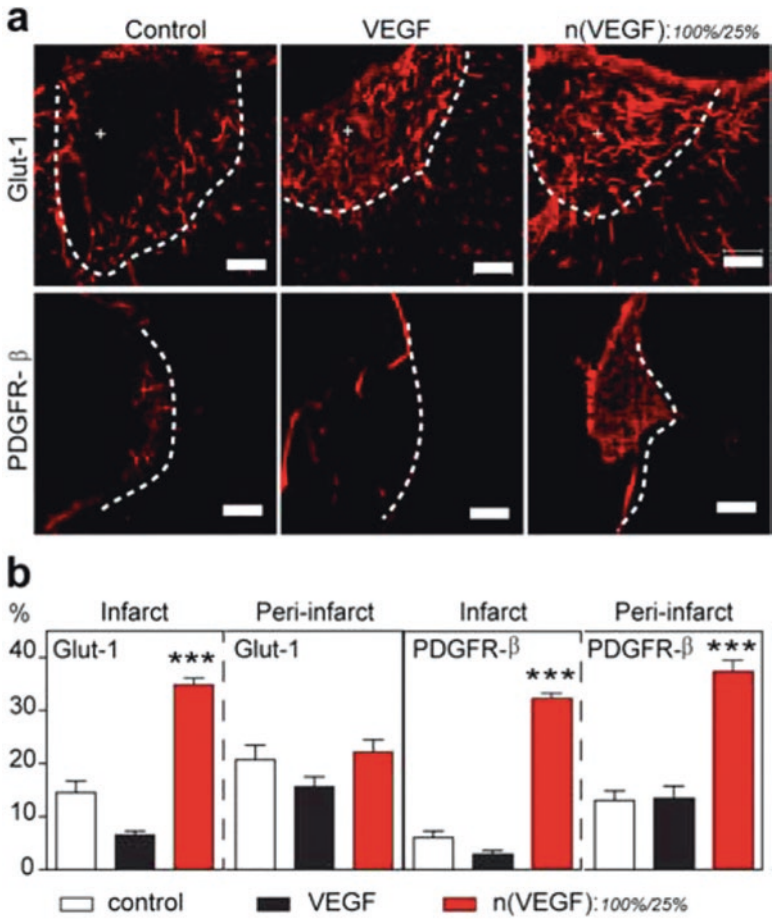

Fig. 7.3 Temporal control of HA-VEGF nanocapsule delivery in a mouse model of ischemic stroke. (**a**) Representative fluorescent images of blood vessels (Glut-1) and pericytes (PDGFR-β) in (+) and around the lesion site injected with HA-RGD alone (control), with soluble VEGF (VEGF), or with nanocapsules of VEGF (n(VEGF)) and (**b**) quantitative analysis. Anova with Tukey test's posttest, mean ± SEM. $*p < 0.05$, $**p < 0.01$, $***p < 0.001$. Scale bars = 100 μm. Figure reprinted from [40] with the permission from Elsevier

focus on fine-tuning the optimal morphological features and to design macro- and microarchitecture that mimics the native matrix and environment. In addition, these materials would be best as an injectable therapy to increase their likelihood of clinical translation in the future and also provide a physical support with mechanical properties similar to brain tissue. Furthermore, long-term studies are needed to fully understand the biological effect of the hydrogels and their degradation over time. Finally, further investigation on dual therapies combining pro-angiogenic and immunomodulator properties is needed to determine the role of

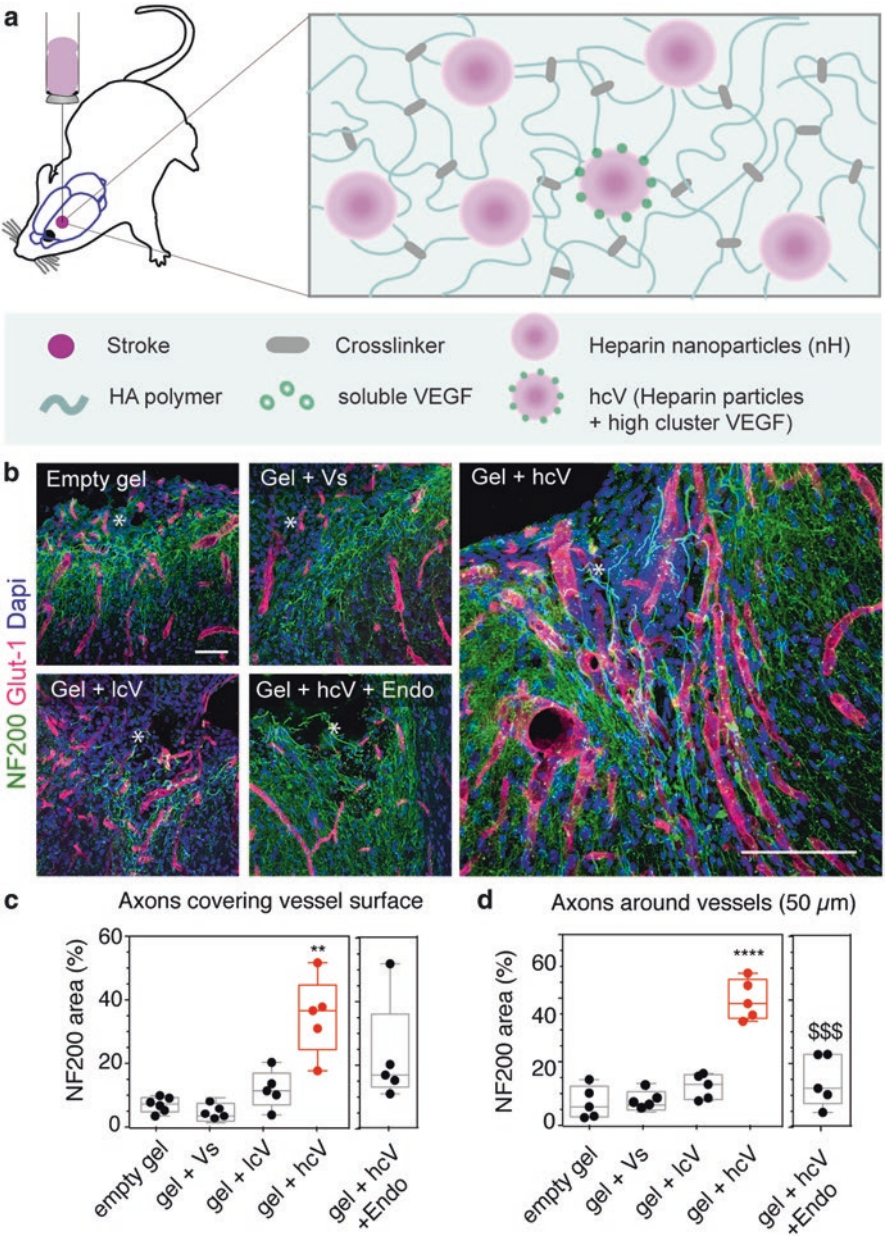

Fig. 7.4 (**a**) Schematic representing a brain injectable hydrogel composed of hyaluronic acid (HA), RGD motif peptide, and metalloproteinase-sensitive cross-linker. The gel was loaded with highly clustered VEGF (hcV) covalently bound onto heparin nanoparticle's surface and injected in a mouse model of ischemic stroke. (**b**) Vascular (Glut-1, red) and axonal growth (neurofilament NF200, green) was evaluated 16 weeks after gel implantation and compared with control groups treated with an empty gel, or gel loaded with soluble VEGF (Vs), low clusters of VEGF (lcV), or hcV and endostatin (angiogenesis inhibitor). The results show a significantly increased tissue growth in the hcV group, with a close association of axonal and vascular networks (**c**, **d**). Data are presented using a minimum-to-maximum box plot. Each dot in the plots represents one animal, and p values were determined by one-way ANOVA with Tukey's post hoc test. $^{**}p < 0.01$, $^{****}p < 0.0001$. Scale bar, 100 μm. Figure reprinted from [25] with the permission from Elsevier

inflammation on angiogenesis-induced tissue repair. Taken together, a tissue engineering approach to provascular therapies presents challenges that need to be overcome, before provascular materials are a valuable alternative for the clinical treatment of brain damage.

References

1. Abe, K., Setoguchi, Y., Hayashi, T., & Itoyama, Y. (1997). Dissociative expression of adenoviral-mediated *E. coli* LacZ gene between ischemic and reperfused rat brains. *Neuroscience Letters, 226*, 53–56.
2. Allen, C. M. (1984). Predicting the outcome of acute stroke: A prognostic score. *Journal of Neurology, Neurosurgery, and Psychiatry, 47*, 475–480.
3. Anderson, M. A., Burda, J. E., Ren, Y., Ao, Y., O'Shea, T. M., Kawaguchi, R., et al. (2016). Astrocyte scar formation aids central nervous system axon regeneration. *Nature, 532*, 195–200.
4. Anderson, S. M., Siegman, S. N., & Segura, T. (2011). The effect of vascular endothelial growth factor (VEGF) presentation within fibrin matrices on endothelial cell branching. *Biomaterials, 32*, 7432–7443.
5. Benjamin, E. J., Blaha, M. J., Chiuve, S. E., Cushman, M., Das, S. R., Deo, R., et al. (2017). Heart disease and stroke statistics-2017 update: A report from the American Heart Association. *Circulation, 135*, e146–e603.
6. Bible, E., Qutachi, O., Chau, D. Y. S., Alexander, M. R., Shakesheff, K. M., & Modo, M. (2012). Neo-vascularization of the stroke cavity by implantation of human neural stem cells on VEGF-releasing PLGA microparticles. *Biomaterials, 33*, 7435–7346.
7. Castellanos, M., Sobrino, T., & Castillo, J. (2006). Evolving paradigms for neuroprotection: Molecular identification of ischemic penumbra. *Cerebrovascular Diseases, 21*(Suppl 2), 71–79.
8. Chopp, M., Li, Y., & Zhang, J. (2008). Plasticity and remodeling of brain. *Journal of the Neurological Sciences, 265*, 97–101.
9. del Zoppo, G. J., & Mabuchi, T. (2003). Cerebral microvessel responses to focal ischemia. *Journal of Cerebral Blood Flow and Metabolism, 23*, 879–894.
10. Dirnagl, U., Iadecola, C., & Moskowitz, M. A. (1999). Pathobiology of ischaemic stroke: An integrated view. *Trends in Neurosciences, 22*, 391–397.
11. Emerich, D. F., Silva, E., Ali, O., Mooney, D., Bell, W., Yu, S. J., et al. (2010). Injectable VEGF hydrogels produce near complete neurological and anatomical protection following cerebral ischemia in rats. *Cell Transplantation, 19*, 1063–1071.
12. Granger, C. V., Hamilton, B. B., & Fiedler, R. C. (1992). Discharge outcome after stroke rehabilitation. *Stroke, 23*, 978–982.
13. Greenberg, D. A. (1998). Angiogenesis and stroke. *Drug News & Perspectives, 11*, 265–270.
14. Greenberg, D. A., & Jin, K. (2007). Regenerating the brain. *International Review of Neurobiology, 77*, 1–29.
15. Hayashi, T., Abe, K., & Itoyama, Y. (1998). Reduction of ischemic damage by application of vascular endothelial growth factor in rat brain after transient ischemia. *Journal of Cerebral Blood Flow and Metabolism, 18*, 887–895.
16. Herz, J., Reitmeir, R., Hagen, S. I., Reinboth, B. S., Guo, Z., Zechariah, A., et al. (2012). Intracerebroventricularly delivered VEGF promotes contralesional corticorubral plasticity after focal cerebral ischemia via mechanisms involving anti-inflammatory actions. *Neurobiology of Disease, 45*, 1077–1085.
17. Issa, R., Krupinski, J., Bujny, T., Kumar, S., Kaluza, J., & Kumar, P. (1999). Vascular endothelial growth factor and its receptor, KDR, in human brain tissue after ischemic stroke. *Laboratory Investigation, 79*, 417–425.

18. Jin, K., Mao, X. O., & Greenberg, D. A. (2006). Vascular endothelial growth factor stimulates neurite outgrowth from cerebral cortical neurons via rho kinase signaling. *Journal of Neurobiology, 66*, 236–242.
19. Ju, R., Wen, Y., Gou, R., Wang, Y., & Xu, Q. (2014). The experimental therapy on brain ischemia by improvement of local angiogenesis with tissue engineering in the mouse. *Cell Transplantation, 23*(Suppl 1), S83–S95.
20. Krupinski, J., Kaluza, J., Kumar, P., Kumar, S., & Wang, J. M. (1994). Role of angiogenesis in patients with cerebral ischemic stroke. *Stroke, 25*, 1794–1798.
21. Ma, Y., Zechariah, A., Qu, Y., & Hermann, D. M. (2012). Effects of vascular endothelial growth factor in ischemic stroke. *Journal of Neuroscience Research, 90*, 1873–1882.
22. Manoonkitiwongsa, P. S., Jackson-Friedman, C., McMillan, P. J., Schultz, R. L., Lyden, P. D., et al. (2001). Angiogenesis after stroke is correlated with increased numbers of macrophages: The clean-up hypothesis. *Journal of Cerebral Blood Flow and Metabolism, 21*, 1223–1231.
23. Moshayedi, P., Nih, L. R., Llorente, I. L., Berg, A. R., Cinkornpumin, J., Lowry, W. E., et al. (2016). Systematic optimization of an engineered hydrogel allows for selective control of human neural stem cell survival and differentiation after transplantation in the stroke brain. *Biomaterials, 105*, 145–155.
24. Nih, L. R., Deroide, N., Leré-Déan, C., Lerouet, D., Soustrat, M., Levy, B. I., et al. (2012). Neuroblast survival depends on mature vascular network formation after mouse stroke: Role of endothelial and smooth muscle progenitor cell co-administration. *The European Journal of Neuroscience, 35*, 1208–1217.
25. Nih, L. R., Gojgini, S., Carmichael, S. T., & Segura, T. (2018). Dual-function injectable angiogenic biomaterial for the repair of brain tissue following stroke. *Nature Materials, 17*, 642–651.
26. Ohab, J. J., Fleming, S., Blesch, A., & Carmichael, S. T. (2006). A neurovascular niche for neurogenesis after stroke. *The Journal of Neuroscience, 26*, 13007–13016.
27. Oshikawa, M., Okada, K., Kaneko, N., Sawamoto, K., Ajioka, I., et al. (2017). Affinity-immobilization of VEGF on laminin porous sponge enhances angiogenesis in the ischemic brain. *Advanced Healthcare Materials, 6*(11), 28488337.
28. Rodriguez-Yanez, M., Castellanos, M., Blanco, M., Mosquera, E., & Castillo, J. (2006). Vascular protection in brain ischemia. *Cerebrovascular Diseases, 21*(Suppl 2), 21–29.
29. Ruhrberg, C., Gerhardt, H., Golding, M., Watson, R., Ioannidou, S., Fujisawa, H., et al. (2002). Spatially restricted patterning cues provided by heparin-binding VEGF-A control blood vessel branching morphogenesis. *Genes & Development, 16*, 2684–2698.
30. Schmidt, R., Schmidt, H., & Fazekas, F. (2000). Vascular risk factors in dementia. *Journal of Neurology, 247*, 81–87.
31. Slevin, M., Krupinski, J., Slowik, A., Kumar, P., Szczudlik, A., & Gaffney, J. (2000). Serial measurement of vascular endothelial growth factor and transforming growth factor-beta1 in serum of patients with acute ischemic stroke. *Stroke, 31*, 1863–1870.
32. Slevin, M., Kumar, P., Gaffney, J., Kumar, S., & Krupinski, J. (2006). Can angiogenesis be exploited to improve stroke outcome? Mechanisms and therapeutic potential. *Clinical Science, 111*, 171–183.
33. Sun, Y., Jin, K., Xie, L., Childs, J., Mao, X. O., Logvinova, A., et al. (2003). VEGF-induced neuroprotection, neurogenesis, and angiogenesis after focal cerebral ischemia. *The Journal of Clinical Investigation, 111*, 1843–1851.
34. Szpak, G. M., Lechowicz, W., Lewandowska, E., Bertrand, E., Wierzba-Bobrowicz, T., & Dymecki, J. (1999). Border zone neovascularization in cerebral ischemic infarct. *Folia Neuropathologica, 37*, 264–268.
35. van Bruggen, N., Thibodeaux, H., Palmer, J. T., Lee, W. P., Fu, L., Cairns, B., et al. (1999). VEGF antagonism reduces edema formation and tissue damage after ischemia/reperfusion injury in the mouse brain. *The Journal of Clinical Investigation, 104*, 1613–1620.
36. Wang, Y., Kilic, E., Kilic, U., Weber, B., Bassetti, C. L., Marti, H. H., et al. (2005). VEGF overexpression induces post-ischaemic neuroprotection, but facilitates haemodynamic steal phenomena. *Brain, 128*, 52–63.

37. Yu, S. W., Friedman, B., Cheng, Q., & Lyden, P. D. (2007). Stroke-evoked angiogenesis results in a transient population of microvessels. *Journal of Cerebral Blood Flow and Metabolism, 27*, 755–763.
38. Zhang, H., Hayashi, T., Tsuru, K., Deguchi, K., Nagahara, M., Hayakawa, S., et al. (2007). Vascular endothelial growth factor promotes brain tissue regeneration with a novel biomaterial polydimethylsiloxane-tetraethoxysilane. *Brain Research, 1132*, 29–35.
39. Zhang, Z., Zhang, L., Jiang, Q., Zhang, R., Davies, K., Powers, C., et al. (2000). VEGF enhances angiogenesis and promotes blood-brain barrier leakage in the ischemic brain. *The Journal of Clinical Investigation, 106*, 829–838.
40. Zhu, S., Nih, L., Carmichael, S. T., Lu, Y., & Segura, T. (2015). Enzyme-responsive delivery of multiple proteins with spatiotemporal control. *Advanced Materials, 27*, 3620–3625.

Index

S. Gerecht (ed.), *Biophysical Regulation of Vascular Differentiation and Assembly*, Biological and Medical Physics, Biomedical Engineering,
https://doi.org/10.1007/978-3-319-99319-5